Improvement of Early Preparedness and Early Warning Systems for Extreme Climatic Events – Flood Warnings

Report to the
Water Research Commission

by

E Poolman*, E de Coning*, E Becker*, G Pegram, S Sinclair**, N Kroese***
*South African Weather Service
** Pegram & Associates (Pty) Ltd

WRC Report No. 2068/1/15
ISBN 978-1-4312-0664-3

APRIL 2015

Obtainable from

Water Research Commission
Private Bag X03
GEZINA, 0031
orders@wrc.org.za or download from www.wrc.org.za

ABSTRACT

This project endeavoured to enhance the early warning system against flash floods in South Africa, which is based on the South African Flash Flood Guidance (SAFFG) system. The SAFFG system models on an hourly basis the likely hydrological response of small river basins to rainfall as estimated in near real time by information obtained from SAWS weather radar systems and the Meteosat weather satellite. The performance of the SAFFG system was investigated and the problem areas identified. This led to the development of an enhanced satellite rainfall-estimation algorithm to address the serious underestimation of stratiform rain in the Western Cape Province, by combining convective rainfall estimation from satellite images with stratiform rainfall forecasts from the Unified Model operated by SAWS. Experiments were also conducted to improve the radar-rainfall relationships. A comparison of the soil moisture modelling of SAFFG with the PyTopkapi model developed by Pegram & Associates revealed some errors in the calibration that were addressed subsequently by the SAFFG developers. The lack of useful information on potential flash floods beyond a six hours horizon was addressed by the development of an ensemble forecasting system based on a single deterministic weather model. Understanding user needs was also an important focus of the project. These user needs were determined through sessions with various municipal and provincial disaster management centres. This led to the development of various user-oriented products, such as a system to forecast the likely impact of a flash flood and not only the occurrence of the flash flood, by linking the potential of flash floods from the SAFFG model with socioeconomic vulnerability indicators through an impact model. The study concludes with recommendations for the enhancement of the entire flash flood early warning system.

EXECUTIVE SUMMARY

INTRODUCTION

Almost 95% of all natural disasters occurring in South Africa are weather related. Of these, the most numerous disasters on record since 1920 involving loss of life and property are due to floods and flash floods. Floods have the most significant impact of all natural disasters on communities and their livelihoods in South Africa. The expected changes in the frequency and intensity of heavy precipitation due to climate change could lead to an increase of flood events worldwide. In South Africa, impacts are exacerbated by progressively increased urbanization over the last hundred years, which has increased the vulnerability of people as more communities settle in flood plains. In response to this threat, this study for the WRC was conducted in order to enhance the early warning system against flash floods in South Africa. The aims of the study are:

- To enhance the early warning systems of extreme flood events, particularly the SAFFG system, based on *in situ* observation and remotely-sensed hydro-meteorological information;
- To enhance the prediction tool to support water resource and disaster managers in flash flood risk evaluation and analyses, river flow forecasting as well as precipitation estimation;
- To review international best practices of early warnings and preparedness for flash flood events, and compare these with available technology such as the South African Flash Flood Guidance system (SAFFG), PyTOPKAPI and others;
- To improve rainfall estimation (from radar and satellite) and the nowcasting input into SAFFG;
- To improve the hydrological input and products of the flash flood guidance warning system, including soil-moisture estimation by SAFFG;
- To enhance the integration of system components to enable seamless dissemination and application of flash flood warnings to end-users such as disaster management and water managers.

The main focus of this study was the improvement of SAFFG implemented at the South African Weather Service (SAWS) in 2010. SAFFG is a hydrometeorological modelling system that simulates the most likely hydrological response of 5366 small river basins to rainfall estimated from weather radars and the Meteosat meteorological satellite. Its domain covers the major economic and heavily populated areas of South Africa and the south coast between Cape Town and Port Elizabeth. SAFFG provides guidance to weather forecasters as to how much rain is required in each small basin for possible flooding to occur at the outlet of the basin (Figure A). Combined with a rainfall forecast, the SAFFG has the potential to provide indicative guidance to forecasters regarding where and when to issue flash flood warnings, with a lead-time of between 1 to 6 hours, to disaster and water managers and the general public. SAFFG thus performs a vital modelling role in the flash flood warning system.

The primary sources of error in SAFFG are the quality of the radar and satellite precipitation estimation, and the calibration of the basins to allow realistic simulation of soil moisture conditions affecting runoff production. These problem areas were a major focus to improve SAFFG either through the project activities, or through collaborative studies with the Hydrological Research Center (HRC) in San Diego, California, USA, the developers of SAFFG. Another important

development area was to devise special products and information, based on the SAFFG output, for enhancing the decision-making capacity of forecasters and disaster managers.

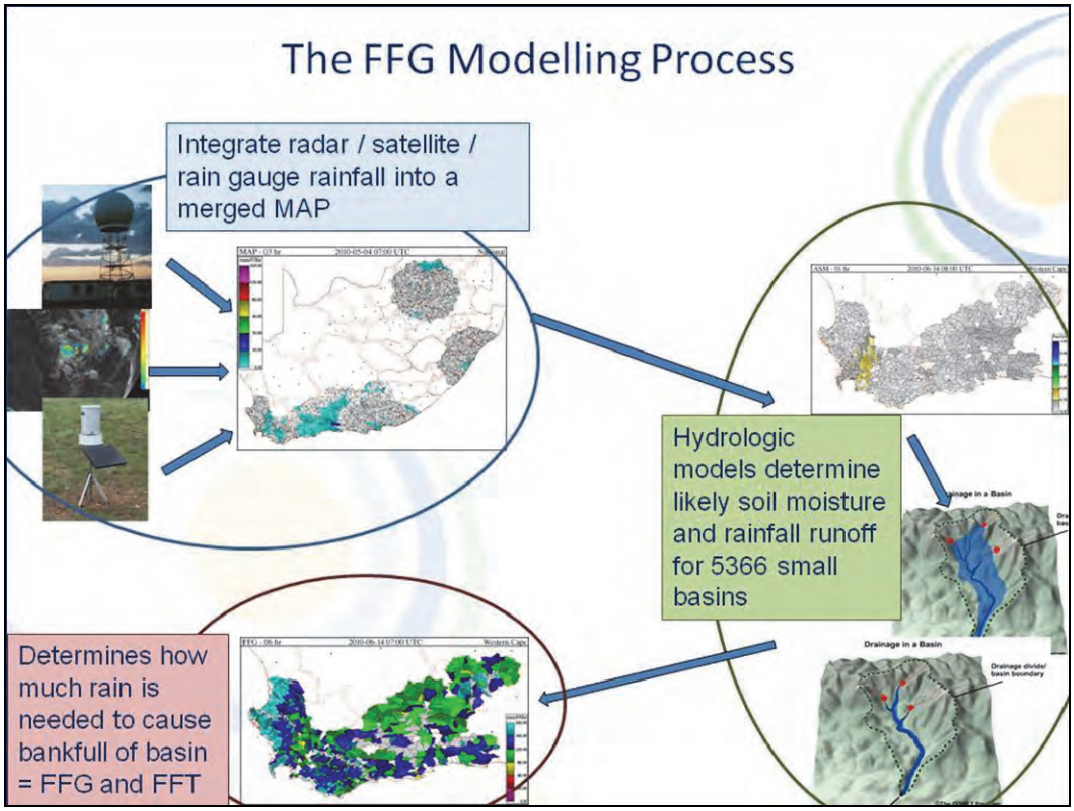

Figure A: Image illustrating the integration of meteorological variables with hydrological modelling in the SAFFG to assist in evaluating FFT.

MAJOR RESULTS

This study succeeded in improving the application of SAFFG in the flash flood warning system in South Africa in two main areas:

(1) The SAFFG modelling system was enhanced through the improvement of the rainfall estimation techniques and identification of calibration issues affecting performance of hydrological models;
(2) User oriented products were developed aimed at improving the application of SAFFG in the decision making systems used by weather forecasters, water managers and disaster managers.

An analysis of the archived output of SAFFG revealed that it performed reasonably well in capturing a climatologically realistic pattern of flash flood potential, particularly during organized convective rainfall situations, when using rainfall estimated by the S-band radars (using a 10 cm wavelength) in the Gauteng Province, KwaZulu-Natal and the eastern parts of the Eastern Cape Province. A number of prominent and serious flash flood events were well captured by SAFFG and provided useful guidance to weather forecasters.

C-band (5 cm wavelength) radars in Port Elizabeth, and for a few months in 2012 in Durban, experienced serious interference from radio LAN operated by private companies and individuals in the radar domain. Filters deployed to reduce this interference led to significant underestimation of rainfall by these radars and their data had to be removed from the rainfall estimation data-field.

Satellite rainfall estimation, which relies heavily on cloud-top temperature measurement, is more effective for convective clouds with high cloud tops than for stratiform clouds with much lower cloud tops. Consequently, serious underestimation of rainfall by satellite occurred during stratiform rainfall situations, as experienced during the winter in the Western Cape Province. This resulted in very few flash flood events being simulated realistically. To overcome this issue, the satellite convective rainfall estimates were blended with the stratiform rainfall forecasts from numerical weather prediction products of the UK Met Office Unified Model run at SAWS. This new combined rainfall product proved to be an improvement, which led to more realistic capturing of flash flood potential in the Western Cape.

A comparison of the soil moisture modelling by SAFFG with the PyTOPKAPI model revealed an error in the soil moisture-modelling component owing to an area specific calibration problem in SAFFG. This caused some underestimation of potential flooding in the Gauteng Province. Relevant modelling issues have been subsequently addressed by the HRC through a separate contract with SAWS. The HRC also recalibrated the bias correction factors for radar rainfall estimation using S-band radars, as well as the bias correction factors for the new combined satellite/Unified Model rainfall estimation scheme.

An important component of any early warning system is the link between the forecaster and the disaster manager, which ensures effective response by communities at risk to the warnings issued. This requires a complete package of user-oriented information that allows disaster management to translate the warning into disaster risk information that allows life-saving decisions to be made. Workshops were conducted with various disaster management centres to determine user needs regarding flash flood forecasting and warning products. This resulted in the development of a series of new user-oriented products, including maps at local municipality level, for alerting users in local municipalities to potential flash flood problems.

Capacity building included workshops with disaster management and water managers, as well as formal post-graduate training at MSc and PhD level.

CONCLUSIONS AND WAY FORWARD

The flash flood warning system in South Africa has brought together the meteorological, hydrological and disaster management sectors, ensuring mutual collaboration. SAFFG is a hydrometeorological model, which provides guidance to forecasters in issuing warnings of flash floods to disaster management and to the public. This WRC project succeeded in making important improvements to the SAFFG modelling system following its initial implementation in 2010. It has been the catalyst for a number of subsequent activities aimed at improving the entire flash flood warning system in South Africa.

A system similar to SAFFG, the Southern African Regional Flash flood Guidance system (SARFFG), has been implemented for nine countries in the southern African region by the World Meteorological Organisation (WMO). Compared to SAFFG, SARFFG uses only satellite information and covers the nine southernmost countries in Southern Africa, but at a lower resolution. Improvements made in the SAFFG system will also benefit the SARFFG.

Parallel to this WRC project, SAWS has entered into a separate project agreement with the Hydrologic Research Center (HRC) in San Diego, USA, who are the developers of SAFFG. The purpose of this project with HRC is to perform additional upgrades to the SAFFG modelling system, based on the recommendations of the WRC project. Other subsequent activities include a project by WMO, to start in 2015, which aims to integrate SARFFG into the Severe Weather Forecasting Demonstration Project (SWFDP), developed as a SADC regional severe weather early warning system, with SAWS as the regional specialised meteorological centre. An innovative outcome of the project is an initiative to move beyond forecasting the hazard towards forecasting the impact of the hazard. An impact forecasting concept will be further developed in a collaboration effort between SAWS and disaster management for operational implementation in South Africa in the next few years.

Based on this study and on previous investigations by other WRC-supported researchers, recommendations have been made that relate to the enhancement of the entire flash flood early warning system. A new proposal has been presented for a comprehensive, integrated, flood warning system, covering all forecasting timescales from seasonal forecasts right down to the nowcasting of severe weather in the next hour or two. Such an integrated system can only be developed and operated as a partnership between the main role players, particularly the South African Weather Service, the Department of Water Affairs and Disaster Management structures.

ACKNOWLEDGEMENTS

The project team would like to thank the Water Research Commission for providing financial support that made this project possible.

Appreciation is also expressed to the following persons who served on the project reference group for their invaluable guidance and support:

Mr C Moseki (WRC – Chairman)
Mr B du Plessis (DWA)
Dr G Green (WRC – Retired)
Dr B Mwaka (DWA)
Mr M Maswuma (DWA
Mr D van der Spuy (DWA
Prof J van Heerden (Retired)
Prof H Rautenbach (UP)
Mr M Tau (NDMC)
Mr V de Beer (Gauteng PDMC)
Mr Mark van Staden (NDMC)
Dr Dennis Dlamini (DWA)

The South African Weather Service (SAWS) provided the computing facilities, data and staff who participated as part of the project team. The project team consisted of:

Mr E Poolman (SAWS)
Dr E de Coning (SAWS)
Mr E Becker (SAWS)
Mr N Kroese (SAWS)
Ms V Phakula (SAWS)
Ms B Maseko (SAWS)
Prof G Pegram (Pegram and Associates)
Dr S Sinclair (Pegram and Associates)

LIST OF ABBREVIATIONS

ASM	Average Soil Moisture
CAPPI	Constant Altitude Plan Position Indicator
COMB	Combination product between the Unified Model and satellite rain
DWA	Department of Water Affairs
FFG	Flash Flood Guidance
FFT	Flash Flood Threat
FFWRS	Flood Forecast Warning and Response System
HRC	Hydrologic Research Center
IFFT	Imminent Flash Flood Threat
IPCC	Intergovernmental Panel on Climate Change
ISDR	International Strategy for Disaster Reduction
MAE	Mean Absolute Error
MDV	Meteorological Data Volume
MHEWS	Multi-Hazard Early Warning System
MMAP	Merged Mean Areal Precipitation
MSG	Meteosat Second Generation
NCAR	National Center for Atmospheric Research
NDMC	National Disaster Management Centre
OFC	Optical Flow Constraints
PDMC	Provincial Disaster Management Centre
QPE	Quantitative Precipitation Estimation
QPF	Quantitative Precipitation Forecast
RMSE	Root Mean Square Error
SADC	Southern African Development Community
SAFFG	South African Flash Flood Guidance system
SARFFG	Southern African Regional Flash Flood Guidance system
SAWS	South African Weather Service
SIMAR	Spatial Interpolation and Mapping of Rainfall
SPE	Satellite Precipitation Estimates
SWFDP	Severe Weather Forecast Demonstration Project
SWWS	Severe Weather Warning System
TRMM	Tropical Rainfall Measuring Mission
VRP	Vertical Reflectivity Profile
WRC	Water Research Commission

Table of Contents

1. INTRODUCTION

1.1 FLOOD DISASTERS IN CONTEXT

The World Meteorological Organization (WMO) recognized that according to the CRED/EMDAT international disaster database 80% of all natural disasters occurring worldwide are weather related (WMO, 2006; Poolman, 2014, section 2.2). Analysing this database from 1920 to 2008 this percentage rises to 95% for South Africa (CRED/EMDAT, 2010). This is mainly due to the low occurrence of earthquakes and volcanoes in the country compared to other parts of the world. The most prominent natural disasters in South Africa are floods, followed by droughts, wind storms (tornadoes, coastal gales, etc.) and wild fires based on both the number of each disaster (as showed in Figure 1.1) and also the relative impact score (Figure 1.2) calculated from the CRED/EMDAT data. Whereas droughts in South Africa affected more people by far, floods were more numerous, and overall have a significantly wider impact on people and their livelihoods. Furthermore, flood disasters constituted 44% of all reported weather related disasters (excluding drought) in South Africa, mostly in the form of flash floods. In the USA, most weather related deaths are associated with flash floods (Davis, 2001).

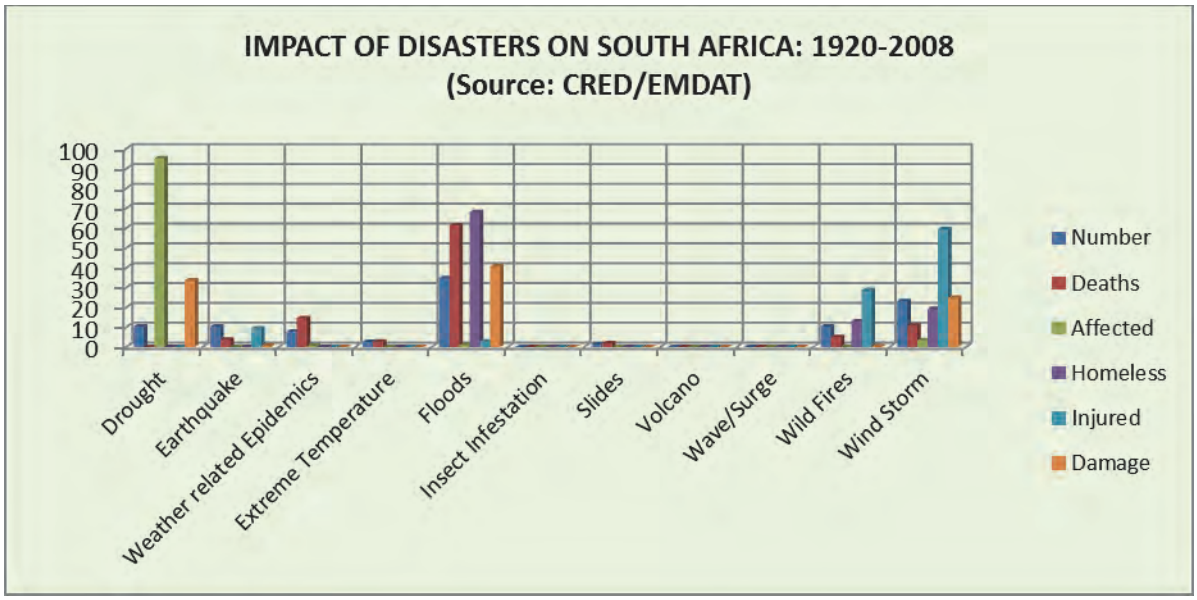

Figure 1.1: Comparison of the impact (as a percentage of the total impact per category) of different natural disasters that occurred in South Africa between 1920 and 2008 on human livelihood, according to the CRED/EMDAT disaster database (Poolman, 2014).

In a detailed investigation by Holloway (2010) on the impact of six disaster events in the Western Cape Province between 2003 and 2008 they found flood and storm damage amounting to more than R2.5 billion (adjusted to 2005 values) in property and infrastructure damage. They concluded that weather systems causing floods and windstorms had significant impact on cities, coastal settlements and rural communities. Flooding caused by tropical cyclone Eline in 2000 caused extreme damage to roads, infrastructure, agriculture and property over Mpumalanga, South Africa, amounting to more than R3 billion (Du Plessis, 2002). Natural hazards will always affect communities simply because humans are living in the volatile natural world, which is dynamic and can be extremely hostile and

violent at times. When these natural hazards disrupt human activity beyond the ability of the community to cope, using its own resources and causing loss of lives and livelihoods, these natural hazards turn into disasters (ISDR, 2005a). According to the ISDR (ISDR, 2010) a hydrometeorological hazard is a potentially damaging event or phenomenon of meteorological, hydrological or oceanographic nature that may lead to the loss of life or property. Vulnerability of communities increase as people settles and develops in risky areas such as flood plains or earthquake zones making them more susceptible to natural hazards such as floods.

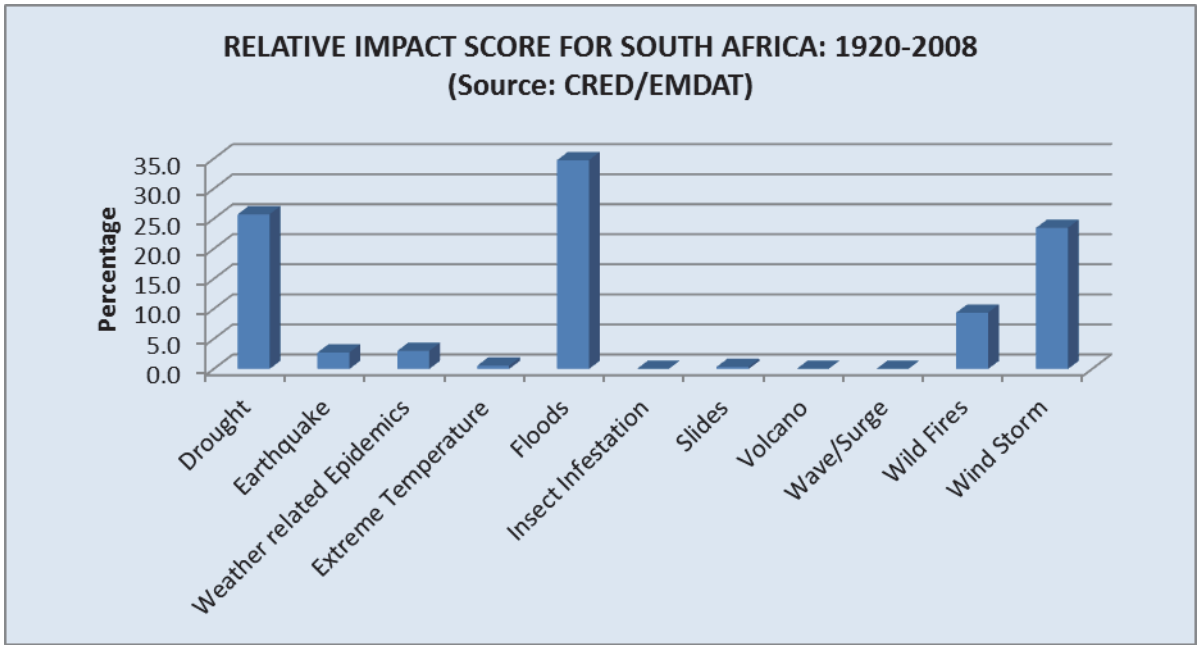

Figure 1.2: Relative impact score based on the data in Figure 1.1 calculated as the average of the various impacts (deaths, people affected, homeless, injured and damage) that each hazard had as a percentage of the total impacts of all the hazards (Poolman, 2014).

In November 2011 the IPCC (2011) released a summary of a Special Report on Managing the Risks of Extreme Events and Disasters, stating "*… a changing climate leads to changes in the frequency, intensity, spatial extent, duration and timing of extreme weather and climate events, and can result in unprecedented extreme weather and climate events*" (IPCC, 2011, p4). They furthermore concluded "*…it is likely that the frequency of heavy precipitation….will increase in the 21st century…*" even despite projected decreases of total precipitation in some regions (IPCC, 2011, p10). This is likely to be exacerbated by the impact of social and demographic changes. Reflected against the increase of the total population of South Africa from 17.4 million in 1960 to 47.8 million in 2008 (World Bank, 2010), the number of people living in areas vulnerable to natural hazards will increase significantly increasing the pressure on disaster risk reduction activities in these regions (Davis, 2001; Pegram *et al.*, 2007). When the vulnerability and risk of disasters increase, then early warnings systems need to be improved to provide timely useful information to disaster managers and vulnerable communities to take action and reduce the negative impact of a hazard. Figure 1.3 show trends of natural disasters versus flood disasters between 1980 and 2007 in Southern Africa as constructed from the CRED/EMDAT database. The increase in disasters can be attributed to a number of causes, including probably climate change, demographic changes and improved reporting. Figure 1.4 show a distribution of flood events as reported in the CAELUM newspaper events database of SAWS (Caelum, 2010).

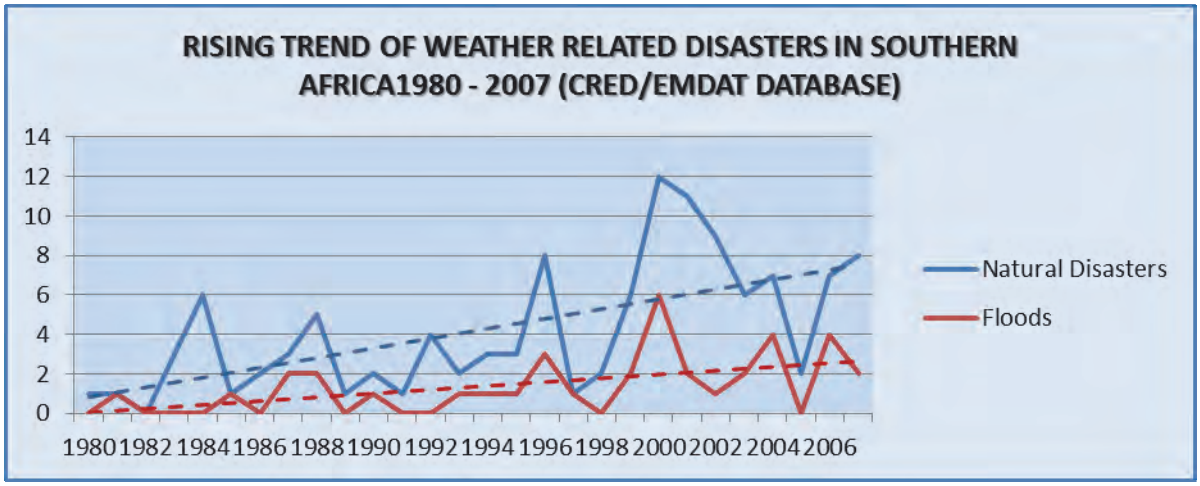

Figure 1.3: Trends of the number of natural disasters in comparison with flood disasters in Southern Africa according to the CRED/EMDAT disaster database.

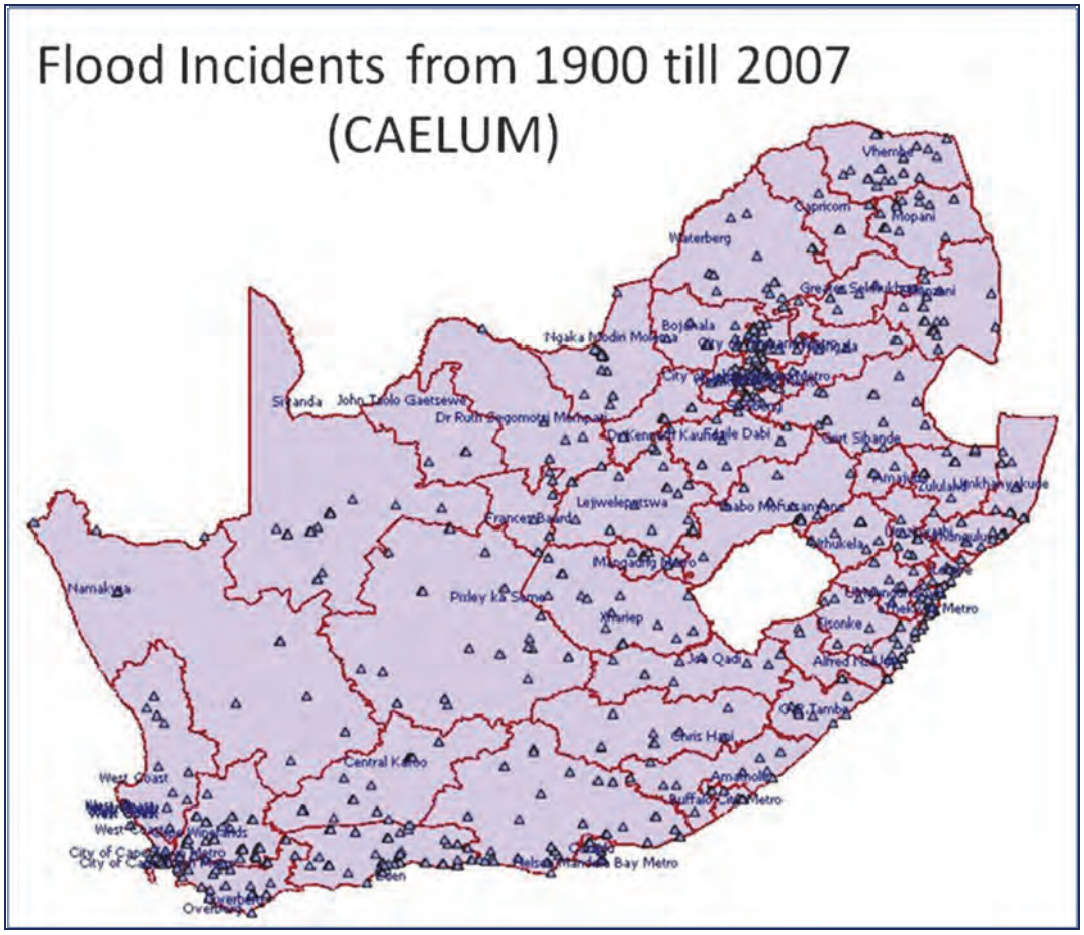

Figure 1.4: Distribution of flood events in South Africa from 1900 until 2007 as reported by newspapers and summarized in the SAWS Caelum. The red lines are borders of district municipalities.

1.2 RECENT DEVELOPMENT OF A FLASH FLOOD WARNING SYSTEM FOR SOUTH AFRICA

Officially, no institution in South Africa is mandated to issue flash flood warnings, i.e. flooding within 6 hours of the causative event such as heavy rain. The Department of Water Affairs (DWA) generally deals with river flooding and related warnings. The South African Weather Service (SAWS) is responsible for issuing heavy rain warnings, and usually adds a general note that "flash flooding is possible in low-lying areas" without any substantiating explanation.

In response to the increasing flash flood threat to South Africa described above, the South African Weather Service (SAWS) and the National Disaster Management Centre (NDMC) embarked on a collaborative project for the development of a flash flood warning system in October 2008. This system is a part of the multi-hazard early warning system of South Africa against weather-related disasters. Central to the flash flood warning system, the South African Flash Flood Guidance (SAFFG) system (Poolman, 2010) has been implemented as a diagnostic modelling tool supporting forecasters with information related to the hydrologic conditions that could lead to flash floods. Another integral part of the end-to-end flash flood warning system is the effective application of flash flood warnings by end users such as disaster managers at local level.

The SAFFG system is a hydro-meteorological modelling system combining in real-time meteorological information, such as quantitative rainfall estimation from weather radars, satellite and rain gauges, with hydrological modelling of the soil moisture conditions and the flash flood potential in 5366 small river basins (on average 50 km^2) in five flash flood prone regions over South Africa. The SAFFG depends heavily on the quality of quantitative precipitation estimation (QPE) products from radar and satellite as input to the hydrologic models, an area identified as a weak point in need of significant improvement in preliminary tests.

The World Meteorological Organization is developing a similar Southern Africa Regional Flash Flood Guidance system (SARFFG) developed by the same contractor in the USA, aiming for implementation in 2014. The SADC SARFFG system will cover the rest of South Africa and nine other countries where there are no radar coverage. Any improvements (apart from radar specific enhancements) implemented for the SAFFG warning system will be valuable in the SADC SARFFG system for the rest of South Africa and for the other SADC countries who do not have the capability to carry out this research and development.

1.3 AIMS OF THE STUDY

This study generally aims to enhance the end-to-end flash flood warning system, and specifically to address the identified weak points of the SAFFG system. It is very important to improve the rainfall estimation from radar and satellite information as a primary input into the hydrological modelling. Testing and validation of the products of the SAFFG modelling system is needed to improve the hydrologic modelling of soil moisture and flash flood guidance. Improving the effective use of SAFFG products in the decision-making processes of end-users such as water resource and disaster managers needs to be addressed, including extending the current lead-time of flash flood warnings from the SAFFG system from 6 hours to 24 hours and beyond. The specific aims of the study are:

- To enhance the early warning systems of extreme flood events, particularly the SAFFG system, based on *in situ* observation and remotely-sensed hydro-meteorological information;
- To enhance the prediction tool to support water resource and disaster managers in flash flood risk evaluation and analyses, river flow forecasting as well as precipitation estimation;
- To review international best practices of early warnings and preparedness for flash flood events, and compare these with available technology such as the South African Flash Flood Guidance system (SAFFG), PyTOPKAPI and others;
- To improve rainfall estimation (from radar and satellite) and the nowcasting input into SAFFG;
- To improve the hydrological input and products of the flash flood guidance warning system, including soil-moisture estimation by SAFFG;
- To enhance the integration of system components to enable seamless dissemination and application of flash flood warnings to end-users such as disaster management and water managers.

1.4 OUTLINE OF THE REPORT

An overview of flood warning systems is provided in Section 2. This is followed in Section 3 by a detailed discussion of the South African Flash Flood Guidance system (SAFFG), and in Section 4 an intercomparison of the soil moisture modelling between SAFFG and the PyTOPKAPI model. In Section 5 information on precipitation estimation using weather radars and the European meteorological satellite is provided. Analysis of problems using these systems for rainfall estimation, and improvements aimed at SAFFG is discussed. In Section 6 the important links with users, particularly disaster management and hydrologists are discussed with developments to provide better information and products to users. The study is concluded in Section 7 with recommendations for improving the flash flood warning system in South Africa.

2. AN OVERVIEW OF FLOOD WARNING SYSTEMS

2.1 INTRODUCTION

The American Meteorological Society (AMS, 2012) as well as the WMO International Glossary of Hydrology (WMO, 2011) defines a flood as the "*overflowing of the normal confines of a stream or other body of water, or the accumulation of water over areas that are not normally submerged*". There are various types of floods identified around the world (WMO, 2011), ranging among others from flash floods and river floods to seasonal floods, multi-event floods, estuarine floods and ice-jam floods. Based on the information provided above and other references (Holloway, 2010), different types of floods affecting South Africa could be identified for this report (Poolman, 2014, section 2.4):

- *River floods* usually occur when heavy rain falls over many days in an upper catchment and increase the water levels in the river channels exceeding the capacity of the channel causing spilling of water over the banks into natural flood plains. As the flood wave moves downstream, adjacent areas to the rivers are inundated by floodwaters, as the water level overflows a river's banks. These floods can be exacerbated when sluice gates in dams have to be opened to prevent them from overtopping;
- *Flash floods* are quick response flood events causing sudden flooding in small river basins. The flooding occurs within 6 hours of the heavy rain event. They could also occur in small streams or dry riverbeds. The short warning and response time lead to high risk of death;
- *Urban floods* are flash floods that occur in basins altered by humans when heavy rain collects on impervious surfaces in cities (like roads, parking areas, etc.) storing more surface water than can drain through the sewer systems. These include flooding of streets, underpasses, low-lying areas or storm drains;
- *Road floods* are similar to urban floods, resulting in flooded roads, highways, underpasses and bridges that are particularly hazardous to traffic. Debris clogging inlets to pipes or channels aggravates the problem;
- *Pooling*, also called *rising floods,* occur when an area is flooded through a build-up of water, but no significant river flow is evident. This happens typically in the Cape Flats in informal settlements close to wetlands;
- *Storm surges* and *coastal floods* are the result of abnormally high levels of water caused by intense storm systems (like tropical cyclones, or intense extra-tropical cyclones) coinciding with high tides, and which surge against the coast line into river mouths and estuaries, or severely damage coastal infrastructure;
- *Estuarine floods* occur when the seaward flow of rivers and streams meet with landward flow of seawater at estuaries during high tides and surges, combined with significant inland rain.

Each of these types of flood needs to be dealt with in a specific manner. The response time of large catchments leading to river floods, vary from many hours to days (Pegram *et al.*, 2007). In comparison, small catchments have response times in the order of hours resulting in flash floods. The forecasting technology used for one type of flooding cannot necessarily be applied to other types of flooding. River floods, flash floods and storm surges are dealt with in different ways with

different technological systems, and even different institutions in some cases. This report will focus more specifically on flash flood warning systems, which are least predictable but the biggest threat of the above flood types (Davis, 2001). A flash flood is defined by the AMS (2012) as "*a flood that rises and falls quite rapidly with little or no advance warning, usually as the result of intense rainfall over a relatively small area*". The WMO (2008, pp. 16) defines flash floods as "*excessive water flow events that develop within a few hours – typically less than 6 hours – of the causative rainfall event*". The simplest definition for a flash flood is "*too much water, too little time*" (Davis, 2001, pp. 482).

2.2 WARNING SYSTEMS AGAINST FLOODING: INTERNATIONAL APPROACHES

A global survey of early warning systems done by the International Strategy for Disaster Reduction (ISDR) in 2006 (ISDR, 2006b) revealed that a number of developed countries operated **river flood** warning systems mostly on large river systems like the Danube, Thames, etc. Floods in large river basins respond slowly to heavy rain events due to the time water takes to travel and accumulate in the main river channel. Warning and forecasting concern predicting the movement of the flood wave down the river as represented by hydrographs at critical points along the river. It is thus primarily a hydrological problem. In many instances rainfall-runoff models, coupled with river-routing models are used (WMO, 2008). They tend to require detailed catchment calibration and can have elaborate data requirements. Invariably, these models are too complex for effective use in flash flood situations, particularly when different rainfall scenarios need to be tested operationally.

The ISDR survey also reported that some countries had systems in place to *monitor* **flash floods**, including using weather radars. Unfortunately, most flash floods occur in areas not covered by radars. The survey found that operational flash flood *forecasting* systems existed, at the time of publication, in only a few countries. Davis (2001) concluded that forecasting and detecting flash floods are the most difficult challenges for forecasters. This can be attributed to the complexity of flash flood forecasting involving hydrological complexity mixed with meteorological challenges. The very short lead-time (less than 6 hours) available for hydrometeorological forecasts to be useful, compared to the long lead time (days) for river floods, exacerbates the problem.

There is a multitude of hydrologic models and approaches to model aspects of floods (WMO, 2011). The most advanced service provides information on inundation areas and the depth of flooding. However, this is the most costly and complex flood warning service and not even developed countries can cover the entire country with this type of service. The complicated modelling and cost of effective instrumentation for the relative small number of events per basin cannot yet justify the necessary investment. According to the WMO (2011), the level of service depends on the technical feasibility and the economic conditions of a country. The following levels of general flood forecasting and warning services are identified in the WMO report in increasing order of complexity:

- Threshold-based flood alert, which is a qualitative estimation of hazard and which requires no hydrologic modelling. It can be based on observations and is location specific to the observation points;
- Flood forecasting, either using simple statistical methods, or performing more complex modelling of the response of streams. Calibration using historical data is required, and the service can be focussed on specified places at risk and is not limited to observation points as in the previous case;

- Map-based visualization, or “vigilance” mapping (as done in France). This is an enhancement of the previous method, and provides information on the severity of the expected flooding;
- Inundation forecasting is the most advanced service. This is the most complex and precise forecasting of flooding, providing information on inundation of different suburbs or critical infrastructure.

Flash floods are caused by rapidly rising floodwaters due to a heavy rain event, and they can occur in any small stream, in mountainous areas, low-lying areas or in urban areas. The WMO further state (WMO, 2008) that due to the short time interval between the heavy rain and the flash flood, accurate detection and prediction of the flash flood event is crucial for a successful warning system. This in turn requires close cooperation between hydrologists and meteorologists, and thus flash floods forecasting is a “truly hydrometeorological endeavour” (WMO, 2008, pp16). To allow for the complications three types of flash flood modelling approaches are broadly identified (Georgakakos, 2011):

- *Site specific modelling*: This approach has a special purpose for a specific site or basin and requires a data rich environment for effective modelling. A typical example is hydrologic forecasting for the Panama Canal.
- *High resolution distributed modelling*: In this approach, flow simulations are forecast for small sub-catchments of larger catchments using hydrologic models and current high-resolution rainfall estimated from radars. Typical examples are the TOPKAPI hydrological model implemented for flood forecasting on some Italian rivers (WMO, 2011). These types of model systems are more complex to use in operational flash flood scenarios for large areas at high resolution, and are better suited for river flood forecasting.
- *Flash flood guidance*: This approach is specifically aimed at flash flood forecasting (Georgakakos, 2006), since the required amount of basin-averaged rainfall over a specific period that will lead to bank full conditions at the outlets of small basins is regularly calculated from observed rainfall and hydrologic parameters. It is thus a diagnostic tool for forecasters to quickly assess the potential for flash floods in relation to expected rainfall in the next few hours. This methodology has been used in the USA since the 1970s to produce flash flood watches and warnings, and has since then been extensively enhanced (Davis, 2001; Georgakakos, 2006). It is also ideal for larger ungauged regions, especially in the absence of weather radars, since useful information can be provided using satellite estimates of rainfall. It is thus well suited for developing regions such as Southern Africa, Central America, and so forth (WMO, 2007).

2.3 FLOOD WARNINGS AS PART OF THE MULTI-HAZARD EARLY WARNING SYSTEM

2.3.1 Summary of previous investigations

Following the floods in the Mpumalanga province of South Africa in 2000, Du Plessis (2002) reviewed the status of a flood forecast, warning and response system (FFWRS) in South Africa at the time. He argued that there was a desperate need for the implementation of such a system as an effective prevention and mitigation strategy to minimize loss of life and reduce damage to property caused by flood disasters. Such a warning system should be integrated to include technical warning, communication issues and effective response by users, and mitigation strategies based on vulnerability assessments and awareness campaigns. Based on examples from elsewhere, Du Plessis proposed a five-stage implementation model of 14 different criteria for South Africa.

At the time of writing his paper, Du Plessis concluded that "very little, if any, formal flood warning (is) available" (Du Plessis, 2002, p134). A flood warning system that was developed by Alexander in 1993 for the Jukskei River has since stopped functioning. The then Department of Water Affairs and Forestry (DWAF) operated an advanced River Forecasting System in the Vaal and Orange Rivers, based on technology used in the USA. There was also some local level interest in flood warning systems, particularly in Alexandria on the Jukskei River, and in Ladysmith on the Klip River. The SA Weather Service (SAWS) at that stage was primarily responsible for forecasting heavy rain, using numerical weather prediction (NWP) models, satellite data and an outdated radar network. The SAWS had some success in providing forecasts of heavy rain from large weather systems with lead-times of up to 5 days, as in the case of the Natal floods of 1987. Apart from the individual efforts mentioned by Du Plessis in the Jukskei and Klip Rivers, there were no flash flood warning systems in South Africa. Du Plessis concluded that effective flood warning required clarification of roles and responsibilities through the anticipated implementation of the new Disaster Management Act, and the implementation of an appropriate FFWRS in flood-prone areas.

A series of WRC reports published in 2004 (Kroese, 2004; Deyzel *et al.*, 2004; Pegram, 2004) described the development of the Spatial Interpolation and Mapping of Rainfall (SIMAR) product over a period of three years. The SIMAR product was a daily rainfall map of 24 hour accumulated rainfall on a resolution of 2 km, over the whole subcontinent, based on satellite, radar and rain gauge information. This was the first attempt to have daily, countrywide high resolution gridded rainfall product available for flood forecasting purposes, among others. The S-band radar at Bethlehem, procured by the WRC in 1994 and decommissioned in the late 2000's, was a prominent part of the SIMAR project. Daily SIMAR products were available until the new weather satellite, MSG, became operational in 2006. The data of MSG were incompatible with the SIMAR algorithms, which resulted in a loss of one of the three main sources of rainfall data.

In a final report to a related WRC project, Pegram *et al.*, (2007) investigated the feasibility of a national flood warning system. A scheme for the implementation of flood forecasting systems for South Africa was proposed in this report. This included a prototype system developed in earlier research in the Mgeni and Mlazi catchments near Durban using the TOPKAPI fully distributed rainfall-runoff model. In their report Pegram *et al.*, (2007) also proposed a methodology to produce flood lines and thus inundation areas for selected high-risk catchments. The final recommendations by the project steering committee included a proposal (Pegram *et al.*, 2007, pp 90-95) for the implementation of a pragmatic national flood nowcasting system, taking into account institutional capacities, roles and responsibilities, and focussing on the main metropolitan areas in South Africa. This proposal included application of flood warnings with lead-times larger than 6 hours, and flash flood warnings with short lead-times – each with its own different technological system. At the time of the proposal, this vision was not realizable on a technical or institutional level. However, the proposal will be revisited in the current project in the light of new developments in the last few years.

2.3.2 The Multi-Hazard Early Warning System

In recent years, significant developments occurred that paved the way for implementing improved flood and flash flood warning systems. First and foremost was that since the implementation of the National Disaster Management Act of 2002 (DPLG, 2002) and the National Disaster Management Framework (DPLG, 2005) the disaster risk management system in South Africa became much more

organized, including the establishment of disaster management centres at national, provincial and district municipal level. Disaster risk management adopted a comprehensive proactive attitude by including prevention and preparedness into the disaster management cycle with the mitigation and response activities. This also organized the roles and responsibilities of disaster managers, thereby simplifying issuing of warnings to *bona fide* disaster managers in specific areas, compared to the less organized emergency management structures of the past.

As part of the drive to improve early warning systems, the National Disaster Management Centre (NDMC) has accepted the concept of a Multi-Hazard Early Warning System (MHEWS) for South Africa. A MHEWS refers to an early warning system that deals with different types of hazards (i.e. meteorological, hydrological, seismic, wild land fires, etc.) within a similar framework of warning preparation, dissemination and response (WMO, 2006a). A MHEWS also implies the involvement of a number of stakeholders, both from the technical hazard monitoring agencies, such as meteorological services, geosciences institutions, hydrological agencies, etc., and from the response structures, for example different government departments that may deal with the impacts of different hazards in many cases. Thus, the word "multi" applies not only to "multiple hazards", but also to "multiple hazard monitoring organizations", "multiple response structures" and "multiple communities at risk". To ensure good coordination between these multiple role-players mentioned above well-developed plans, clear mandates and efficient coordinating mechanisms needs to be established between all stakeholders.

Each of the different types of flood warning constitutes a typical hazard in the MHEWS. Through the MHEWS coordination framework, they will be dealt with in similar ways regarding institutional coordination, warning dissemination and response mechanisms, even if different institutions have technical responsibility for each hazard.

2.3.3 Riverine flood warning systems

The Department of Water Affairs (DWA) has the responsibility for riverine flood warnings and the subsequent management of the large reservoirs in the large rivers in South Africa, such as the Vaal and Orange Rivers (Pegram *et al.*, 2007). This is done through the Flood Room of DWA. In the mid-1990s, the DWA implemented the US River Forecasting System (RFS) in the Vaal and Orange Rivers. Using the Sacramento rainfall-runoff model, manual imported rainfall values were ingested to produce flow forecasts and information used to manage the main reservoirs in these rivers and to warn disaster management and the public in danger of flooding along riverbanks. A number of major events occurred in the past two decades, notably in 1996, 2000 and 2011.

Apart from this system, Pegram *et al.* (2007) concluded at the time of their report there were no other riverine flood warning systems in South Africa. The main reasons for this situation include the complexity of implementing and calibrating rainfall-runoff models in large catchments, as well as the lack of river flow and adequate rainfall data needed by these systems. As noted in the WMO report (WMO, 2011) the complicated modelling and cost of effective instrumentation for the relative small number of events per basin have not justified the necessary investment yet. However, this situation needs to be evaluated from time to time and selected large river catchments may need special attention in this regard in future, particularly for catchments with vulnerable communities.

2.3.4 Flash flood warning systems

Since flash floods are hydrometeorological events with little lead-time and require direct and quick involvement from weather forecasters, they are dealt with by the SAWS through their Severe Weather Warning System (SWWS). The SWWS is also a part of the national MHEWS. The typical early warning system for flash floods South Africa used to be based on heavy rain warnings, such as "with potential for flash flooding", without any knowledge which river basins were prone to flash flooding at the time. This vaguely worded warning inadvertently weakens the effect of the early warning to prompt reaction among communities at risk, or vigilance from disaster management structures at the river basins in danger of being flooded. Thus, a real need existed for a flash flood warning system, which combines meteorological heavy rainfall warnings with hydrological information in a robust way to guide the preparation of more accurate warnings about imminent flash floods in affected river basins.

In October 2010, the South African Flash Flood Guidance system (SAFFG) was implemented in the main metropolitan areas of South Africa. This implementation was funded by the National Disaster Management Centre (NDMC) and SAWS. This system provides guidance on potential flash floods to forecasters, based on meteorological information and hydrological modelling. Subsequently, the WMO has adopted the flash flood guidance concept for regional implementation in various parts of the world (WMO, 2007), including seven countries in the Southern Africa Development Community (SADC). This project aims to increase the abilities of various developing regions in the world to prepare flash flood warnings based on diagnostic evaluation of flash flood potential of small basins. Through this Southern African Regional Flash Flood Guidance (SARFFG) system, based on the same concepts as SAFFG, the remainder of South Africa will also be covered by a flash flood warning system by 2012.

The concept of SAFFG will be discussed in more detail in section 4. However, this system has the potential to fulfil an important component of the proposed National Flood Warning System of Pegram *et al.*, (2007).

2.3.5 Storm surge warning system

The development of guidelines for a storm-surge warning system, as a component of the MHEWS, was put forward in 2011 by the SAWS, Department of Environment Affairs Oceans and Coasts branch, the CSIR, the Navy's Hydrographical Office, and relevant Disaster Management Centres (SAWS, 2011). These guidelines involve a technical forecasting capability developed between SAWS and the CSIR. It also includes agreement on all the relevant dissemination and coordination mechanisms with disaster management structures.

2.3.6 Tsunami warning system

In the same vein, guidelines for a tsunami early warning system were also developed in 2011 as part of the MHEWS. The collaborators in this case were the SAWS, NDMC, Council for Geosciences, with input from coastal Disaster Management Centres (SAWS, 2011a). These guidelines include the evaluation of international tsunami guidance by the relevant role-players to assess the potential need for a local warning. Agreement between stakeholders on the relevant dissemination and coordination mechanisms are described in the guidelines.

3. THE SOUTH AFRICAN FLASH FLOOD GUIDANCE SYSTEM (SAFFG)

3.1 BACKGROUND

A summary of the concepts of the SAFFG modelling system is provided by Poolman (2014, Chapter 2). Excerpts of this summary are provided in Section 3.1 and 3.2.

In order to issue flash flood warnings weather forecasters need to know "how much rainfall over a small catchment could lead to potential flooding in that catchment?" The answer to this basic question requires a hydrometeorological solution that has evaded forecasters generally. Flash flood guidance computations attempt to provide such guidance and the concept has been used in the USA since the 1970s (Georgakakos, 2006). The arrival of satellite- and radar-based precipitation estimates, and GIS-based databases related to catchment properties have allowed the development of operational systems that could simulate the flash flood guidance concept distributed over numerous small river basins in real-time (Georgakakos, 2004). The Flash Flood Guidance System (FFGS) was introduced in the Central American Flash Flood Guidance system (CAFFG) in 2004. The FFGS provides flash flood guidance, not as a forecast, but as diagnostic information to be used by experienced forecasters as guidance along with other data, tools and systems to determine the short-term risk of flooding in small basins.

The SAWS upgraded its weather radar network in the mid 2000's by installing a number of new S-band weather radars, which enhanced its rainfall estimation ability within the radar detection range. Technology implemented on the products of the new MSG-satellite (Meteosat Second Generation) in the same period allowed for more skilful satellite-based rainfall estimation in Southern Africa (De Coning *et al.* (2011). This paved the way for the operational implementation by the Hydrologic Research Center (HRC) in San Diego, USA, of the South African Flash Flood Guidance system (SAFFG) based on FFGS in South Africa by October 2010, and the SADC Southern Africa Regional Flash Flood Guidance system (SARFFG) over SADC in 2012. SAFFG covers 5366 small catchments (averaging from 50 to 100 km^2) over the main metropolitan areas of South Africa, as well as the flash flood prone Cape South Coast (see Figure 3.1(a)). Precipitation estimation based on the weather radars, the MSG satellite and real-time rain gauges are used to update the flash flood guidance information hourly for each of the 5366 small river basins.

The major difference between the SAFFG, and the SADC regional SARFFG implemented by HRC under the WMO project in Southern Africa, is that whereas the latter covers the entire South Africa (Figure 3.1(b)), it updates the flash flood guidance for its larger catchments (around 200 km^2) only every 6 hours using only satellite rainfall estimation. In the context of South Africa, the SAFFG thus compliments, as a high-resolution product (in space and time) the SADC SARFFG version , zooming into more detail at the flash flood prone metropolitan regions.

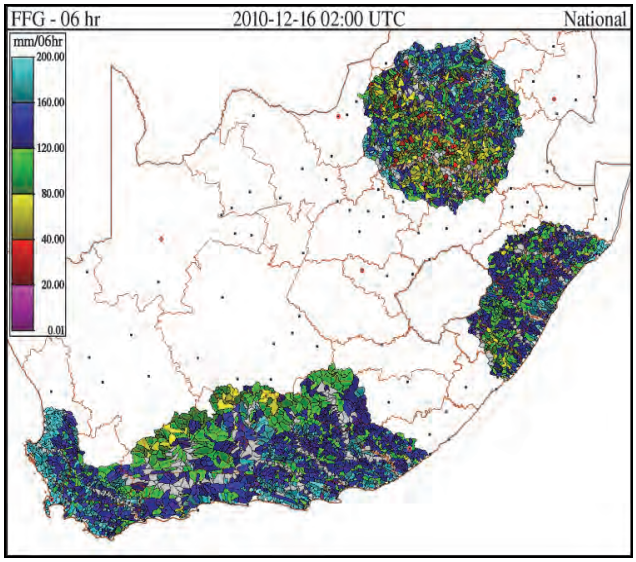

Figure 3.1(a): Domain of the SAFFG, covering flash flood prone regions in South Africa with high resolution catchments of 50-100 km^2 area

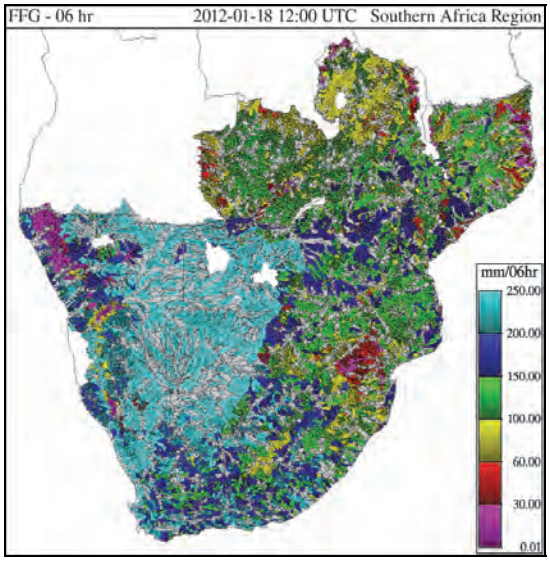

Figure 3.1(b): Domain of the regional SARFFG covering nine countries, but at a lower resolution of approximately 200 km^2 compared to SAFFG.

3.2 OVERVIEW OF THE SAFFG SYSTEM

3.2.1 Overview

The FFGS models the hydrologic response of small river basins to the rainfall received and provides guidance to weather forecasters and disaster managers on the potential for flash flooding for each of these basins. It is thus a true hydro-meteorological system, designed to answer the basic question of weather forecasters, mentioned above: "how much rainfall over a small catchment could lead to potential flooding in that catchment?". Georgakakos (2004, 2006) describes in detail the modelling concepts applied in the FFGS, and Sperfslage *et al.* (2010) provide information on the SAFFG. A summary is provided in this section, based on these references.

There are essentially four main components in the hydro-meteorological modelling system as it is implemented in the SAFFG and SARFFG, namely:

- Consolidation and ingestion of rainfall estimation;,
- Modelling the soil moisture deficit based on the rainfall estimation;
- Relating the basin's unique threshold runoff (the effective rainfall amount needed should the basin be completely saturated) to flash flood guidance (FFG) given the soil moisture deficit;
- Comparing the flash flood guidance value with observed rainfall as an indicator of possible imminent flash flood threat (FFT), or to a nowcast of rainfall for possible flash flood threat up to the next six hours. Figure 3.2 (similar to Figure A in the Abstract) provides a graphical description of the modelling process.

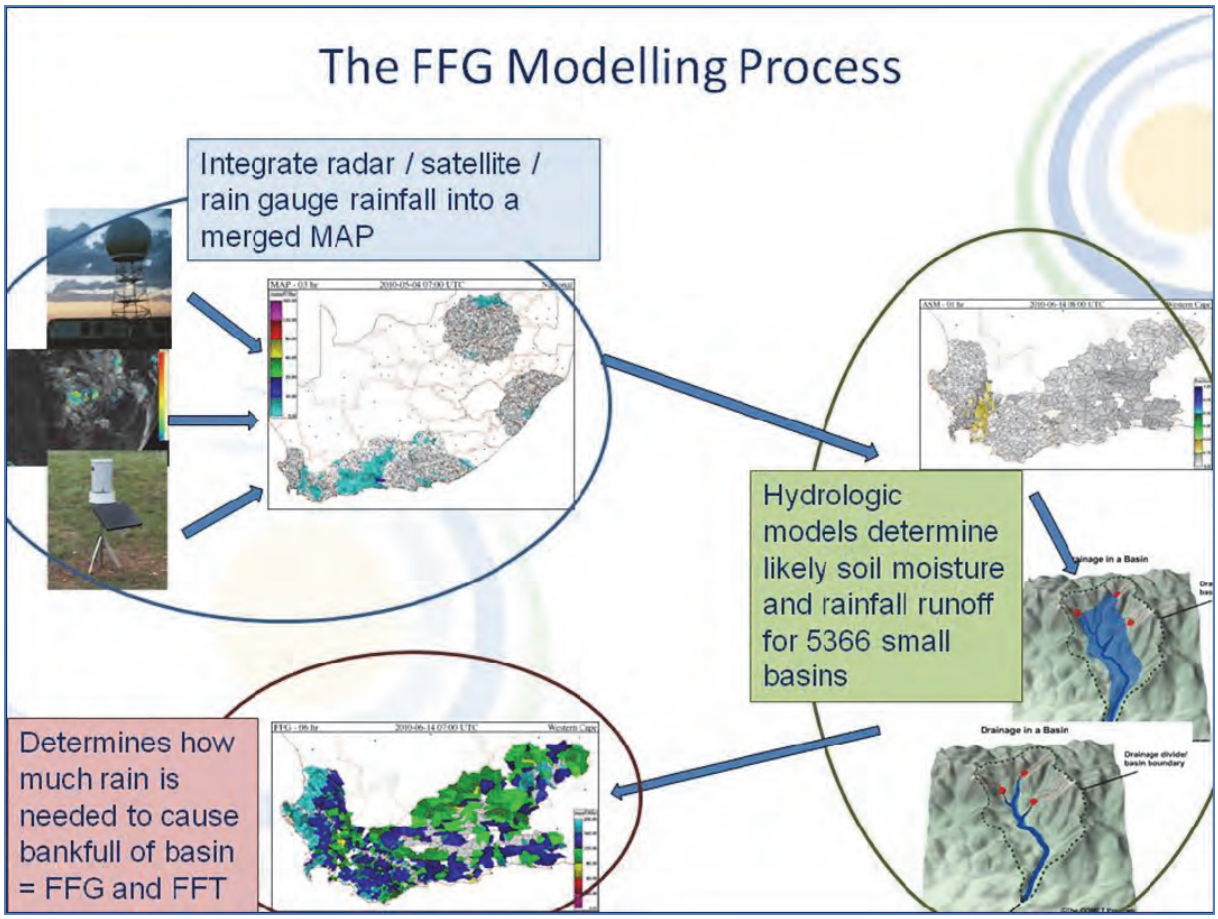

Figure 3.2: The hydrological modelling through integration of meteorological variables is shown in the graphic. In the case of the SAFFG this process is repeated every hour with the latest rainfall information available, and for SARFFG this is repeated every six hours with satellite rainfall estimation information only.

3.2.2 System preparation

The FFGS as implemented in SAFFG and SARFFG is essentially a spatially distributed modelling system. This means that it models the hydrologic response to rainfall of each of the small river catchments over a large area to provide spatial information on the potential for flash floods. The flash flood prone regions in South Africa (for SAFFG) were delineated into small catchments using a Geographical Information System (GIS) and digital elevation data of 90 m resolution. The minimum basin size was set to 30 km^2 for areas where radar precipitation data are available (at 1 or 2 km grid scale) and 100 km^2 where only satellite precipitation data (at 2 to 4 km grid scale) are available. The catchment scales are a few grid lengths of either the radar or satellite data to allow acceptable precipitation estimates.

Characteristics of the catchment geometric properties and stream cross-section geometric properties (including catchment size, channel length, channel slope, stream top width and hydraulic depth at bank full) were determined through GIS processing of the digital elevation data, or through regional relationships (Carpenter *et al.*, 1999). Other information needed for catchments including soil type and depth, land-use, vegetation, etc., were received from various official sources in GIS

friendly format. This information needed in the hydrological modelling of the catchments was interpreted to corresponding information for each FFGS catchment.

3.2.3 Rainfall estimation

In the SAFFG, rainfall estimation is based on remote sensing platforms such as weather radars and the MSG satellite, both of which are indirect methods of rainfall measurement, but with the advantage of good spatial and temporal detail (Pegram *et al.*, 2007; De Coning *et al.*, 2011). Radar and satellite based rainfall estimation is provided to the SAFFG system and are assumed by the latter to be the best available rainfall estimation from these platforms. Still, to compensate for the errors in precipitation estimation by radars and satellite, dynamic and climatologic bias correction schemes are employed on both sets of data using available rain gauge information received at either hourly, or at most daily, intervals.

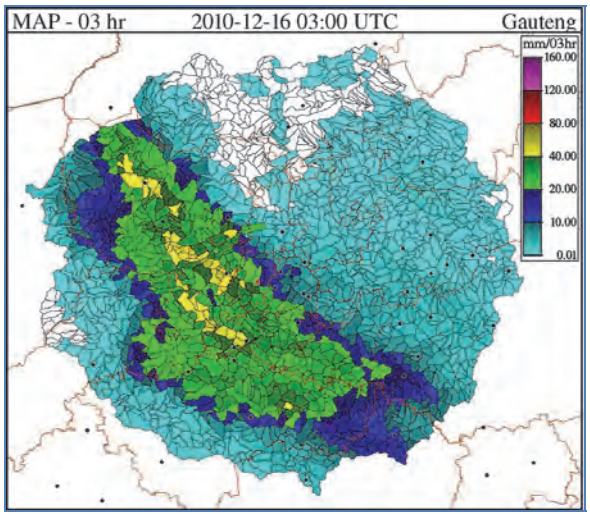

Figure 3.3(a): An example of a 3-hour accumulated mean areal precipitation (MAP) field for the SAFFG covered by the Irene radar near Pretoria.

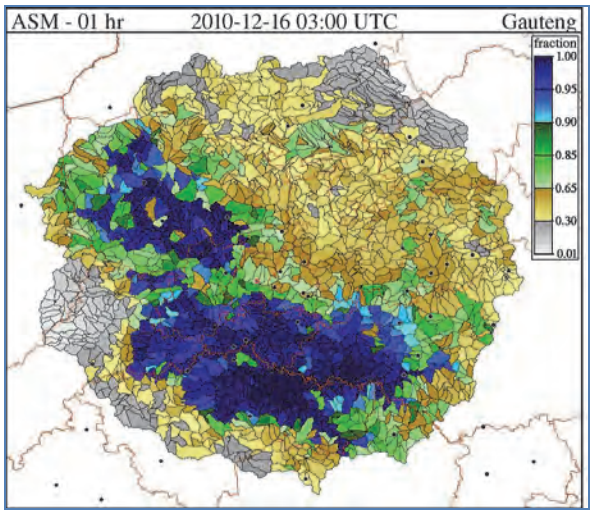

Figure 3.3(b): A 3-hour soil moisture fraction (ASM) for the same area and date as in Figure 3.3(a)

Bias corrected radar and satellite rainfall estimation data are processed every hour to provide the latest mean areal precipitation (MAP) estimates for the previous 1-hour, 3-hours and 6-hours, used as the precipitation forcing in the soil moisture and flash flood guidance models (see example Figure 3.3(a)). In regions where radar estimates are available, the radar based bias-corrected MAP fields are used as the precipitation field for the subsequent models. However, should the radar not be available, the system will automatically default to using the corresponding satellite MAP fields. The SADC regional SARFFG uses only satellite MAP fields, bias corrected with available rain gauge data.

Precipitation estimation by radar and satellite are key ingredients to the FFGS system, and are assumed by the system to be pseudo “observations”. Therefore, significant effort is needed to produce radar and satellite precipitation estimation fields that are as accurate as technologically possible. This will be a major feature of subsequent sections in this project.

3.2.4 *Modelling soil moisture deficit*

Soil moisture deficit is modelled with the Sacramento Soil Moisture Model adapted for use in the FFGS as described by Georgakakos (2006). Runoff is modelled in the upper and lower soil zone components (direct and saturation excess surface runoff, interflow, base flow, see Figure 3.4) from the mean areal precipitation and evapotranspiration estimates for the catchment. Evapotranspiration is computed from location, climatological and vegetation properties of each catchment. The state of the soil moisture is computed every hour (SAFFG) and every six hours (SARFFG) for each small FFGS catchment and provided to the FFG model as the current state of soil moisture deficit (see the example in Figure 3.3(b)) to compute the FFG values.

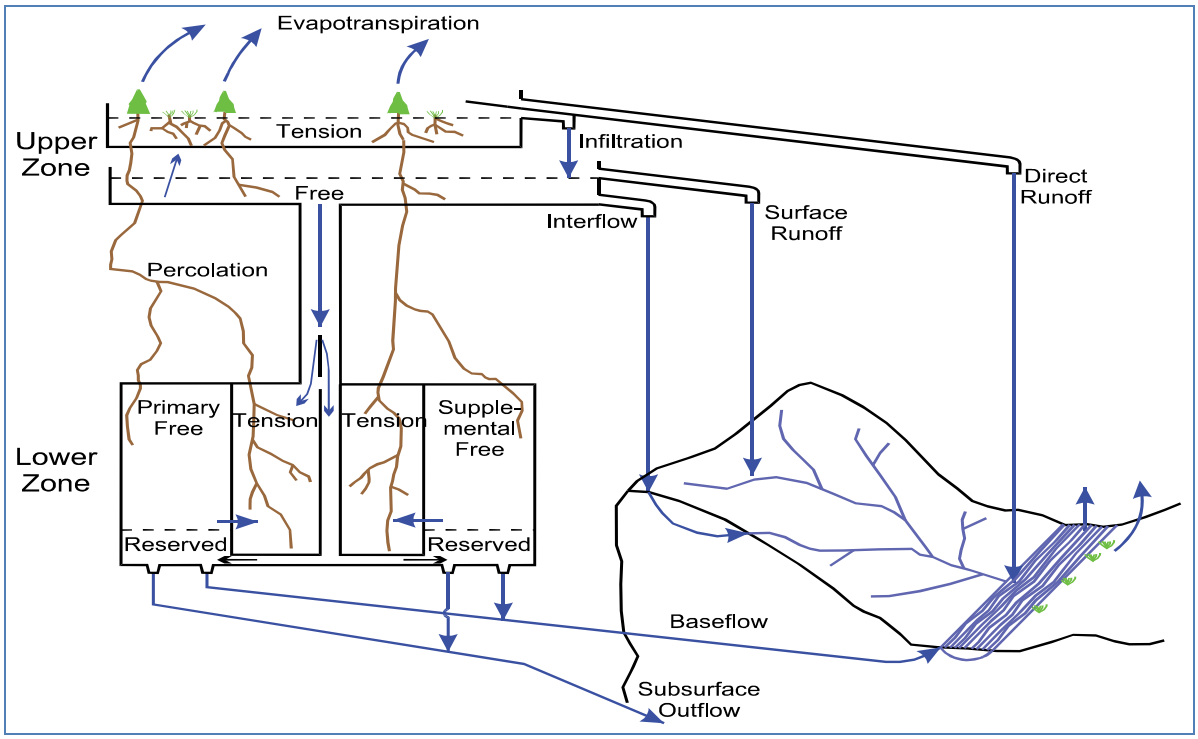

Figure 3.4: Graphical representation of the Sacramento Soil Moisture Accounting Model components (COMET, 2010)

3.2.5 *Flash flood guidance model*

Flash flood guidance (FFG) is defined as *the average amount of rainfall (MAP) of a given duration (1, 3 or 6 hours) over the catchment required to cause bank full flows (i.e. minor flooding) at the outlet of the catchment*. FFG is thus a conservative estimate of the amount of rainfall needed to cause minor flooding, answering the question typically asked by forecasters, as mentioned in Section 3.2.1: "how much rainfall over a small catchment could lead to potential flooding in that catchment?".

FFG is determined using the relationship of the fixed *Threshold runoff* value of the basin and the *soil moisture deficit* at the time. Threshold runoff is the runoff volume (and thus effective rainfall) needed for bank full discharge after accounting for all losses of water such as interception and soil moisture storage. Threshold runoff is thus the residual rainfall amount needed for bank full at the catchment outlet if the catchment is completely saturated, and is a one-time calculation for a given catchment done during the setup of the system. FFG, on the other hand, is the actual rainfall

needed (some part of which will sink into the unsaturated soil) and is computed on a real-time basis since it depends on the saturation level of the catchment. FFG will thus by definition be more than or equal to the threshold runoff amount.

To find the FFG, basic rainfall-runoff curves are needed for the basin with the given soil moisture deficit calculated for the catchment in the previous model (to be detailed in section 4.2.3). The flash flood guidance model uses this soil moisture deficit to determine this basic rainfall-runoff curve for the particular basin at that particular time. This is done by running "what if" scenarios using the hydrologic model to calculate the runoff that different (increasing) rainfall values will generate, given the same soil moisture state at the time. From these estimates, rainfall-runoff relationships (the curves in Figure 3.5) can be determined for the particular catchment given the current state of soil moisture. The effective rainfall needed (i.e. the Flash Flood Guidance value, or FFG) can then be determined through these relationships (the curves) from the pre-determined runoff value that will lead to bank full (i.e. threshold runoff). This is done for 1, 3 and 6 hour rainfall durations (see example in Figure 3.6(a)).

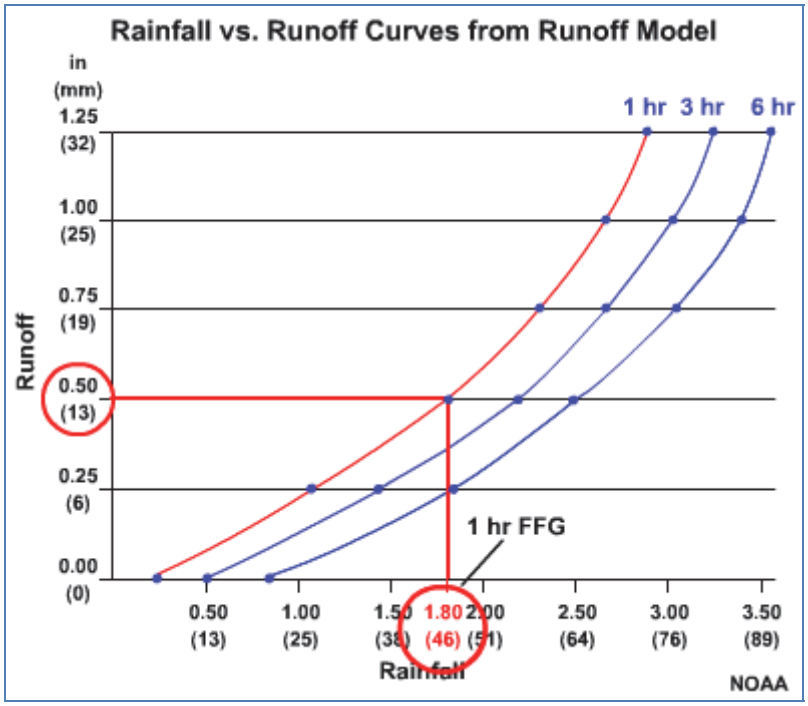

Figure 3.5: Example rainfall-runoff curves for 1, 3, and 6 hour durations calculated for a specific soil moisture deficit for a specific FFGS basin (COMET, 2010). The 1 hour FFG is determined by relating the threshold runoff (i.e. runoff that will cause bank full flow at the catchment outlet) with the rainfall through these curves for the given soil moisture deficit.

Threshold runoff calculations assume natural stream channels, and therefore they cannot be applied to modified channels and river sections. Fire burn areas temporarily modify the runoff characteristics of a catchment, which cannot be taken into account by the FFG model system assuming the natural conditions. Similarly, streams that are channelled are still treated by the FFG model system as if they were natural streams, and therefore the modelled FFG values will be unrepresentative and considerably higher in these cases than should be if channelling was taken into account. This applies for a very small number of streams (less than 0.1% of all the catchments in

SAFFG), however they tend to be important as they relate to urban flooding in cities with high impact to people and infrastructure. Reservoirs in streams also interrupt the geomorphologic relationships and therefore basins with reservoirs are excluded from FFG calculations.

3.2.6 Determining flash flood threat

To determine whether a flash flood is imminent in the particular catchment or not, the most recent rainfall estimates (MAP) must be compared with the corresponding period's Flash Flood Guidance value (FFG). Areas with excess rainfall, i.e. where the observed rainfall amount is larger than the FFG value (positive Flash Flood Threat – FFT), are potentially experiencing a flash flood. Maps of the basins with positive FFT provide spatial insight into potential problem areas (see example in Figure 3.6(b)). Similarly, if a nowcast of MAP for the next few hours is compared with the similar period's FFG, then a potential for future flash floods up to the next 6 hours can be determined, and predicted FFT maps can be prepared. In the SAFFG and SARFFG, the nowcast MAP is produced by repeating the previous 1, 3, or 6 hours accumulated rain in the next 1, 3, and 6 hours respectively. In general, for convective conditions, this is not a realistic forecast because convective storms tend to move relatively quickly. During strong synoptic forcing, the persisted rainfall nowcast has more value and tends to produce useful FFT values for the next few hours. A predictive element using either (i) a forecaster's predicted MAPs or (ii) MAP generated from numerical weather prediction should be chosen and this is dealt with in another section in this project (Section 6.2).

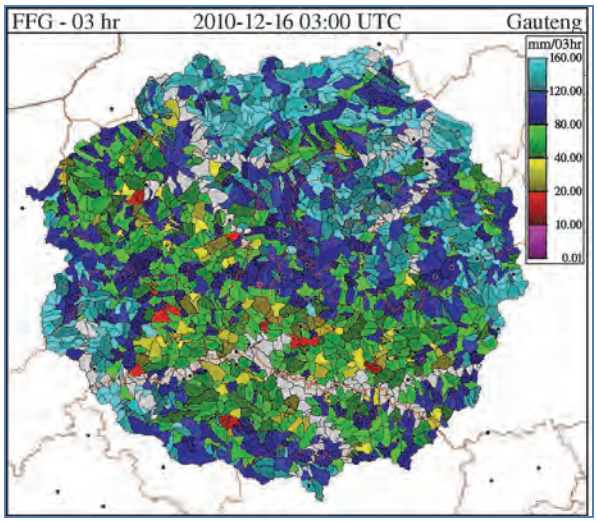

Figure 3.6(a): 3-hour flash flood guidance (FFG) for the same area and date as in Figure 3.3(a)

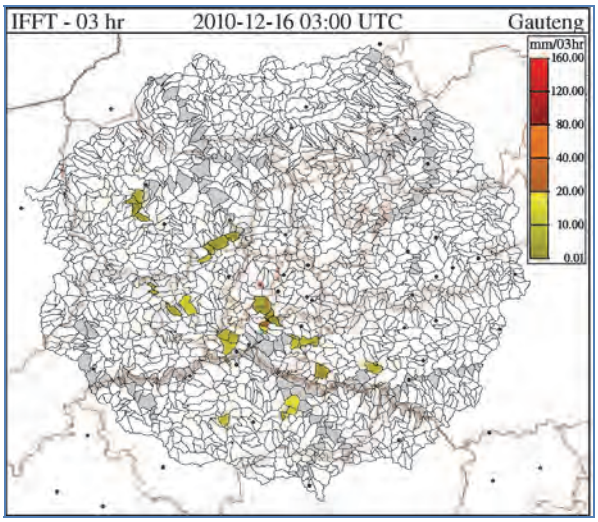

Figure 3.6(b): 3-hour imminent flash flood threat (FFT) for the same area and date as in Figure 3.3(a)

3.3 A RECENT CLIMATOLOGICAL ANALYSIS OF THE SAFFG PRODUCTS

3.3.1 Data and products

The SAFFG system provides a number of products to the forecaster on a web-based forecaster interface (Figure 3.7). These products are related to the four main components of the SAFFG as described above. All these products are archived in a database at SAWS since April 2011 until present with a loss of data due to unforeseen circumstances for August 2012 and January 2013. The product information is available in the form of text files as single averaged values for each of the

5366 basins in SAFFG, for each hour of the day. This provides the opportunity to perform a climatological analysis on the data to establish trends and patterns.

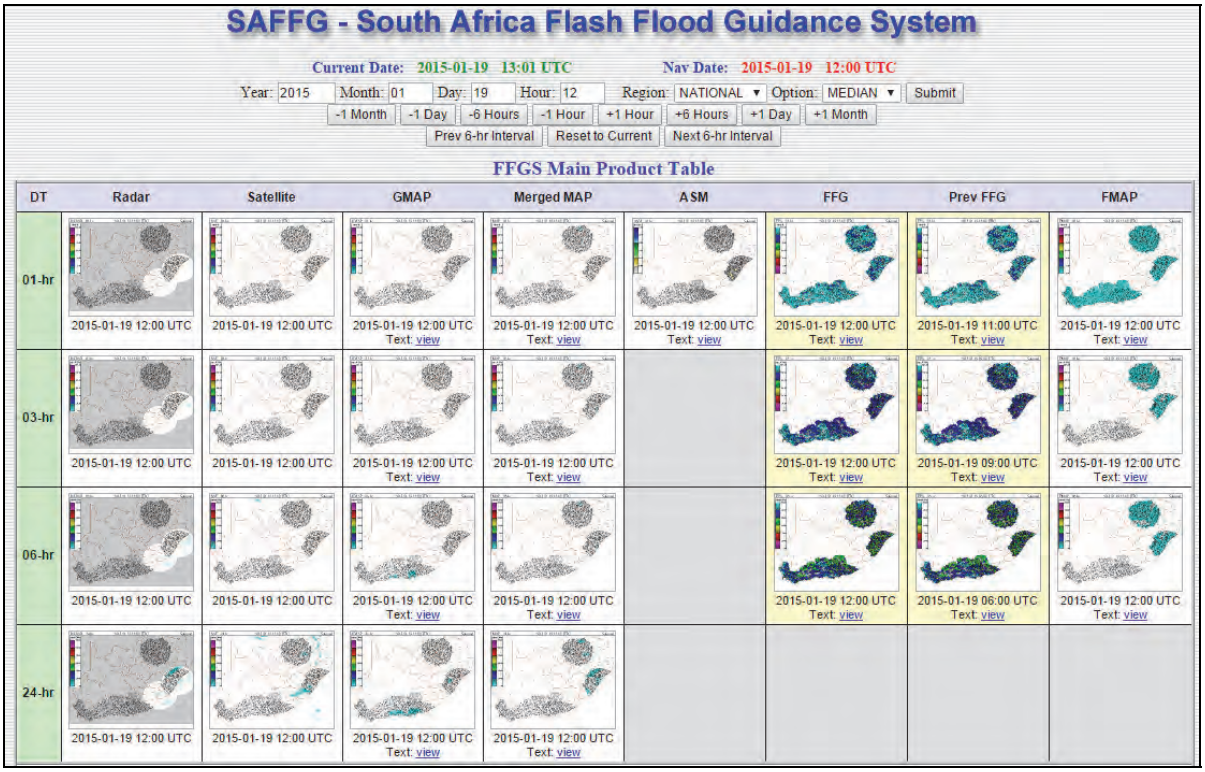

Figure 3.7: The forecaster interface of the SAFFG system, showing the thumbnails of the different products that the forecasters can enlarge, or scroll through in time.

The first group of products related to the precipitation estimation process, and the final Merged Mean Areal Precipitation (MMAP) over a given period (1, 3, 6 or 24 hours) are used in the climatology assessment. This final merged MAP is based in hierarchical order on radar rainfall estimation values if available, otherwise on satellite rainfall estimation products. Radar information is available for the SAFFG domains around Pretoria/Johannesburg (S-band Gematronik radar), Durban (S-band Gematronik radar for most of the period, otherwise a C-band Enterprise radar) and Port Elizabeth (C-band Enterprise radar, but the East London S-band Gematronik covered the eastern parts of this domain east of Port Elizabeth for most of this period). Figure 3.8 provides information on the radar availability during the archive period. For the remainder of the domain (Cape South Coast and around Cape Town), satellite rainfall estimation from the Meteosat Second Generation (MSG) was used through the Hydro-Estimator (HE) system used in SAWS.

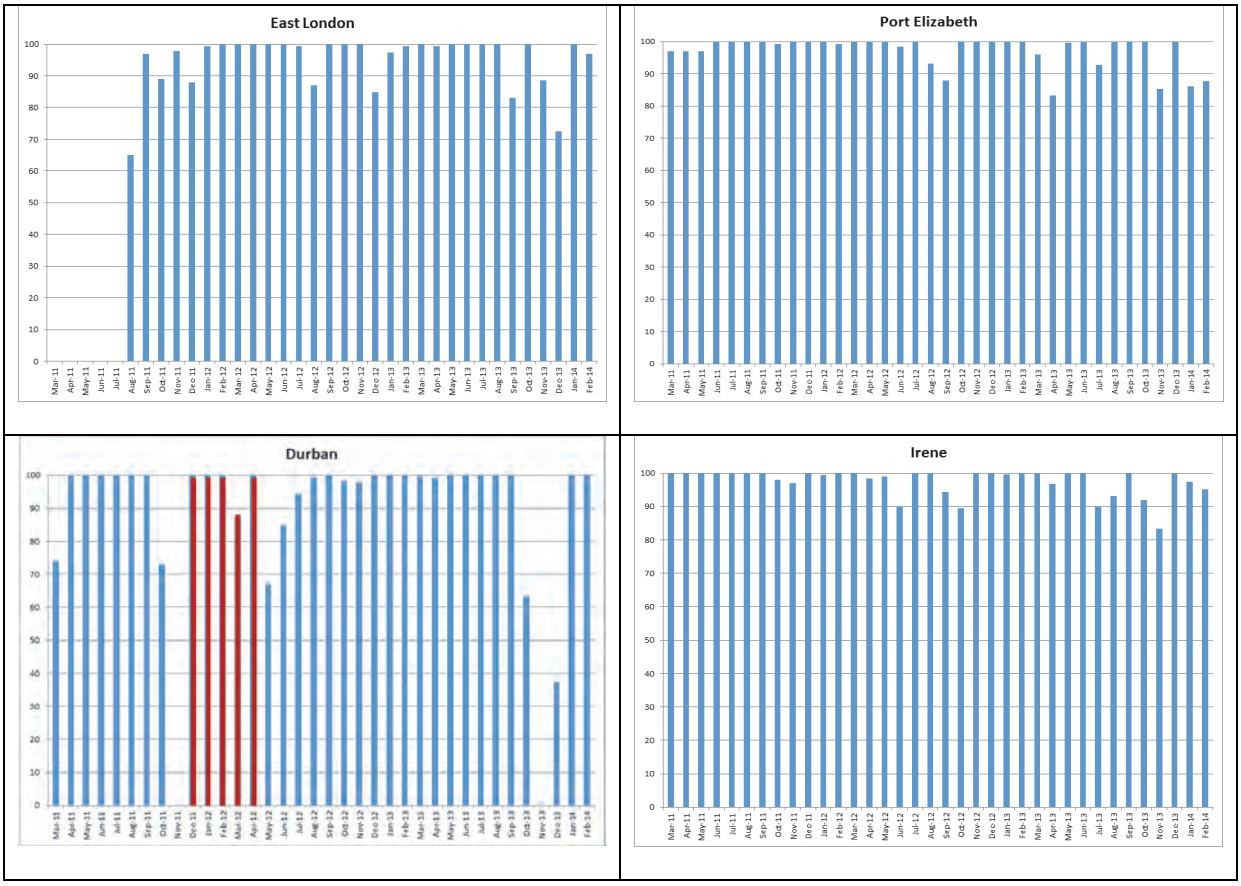

Figure 3.8: Radar availability from the four main radar systems used in the SAFFG since March 2011. The radar at Port Elizabeth is and older C-band Enterprise radar. In Irene, Durban and East London newer S-band radars are operational, except for the short time in Durban (red bars) between November 2011 and April 2012 when the S-band radar was unserviceable and a C-band operated temporarily.

The second product used in the climatological analysis is the basin Averaged Soil Moisture (ASM) product, which is the result of the hourly soil moisture modelling through the Sacramento soil moisture accounting model for each of the 5366 small basins. ASM is the soil moisture fraction for the upper soil moisture layer at the hour based on the recent rain as reflected in the MMAP fields, as well as on the soil, vegetation and land-use conditions.

The third product is the Flash Flood Guidance (FFG), which is determined by the rainfall runoff model, using the ASM as input with basin properties such as slope, etc. FFG provides the amount of rainfall needed in a basin over a given period (1, 3 or 6 hours) that, if received, would lead to bank full conditions (i.e. minor flooding) at the outlet of the basin.

The final product used is the Imminent Flash Flood Threat (IFFT), which is the difference between rainfall over the 1, 3 or 6 hours period, and the corresponding FFG for the same period. Where more rain has fallen than needed according to the FFG, the amount of excess rain will be indicated as a positive IFFT, implying flash flooding could have occurred in those basins.

ASM is an hourly evaluation of soil moisture fraction at that specific time, and thus not related to the period accumulations as in the other three products.

3.3.2 Analysis procedure

The four products (MMAP, ASM, FFG and IFFT) were extracted for each basin over the entire archive period and daily and monthly values were calculated for each of these products as follows:

- MMAP: The 24-hour total rainfall at 23:00 UTC was extracted and monthly total rainfall was calculated;
- ASM: The daily highest values were determined from the hourly information, and then the average per month was calculated per basin;
- FFG: The daily lowest 1, 3 and 6 hour FFG values were determined from the hourly archived information, and then a monthly average was calculated for each of the three periods;
- IFFT: The daily highest 1, 3 and 6-hour IFFT values was determined from the hourly archived information, and then a monthly maximum value was determined. The number of days that a positive IFFT was recorded any time in the day was also counted and reflected as a monthly value.

The products were depicted either as maps using a GIS system, or as graphs. Useful information can be determined from these maps and graphs relating to the distribution of potential flooding as modelled by SAFFG, both in space and in time. It also provided information about potential deficiencies in the system.

3.3.3 Results

3.3.3.1 Rainfall estimation

The rainfall distribution for the entire period from April 2011 to December 2012 as presented in Figure 3.9 clearly shows an expected preference for higher rainfall over the eastern parts of the country, with a typical summer/winter distribution. Figure 3.10 is a comparison of the annual rainfall measured for 2012 by climate stations, to the SAFFG 24-hour merged MAP rainfall total for the same period.

It is clear that the S-band radar at Irene in the Gauteng region overestimated the rainfall somewhat, in some cases by almost double the measured amount as shown for only a few stations in Table 3.1. The rainfall pattern for KwaZulu-Natal appears to be more realistic, although the Durban S-band radar was defective during the first three months of 2012 and it was replaced by the older C-band radar. The latter most probably underestimated the rainfall (discussed further down) and consequently the rain for the KwaZulu-Natal region would have been higher according to the SAFFG MAP than is shown in Figure 3.10.

The S-band radar in East London covering the eastern parts of the Eastern Cape (east of Port Elizabeth – see Figure 3.11) also appears to have overestimated the rainfall compared to the climate stations. West of Port Elizabeth, however, the SAFFG MAP rainfall generally underestimated the rain measure by the climate stations, particularly along the coast and in the Cape Town region (Figures 3.9, 3.10 and 3.11).

Total 24-hour MAP April 2011 to December 2013	Total 24-hour MAP Summer: 2011/12, 2012/13	Total 24-hour MAP Winter: 2011, 2012, 2013	
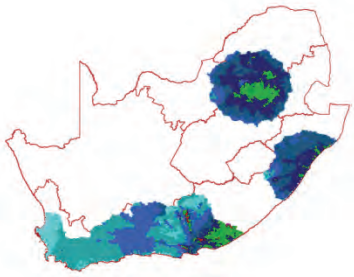	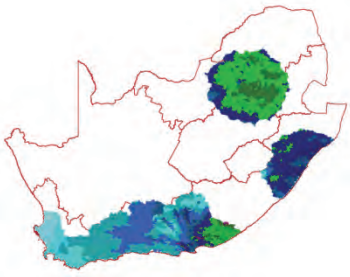	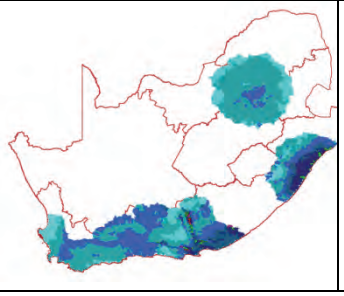	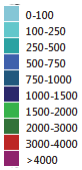

Figure 3.9: Total 24-hour Merged MAP values over the relevant period

Total MAP for 2012 from SAFFG	Climate stations total rainfall for 2012
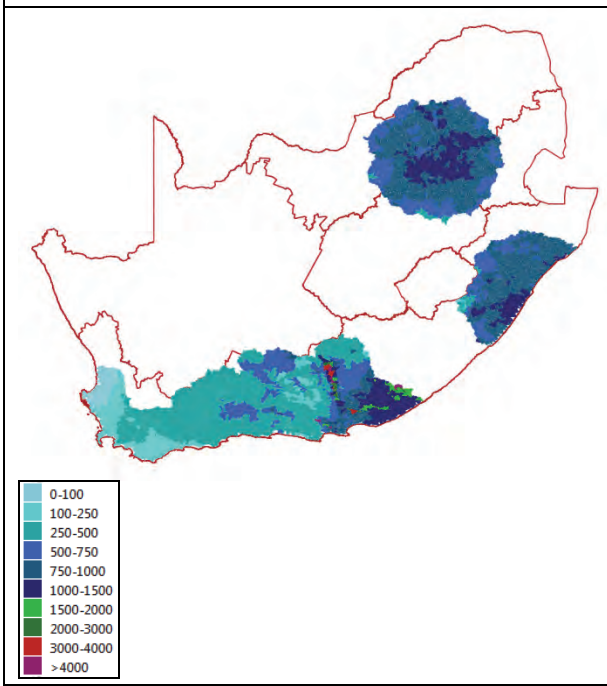	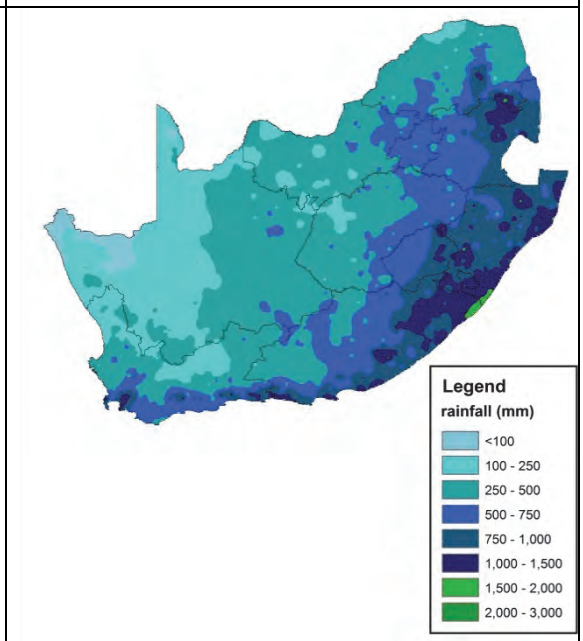

Figure 3.10: Comparison of SAFFG MAP rainfall total and climate station annual rainfall for 2012

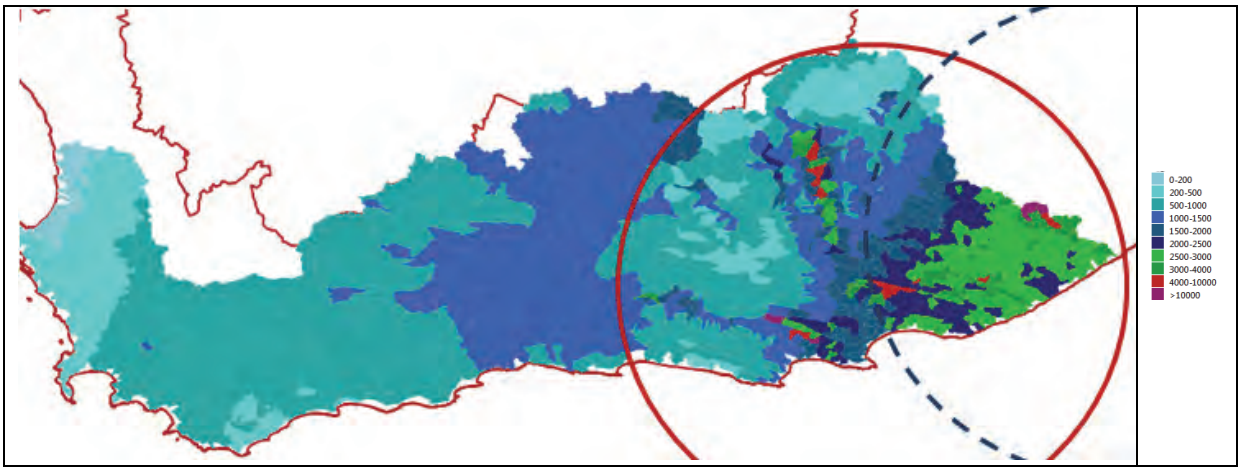

Figure 3.11: Total 24-hour Merged MAP values over the entire period for the southern coastal areas.

Table 3.1 Comparison of a few climate rainfall stations with corresponding SAFFG basin average rainfall.

Location	Climate Station Annual Rainfall	SAFFG Basin Rainfall Total
Pretoria CBD	593.5	896
O. R. Tambo International Airport	666.0	1194
Heidelberg	479.5	975
Cape Town Weather Office	466.2	119.8
Stellenbosch	868.2	275.4
George Weather Office	688.7	430

What is evident in Figure 3.11 is the change of rainfall distribution over the southern coastal areas from Cape Town in the west towards East London in the east. This coastal area experiences a climatological change from the drier, winter rainfall area in the west, to an all season rainfall area over the central and eastern coastal regions. There is also a preference for more thunderstorms over the eastern parts during summer. There is another reason for this rainfall difference, which relates to the different rainfall estimation systems used in this area:

- Over just more than the western half of the southern coastal region the rainfall estimation is satellite based (west of the red circle in Figure 3.11), using the Hydro-Estimator rainfall estimation system described in Section 5.1. Rainfall estimation techniques using satellite data, such as the Hydro-Estimator, are generally based on cloud top temperatures. They are therefore better suited for convective clouds. This coastal area receives most of its rain in the form of stratiform rainfall with much lower cloud tops. Consequently, the Hydro-Estimator general underestimates the rainfall in this region (Figure 3.11 and Table 3.1). Attempts to deal with this problem are described in Section 5.1 (De Coning and Poolman, 2011).
- Rainfall estimation over the eastern parts of this region, around Port Elizabeth (covered by the red solid circle showing the Port Elizabeth C-band radar domain) and East London (covered by the blue dotted semicircle showing the overlapping East London S-band radar domain), is based on radar estimation techniques. These are generally far more accurate, since it is based on the radar reflectivity of the water droplets inside the clouds. It tends to work better for convective rain than stratiform rain.

The problem in this southern coastal region in Figure 3.11, however, is that the rainfall based on radars in this area shows unrealistic patterns. The area under the Port Elizabeth C-band domain (within the red solid circle), but outside the overlapping coverage of the East London S-band radar (blue dotted semicircle), shows less rainfall than the area just west of the red circle. This is not what is expected from the regular rainfall climatology. There are also clear “spikes” of high rainfall to the north and west-northwest of Port Elizabeth. These erroneous values are caused by interference by radio Local Area Network (radio LAN) within the Port Elizabeth area (Figure 3.12). Radio LAN

interference is a well-known problem for C-band radars in South Africa, and efforts to deal with the problem with filters led to a general under estimation of rainfall. C-band radars also suffer more from attenuation of the radar beam than S-band radars, exacerbating the under estimation of rainfall. The overlapping East London S-band radar domain under the blue dotted circle shows a far more regular rainfall pattern (apart from the couple of red coloured basins).

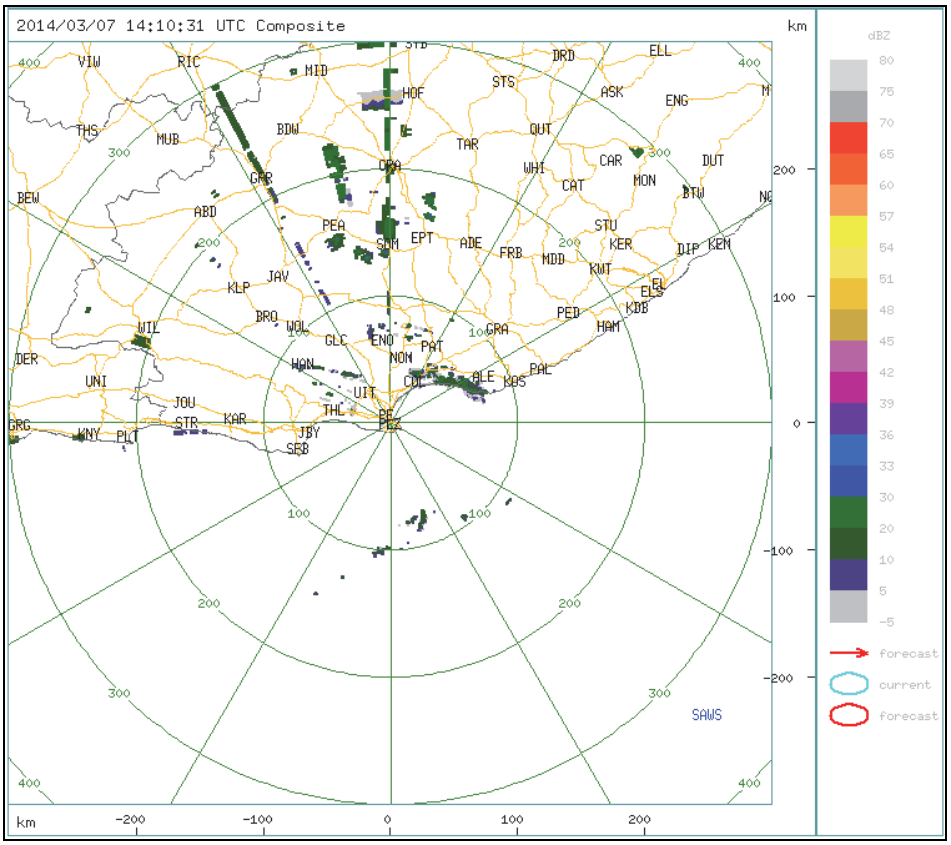

Figure 3.12: Radio LAN interference from the Port Elizabeth C-band radar on a clear day.

3.3.3.2 Soil moisture modelling

As mentioned earlier, soil moisture modelling will be directly affected by inaccurate rainfall estimation. There are other factors, however, that could also influence the soil moisture modelling. These are related to the basin specific parameters used by the Sacramento soil moisture accounting model to describe the characteristics of each basin.

Figure 3.13 show graphical representations of the highest daily soil moisture fraction (ASM), averaged over the relevant periods. The patterns of soil moisture fraction in the top layer follow largely the rainfall distribution, as expected. Once again, the higher soil moisture values are over the eastern parts, which received more rain. Higher soil moisture values occurred in the summer than in the winter over the eastern parts of the country, but as expected, soil moisture values were higher in winter over the southern Cape region.

Average ASM April 2011 to December 2013	Average ASM Summer: 2011/12, 2012/13	Average ASM Winter: 2011, 2012, 2013	
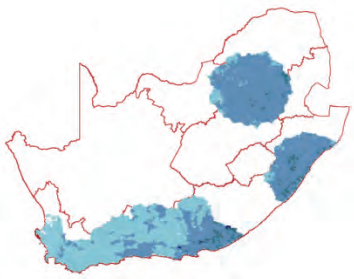	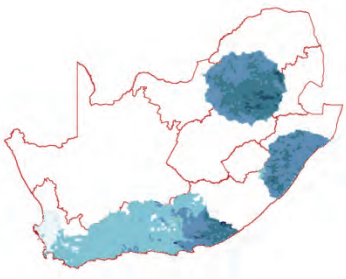	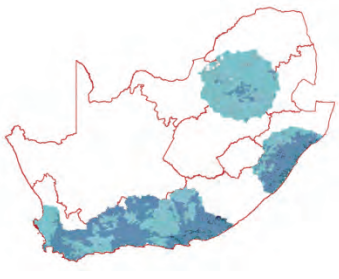	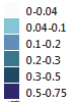

Figure 3.13: Highest daily ASM values, averaged over the relevant period

3.3.3.3 Flash flood guidance

Figure 3.14 provide a graphical description of the FFG distributions. The FFG of a basin is the average amount of rainfall needed over the basin over a specified period (1, 3 or 6 hours) that could lead to bank full at the outlet of the basin. Lower values of FFG imply less rain is required to cause flash flooding, and is thus more dangerous. It is closely related to the soil moisture fraction of the basin and other basin properties. Surprisingly low FFG occurred over many parts of the Karroo. It has to be related to soil conditions in that area.

The small variation in FFG values between summer and winter is also unexpected. Clearly, other soil parameters have a strong influence in these cases. Typically, the average lowest daily 6-hour FFG for basin 2001800692 is only 77.5 mm with a standard deviation of only 3.8 mm throughout the entire period from April 2011 to December 2013.

Average FFG6 Apr 2011 to Dec 2013	Average FFG6 Summer: 2011/12, 2012/13	Average FFG6 Winter: 2011, 2012, 2013	
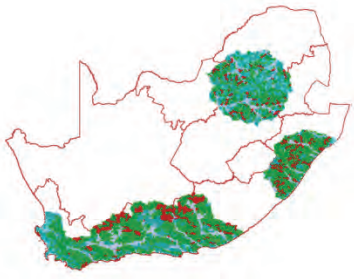	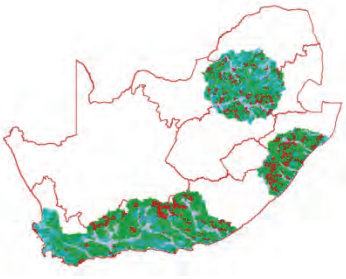	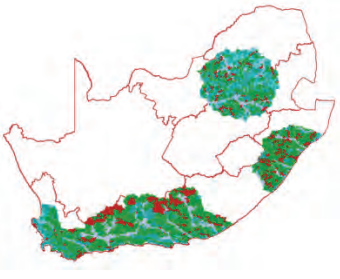	

Figure 3.14: Lowest daily FFG 6-hour values, averaged over the relevant period

3.3.3.4 Flash flood threat

Despite the high number of basins with low FFG values, and the over estimation of rainfall in the Irene radar region, very few basins had a positive 6-hour IFFT (Figure 3.13). Only 43 of the 2101 basins in this area had a day with positive 6-hour IFFT values, none in the Pretoria-Johannesburg area even though that area has experienced flash floods during this period. The best response came from the KwaZulu-Natal region as covered by the Durban S-band radar (Figure 3.15). A clear

difference emerged in which basins indicated a positive 6-hour IFFT during summer and during winter, which corresponds to the rainfall difference between these seasons in the area. In summer, thunderstorms are largely the driving factor and consequently the basins with positive IFFT were spread over the entire domain. During winter, frontal activity is the main driving force and consequently most basins that responded were along the coast.

Max IFFT6 Apr 2011 to Dec 2013	Max IFFT6 Summer: 2011/12, 2012/13	Max IFFT6 Winter: 2011, 2012, 2013	
	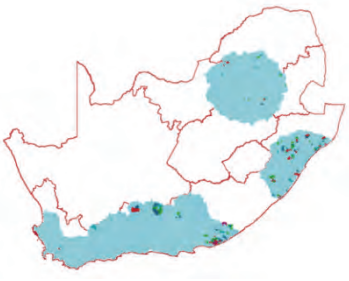		

Figure 3.15: Maximum IFFT 6-hour values over the relevant period

Nr Days IFFT6 Apr 2011 to Dec 2013	Nr Days IFFT6 Summer: 2011/12, 2012/13	Nr Days IFFT6 Winter: 2011, 2012, 2013	
		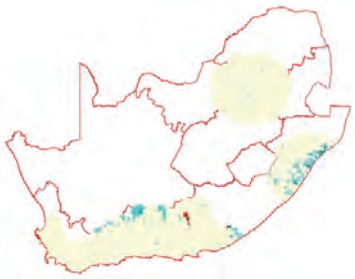	

Figure 3.16: Number of days with a positive IFFT 6-hour value over the relevant period

Nr Days IFFT6 Summer: 2011/12	Nr Days IFFT6 Summer: 2012/13	
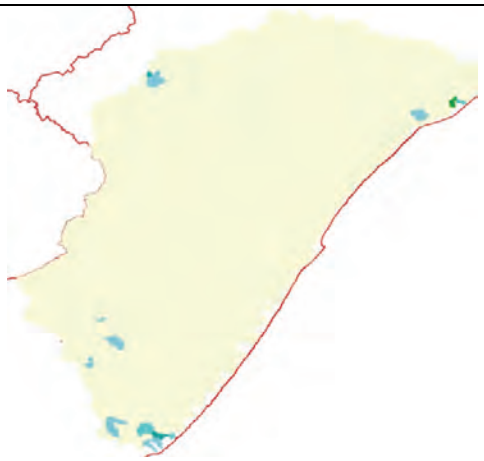	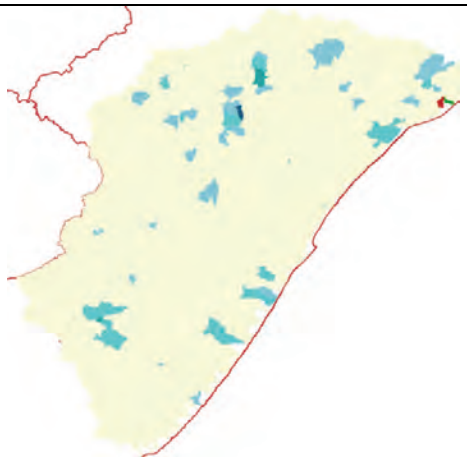	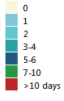

Figure 3.17: Number of days with a positive IFFT 6-hour value over the relevant period over KwaZulu-Natal.

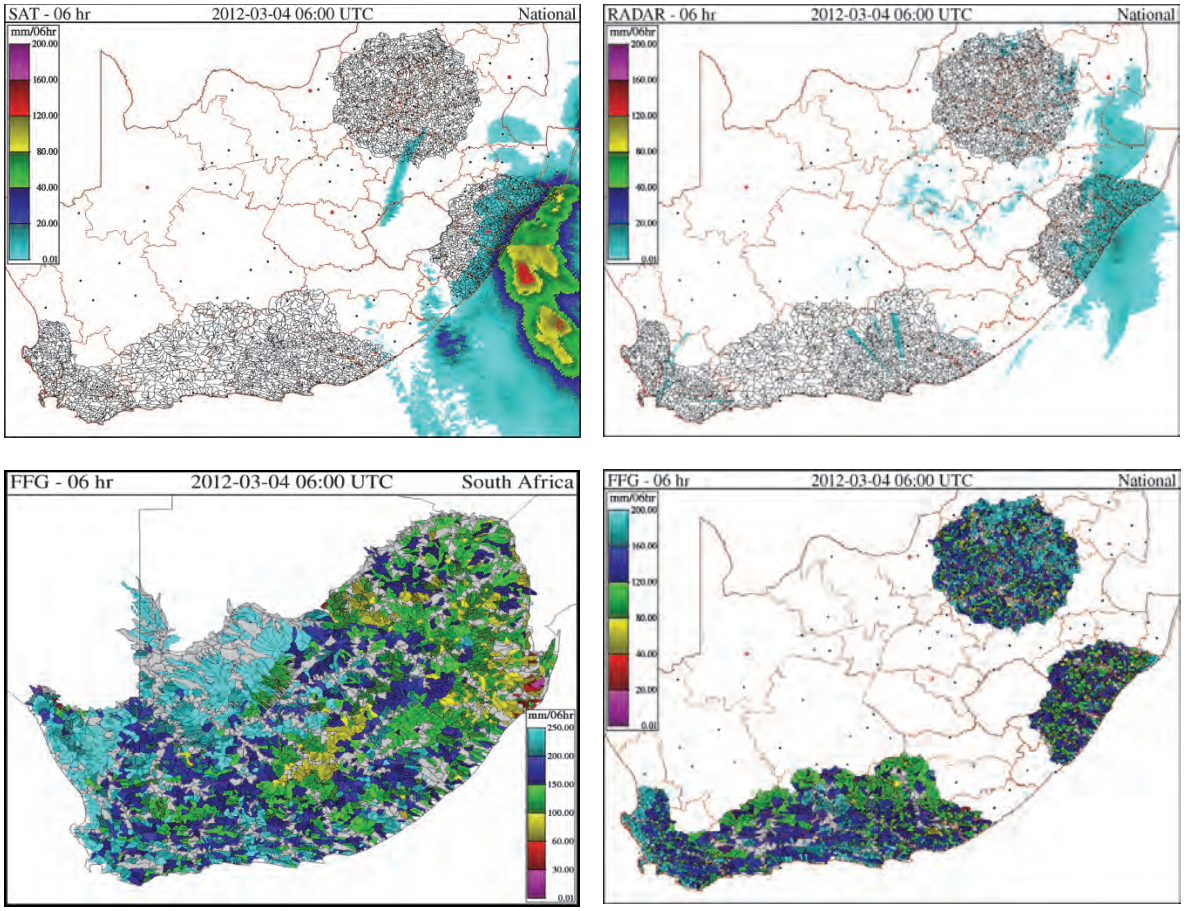

Figure 3.18: The satellite rainfall estimation (top left) and C-band radar rainfall estimation (top right) of tropical cyclone Irina on 4 March 2012. In the bottom row the resultant 6-hour FFG of the regional SARFFG (bottom left) based only on satellite rainfall and the FFG of SAFFG based on radar rainfall for KwaZulu-Natal are shown (bottom right).

During the summer of 2011/12, the S-band radar at Durban was down from November to April, and replaced by the older C-band radar. Figure 3.17 shows the number of days basins in KwaZulu-Natal had a positive 6-hour IFFT for the two summer seasons of 2011/12 and 2012/13, for comparison. Where the summer of 2012/13 (right-hand image in Figure 3.17) had numerous basins with a positive response, there were very few responses during the summer of 2011/12, except a few basins at the edge of the domain. Against the backdrop of the typical rainfall season experienced in particular by KwaZulu-Natal in 2012 (Figure 3.10), this lack of positive response is unrealistic, and points towards poor rainfall estimation by the C-band radar compared to the S-band radar. This is corroborated by the case of Tropical Cyclone Irina on 4 March 2012. On this day, Tropical Cyclone Irina brushed the coast of KwaZulu-Natal causing flooding on the north coast. The huge difference in rainfall measurement between the C-band radar and satellite is quite evident (Figure 3.18), as are the high 6-hour FFG values still prevalent for the SAFFG, when compared to the low FFG values of the regional SARFFG system that uses only satellite rainfall estimates. These results support the earlier conclusion regarding the poor performance of the C-band radar in Port Elizabeth. It can thus be concluded that the current C-band radars of SAWS are unsuited for effective rainfall estimation as needed in the SAFFG system.

In the Eastern Cape the basins that indicated a positive 6-hour IFFT were limited to the regions covered by the East London S-band radar, and the area in the Karroo covered only by the METEOSAT satellite. Along the southern and south-western coastal areas there was virtually no basin with positive 6-hour IFFT, except in the mountains near Cape Town where two basins responded on two days each. This reinforces the observation that the satellite estimates of rainfall over the south-western parts of the country do not properly pick up the rainfall as measured on the ground.

3.3.4 Discussion

The following conclusions can be made at this point regarding the SAFFG products:

- Rainfall estimation is a crucial input variable into the SAFFG modelling system, so it therefore has to be made as accurately as possible. Any inaccuracies in the rainfall field have an adverse impact on all the other products produced by models downstream, such as soil moisture fraction, flash flood guidance and flash flood threat, since these models accept the rainfall field to be the best estimate at the time.
- It is evident that the rainfall measured by the S-band radars of East London, Irene in Gauteng, and Durban in KwaZulu-Natal generally showed realistic rainfall patterns, although they appear to be overestimating the rainfall. There is thus a need to recalibrate these instruments to enable realistic bias correction within SAFFG.
- The C-band radars at Port Elizabeth, and the one used for a short time in Durban, vastly underestimate the rainfall due to attenuation and attempts at filtering to reduce the excessive radio LAN interference. These radars should be replaced with S-band radars, which are not affected by radio LAN frequencies.
- The Hydro-Estimator significantly underestimates the rainfall over the south-western region of South Africa, where rainfall is mostly stratiform in nature, being linked to frontal systems in the winter. Adjustments to the Hydro-Estimator methodology are needed to find a more suitable rainfall estimation system for this part of the country. Currently, the hybrid NWP/Hydro-Estimator technique developed in Section 5 is one such option.
- The soil moisture modelling results, particularly under the Irene radar in Gauteng, respond quite slowly to rainfall events, and as a result basins seldom indicate potential for flash flooding, even though this threat does occur more often. This should be investigated.

There have been a number of cases where the SAFFG provided positive guidance to forecasters, particularly in KwaZulu-Natal, and the eastern parts of the Eastern Cape. If the deficiencies mentioned above can be properly addressed, then SAFFG will be able to provide useful guidance information to forecasters. A pattern of areas that are more prone to flash flooding is emerging, particularly for KwaZulu-Natal, and the eastern parts of the Eastern Cape.

4. INTER-COMPARISON OF SAFFG AND PyTOPKAPI SOIL MOISTURE ESTIMATES

4.1 INTRODUCTION

In this section, model intercomparison of daily soil moisture, estimated over selected SAFFG catchments and sub catchments, is made respectively by (i) the SAFFG and (ii) the PyTOPKAPI model adapted by Pegram *et al.* (2010) from the TOPKAPI model of Liu and Todini (2002).

This intercomparison was made in the following steps:

- Obtain SAFFG data for the period 2011/03/07 to 2012/12/31
- Generate PyTOPKAPI simulations for selected catchments during this period (at 1km^2)
    - using the Tropical Rainfall Measuring Mission (TRMM) 3B42RT rainfall estimates forcing HYLARSMET (developed in WRC project K5/2024)
    - using the rainfall forcing from the SAFFG catchment model
- Average PyTOPKAPI estimates over the SAFFG sub catchments, a day at a time
- Compare time-series on each SAFFG catchment in the study area by computing the R^2 values on each sub catchment and display them on maps

4.2 THE MAIN CATCHMENTS AND THEIR SUBCATCHMENTS

The map in Figure 4.1 gives the layout of the SAFFG monitored regions coloured blue, overlaid on the WR 2005 quaternary catchments. They are clustered within the areas of coverage of the Irene, Durban, Port Elizabeth and Cape Town radars. There are also SAFFG catchments in the fold mountain region of the Western Cape outside the radar range – these catchments are larger because the only available rainfall input there is satellite-, not radar-based.

Figure 4.2 displays 4 mesoscale sized catchments within the range of the Irene radar and Figure 4.3 shows their drainage patterns determined by the streamflow networks. Clearly, one of the highest points in the region is close to where the watersheds (perimeters) of the four main catchments intersect. Note that these coloured catchments are formed from the tessellation of the region into 1 km^2 areas, which is the scale of PyTOPKAPI as applied routinely.

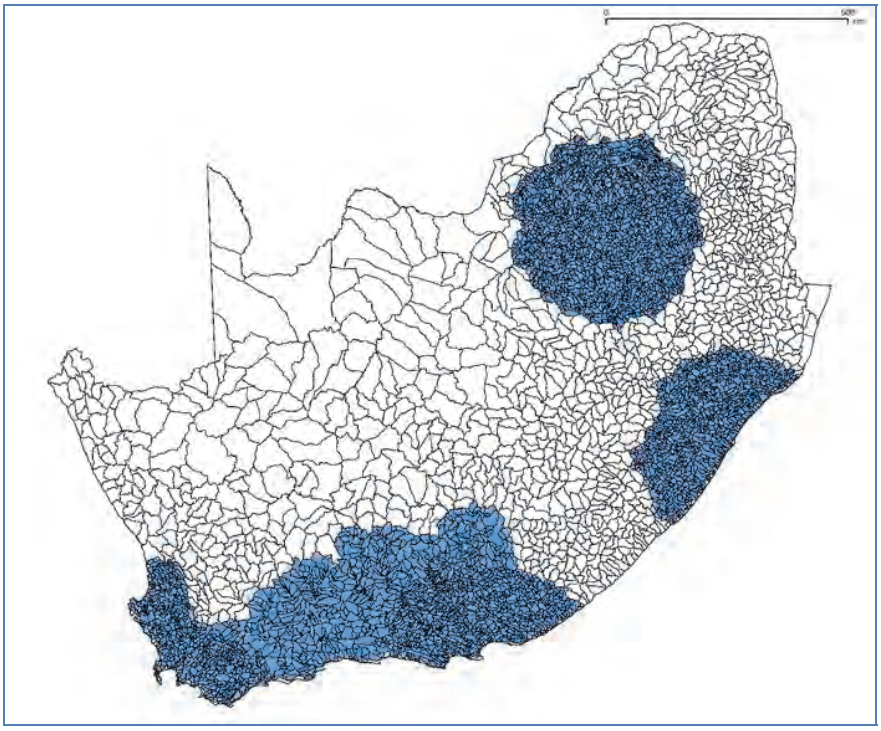

Figure 4.1: Overview of the SAFFG catchments in South Africa, Lesotho and Swaziland. The highly divided SAFFG catchments are the blue coloured polygons, shown overlaid on the WR2005 quaternary catchments. [The horizontal bar, top-right, denotes 500 km.]

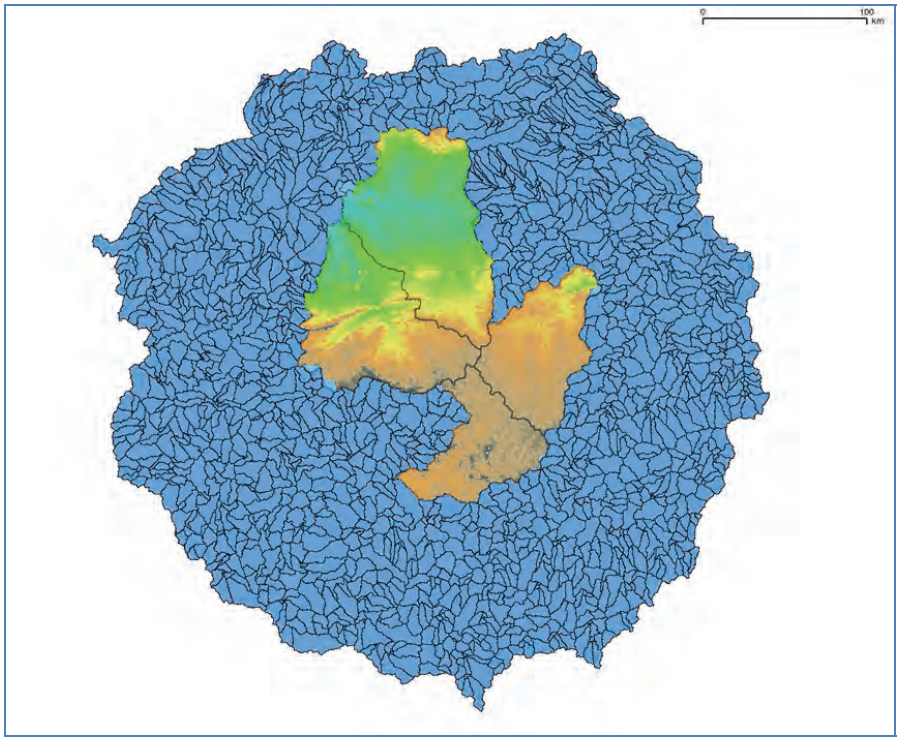

Figure 4.2: A more detailed view of the SAFFG catchments within range of the Irene radar, showing the four WR2005 tertiary level catchments we chose for the modelling process. The elevation is shown by the green (lower) through dark brown (higher) colour scale, derived from the Shuttle Mission Digital Elevation Map. The catchment labelling and areas appear in the Table below. [The horizontal bar top right denotes 100 km.]

Tertiary catchment	Area (km^2)
A23 (North)	6282
A21 (West)	7505
B20 (East)	4360
C21 (South)	3485

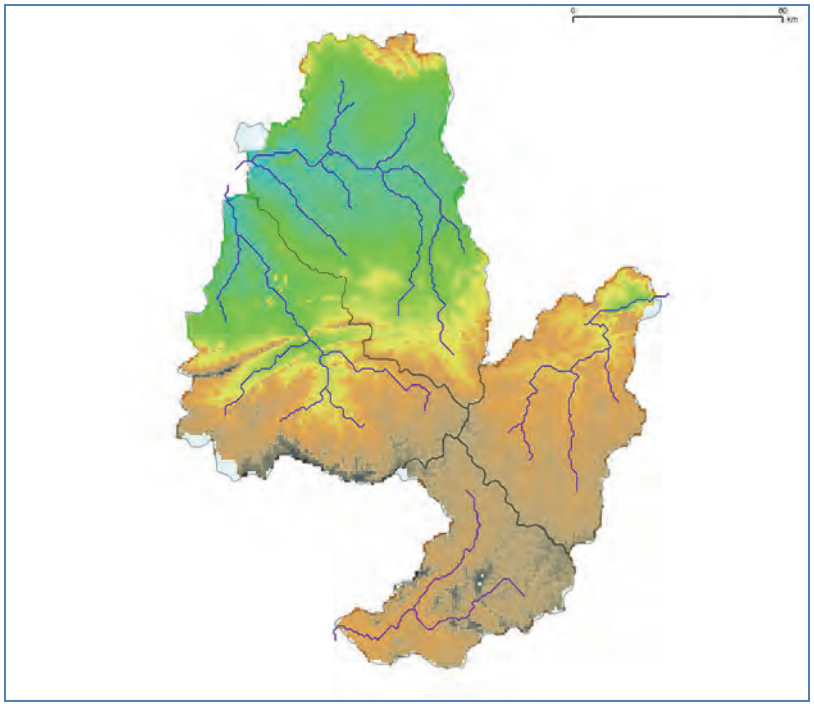

Figure 4.3: A more detailed view of the four extracted catchments coloured in Figure 4.2 and their stream networks, obtained via automated GIS analysis of the DEM. [The horizontal bar denotes 80 km.]

4.3 THE HYDROLOGICAL MODELS

The PyTOPKAPI model structure is shown in Figure 4.4 as applied to the Liebenbergsvlei in Pegram *et al.* (2010).

In PyTOPKAPI, each 1 km^2 pixel is modelled in the A & B soil horizons (about 800 mm depth from the surface) using hydraulic principles of continuity and energy, exploiting the natural parameters of the soil and surface. The inputs are rainfall and upstream flow, the outflows are actual evapotranspiration and down-slope drainage, and the calculation interval is 3 hours, matching the TRMM frequency.

By contrast, the Sacramento model is a modified tank-storage model, depicted in Figure 4.5. It has two soil stores, labelled 'upper' and 'lower' in the Figure. SAWS was unable to provide details of the

depths and porosities in the soil layers, so only relative values of Soil Moisture can be compared in the sequel.

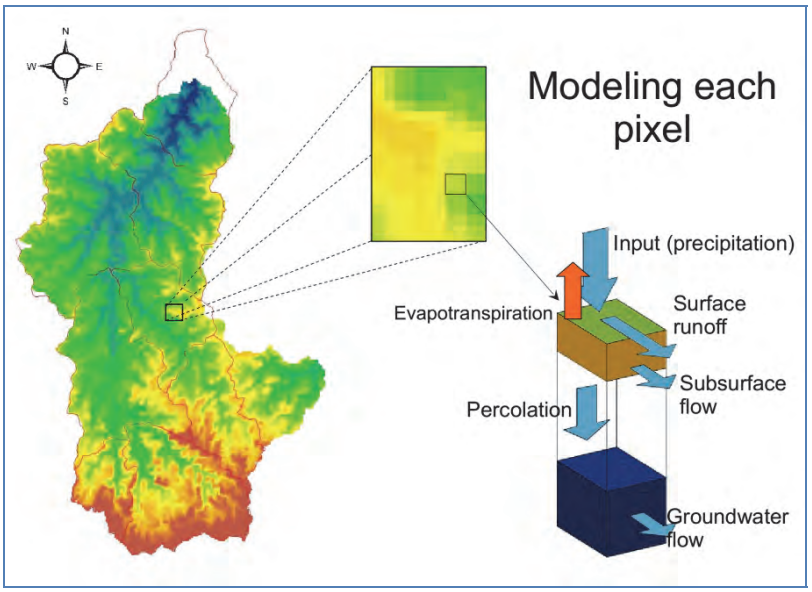

Figure 4.4: Set up PyTOPKAPI in full Hydrological mode.

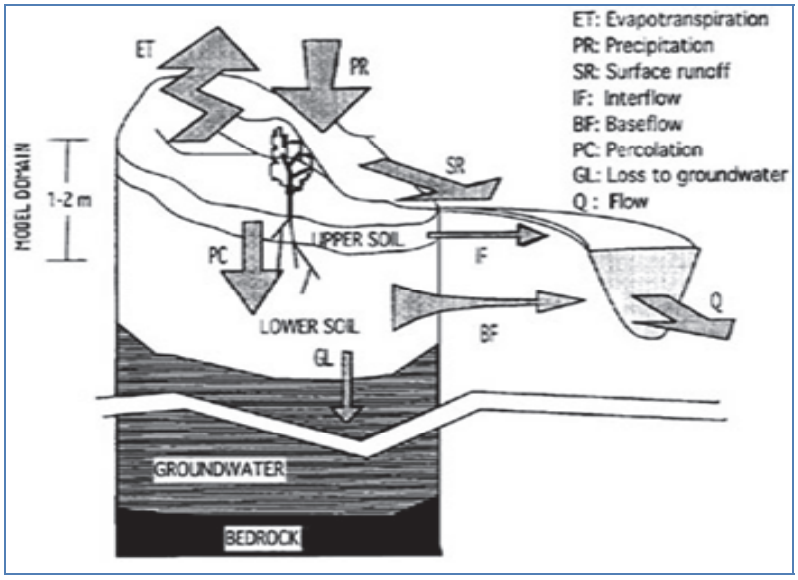

Figure 4.5: Sacramento Model soil zones in context

4.4 MODELLING SOIL MOISTURE AS A RELATIVE QUANTITY

To display the power of the PyTOPKAPI modelling procedure, the southern-most tertiary level catchment of the four in Figure 4.3 was modelled and then the average Soil Moisture (SM) for each SAFFG catchment was computed from these simulation results. The example of a snapshot of SSI (relative SM) over catchment C21 is shown in Figure 4.6.

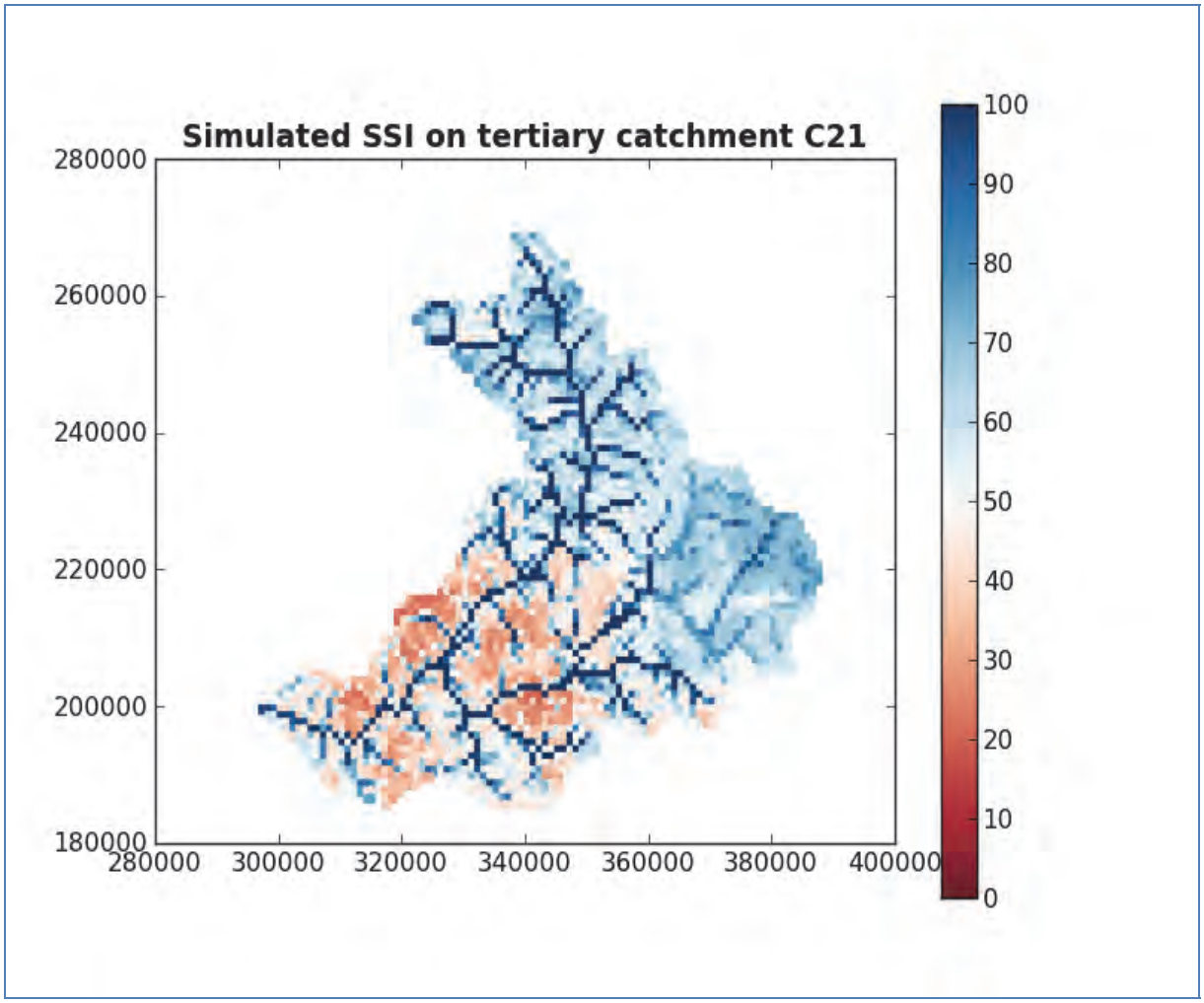

Figure 4.6: SSI modelled by PyTOPKAPI at 1 km^2 resolution for the Southern C21 tertiary catchment shown in Figure 4.3. This is a snapshot of one of the 3-hour time-steps during the 2-year simulation reported here. (The horizontal and vertical scales are in metres. The colour-scale is SSI in percentages.) Note the relatively very wet river channels.

Figures 4.7 and 4.8 following were produced by spatially averaging the SSI over each SAFFG catchment, based on a 3-hour time-step simulation over a period of 2 years using PyTOPKAPI forced by TRMM. They show the status of SSI averages at the start (00:00 UTC) on different days.

In Figure 4.7, the change in SSI state with time is shown during a wetting-up period. The top-left panel shows the SSI snapshot on day 0, the top-right day 1, the bottom left day 7 (one week later) and the bottom right day 30 (approx. one month later).

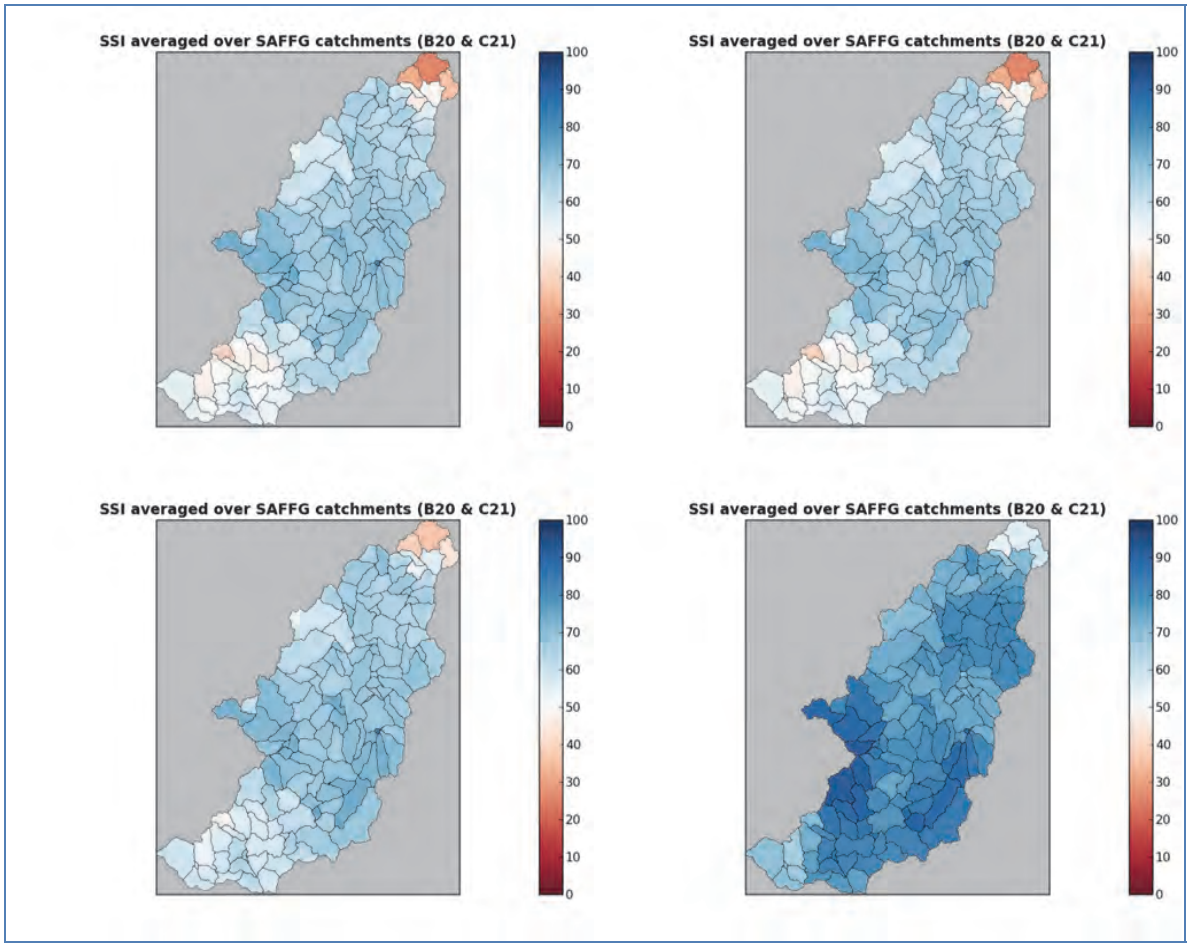

Figure 4.7: Soil Moisture as SSI is typically a slowly varying quantity. This Figure shows the SSI averaged over each of the SAFFG catchments, which fall within tertiary catchments C21 (Southern parts) and B20 (Eastern parts).

In Figure 4.8, the change in SSI state with time, on tertiary catchments B20 and C21, is shown over a calendar year (2010) at monthly intervals. Starting relatively wet in January, peaking in February, the catchment slowly dries out until the beginning of October, then gradually wets up again towards the end of the year. This slow change in SSI response was also a feature of the Liebenbergsvlei, as reported in Pegram *et al.* (2010).

In summary, this section illustrates the results of the calculation procedure to derive SSI estimates over SAFFG catchments using PyTOPKAPI forced by TRMM 3B42RT rainfall at 3-hour intervals, as was done in the WRC project HYLARSMET: K5/2024.

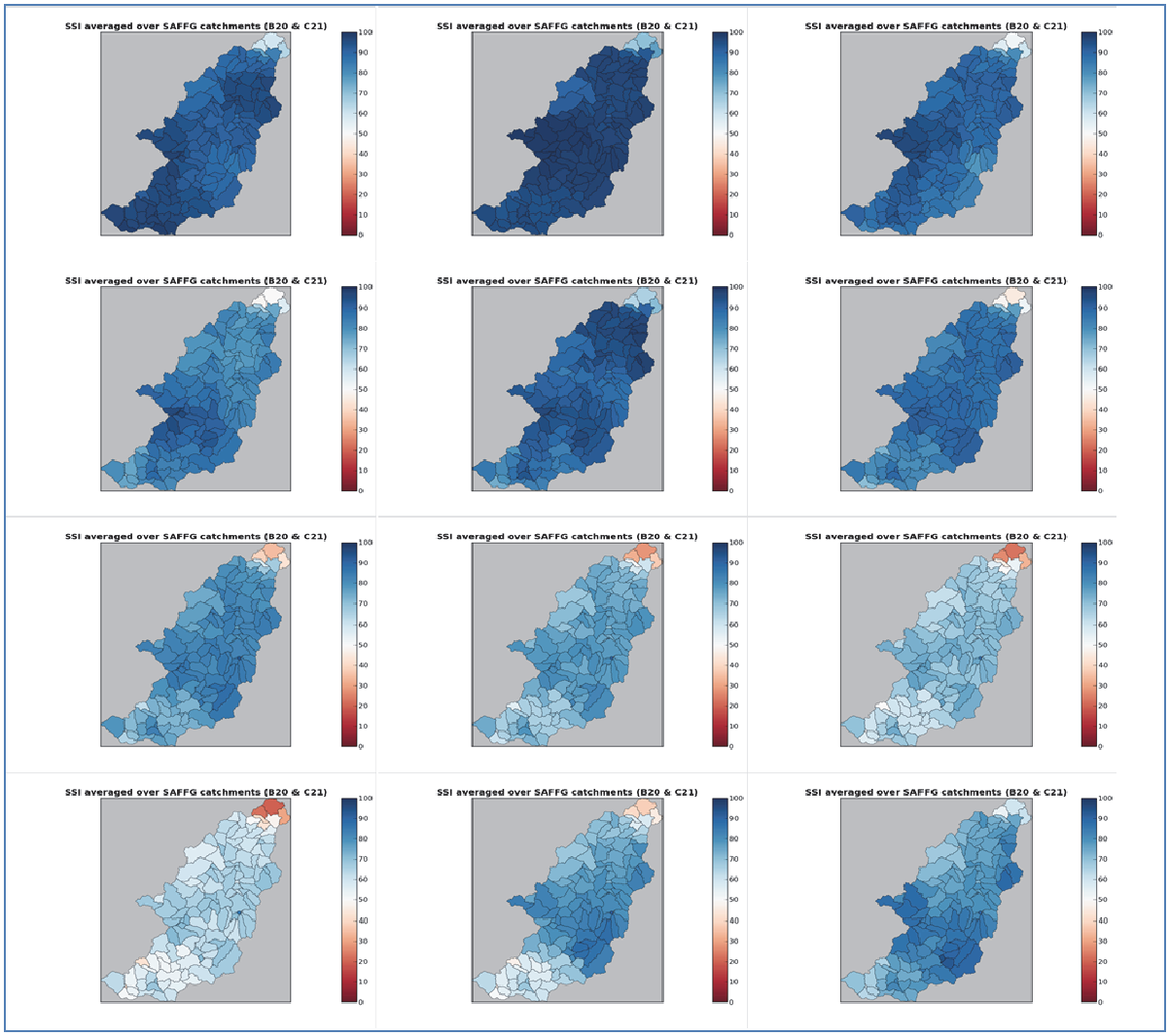

Figure 4.8: Monthly evolution of SSI averaged over (approximately 140) SAFFG catchments lying within tertiary catchments B20 and C21. Each panel is a snapshot of conditions at 00:00 on the first day of the month during 2010. The sequence starts with 1st January 2010 at the top left panel and proceeds in month order from left to right to end with 1st December 2010 in the bottom right panel.

In Section 4.5 following, three new sets of time series are compared: the Relative Soil Moisture estimates computed using SAFFG by SAWS on the same catchments as above, but using the SAWS rainfall estimates averaged over the catchments (i) for the upper layer, and (ii) for the lower layer of the Sacramento model. (iii) The SSI estimates over the same catchments are recalculated using PyTOPKAPI forced by the SAWS rainfall, instead of TRMM.

4.5 COMPARE SM ESTIMATES BY TWO MODELS FORCED BY TWO RAINFALL SEQUENCES

A start is made with tertiary catchment C21 by way of introducing the ideas, which are fully developed in Section 4.5.1, and the analysis for tertiary catchment B20 is repeated in Section 4.5.2. Figure 4.9 indicates the SAFFG catchment 2001803424, highlighted in red. Figure 4.10 shows the contemporaneous traces of the estimates of the Soil Moisture estimated by the PyTOPKAPI model and the SAFFG model. The latter's upper layer response is shown both as raw and temporally filtered (by an exponential filter with a dwell time of 20 days).

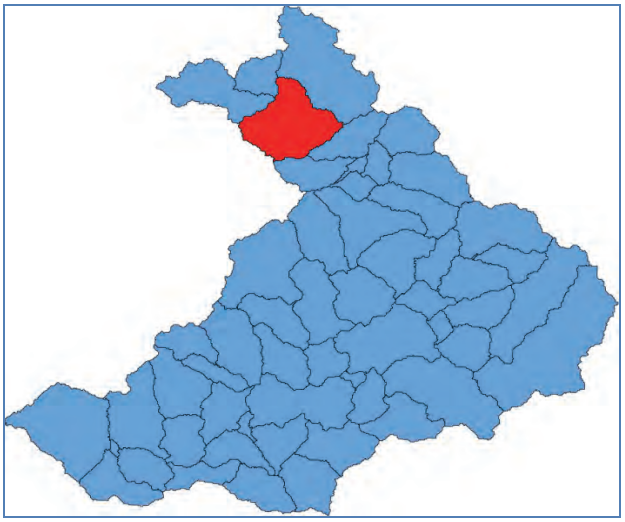

Figure 4.9: Choose an SAFFG catchment (coloured red) in tertiary catchment C21

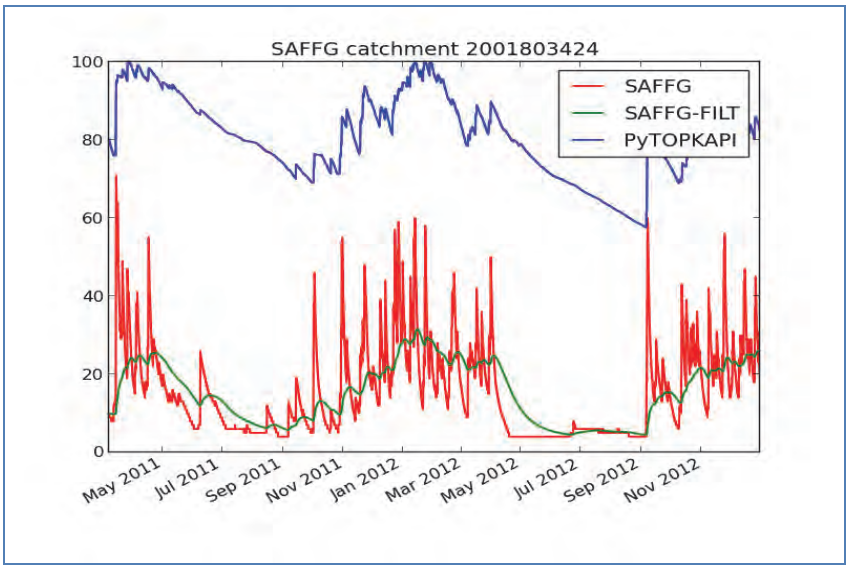

Figure 4.10: Time series of daily estimates of percentage SM, in the SAFFG catchment highlighted in Figure 9, over 21 months, estimated by PyTOPKAPI forced by TRMM (blue line), raw SAFFG upper layer (red line) and filtered [exponential filter with 20-day residence time] SAFFG upper layer (green line). Note the unrealistic limiting lower threshold of the unfiltered SAFFG estimate, which plateaus at about 5%

Figure 4.11 shows the scatterplots of the PyTOPKAPI daily estimates of SSI, compared with those in the upper and lower layers of the SAFFG model; the data are drawn from Figure 4.10.

Figure 4.12 summarises the calculation for all the SAFFG catchments in C21, showing the position of the one selected for the calculations leading to Figures 4.10 and 4.11.

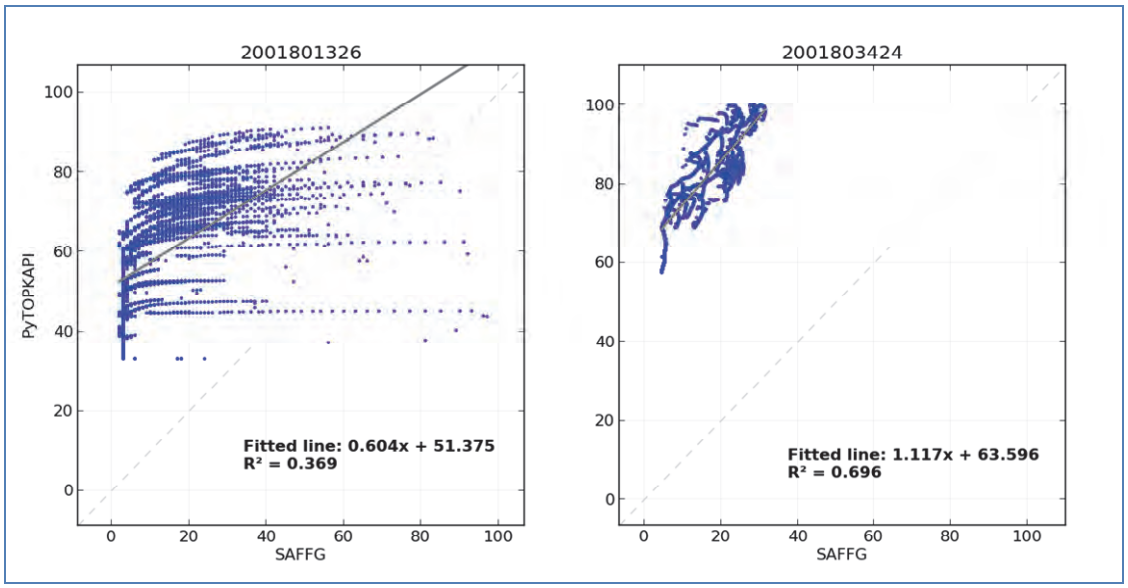

Figure 4.11: Scatterplots, fitted regression lines and R2 values derived from plotting PyTOPKAPI versus SAFFG unfiltered (left) and filtered (right) derived from the data creating Figure 4.10.

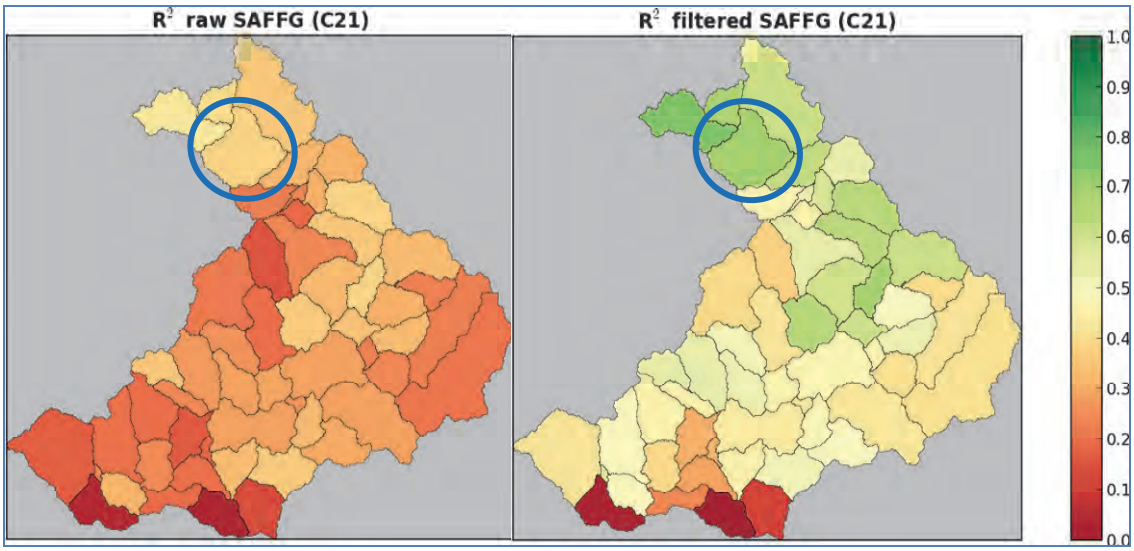

Figure 4.12: Summary C21 catchment-dependent plots, based on R2 values derived from plotting PyTOPKAPI versus SAFFG unfiltered (left) and filtered (right) similar to those taken from Figure 4.11; the ringed SAFFG catchment is the highlighted one in Figure 4.9.

Note that these results are only for the Upper layer of the SACRAMENTO model and outline the methodology devised to make the model intercomparison. The results for the full set including the Lower model layer, extended over tertiary catchment B20, follow.

First, it was decided to compare the rainfall products forcing the two models: PyTOPKAPI & SACRAMENTO. Figure 4.13 compares the radar product used in SAFFG and the TRMM 3B42RT product forcing PyTOPKAPI. The radar product is spatially averaged over the SAFFG catchments, while the TRMM estimates at 3-hour intervals are averaged over the 0.25° squares, which is the spatial resolution of TRMM. The period covered is 21 months long, from 1 April 2011 to 31 December 2012.

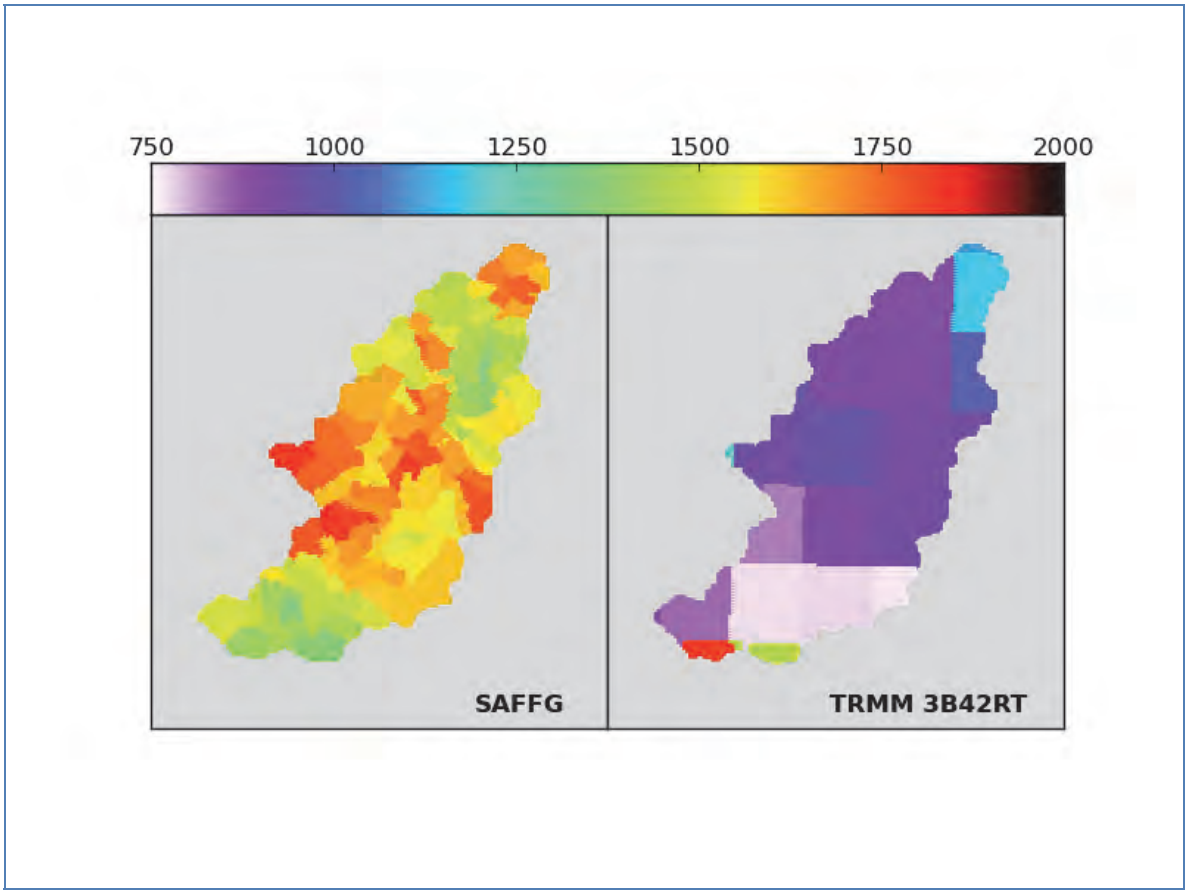

Figure 4.13: Comparison of total rainfall accumulation on tertiary catchments B20 and C21 for period 2011/04/01 - 2012/12/31 for SAFFG rainfall (predominantly Irene weather radar) and TRMM 2B42RT.

Note the discrepancy between the rainfall inputs in the two models shown in Figure 4.13. SAFFG's SACRAMENTO model receives nearly double the rainfall estimated by the radar compared to that which PyTOPKAPI receives from TRMM.

4.5.1 Tertiary catchment C21

In this section, a new SAFFG catchment 2001803435 is chosen, highlighted in Figure 4.14, and the Soil Moisture estimates of PyTOPKPAI are estimated, forced by both (i) TRMM and the (ii) SAFFG input against the SAFFG record of (iii) the Upper and (iv) the lower layer store of the SACRAMENTO model.

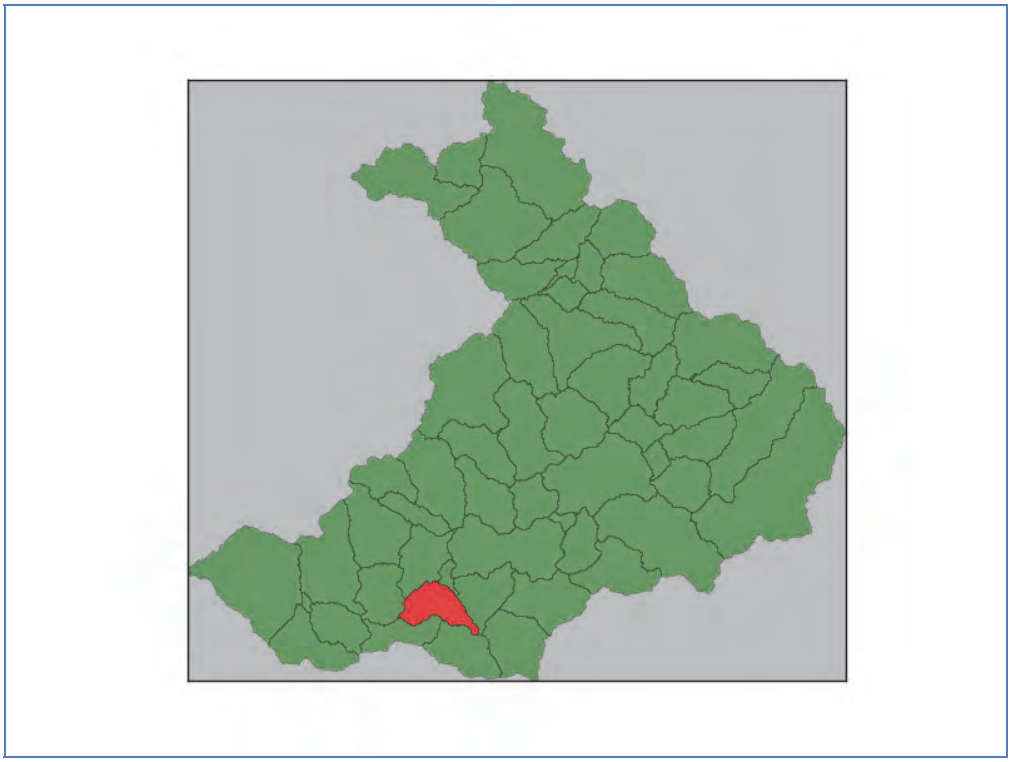

Figure 4.14: SAFFG catchments falling within tertiary catchment C21; the red coloured catchment is the one that is discussed with the assistance of Figures 4.15 to 4.21.

Figure 4.15 compares the rainfall inputs to the models: TRMM and radar-based. There seems to be reasonable correspondence in the timings, but the amounts are different.

The PyTOPKAPI simulations were forced by both TRMM and SAFFG rainfall in turn, whereas the SAFFG SACRAMENTO model was only forced by the radar input. These comparisons follow from Figure 4.17 onward. The comment on Figure 4.13 also applies to Figure 4.15; the radar is estimating nearly twice the rainfall offered by TRMM.

Figure 4.16 shows temporal traces of the SSI, obtained from a selection [of the order of 50] of the PyTOPKAPI 1 km^2 elements comprising SAFFG catchment 2001803435, together with their average, which is used in the sequel.

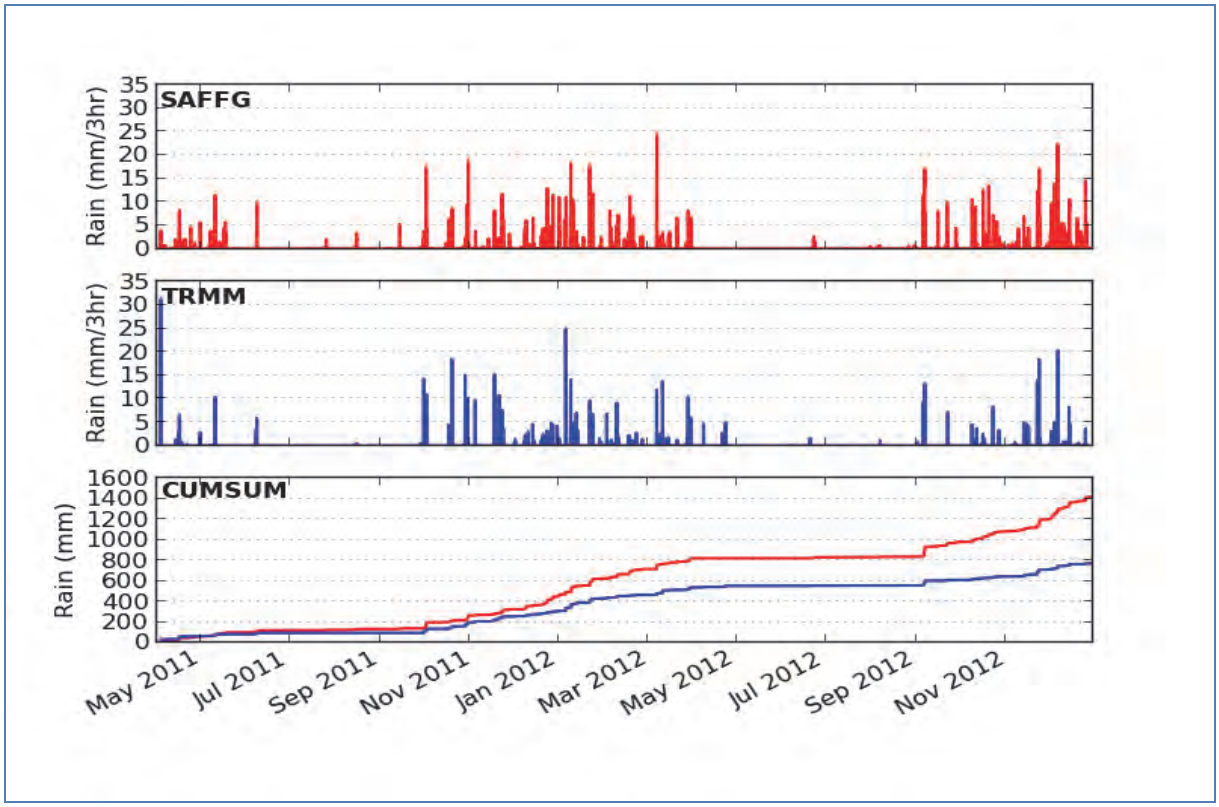

Figure 4.15: Rainfall sequences averaged over the SAFFG catchment highlighted in Figure 4.14

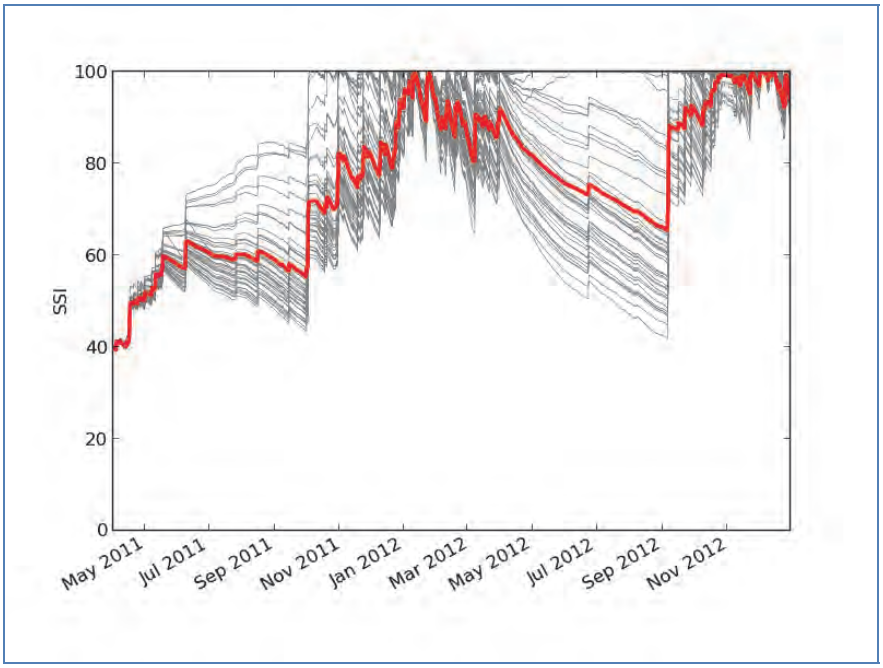

Figure 4.16: Traces of Soil Saturation Index (SSI) for each of the PyTOPKAPI cells inside the SAFFG catchment 2001803435 (grey lines), and the mean value for the catchment (heavy red line, which turns to a blue line in Figure 4.17's lower two panels).

Comment on Figure 4.17. Given that the radar gives nearly twice the rain that TRMM offers, it is surprising that the SAFFG Soil Moisture estimates are so much lower than those of PyTOPKAPI. This observation applies to both the upper and lower layer of the SACRAMENTO model. In addition, it is disturbing that the raw (unfiltered) SAFFG estimate of Soil Moisture has at least two periods of flat response, intimating that there are no losses from the soil store even though the saturation level is as high as 60% in the lower layer. These anomalies seem to occur during times of little rain.

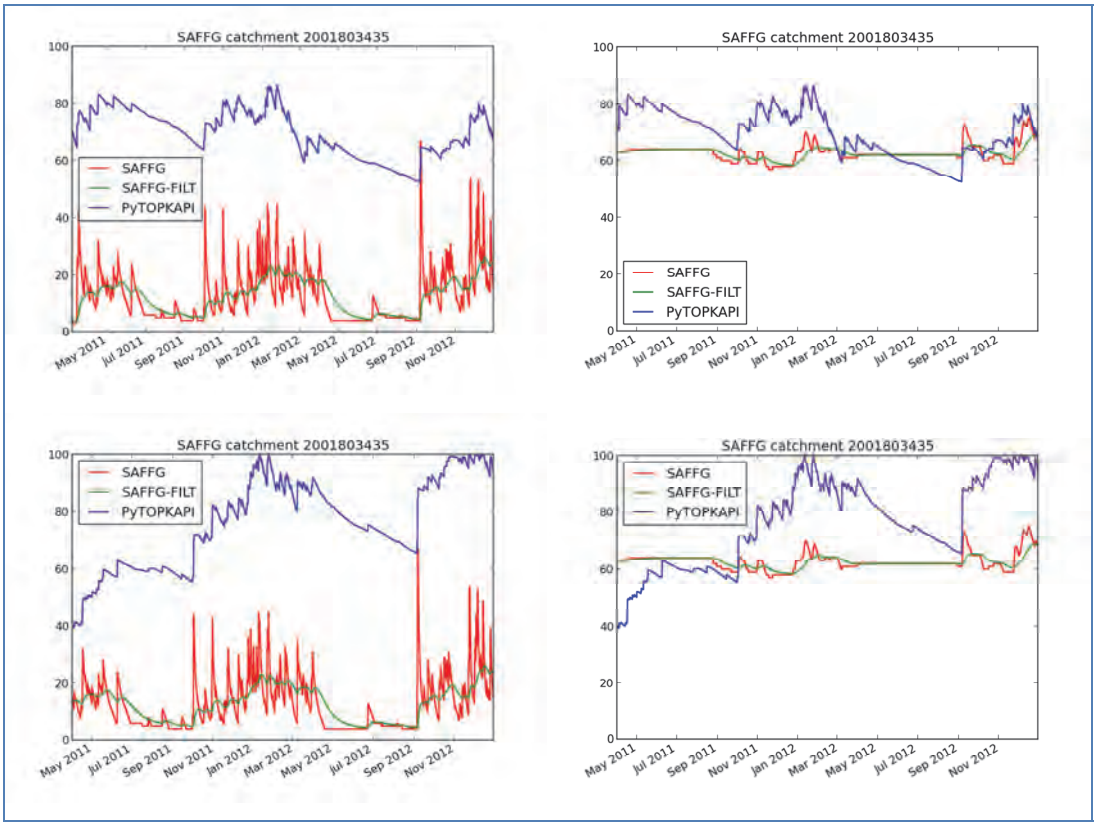

Figure 4.17: Time series of percentage Soil Moisture estimates. Top left: TRMM forced PyTOPKAPI versus SAFFG upper soil layer. Top right: TRMM forced PyTOPKAPI versus SAFFG lower soil layer. Bottom left: SAFFG forced PyTOPKAPI versus SAFFG upper soil layer. Bottom right: SAFFG forced PyTOPKAPI versus SAFFG lower soil layer

These observations suggest that the model is not responding to Evapotranspiration, nor is it draining, during periods of low rainfall from May to September. These occurrences of constant Soil Moisture levels over protracted periods cause a marked reduction in the correlation between the two model outputs, in whichever mode PyTOPKAPI is forced, particularly obvious in Figures 4.19 and 4.21.

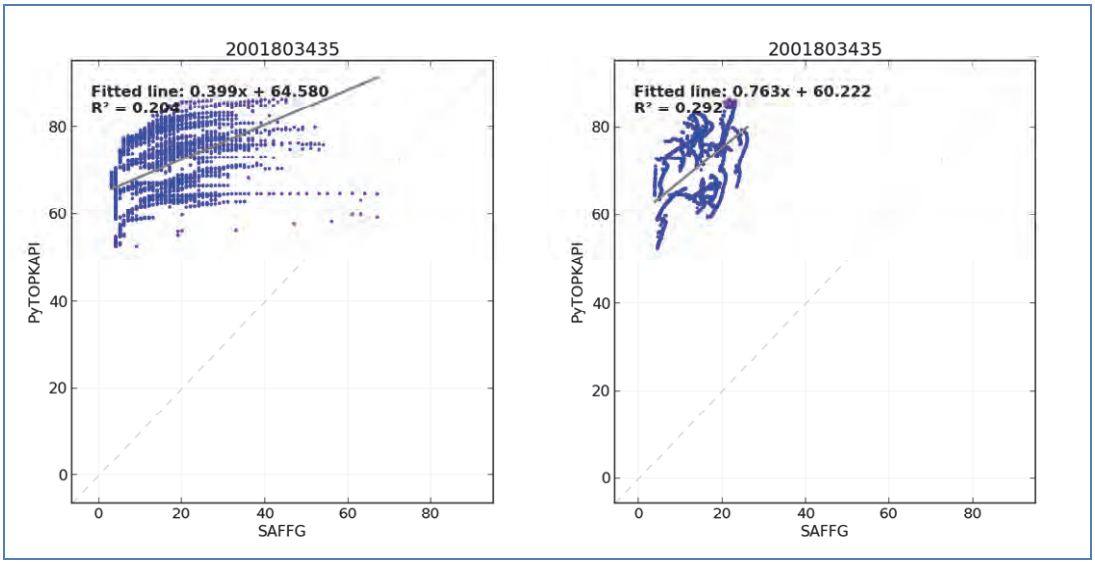

Figure 4.18: Scatter plots of TRMM forced PyTOPKAPI versus SAFFG upper soil layer from top-left image of Figure 4.18. Left: SAFFG raw data. Right: SAFFG temporally filtered data.

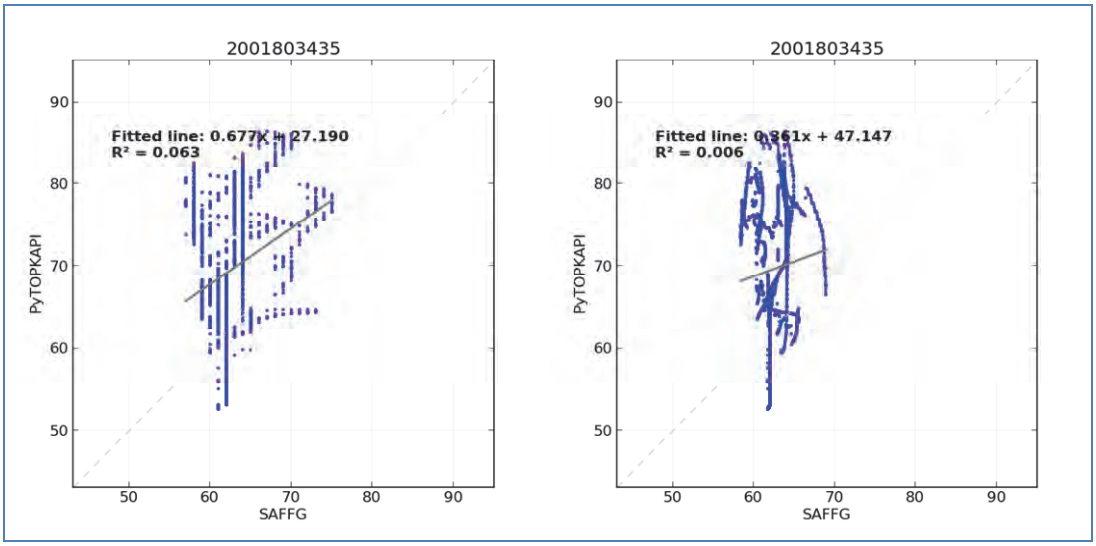

Figure 4.19: Scatter plots of TRMM forced PyTOPKAPI versus SAFFG lower soil layer from top-right image of Figure 4.18. Left: SAFFG raw data. Right: SAFFG temporally filtered data.

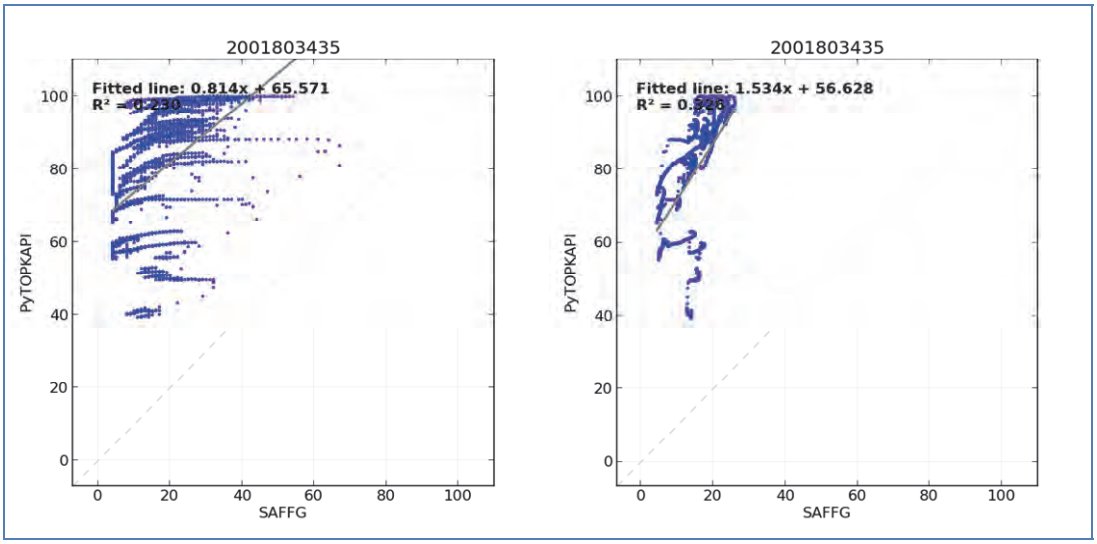

Figure 4.20: Scatter plots of SAFFG forced PyTOPKAPI versus SAFFG upper soil layer from lower-left image of Figure 4.18. Left: SAFFG raw data [R2 = 0.230]. Right: SAFFG temporally filtered data [R2 = 0.326].

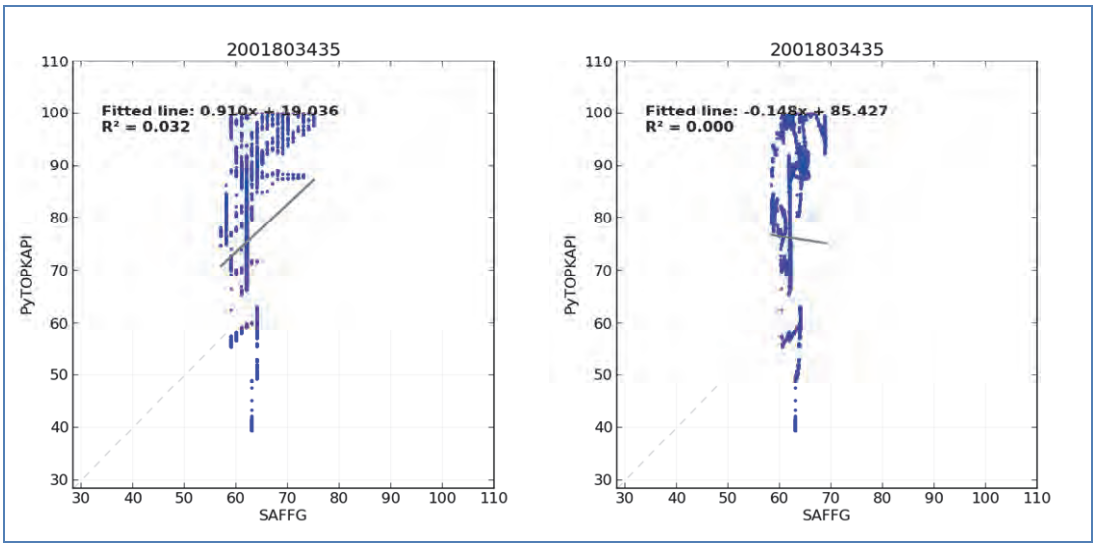

Figure 4.21: Scatter plots of SAFFG forced PyTOPKAPI versus SAFFG lower soil layer from lower-right image of Figure 4.17. Left: SAFFG raw data. Right: SAFFG temporally filtered data.

The values of R^2 computed in Figures 4.18 to 4.21 appear in the ringed SAFFG catchments of Figures 4.22 and 4.23, whose eight panels summarise the comparative results for all SAFFG catchments on tertiary catchment C21. To read Figures 4.22 and 4.23, the raw SAFFG results appear in the left column of 4 panels and the filtered ones appear in the right column. Figure 4.22 treats the results of PyTOPKAPI forced by TRMM, while Figure 4.23 deals with PyTOPKAPI forced by SAFFG inputs. In each Figure, the upper/lower row displays results for the upper/lower soil store of the SACRAMENTO model.

A general comment is that (unexpectedly) filtering seems to improve the correspondence when the upper layer is treated, but has little effect on the lower. Another paradox is that PyTOPKAPI has a better correspondence with SAFFG when forced by TRMM than by the SAFFG forcing.

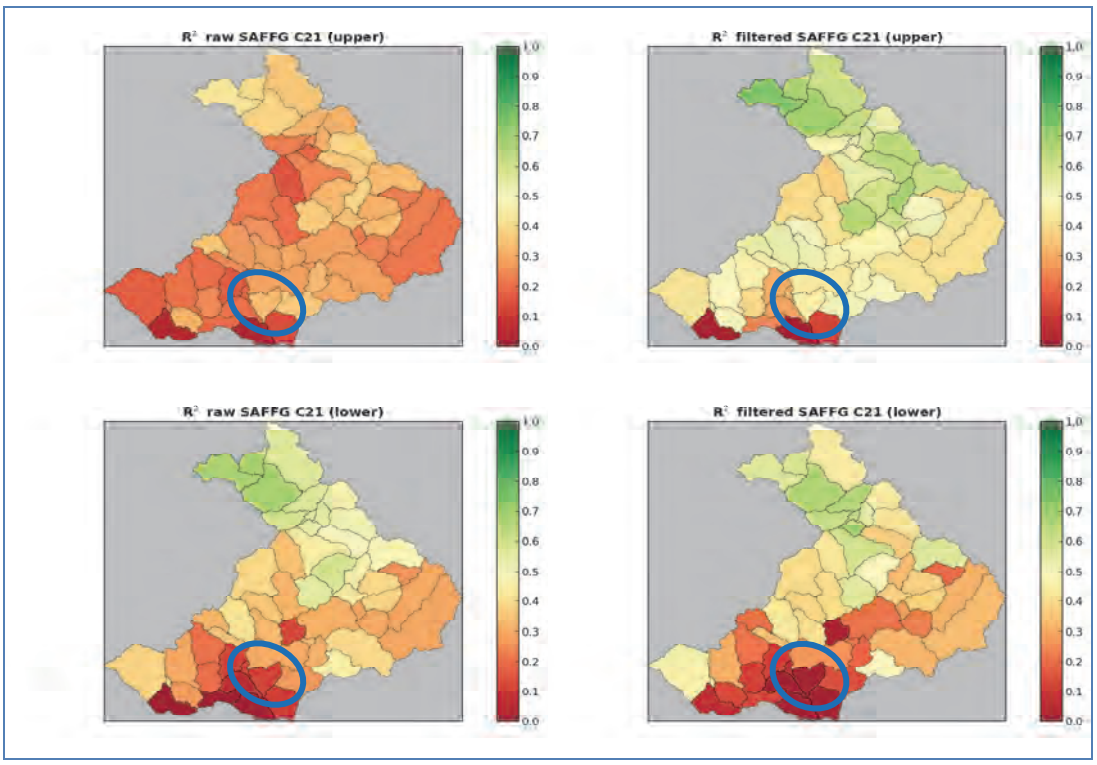

Figure 4.22: Summarized R2 for SAFFG catchments in tertiary catchment C21, following the order of Figures 4.18 and 4.19. Top left: TRMM/PyTOPKAPI ~ raw SAFFG upper soil layer. Top right: TRMM/PyTOPKAPI ~ filtered SAFFG upper soil layer. Bottom left: TRMM/PyTOPKAPI ~ raw SAFFG lower soil layer. Bottom right: TRMM/PyTOPKAPI ~ filtered SAFFG lower soil layer. The ringed catchment is red in Figure 4.14.

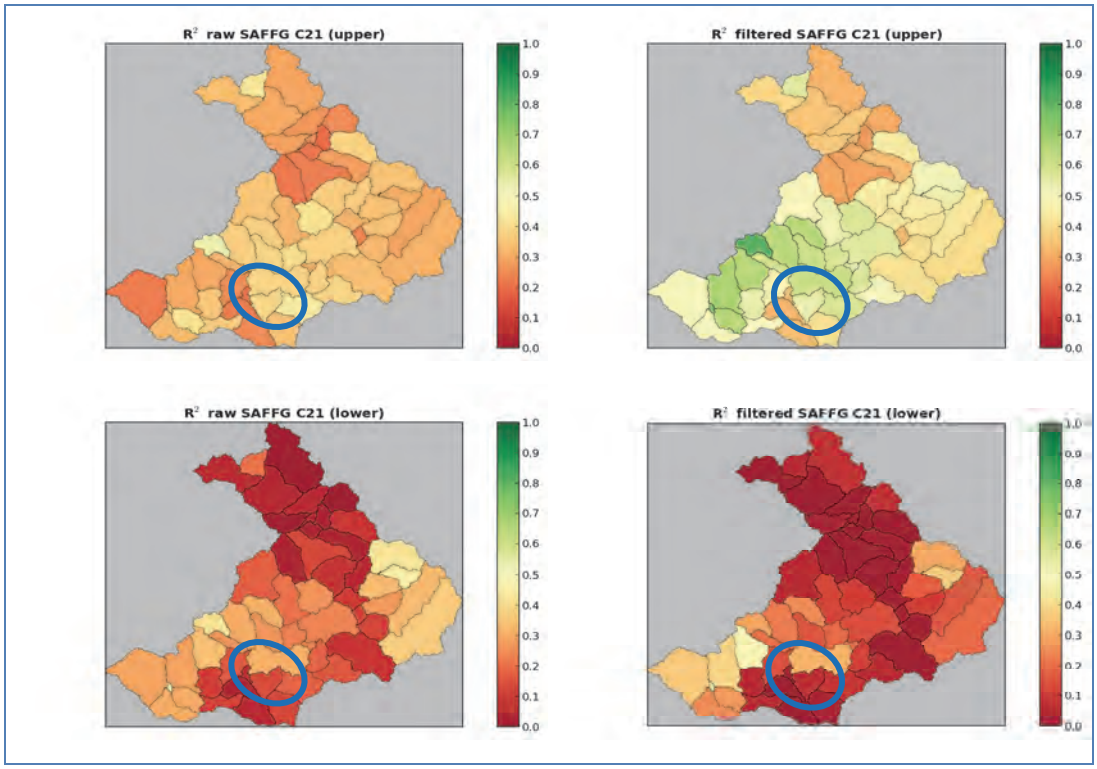

Figure 4.23: Summarized R2 for SAFFG catchments inside tertiary catchment C21, following the order of Figures 4.20 and 4.21. Top left: SAFFG forced PyTOPKAPI ~ raw SAFFG upper soil layer. Top right: SAFFG forced PyTOPKAPI ~ filtered SAFFG upper soil layer. Bottom left: SAFFG forced PyTOPKAPI ~ raw SAFFG lower soil layer. Bottom right: SAFFG forced PyTOPKAPI ~ temporally filtered SAFFG lower soil layer.

4.5.2 Tertiary catchment B20

In this section we repeat the analysis of Section 4.5.1 on the second tertiary catchment B20, reinforcing the above observations.

Figure 4.24: SAFFG catchments falling within tertiary catchment B20. The red coloured catchment is 2001801338, the one whose SM response the following treatment describes

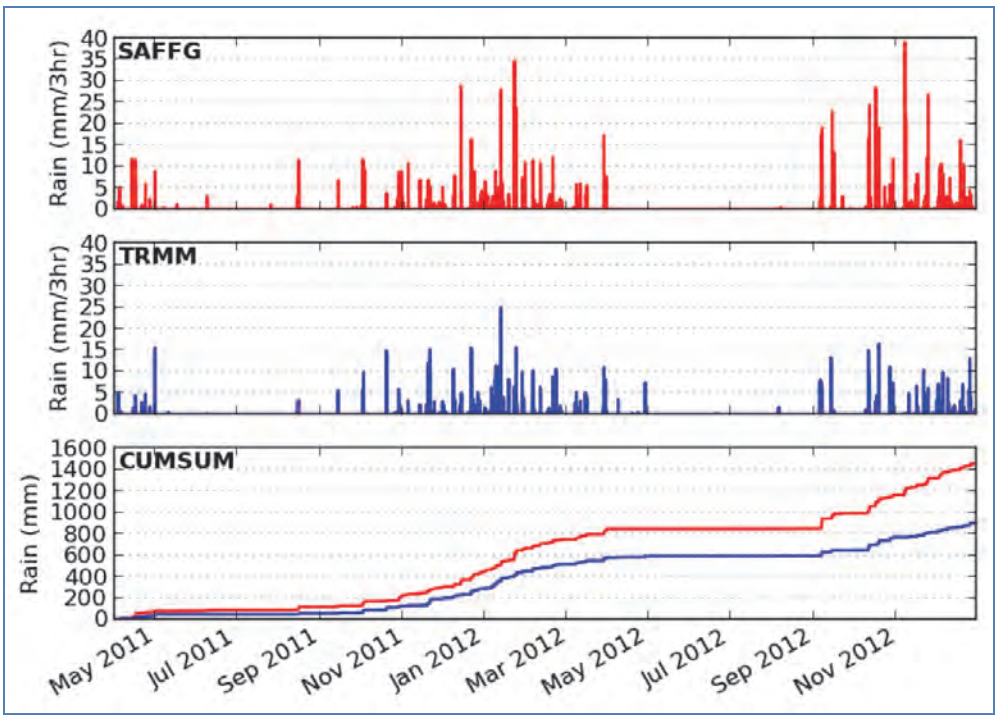

Figure 4.25: Rainfall sequences averaged over the SAFFG catchment highlighted in Figure 4.24. The PyTOPKAPI simulations were forced by both TRMM and SAFFG rainfall in turn

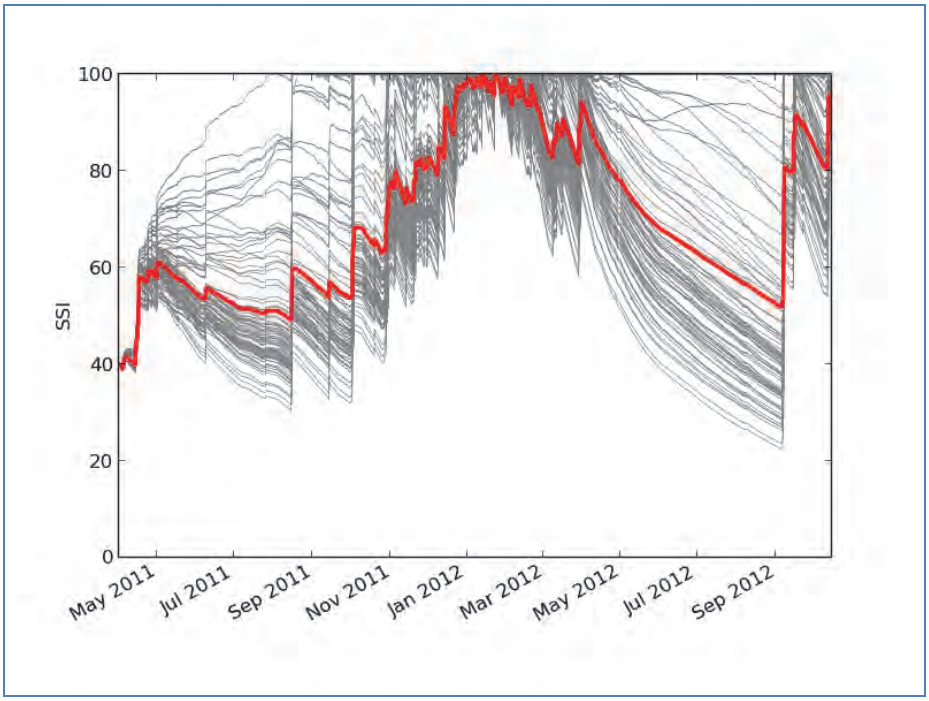

Figure 4.26: Traces of Soil Saturation Index (SSI) for each of the PyTOPKAPI cells inside the SAFFG catchment 2001801338 (grey lines), and the mean value for the catchment (heavy red line).

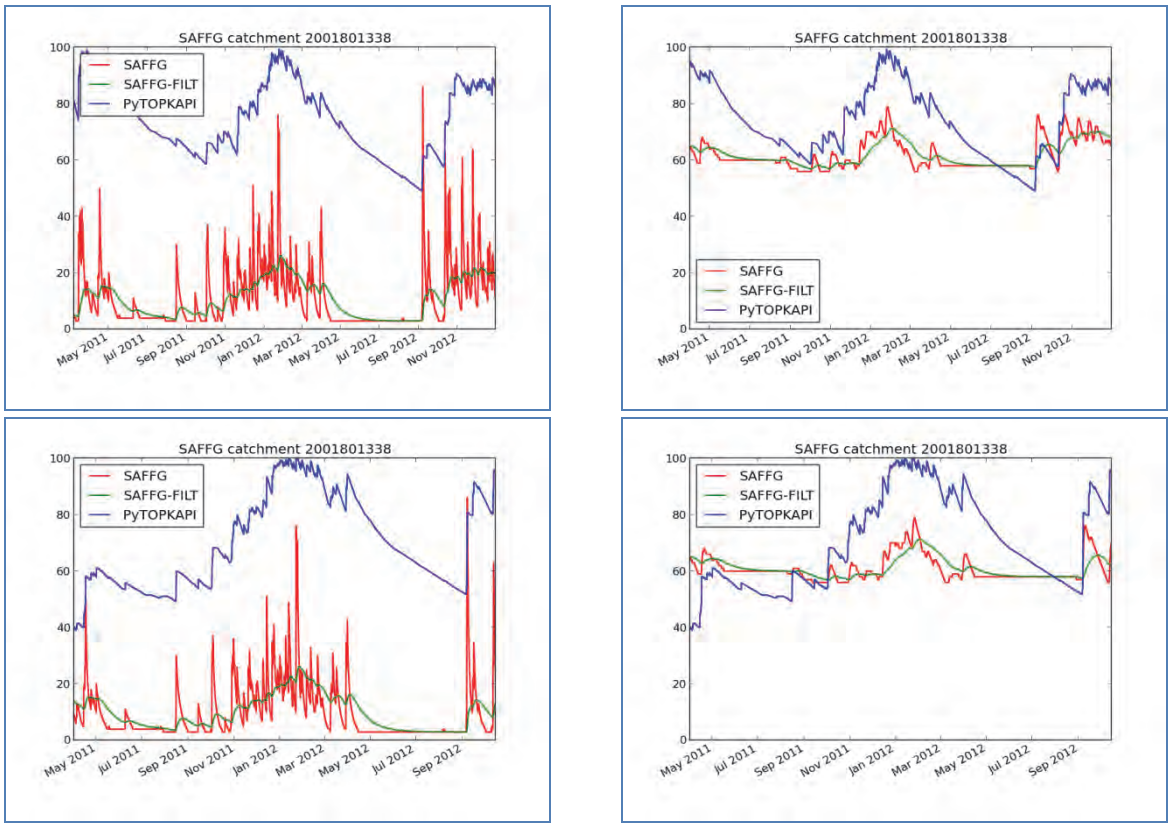

Figure 4.27: Time series of Soil Moisture estimates. Top left: TRMM forced PyTOPKAPI versus SAFFG upper soil layer. Top right: TRMM forced PyTOPKAPI versus SAFFG lower soil layer. Bottom left: SAFFG forced PyTOPKAPI versus SAFFG upper soil layer. Bottom right: SAFFG forced PyTOPKAPI versus SAFFG lower soil layer.

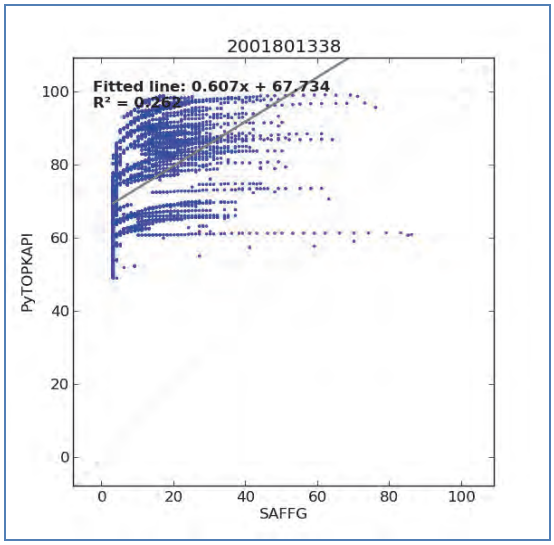

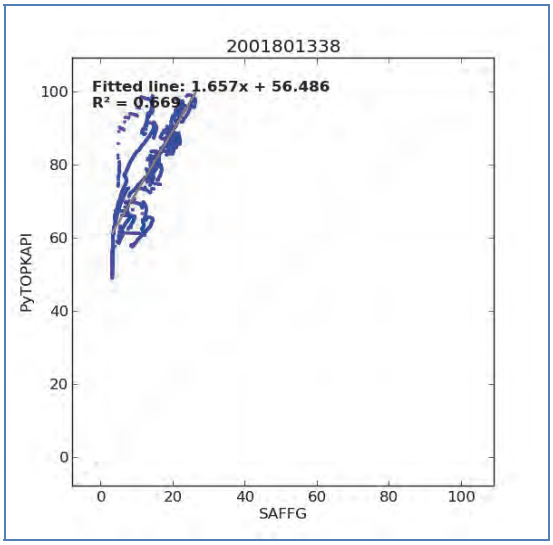

Figure 4.28: Scatter plots of TRMM forced PyTOPKAPI versus SAFFG upper soil layer. Left: SAFFG raw data. Right: SAFFG temporally filtered data.

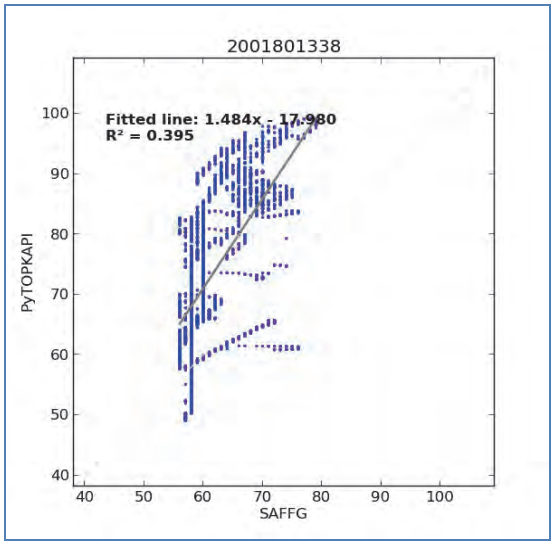

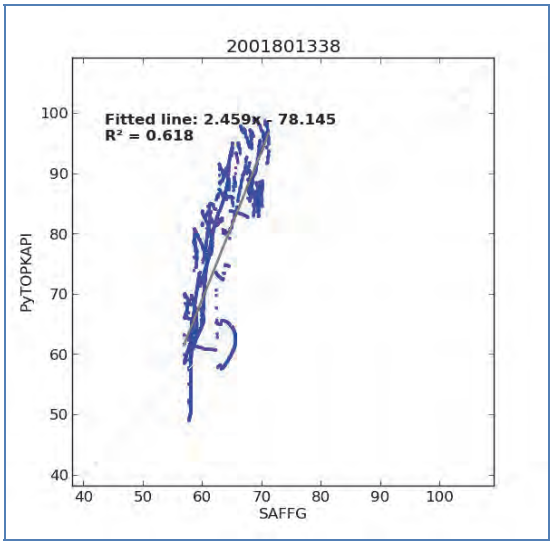

Figure 4.29: Scatter plots of TRMM forced PyTOPKAPI versus SAFFG lower soil layer. Left: SAFFG raw data. Right: SAFFG temporally filtered data.

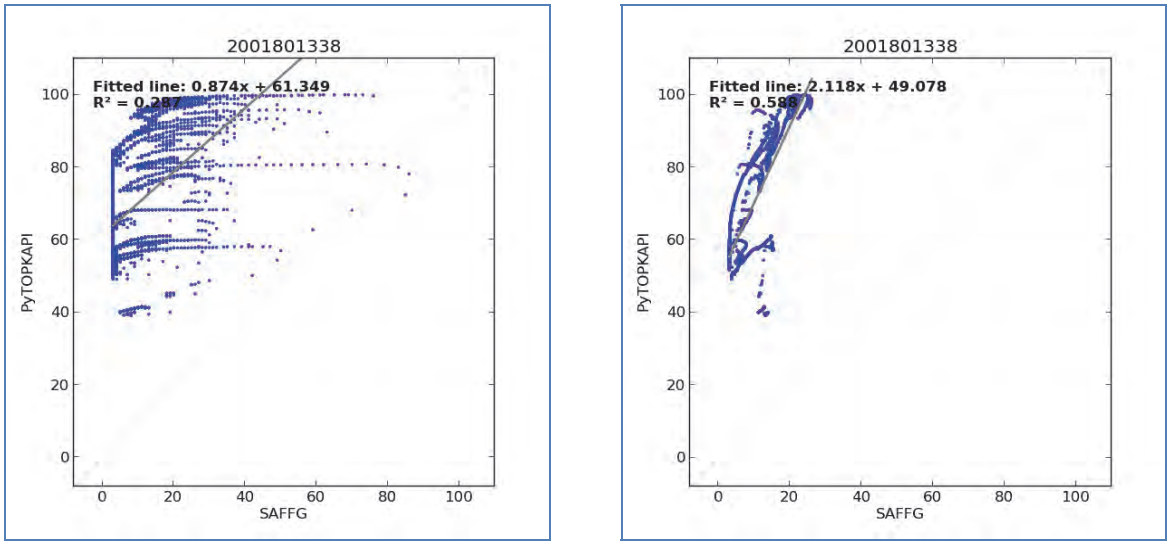

Figure 4.30: Scatter plots of SAFFG forced PyTOPKAPI versus SAFFG upper soil layer. Left: SAFFG raw data. Right: SAFFG temporally filtered data.

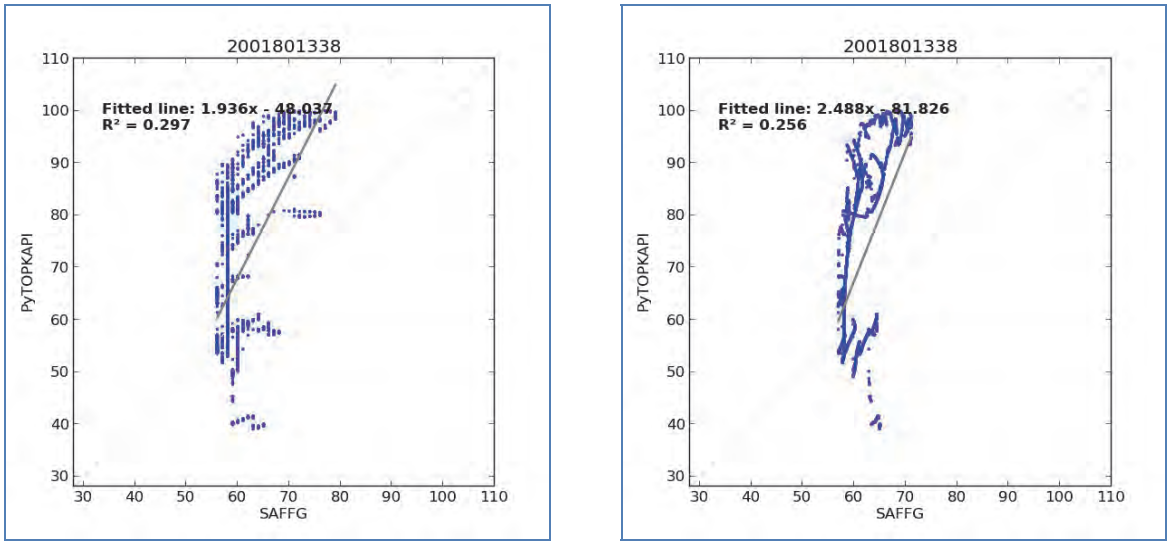

Figure 4.31: Scatter plots of SAFFG forced PyTOPKAPI versus SAFFG lower soil layer. Left: SAFFG raw data. Right: SAFFG temporally filtered data.

An obvious comment on these Figures is that yet again filtering seems to improve the correspondence when the upper layer is treated, but has little effect on the lower. Again, PyTOPKAPI has a better correspondence with SAFFG when forced by TRMM than by the SAFFG forcing. This is more pronounced in the lower panels of Figure 4.33 than the corresponding panels in Figure 4.23.

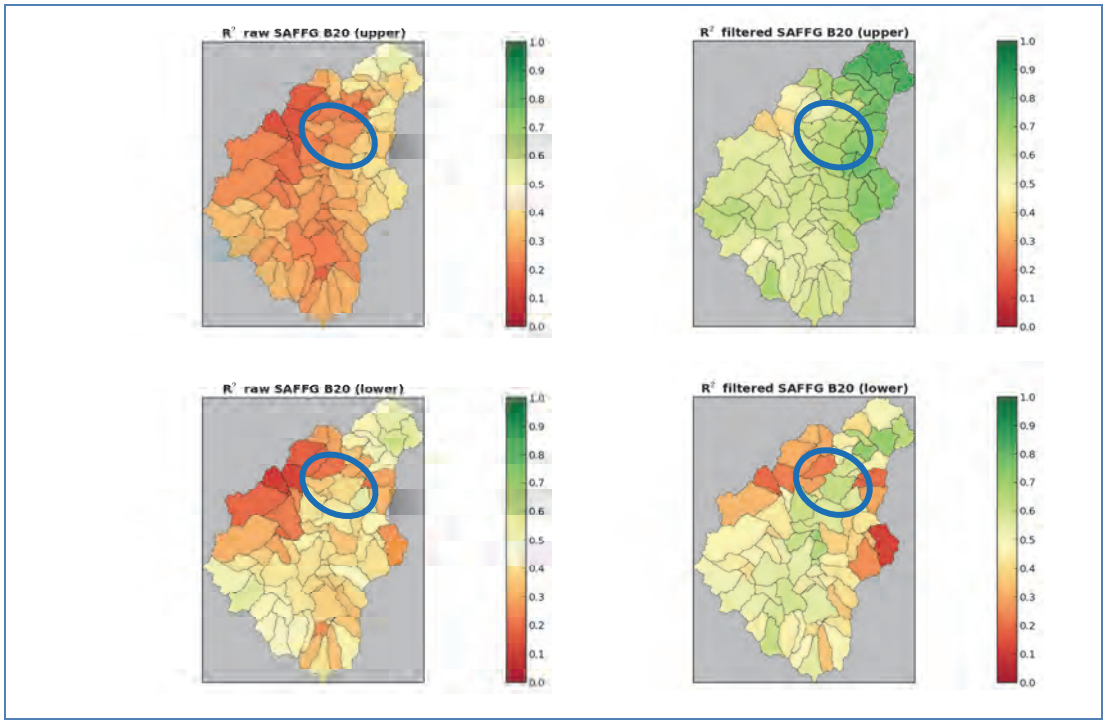

Figure 4.32: Summarized R2 for SAFFG catchments inside tertiary catchment B20. Top left: TRMM forced PyTOPKAPI compared with SAFFG upper soil layer. Top right: TRMM forced PyTOPKAPI compared with temporally filtered SAFFG upper soil layer. Bottom left: TRMM forced PyTOPKAPI compared with SAFFG lower soil layer. Bottom right: TRMM forced PyTOPKAPI compared with temporally filtered SAFFG lower soil layer.

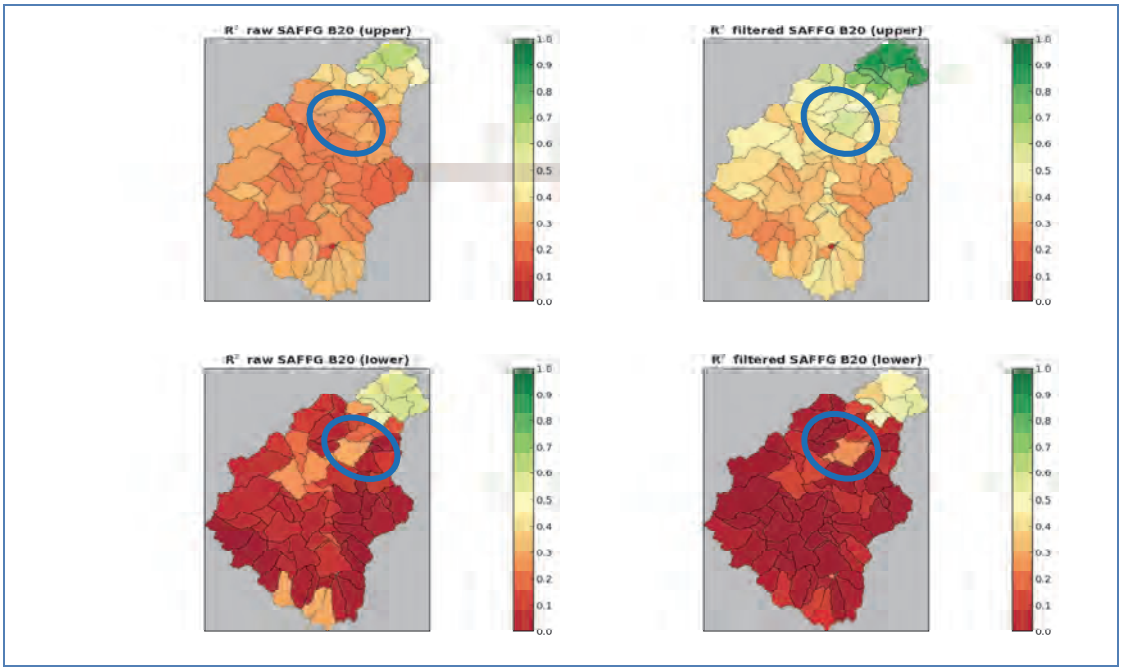

Figure 4.33: Summarized R2 for SAFFG catchments inside tertiary catchment B20. Top left: SAFFG forced PyTOPKAPI compared with SAFFG upper soil layer. Top right: SAFFG forced PyTOPKAPI compared with temporally filtered SAFFG upper soil layer. Bottom left: SAFFG forced PyTOPKAPI compared with SAFFG lower soil layer. Bottom right: SAFFG forced PyTOPKAPI compared with temporally filtered SAFFG lower soil layer.

4.6 SUMMARY

The following conclusions can be drawn from the model intercomparison study conducted under this section:

- The SAFFG rainfall is similar to the TRM 3B42RT, which forces PyTOPKAPI, but is about twice as heavy when averaged over a contemporaneous 21-month period.
- Filtering the upper layer (compared to the lower layer) of the SACRAMENTO model always gives an improvement in the R^2, when compared to the PyTOPKAPI estimates of Soil Moisture, irrespective of that model's forcing. Presumably, this is because the upper layer of the SAFFG model responds to the rainfall input more directly than the lower.
- The SAFFG lower and upper layers are more highly correlated when PyTOPKAPI is forced by TRMM than by the SAFFG input
- Given that the radar gives nearly twice the rain that TRMM offers, it is surprising that the SAFFG Soil Moisture estimates are so much lower than those of PyTOPKAPI. This observation applies to both the upper and lower layers of the SACRAMENTO model.
- Overall, the correlations are disappointingly low, mainly because of the explanation in the next paragraph.

A distinct plateau is observed in all of the time series of the SAFFG Soil Moisture traces, more obvious in the upper layer than the lower one. This is a worry, because when a soil store is above zero and there is no input, evapotranspiration and drainage do not switch off – that would be physically impossible. This paradox has been shared with the developers of SAFFG for possible explanation or modification if needed.

5. REMOTELY SENSED PRECIPITATION ESTIMATION

5.1 ENHANCING SATELLITE-BASED PRECIPITATION ESTIMATION

5.1.1 Introduction

Hourly rainfall estimates constitute a vital input to the SAFFG hydro-meteorological modelling system. They are used to calculate the soil moisture fraction compared to saturation in each of the small river basins in the SAFFG modelling system. The accuracy and quality of the rainfall estimation has a significant impact on the quality of the flash flood guidance derived by the modelling system. On the spatial scale of the SAFFG basins, sufficient rainfall estimation coverage can only be reached by remote sensing systems such as radar and satellite. However, these techniques are indirect measurements of rainfall and are highly sensitive to location and weather systems.

Satellite precipitation estimates (SPE) offer an excellent way to compensate for some of the limitations of other sources of quantitative precipitation information. SPE should not be considered as a replacement for radar estimates and gauges but as a complement (Scofield and Kuligowski, 2003). The National Environmental Satellite, Data and Information Service (NESDIS) developed an automated SPE algorithm for high-intensity rainfall called the Autoestimator (AE). The original AE, developed by Vicente *et al.* (1998), computes rain rates from 10.7 µm brightness temperatures based on a curve that was derived from more than 6000 collocated radar and satellite pixels. The dependence of the initial AE on radar was a significant problem, because one of the advertised strengths of satellite QPE (Quantitative Precipitation Estimation) is its usefulness in regions for which radar and/or rain gauge coverage is unavailable. Another version of the AE, called the Hydroestimator (HE) has been developed which can be used outside regions of radar coverage without compromising accuracy. The HE is mainly dependent on temperature (the higher the cloud, the colder the temperature and the greater the rain rate). Despite the simplicity of this precipitation estimation algorithm, it is still used in many countries around the world. During September 2007 a local version of the Hydroestimator was installed and tested at the South African Weather Service using numerical weather prediction output from the local version of the Unified Model and has been running operationally ever since.

One of the weak points of the HE is that it is known to overestimate precipitation. In this study, the bias of the HE was estimated using two years of data compared to the rain gauges. Another disadvantage of the HE is that it is mainly aimed at estimation of convective precipitation and it often misses stratiform rain events where the cloud tops are not so high. The bias corrected stratiform precipitation field from the Unified Model was used in combination with the bias-corrected HE field to supply the SAFFG with more comprehensive precipitation estimation to cover not only the convective events, but also the stratiform events more accurately.

5.1.2 Initial developments

5.1.2.1 Bias correction of the HE

Data from the HE are available since January 2008. The HE output from January 2008 until December 2009 was used to determine the average area ratio between the HE and the rain gauges in 0.5 x 0.5

degree grid boxes. Since this is a very short “climate” on which to base findings, it was decided to divide the data into six-month periods instead of individual months for all bias correction calculations. It was clear that the months from November to April and May to October, respectively, had similar ratios in the summer rainfall region and thus November to April will be termed the “summer” months and May to October will be termed the “winter” months.

In Figure 5.1, the two-year rainfall total estimated by HE over the country for the winter months is shown in a) and for comparison, the two-year rain gauge total is shown in b). Figure 5.2 is similar for the summer months. The area average of the ratio (HE to gauge) for the summer months (November to April) is 1.3 and the area average for the winter months (May to October) is 2.1. The HE is thus overestimating by a factor 1.3 in summer and a factor of 2.1 in winter. Using the data of these two years, it seems that if 75% (~1/1.3) scaling of the HE is used in summer months and 50% (~1/2.1) in winter months, the HE totals and rain gauge totals might be more aligned.

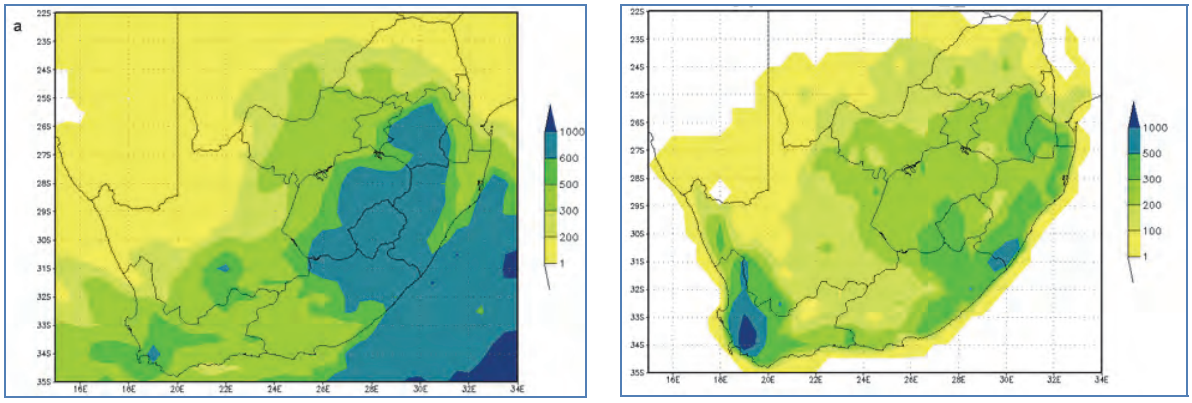

(a) **(b)**

Figure 5.1: HE winter rainfall for 2008 and 2009 (a) and rainfall measured by the gauges in the winters of 2008 and 2009 (b).

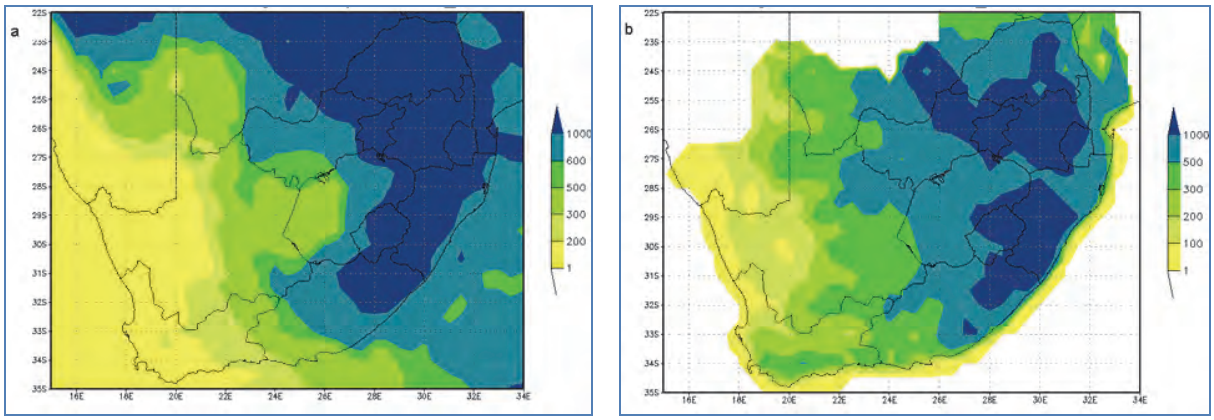

(a) **(b)**

Figure 5.2: HE summer rainfall for 2008 and 2009 (a) and rainfall measured by the gauges in the summers of 2008 and 2009 (b).

5.1.2.2 Bias correction of the stratiform rainfall field from the UM

The bias correction of the stratiform rainfall field provided by the Unified Model can be achieved using the rain rate of the automatic rain gauges and attempting to identify those periods in which the rain rate approximates that expected from stratiform rainfall. Unfortunately, there are not yet enough of these gauges operational over the country to make an impact.

An alternative solution is to use the ratio of the UM stratiform field to the UM total rainfall field to estimate the percentage of the observed rainfall that can be attributed to stratiform rainfall. Figure 5.3 shows this ratio for the months from May to October and November to April. This was calculated using the hourly UM derived rainfall fields from January 2008 to December 2009. It is evident that the frontal systems contribute more to stratiform rainfall during the winter months in the south-western parts of the country. During the summer months stratiform rainfall also occurs along the eastern and north-eastern escarpment of the country.

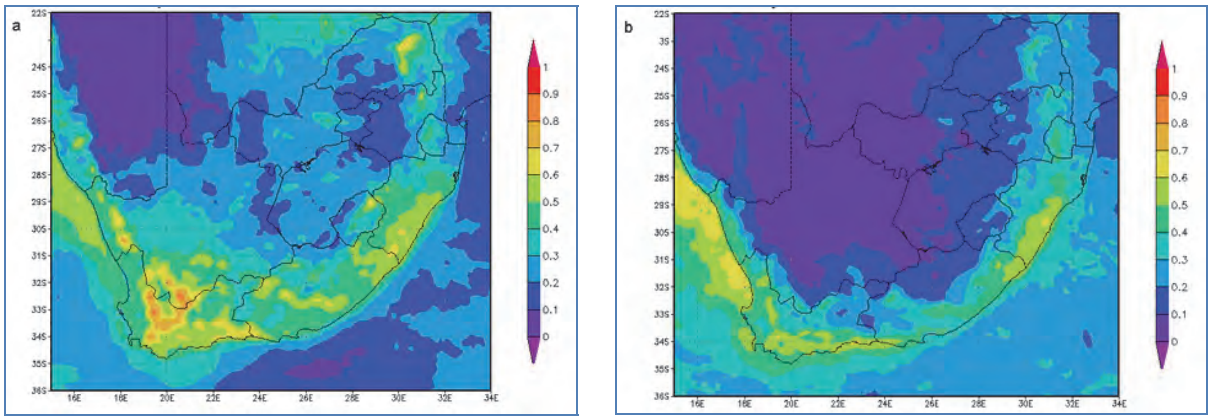

(a) **(b)**

Figure 5.3: Ratio of UM stratiform rainfall divided by UM Total rainfall (a) for winter months and (b) for summer months, during 2008 and 2009.

If these winter and summer ratios are applied to the available rain gauge totals for the winters and summers of the same two year period, a pseudo stratiform observation can be calculated for winter (Figure 5.4a) and summer (Figure 5.4b). Figure 5.5 shows the UM stratiform fields for winter (a) and summer (b). Comparing Figures 5.4 and 5.5 it is evident that the precipitation field provided by the model also overestimates the rainfall measured by gauges, but less so than the HE. Calculating the ratio of the UM stratiform field over this pseudo stratiform observation in areas where more than 150 mm were recorded in this two years period (i.e. in regions where stratiform rainfall makes a significant contribution), provides a bias-correction for the UM stratiform field of 1.25 (~80%) for winter months and 1.4 (~70%) for summer months.

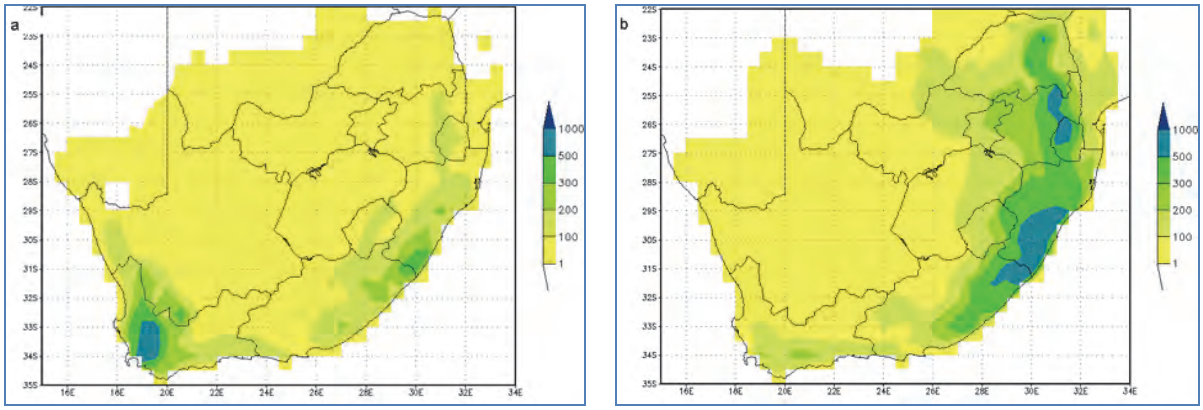

(a) **(b)**

Figure 5.4: Pseudo stratiform rainfall from gauges for winter months (a) and summer months (b) for 2008 and 2009.

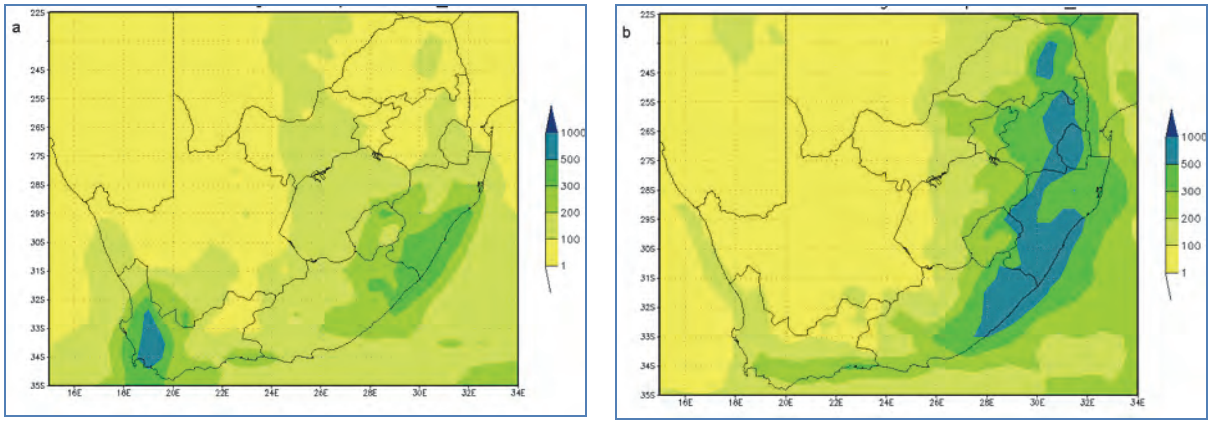

(a) **(b)**

Figure 5.5: UM stratiform rainfall for winter months (a) and summer months (b) for 2008 and 2009.

5.1.2.3 Combining the bias corrected HE and UM stratiform fields into a new precipitation field

The maximum value of either the bias-corrected HE or the bias-corrected UM stratiform rainfall field is used to compute a new rainfall field for each grid box. The maximum of the two values is used to ensure that the extreme values captured by either rainfall mechanism are not missed in areas where both rainfall types occur during a given period. It should be remembered that the HE is primarily designed for cold cloud top convective rainfall although it sometimes captures a small fraction of the stratiform rainfall that are associated with cold cloud tops. This combined product presents a rainfall field, which reflects both bias corrected convective as well as bias corrected stratiform rainfall. This calculation can be done every 15 minutes (when a new HE field becomes available) and the hourly accumulation files of these individual 15-minute files make it useful for the SAFFG system. This combination product will be referred to as COMB in the rest of the text.

5.1.2.4 Method of evaluation of the new precipitation product

The IPWG uses 0.25°X0.25° grid boxes for evaluation purposes and evaluates on an hourly basis. Due to the relative shortage of rain gauges in South Africa compared to the USA, it was decided to accumulate the hourly fields into 24-hour totals for each day using 0.5°x0.5° grid boxes. Daily rainfall totals of the HE and the COMB could then be compared to the daily rainfall totals from the rain gauges. The 24-hour totals were calculated from 0600Z to 0600Z each day. Rain gauges are only available inside the borders of South Africa. A mask was thus created to outline the country to ensure that only values of HE or the combined precipitation product were taken into account where it could be evaluated against rain gauge measurements.

Similar to the approach followed by the IPWG (http://www.isac.cnr.it/~ipwg/) the daily rainfall fields were evaluated using the contingency table approach, calculating the traditional scores such as probability of detection, false alarm ratio, Hanssen-Kuipers score (also known as True Skill Statistic, or Pierces' skill score), Equitable threat score and Heidke Skill Score (Wilks, 2005). The correlation coefficient, mean absolute error and number of points with and without rain were also calculated. All the statistical calculations were done setting rainfall of less than 1 mm per day to no rain and anything more than 1 mm implying rainfall.

5.1.3 New developments

Following analysis of the hybrid precipitation product described in Section 5.1.2, which combines the stratiform rainfall field from the local version of the UM and the Hydroestimator to produce a real time precipitation estimation which can capture both stratiform and convective rainfall events, improvements were made to the system during 2012/13. This resulted in an improved satellite QPE to be used in the SAFFG hydro-meteorological modelling system.

A new way of combining the HE and UMS fields was proposed, based on the results obtained with five years of data from 2008 to 2012, to calculate a 0.25° × 0.25° grid box-based bias ratio for the HE and UMS precipitation fields on a monthly basis. The new methodology takes into account that the HE and UMS fields can overestimate as well as underestimate the rainfall intensity and that this bias correction can change temporally (for different months) as well as spatially.

Sixty cases from 2010, five cases in each month of the year, were used to compare the uncorrected HE, the old combination (Old Comb) and the new combination (New Comb) of the HE and UMS fields to the rainfall observed by the rain gauges. The monthly averages of the HSS indicate that the New Comb is more accurate than the Old Comb as well as better than the uncorrected HE for the 1 mm, 10 mm and 20 mm thresholds in most months. The monthly averages of the Bias Score show that the New Comb improves the Bias Score for the majority of the months. The biggest improvement is in the winter months when stratiform rainfall events influence the coastal areas of the country.

Five daily cases were considered in more detail and in these the advantage of using monthly, grid box-based bias ratios is evident since the contributions of the UMS and HE were allowed to vary spatially. It shows that the New Comb can provide a more accurate and representative rainfall field than the uncorrected HE and the Old Comb on a daily basis.

Remotely sensed rainfall estimation is a valuable tool for forecasters in order to nowcast precipitation. The combination of rainfall fields from HE and UMS presented here can be calculated

on an hourly basis and will provide a comprehensive rainfall field needed for the nowcasting of precipitation. The SAFFG system requires input of rainfall observations at time scales of less than 6 h in order to provide a nowcast of such events. Rainfall fields from rain gauges, radar rainfall as well as satellite rainfall are used as input to the SAFFG on an hourly, 3-hourly and 6-hourly basis. It would have been good to validate the new combination product on this shorter time scale, but unfortunately, not enough observation data are available for such a validation. Given the improvement shown on a daily basis, it is suggested that the combination of HE and UMS rainfall field should benefit the nowcasting of precipitation, as well as enhance input to the SAFFG system, if it is used on an hourly, 3-hourly and 6-hourly basis as a supplement to input from radar rainfall and rain gauge data.

5.1.3.1 Background to the new methodology

In South Africa both convective and stratiform precipitation events play a role in different seasons and different areas of the country. Experience has shown that the Unified Model is most useful for synoptic-scale driven systems and the associated stratiform rainfall fields. The HE tends to be best for convective events and does not capture the stratiform events along the coast lines well. An attempt to improve the satellite-based rainfall as input to the SAFFG was made in 2011 by de Coning and Poolman (2011) by combining the HE with the stratiform rainfall field by the Unified Model (UMS). Using a combination of the HE and the UMS, a more comprehensive rainfall field was created.

5.1.3.2 Short-Comings and Improvements to Previous Methodology

In this subsection an improved methodology is described to combine the HE with the UMS in order to enhance the input to the South African Flash Flood Guidance system, especially along the coastline where wintertime stratiform rainfall events are often not captured by the HE. The new method will aim to address the shortcomings of the previous effort and results will be shown to demonstrate the improvement in validation scores using sixty cases during the course of 2010.

In the initial attempt to improve the satellite-based rainfall as input to the SAFFG, it was shown that a combination of the HE and UMS (both bias corrected against the available rain gauges) performed better against rain gauge measurements than the HE on its own. This was particularly beneficial in cases when stratiform rainfall played a role along the coastlines of South Africa during the winter months.

Despite the improvements achieved by the combination of satellite and NWP rainfall fields, the method had its shortcomings:

(a) The initial data set only focused on two years (2008 and 2009) for which the required data were available for the calculation of the biases.

(b) An area average of the biases was calculated over the entire country, using a 0.5° × 0.5° grid box resolution.

(c) For both rainfall fields, the area average bias corrections indicated that the HE and UMS always overestimate and thus the intensity of rainfall was always diminished in the combined product. However, applying an area average bias correction ignores the fact

that the HE and the UMS fields overestimate in some regions and/or times of the year and underestimates in other regions and/or times of the year.

(d) The data were divided into two 6-month seasons, November to April was treated as "summer", May to October was treated as "winter", and the same bias correction was applied for the entire area for these two seasons.

As more data became available, new approaches were considered, which were applied in this study:

(a) Five years of data (2008 to 2012) from the HE, the UMS and rain gauges were processed in order to establish whether a new, more realistic approach to an optimal satellite-based precipitation field, in combination with the NWP rainfall field, could be obtained.

(b) The calculations were done on a monthly basis, instead of "seasonal"—in other words the monthly totals of rainfall from the different sources were compared to one another for the five year period. For the bias ratio of the HE, the total HE for each month was simply divided by the rainfall as measured by the rain gauges in that month for each grid box. A positive (negative) bias ratio indicated that the HE overestimated (underestimated) the rainfall.

(c) The resolution was improved to 0.25° × 0.25° grid boxes (similar to the IPWG validation methodology) for all calculations. This would imply that spatial variations in the bias patterns (over- and under-estimations) could be taken into account.

5.1.4 Results

5.1.4.1 Bias Ratio corrections for different months

The bias ratios of the HE and UMS for January and July, respectively, are shown in Figure 5.6.

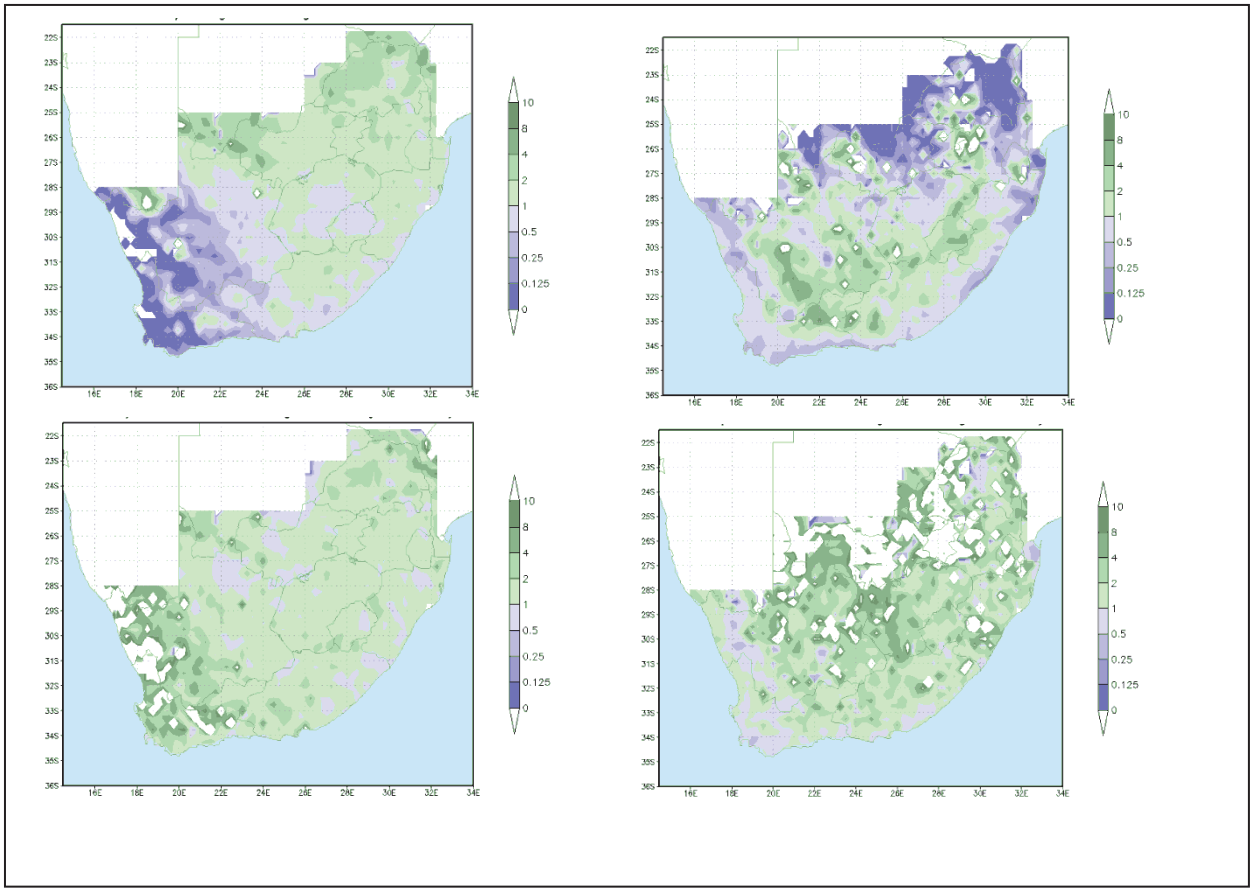

Figure 5.6. Bias ratios for HE in January (top left) and July (top right). Bias ratios for UMS in January (bottom left) and July (bottom right). Purple colours indicate underestimation and green colours indicate overestimation on an exponential scale.

From Figure 5.6 it is clear that the HE underestimates the rainfall in the south-western parts of the country in January (top left), but overestimates the rainfall over the north-eastern half of the country. In the summer months the dominant cause for rainfall is convection. In July (top right) overestimation occurs over the southern interior of the country and underestimation along the coastlines as well as in the far north-eastern parts. It was previously shown that overestimation often occurs in winter months when cold fronts approach the country in combination with a deep upper air trough, which causes widespread rainfall over the south-western interior of the country. These cloud systems often reach high altitudes and consequently the very cold cloud top temperatures cause the HE to overestimate. Stratiform rainfall along the coastlines, which often accompanies the passage of shallow cold fronts and ridging surface high-pressure systems, is often missed or underestimated by the HE. Also evident from Figure 5.6 is that the UMS generally overestimates slightly in January (bottom left) as well as in July (bottom right). However, in July underestimation also occurs along the southern coast lines.

5.1.4.2 Combination of the HE and UMS fields

Combining the two rainfall fields (HE and UMS) and their respective monthly bias corrections to create a more comprehensive rainfall pattern, was accomplished in the following manner:

- If the bias ratio was in the range of 0.125 and 8, the bias correction was applied to the rainfall amount of the HE or UMS fields, respectively.
- If the bias correction was less than 0.125 or more than 8, then four surrounding grid boxes were used to calculate an average of the bias ratio, if this average bias ratio was within the 0.125 to 8 range, the four-grid-boxes-average bias ratio was applied to the respective HE or UMS rainfall amounts.
- If neither of the two previous calculations were within the 0.125 to 8 range, no bias correction was applied to the HE or UMS and the original rainfall value was kept unchanged.

The final combination field was simply the maximum value of the bias corrected HE or UMS fields. In this way, the combined precipitation field includes the convective rainfall events (best covered by the HE) as well as the stratiform rainfall events (best covered by the UMS) and extreme values are not missed.

5.1.4.3 Comparing the Old Combination Methodology to the Proposed New Combination Methodology

In order to test whether the new methodology (using grid box-based, monthly bias ratios to combine the HE and UMS fields) would improve on (a) the HE without any corrections and (b) the previous methodology (using an area average bias ratio for two “seasons”), sixty cases were selected during 2010, five cases from each month of the year. Five days from each month were chosen when rainfall of different intensities was recorded over a significant area across the country.

Cases from all the months were chosen to represent all the rain producing systems—convective as well as stratiform in nature. For each of these days, the HE, the new combination (New Comb) and the old combination (Old Comb) were statistically evaluated against the 24 h rain gauge totals. Daily totals were used for the validation purposes due to a lack of enough automatic rainfall reports to evaluate hourly rainfall. Daily thresholds of 1 mm, 10 mm and 20 mm were also chosen to evaluate the skill of the methods to estimate rainfall intensity.

In Figure 5.7 the HSS of the five cases per month was used to calculate an average for each month and for the three different thresholds. Figure 5.7(top) a shows the skill of the different methods using 1 mm threshold. Using the HE without any bias correction (blue bars) has the smallest HSS in all the months, the Old Comb (red bars) show some improvement while the New Comb (green bars) performed the best in all the months. The only exceptions are July and August, where New Comb is slightly worse than Old Comb. From Figure 5.7 (middle) it is clear that New Comb also outperforms the HE and Old Comb for the 10 mm threshold in most months. In Figure 5.7 (bottom) the indication is that the HSS of New Comb is better than the others for the 20 mm threshold in all the months.

A significant improvement is noted in the months of May to September, which are the months when the frontal passages along the coastlines of the country are accompanied by stratiform rainfall. These are the cases that the HE alone could have missed and that Old Comb (using seasonal, area averaged bias ratios) could have underestimated. The New Comb (using grid box-based bias ratios) shows that both the HE and UMS are underestimating in these regions and should be corrected upwards. The effect of this approach is that rainfall along the coastal areas is augmented.

It was shown that New Comb improves the Bias score (gets it closer to 1) in almost all the months for 1 mm and 10 mm thresholds. In general, the New Comb improves the bias score, *i.e.*, lowers it if it is more than 1 and augments it when it is less than 1 in most months.

Figure 5.8 summarizes the HSS for all the cases and it is clear that the New Comb outperforms the other methods. Table 5.1 summarizes the percentages cases for which the HSS of the New Comb was better than or the same as the Old Comb and the uncorrected HE for the different thresholds.

Figure 5.7: Heidke Skill Scores for (top) 1 mm threshold, (middle) 10 mm threshold and (bottom) 20 mm threshold for all 60 cases (5 cases per month). HSS of the HE is in blue, for Old Comb in red and for New Comb in green

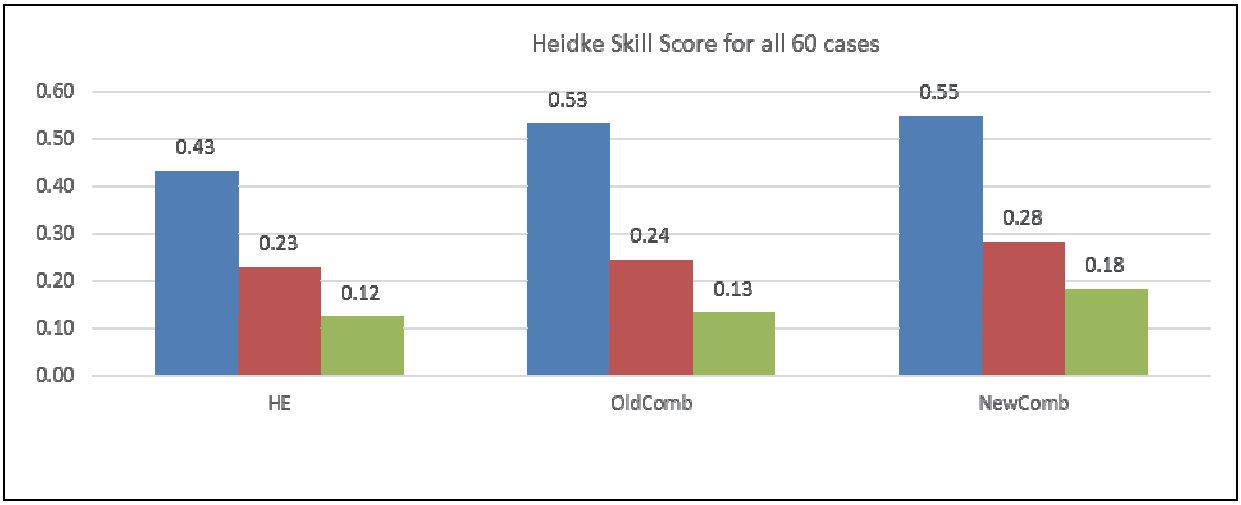

Figure 5.8: HSS for all 60 cases for 1 mm, 10 mm and 20 mm thresholds

Table 5.1: Summary of the percentages cases for which the HSS of the New Comb is the same as or exceeds the HSS of the other two methods.

	New Comb Has a Better HSS than Old Comb	New Comb Has a HSS the Same as Old Comb	New Comb Has a Better HSS than Uncorrected HE
1 mm threshold	67%	13%	93%
10 mm threshold	54%	25%	51%
20 mm threshold	48%	41%	53%

5.1.5 Summary of results

The HE is based on a single channel (IR10.8) from MSG and mainly uses the temperature of cloud tops to estimate precipitation rate every 15 minutes. Although improvements have been incorporated into the HE to avoid the possibility of getting rain from high-level Cirrus clouds, but to include lower clouds, which can cause precipitation, it is still considered to be mainly useful for convective precipitation. The HE has been available in southern Africa since the end of 2007. Shortcomings of the HE include the overestimation of precipitation amounts and the underestimation or missing of some stratiform events.

For any flood of flash flood warning system such as the SAFFG hourly accumulations of both radar rainfall and satellite based rainfall should be used. Unfortunately, radars do not cover the entire South Africa and are very scarce in the rest of Africa. The quality of satellite based precipitation estimations for South and southern Africa are crucial to ensure the accuracy of flood and/or flash flood warnings. In order to provide a more accurate and more comprehensive satellite precipitation based input field, a new combination product was developed. The new product aims to combine the strengths of the HE and the stratiform precipitation field from the Unified Model. The respective bias corrections of the HE as well as the UM stratiform field were determined and these bias corrected products were combined into a new precipitation estimation field.

Subsequently, a new way of combining the HE and UMS fields was proposed, based on the results obtained with five years of data from 2008 to 2012 to calculate a 0.25° × 0.25° grid box-based bias ratio for the HE and UMS precipitation fields, on a monthly basis. The new methodology takes into account that the HE and UMS fields can overestimate as well as underestimate the rainfall intensity and that this bias correction can change temporally (for different months) as well as spatially.

Sixty cases from 2010, five cases in each month of the year, were used to compare the uncorrected HE, the old combination (Old Comb) and the new combination (New Comb) of the HE and UMS fields to the rainfall observed by the rain gauges. The monthly averages of the HSS indicate that the New Comb is more accurate than the Old Comb as well as better than the uncorrected HE for the 1 mm, 10 mm as well as the 20 mm thresholds in most months. The monthly averages of the Bias Score show that the New Comb improves the Bias Score for the majority of the months. The biggest improvement is in the winter months when stratiform rainfall events influence the coastal areas of the country.

Five daily cases were considered in more detail and in these the advantage of using monthly, grid box-based bias ratios is evident since the contributions of the UMS and HE were allowed to vary spatially. It is shown that the New Comb can provide a more accurate and representative rainfall field than the uncorrected HE and the Old Comb on a daily basis.

Remotely sensed rainfall estimation is a valuable tool for forecasters in order to nowcast precipitation. The combination of rainfall fields from HE and UMS presented here can be calculated on an hourly basis and will provide a comprehensive rainfall field needed for the nowcasting of precipitation. The SAFFG requires input of rainfall observations on time scales of less than 6 h in order to provide a nowcast of such events. Rainfall fields from rain gauges, radar rainfall as well as satellite rainfall are used as input to the SAFFG on an hourly, 3-hourly and 6-hourly basis. It would have been ideal to validate the new combination product on this shorter time scale, but unfortunately not enough observation data are available for such a validation. Given the improvement shown on a daily basis, it is believed that the combination of HE and UMS rainfall field should benefit the nowcasting of precipitation as well as enhance input to the SAFFG system if it is used on an hourly, 3-hourly and 6-hourly basis as a supplement to input from radar rainfall and rain gauge data.

5.2 MULTIPLE SATELLITE PRECIPITATION ESTIMATION

5.2.1 Introduction

The South African Weather Service issues operational forecasts on a regular basis. Satellite precipitation estimates (SPE) offer an excellent way to compensate for some of the limitations of other rainfall data sources such as point measurements by gauges or radar rainfall. In an operational environment where forecasters have to make decisions for nowcasting purposes, all information needs to be updated as regularly as possible. Although methods exist to estimate precipitation very accurately by low-level orbiting satellites, the drawback is that the information is only available during an overpass, which can be two to four times per day. Geostationary satellites such as Meteosat Second Generation (MSG) provide updated information every 15 minutes and offer a full view of the African continent. Satellite based Quantitative Precipitation Estimation (QPE) from MSG is thus ideally suited for nowcasting purposes, although less accurate than the estimates from polar

orbiting satellites. For nowcasting purposes in an operational weather office, SPE based on geostationary satellites are best suited in order to have updates on a regular basis.

5.2.1.2 Convective Rain Rate (CRR)

Another geostationary satellite based algorithm used operationally (mostly in European countries) is the Convective Rainfall Rate product, which was developed by the Nowcasting and Very Short Range Forecasting SAF (or SAFNWC). Compared to the single channel HE algorithm, the CRR makes use of either two (IR108 and WV062) or three MSG channels (including VIS006 during day light hours).

As part of another WRC funded project (K5-2235/1), the SAFNWC software was installed at SAWS during 2013 for running case studies with another of the SAFNWC products. This implies using the code as supplied by the SAFNWC, but with the local version of the Unified Model, instead of ECMWF as input to the algorithm. Testing of the CRR could thus be done using the updated version of the software (original coded C-programs).

To take into account the influence of environmental and orographic effects on the precipitation distribution, some corrections can be applied to the basic CRR value, based on input from numerical weather prediction models. The possible corrections are:

- The moisture correction;
- The cloud top growth/decaying rates or evolution correction;
- The cloud top temperature gradient correction;
- The orographic correction.

At the end of the process CRR product produces information on the instantaneous rain rate in mm/h in each pixel of the image. The target of this output can be used to compute the hourly accumulations in mm.

The local version of the UM does not have the required 925 hPa level and thus the abovementioned moisture correction could not be utilized. However, from personal communication with SAFNWC it is clear that this could adversely affect the rainfall rate. In the case studies which were conducted, the moisture correction is thus not done. If/when a newer version of the UM is implemented in SAWS, the 925 hPa level will be included and this should improve of the product to some extent.

5.2.2 Methodology

For each case study, daily (24-hour) total rainfall was used, from 0600 UTC to 0600 UTC. For the South African cases, the validation was done against rain gauge data. For the southern African cases, there is not enough rain gauge data available to make validation meaningful, thus the rainfall data from TRMM was used.

All the fields from the CRR, HE, rain gauges over South Africa as well as TRMM were interpolated to a 0.25°X0.25° grid resolution using a Cressman interpolation. A mask was applied to the field to exclude QPE rainfall outside the boundaries of South Africa where rain gauges are not available.

To evaluate the satellite QPE fields against rain gauge or TRMM data in a quantitative manner, a number of contingency table scores were calculated for three thresholds – 1 mm, 10 mm and 20 mm. These scores are listed in Table 5.2. In addition to the contingency table scores, the Correlation

Coefficient, Root Mean Square Error (RMSE), Mean Absolute Error (MAE) and Bias for the three thresholds were also calculated.

5.2.3 Results over South Africa

Fourteen different cases were chosen to compare the CRR and the HE against daily totals of the rain gauges. All the cases were summer cases. Both the CRR and HE algorithms are intended for convective rainfall events, but not for warm rainfall processes in lower clouds. Events, which are the result of cold fronts and occur in winter months, were thus not included in the study.

Table 5.2: Contingency table scores with their meanings, acronyms perfect score values.

Score	Acronym	Ideal score
Probability of Detection (What fraction of the observed yes events were correctly forecast?)	POD	1
False Alarm Ratio (What fraction of the predicted "yes" events did not occur?)	FARatio	0
False Alarm Rate or Probability of False Detection (What fraction of the observed "no" events were incorrectly forecast as "yes"?)	FARate	0
Hanssen Kuiper Score (How well did the forecast separate the "yes" events from the "no" events?)	HK	1
Equitable Threat Score (How well did the forecast "yes" events correspond to the observed "yes" events accounting for hits due to chance?)	ETS	1
Heidke Skill Score (What was the accuracy of the forecast relative to that of random chance?)	HSS	1
Threat Score (How well did the forecast "yes" events correspond to the observed "yes" events?	TS	1

Table 5.3: Case study dates and type of precipitation

Case date	Type of Convection
18 Nov 2013	Convective rainfall in Limpopo
19 Nov 2013	Widespread convective activity over central parts of SA
20 Nov 2013	Heavy falls over the NE parts of SA
21 Nov 2013	Convective rainfall over the NE parts of SA
9 Dec 2010	Light rain associated with convection over SA
10 Dec 2010	Light rain associated with convection with heavier falls in places
11 Dec 2010	Widespread convective activity with heavy falls in places
12 Jan 2010	Convection with heavier falls in some places
13 Jan 2010	Widespread convection
22 Jan 2010	Widespread convection with heavier falls in some places
26 Jan 2010	Heavy falls in many places
28 Jan 2010	Convective activity with heavier falls in Mpumalanga
23 Feb 2010	Widespread convection with heavier falls over the central interior
24 Feb 2010	Widespread convection with heavier falls over the central interior

5.2.3.1 Example: 19 November 2013

Figure 5.9 shows the rainfall distribution and intensity for the 24 hours for 19 November 2013 on a 0.25-degree resolution. Figures 5.10 and 5.11 show the contingency table scores for this case, using the 10 mm and 20 mm thresholds, respectively.

For this case, it is clear that the CRR performs better than the HE in most of the contingency table scores (Figures 5.10 and 5.11). However, the RMSE is bigger for CRR than HE. The Bias score for 1 mm is best with CRR, but for the 10 and 200 mm thresholds the HE is better (closer to 1). The scatterplots (not provided) show that the CRR might be underestimating in this case.

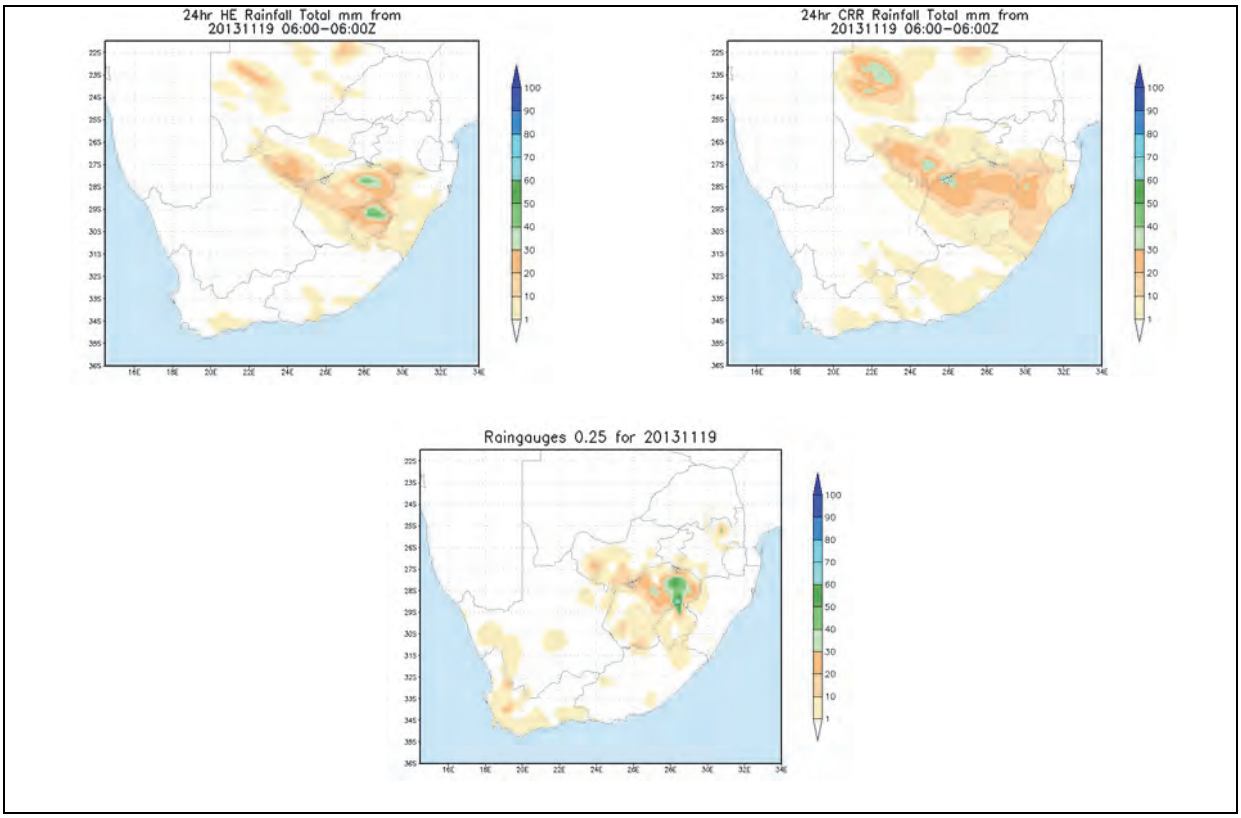

Figure 5.9: HE (top left), CRR (top right), rain gauge (bottom) daily totals for 19 Nov 2013.

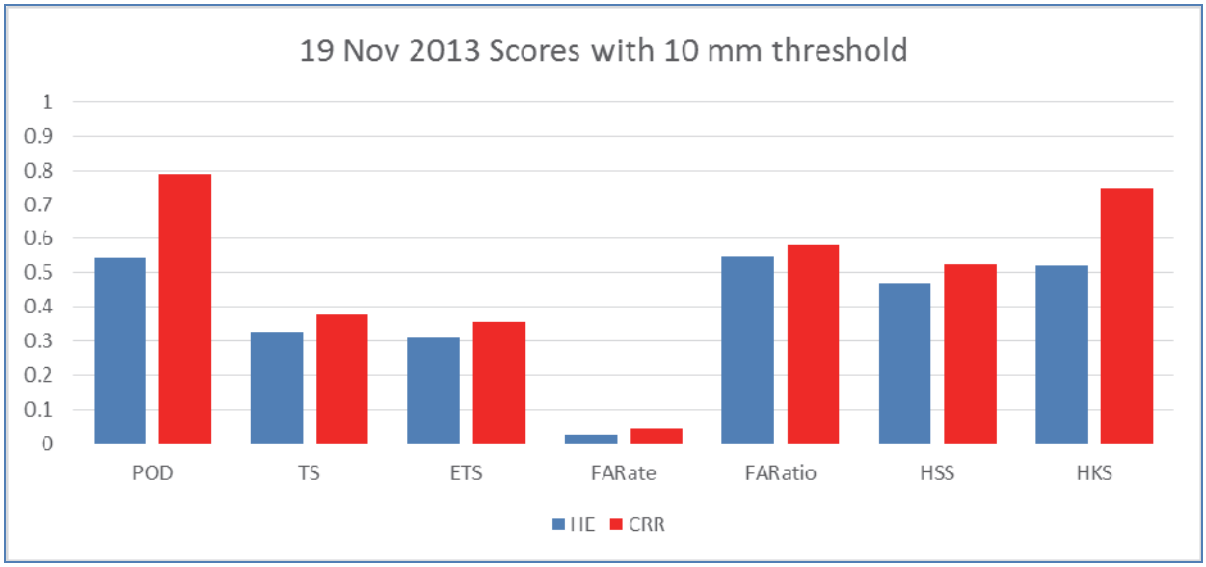

Figure 5.10: POD, TS, ETS, FARate, FARatio, HSS, HKS and Correlation coefficient for 19 Nov 2013 using a 10 mm threshold. HE is indicated in blue and CRR in red bars.

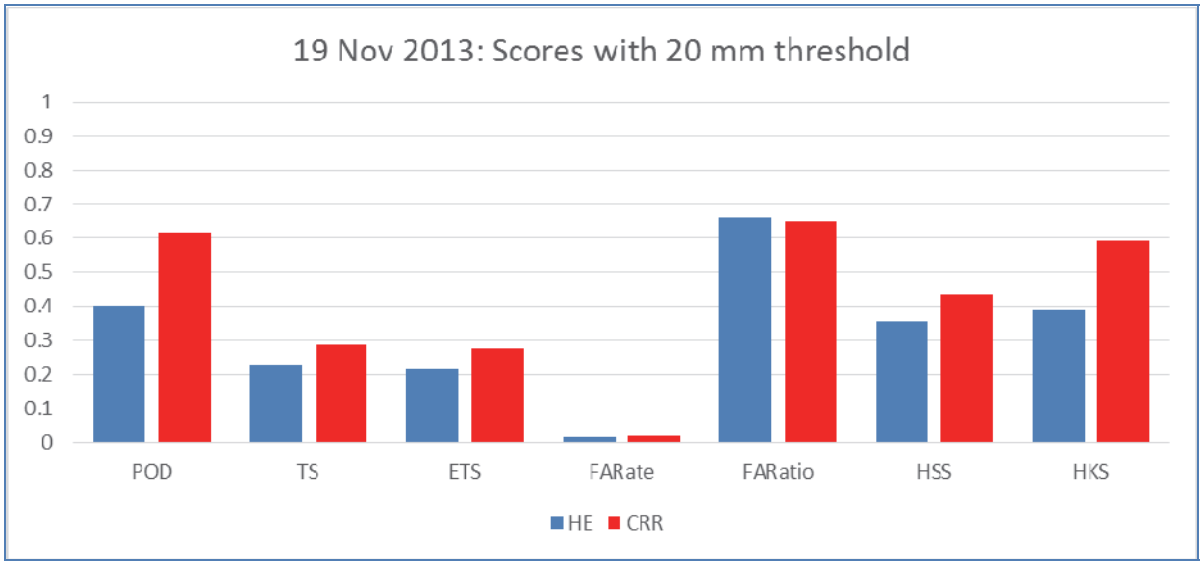

Figure 5.11: As Figure 5.10 but for 20 mm threshold

5.2.3.2 Example: 22 January 2010

In this case the HE outperformed the CRR in all the contingency table scores (Figure 5.13 and 5.14), but the RMSE and MAE of the CRR were smaller than the errors of the HE. The Bias score for 1 mm indicated that HE was the closest to 1 (best), but for the 10 and 20 mm thresholds it is clear that the HE was overestimating and the CRR underestimating. The scatterplots (not provided) indicate that the CRR might be underestimating, while the HE is overestimating.

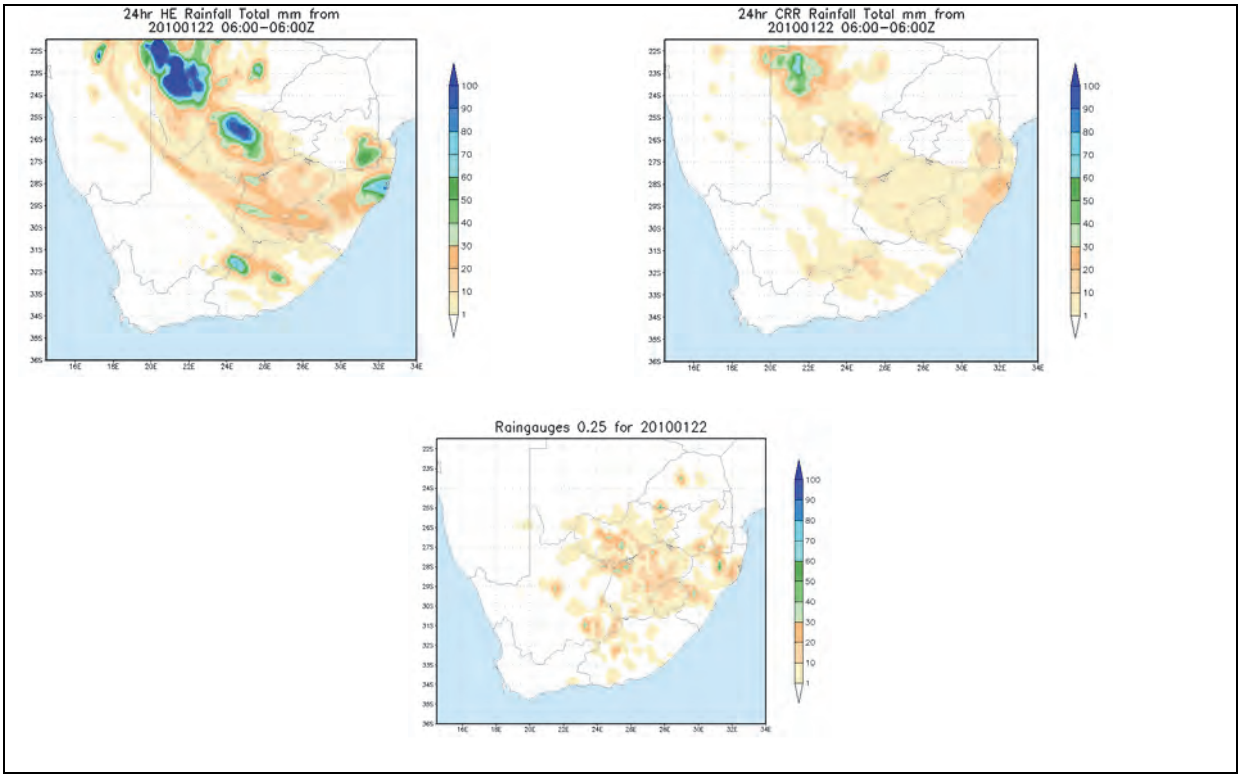

Figure 5.12: As Figure 5.9, but for 22 January 2010

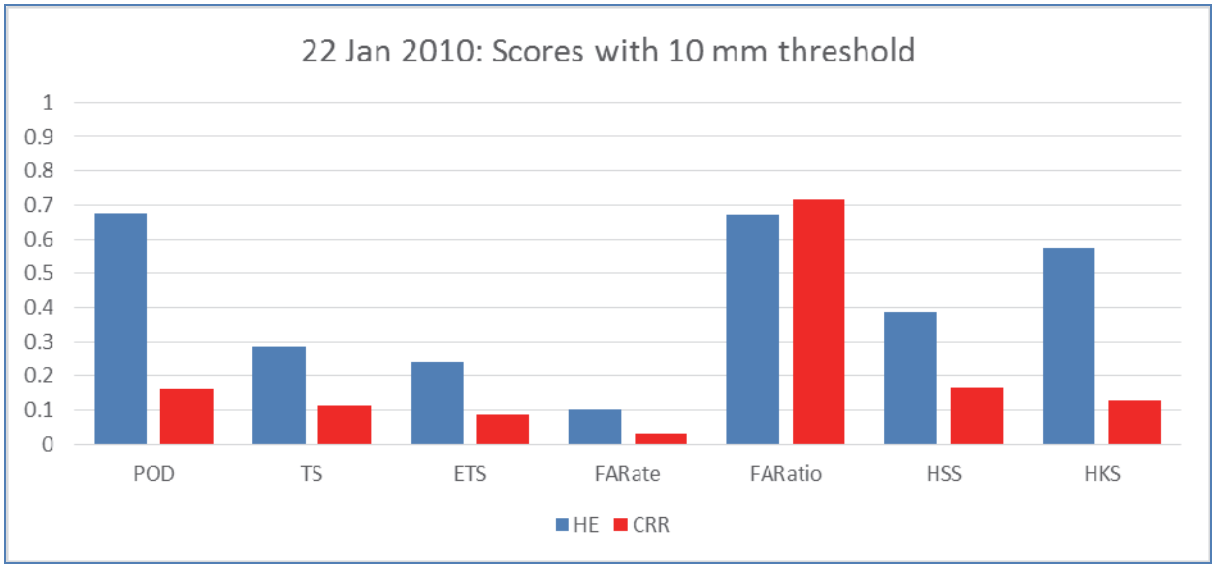

Figure 5.13: As Figure 5.10 but for 22 January 2010

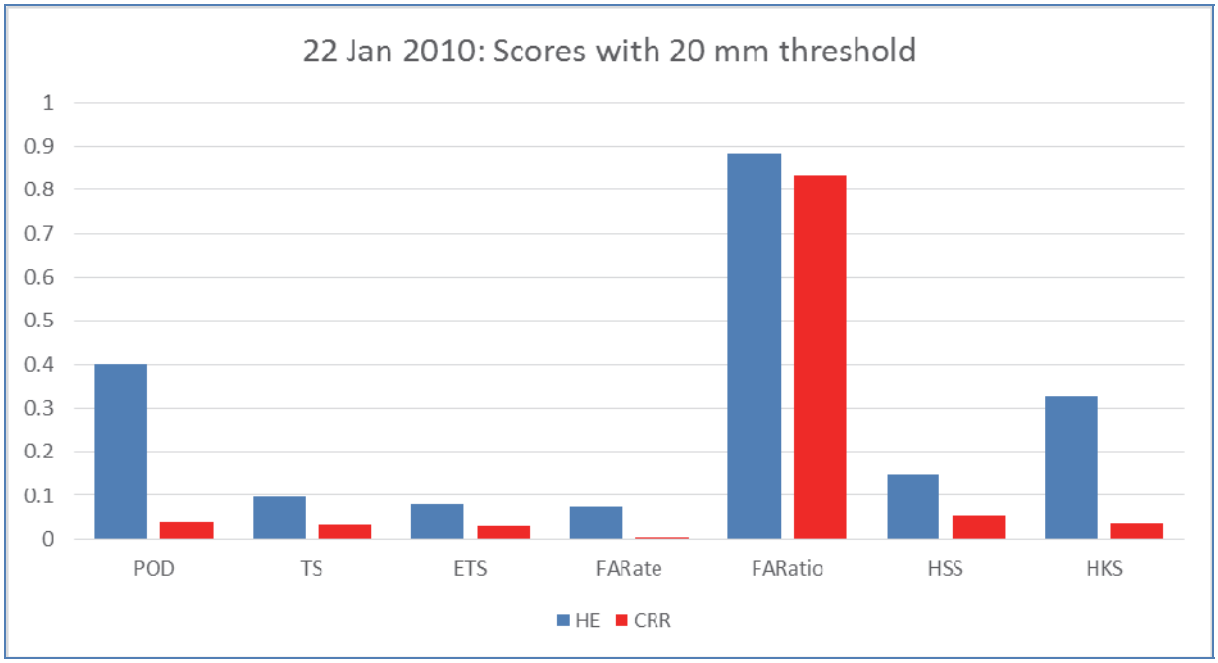

Figure 5.14: As Figure 5.11 but for 22 January 2010

5.2.3.3 Summary of all cases over South Africa

A summary of the scores of all fourteen cases done over the South African domain is shown in Figures 5.15-5.17. The HSS for the 1 mm threshold (Figure 5.15) is the best (blue), followed by the 10 mm (red) and 20 mm (green) thresholds. Although the CRR (dashed lines) are sometimes better than the HE (solid lines) for the relevant thresholds, this is not always the case.

The Correlation Coefficients for the CRR (light blue) is better than for the HE (darker blue) in ten of the fourteen cases. The RMSE and MAE of the CRR is smaller (better) than the HE in nine of the cases. The average scores of all fourteen cases indicated in Figures 5.18 and 5.19 indicate that in general, despite the fact that the CRR is not better than the HE in all cases, the CRR performs just as well or better than the HE on average. For the CRR the HSS for all thresholds are the same or better than those of the HE and the correlation coefficient better. The MAE and RMSE are smaller for CRR and the BIAS of the CRR is closer to one than the HE. The RMSE and MAE of the CRR are better/smaller than the HE. The Bias scores for all thresholds also indicate that the CRR is better.

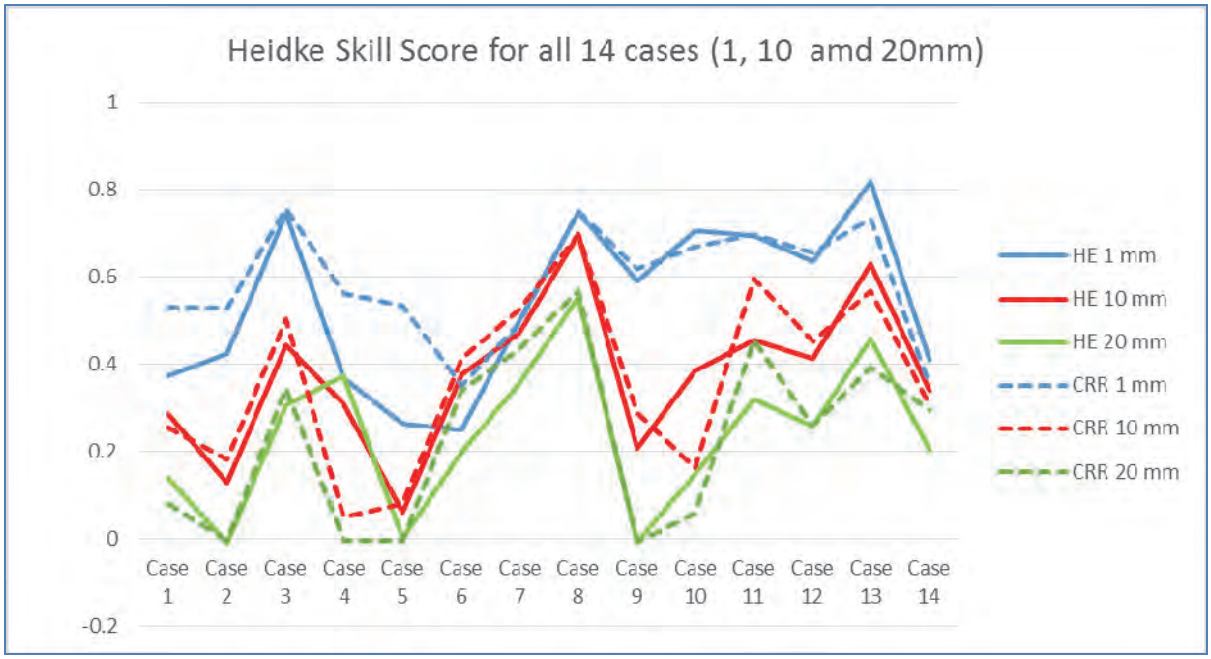

Figure 5.15: Heidke Skill Score for 1 (blue), 10 (red) and 20 (green) mm threshold for all 14 cases. HE in solid lines and CRR in dashed lines

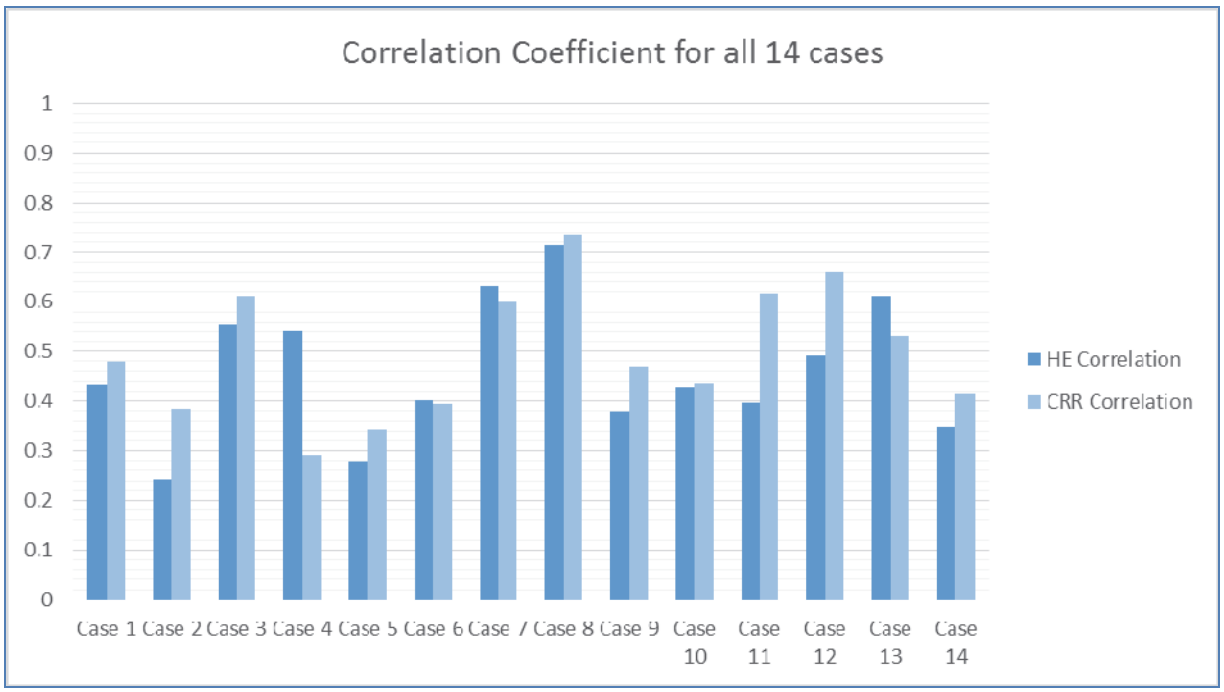

Figure 5.16: Correlation Coefficients for all 14 cases. HE in dark blue and CRR in light blue.

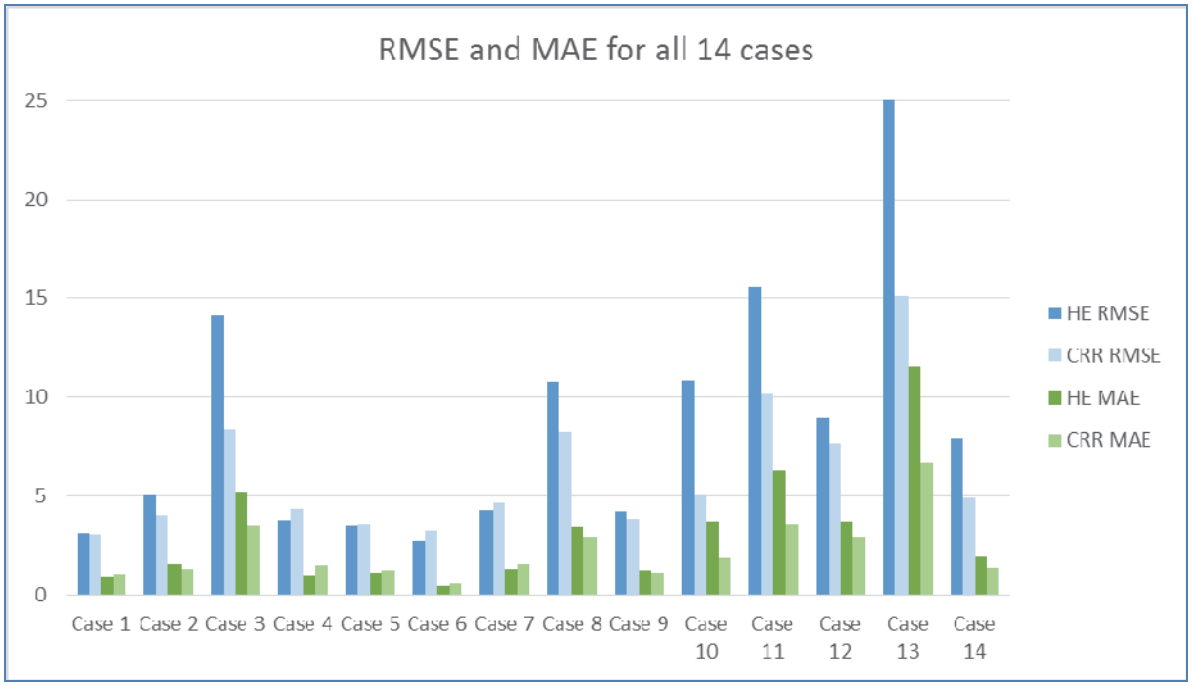

Figure 5.17: The RMSE (Blue) and MAE (Green) for HE (darker bar) and CRR (lighter bar) for all 14 cases.

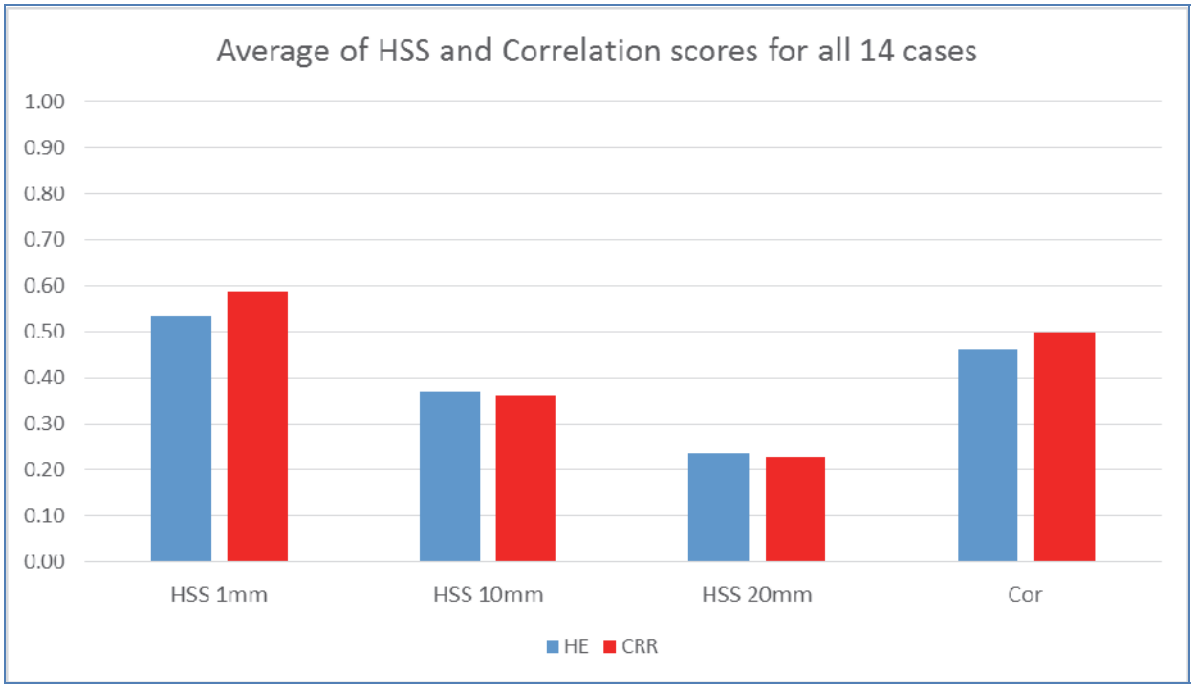

Figure 5.18: Average of the HSS and Correlation Coefficients for all 14 cases

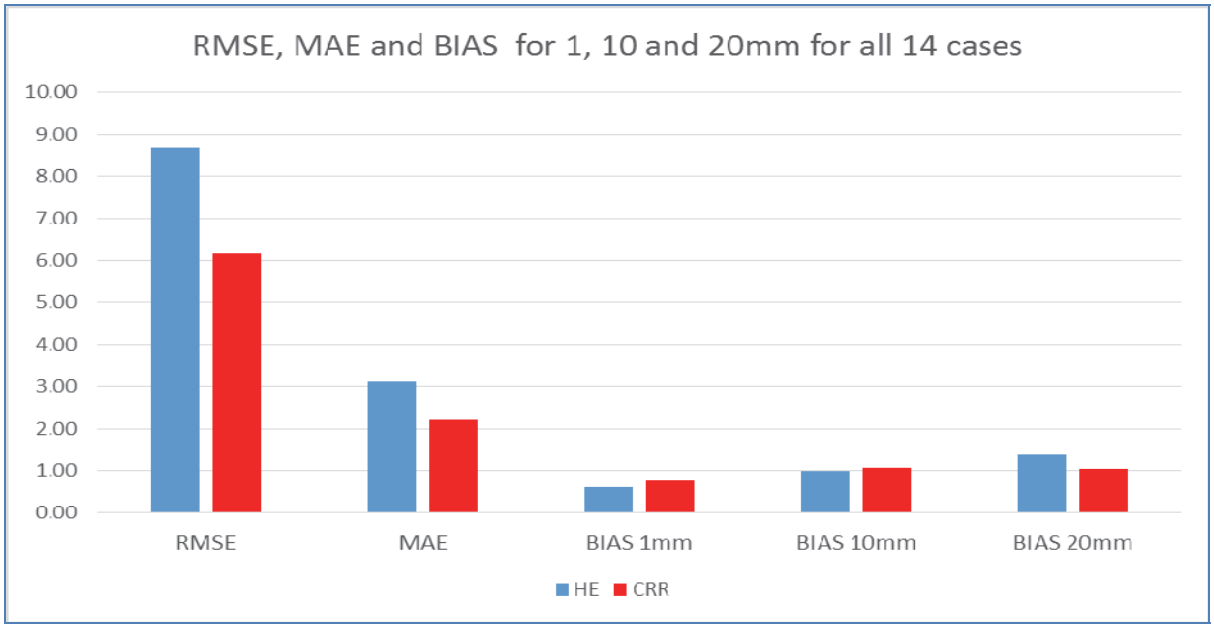

Figure 5.19: Average of the RMSE, MAE and BIAS scores for all fourteen cases.

5.2.4 Results over Southern Africa

Over the Southern African domain outside South Africa, rain gauge measurements are not available for validation purposes. The TRMM Multi-satellite Precipitation Analysis 3B42RT product uses combined IR and microwave satellite signatures. The microwave data is processed and the IR data averaged over 0.25° grid before converted to precipitation. This was taken as "ground truth" for the comparison against HE and CRR for the SADC region.

Ten cases were selected from the November 2013 to January 2014 period to compare the CRR, HE and TRMM (3B42RT) data in daily accumulations for 24 hours (Table 5.4).

Table 5.4: List of SADC case studies

Case date
8 Nov 2013
18 Nov 2013
19 Nov 2013
20 Nov 2013
21 Nov 2013
24 Dec 2013
31 Dec 2013
2 Jan 2014
4 Jan 2014

5.2.4.1 Example: 19 November 2013

Figure 5.20 shows the rainfall distribution and intensity for the 24 hours for 19 November 2013 as depicted by HE, CRR and TRMM. Figure 5.21 and 5.22 show the contingency table scores for this case, using the 10 mm and 20 mm thresholds.

The contingency table scores for 1 mm indicate that the CRR is better than the HE. For 10 mm and 20 mm thresholds, however, the HE outperforms the CRR. The RMSE, MAE of the CRR is smaller than the HE and the BIAS scores of the CRR is closer to 1 (perfect score).

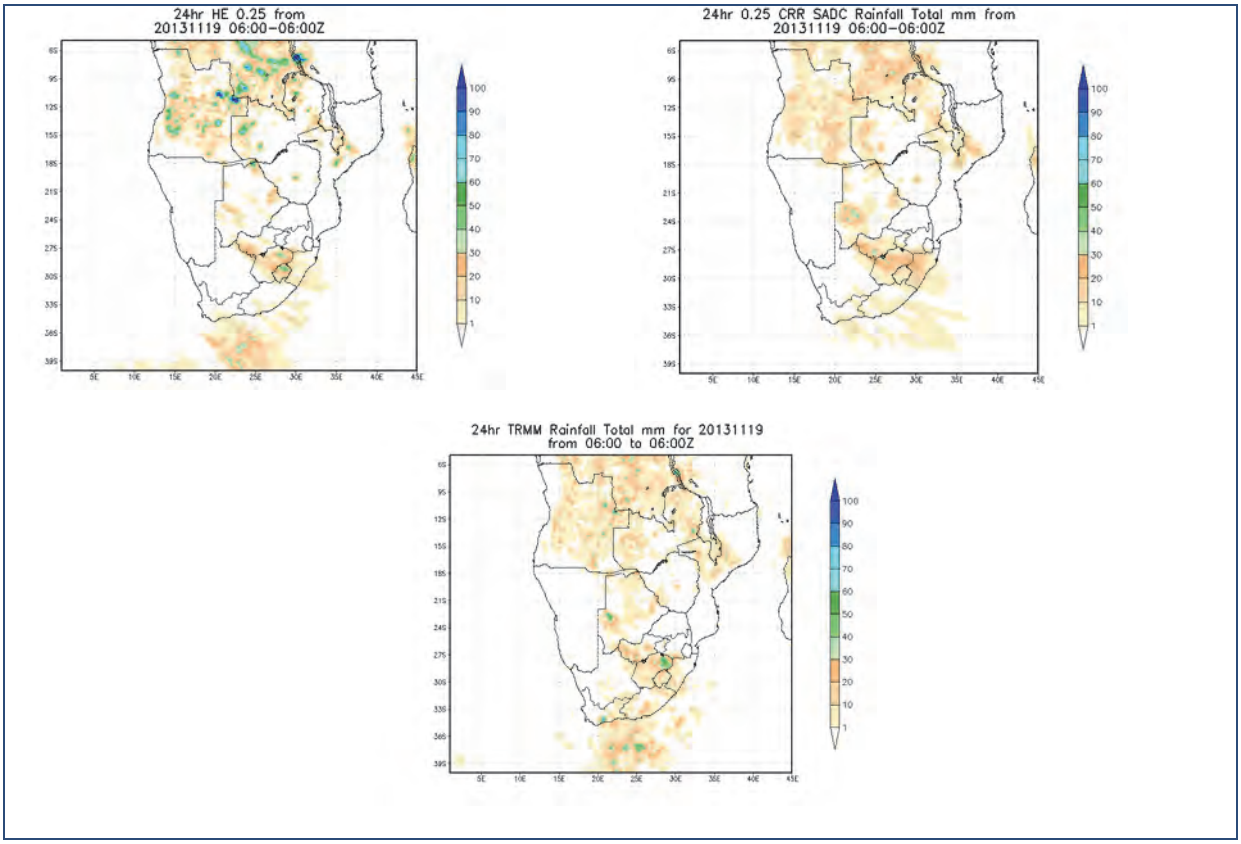

Figure 5.20: HE (top left), CRR (top right) and TRMM (bottom) daily total rainfall for 19 November 2013

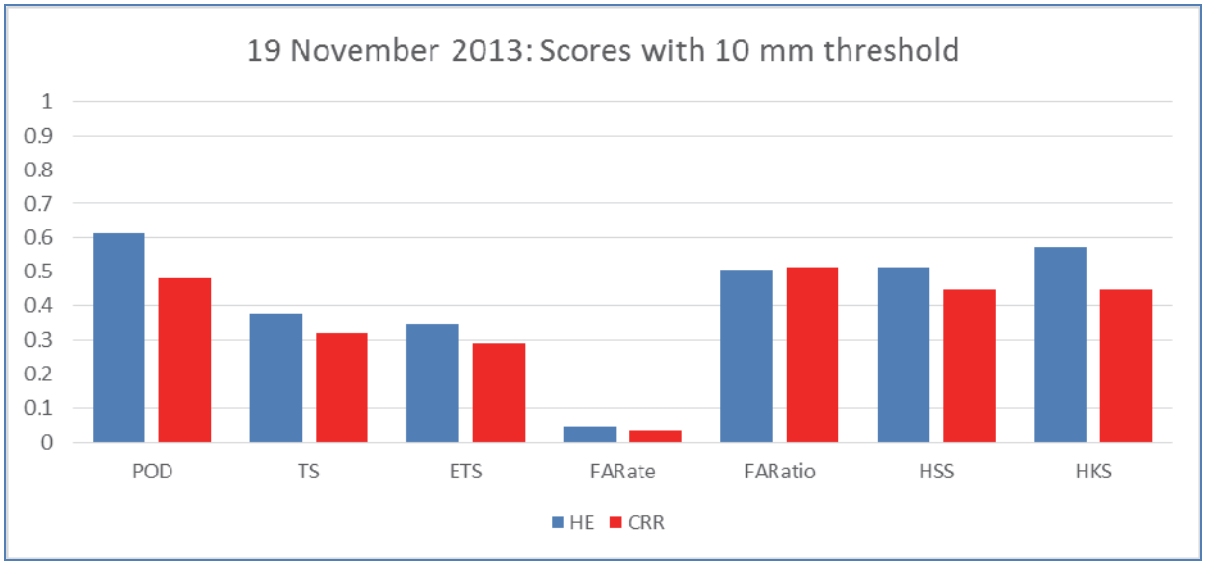

Figure 5.21: Contingency table scores for 1 mm threshold for HE (blue) and CRR (red) for 19 November 2013 over the SADC region

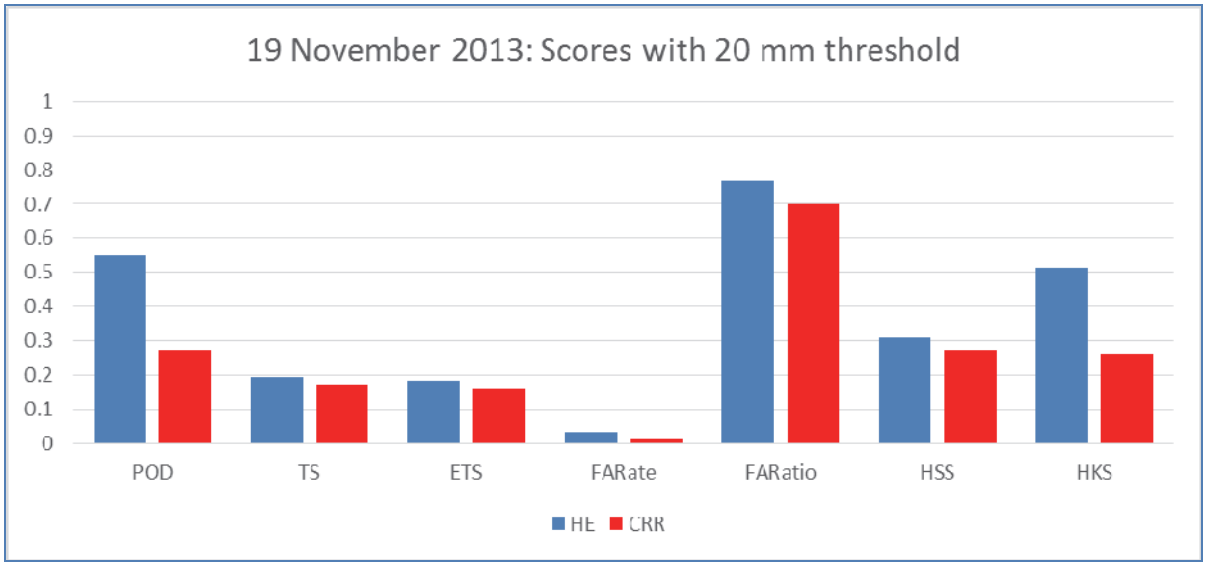

Figure 5.22: As for Figure 5.21 but for 20 mm threshold

5.2.4.2 Summary of all ten cases over the SADC region

As summary of all ten cases are shown in Figures 5.23-5.25. The HSS for 1 mm are the best and it gets lower for the 10 mm and 20 mm thresholds. The CRR scores (Figure 5.23, dashed lines) are sometimes better than the HE (solid lines), but not always. In general, the scores for the different thresholds are very similar. The Correlation Coefficients for the CRR (light bars) are better than the HE (darker bars) in 5 of the ten cases. The RMSE and MAE for the CRR (lighter bars) are always significantly better (i.e. smaller) than the RMSE and MAE scores of the HE (darker bars).

The average of all ten cases (Figure 5.26) shows that the HSS scores are very similar for HE and CRR. The Correlation Coefficient of the CRR is slightly better than the HE. The average of all ten cases (Figure 5.27) confirms that the RMSE and MAE of the CRR are significantly better (smaller) than the HE. For the 1 mm threshold the BIAS of CRR and HE are very similar, but for the 10 mm and 20 mm threshold CRR is better than HE (i.e. closer to 1). The HE is clearly overestimating.

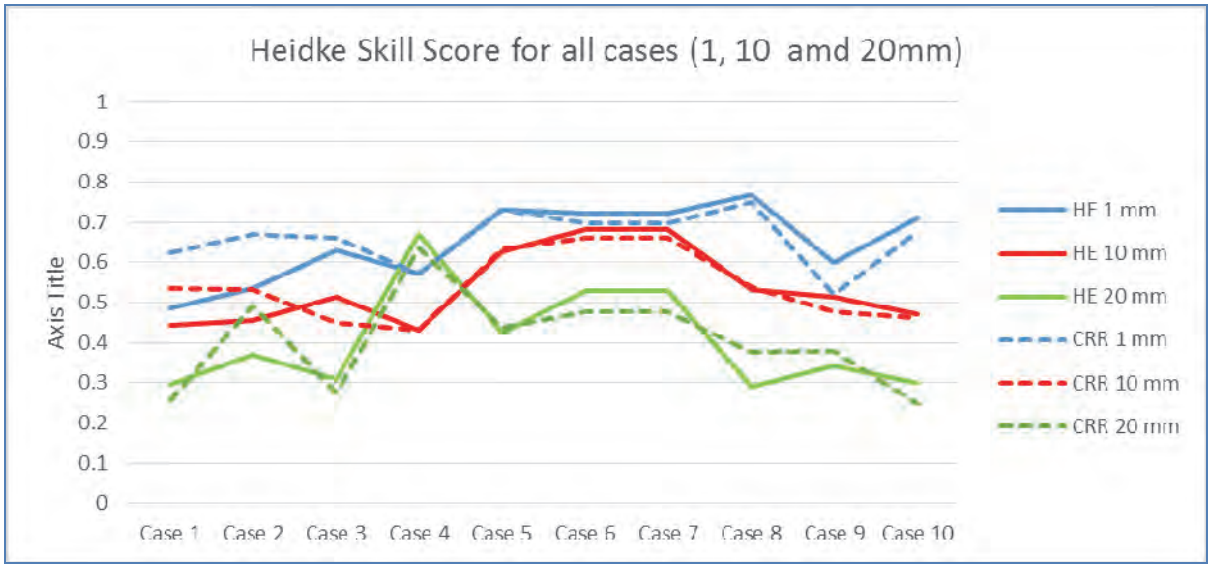

Figure 5.23: As Figure 5.15 but for the SADC cases

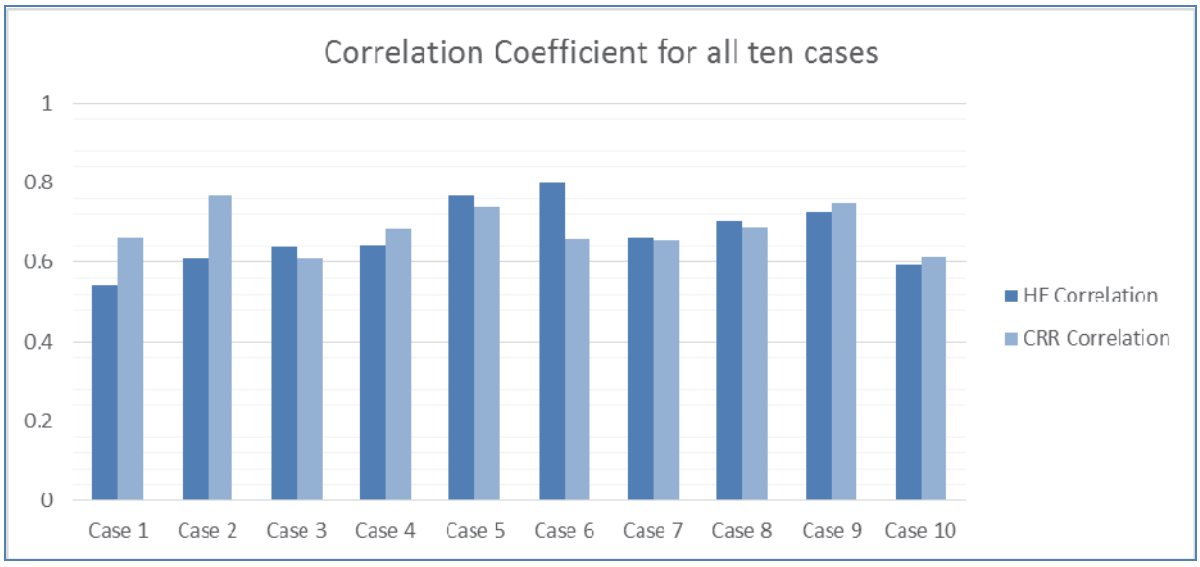

Figure 5.24: As Figure 5.16 but for SADC cases

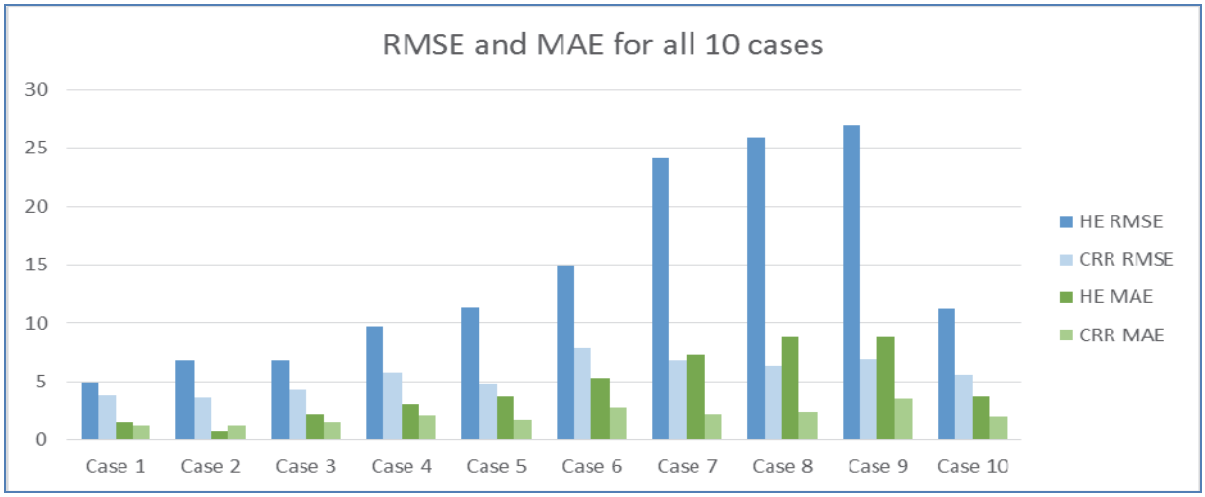

Figure 5.25: As Figure 5.17 but for SADC cases

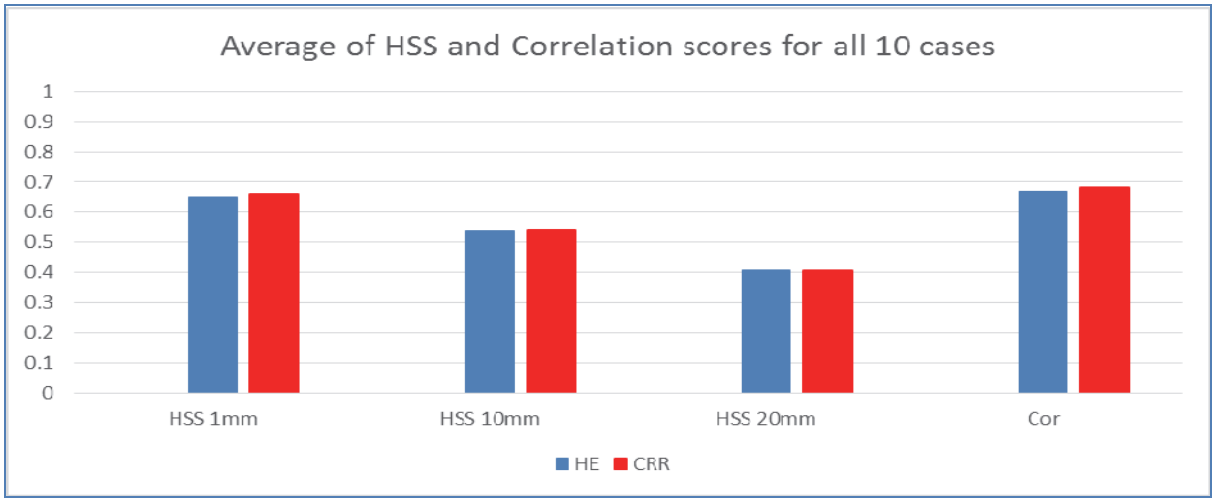

Figure 5.26: As Figure 5.18 but for SADC cases

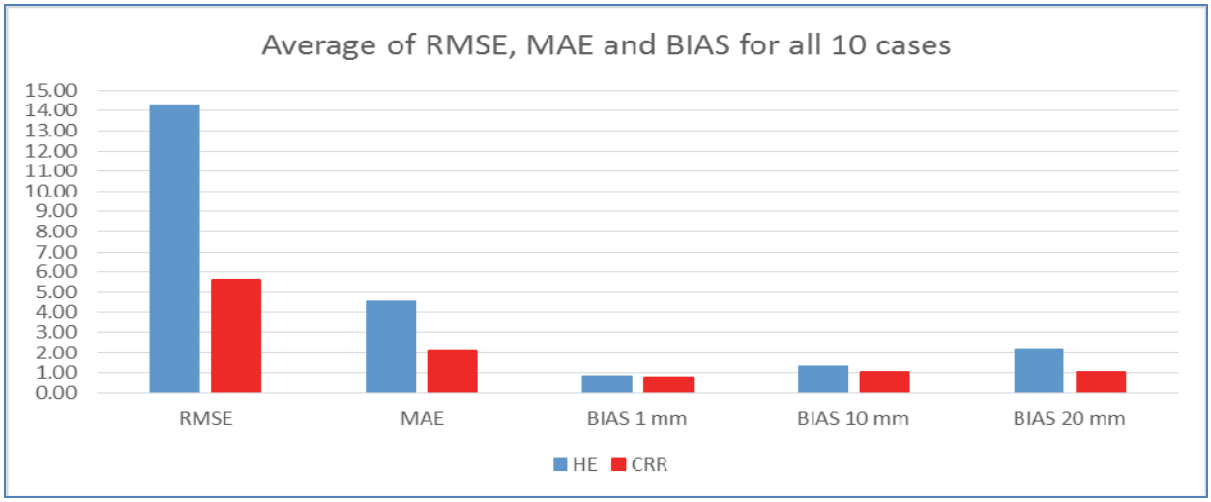

Figure 5.27: As Figure 5.19 but for SADC cases

5.2.5 Summary

Subsequent to the tests which were done with the CRR product in 2012, the Nowcasting SAF software was installed (in research mode) in SAWS. The FORTRAN programs used previously were based on the 2011 version of the software while the installed version (using the original C programs) is the upgraded 2012 version.

Fourteen cases were tested over the South African domain and validated against rain gauge data. The comparisons were done on a 0.25-degree resolution for daily rainfall totals (24 hours). Light, medium and heavy rainfall cases were used during the summer months November to February. Judging by the HSS it is not conclusive that the CRR is better than the HE. The correlation scores as well as the RMSE, MAE and BIAS scores, however, indicate that in the majority of the cases the CRR performs better than the HE.

Ten cases were selected for the entire SADC region during the months November, December and January. Due to the lack of rain gauge data over this region, the CRR and HE were validated in similar fashion as the SA cases against TRMM data. The HSS scores were again inconclusive about the performance of the products. The Correlation Coefficients were better for CRR in half of the cases. The RMSE, MAE and Bias scores, however, were significantly better for CRR than for HE. Although the TRMM data set (3B42RT) is not the "absolute truth" of rainfall over the SADC region, it is seen as a very good, reliable source of rainfall data.

Although the 2012 version of the CRR is better than the 2011 version, it still lacks more cloud microphysical properties in the algorithm. The latter is included in the 2013 version of the CRR. We hope to install the 2013 version operationally during the course of 2014 and the CRR from this version should show considerable improvement to the 2012 version. Using additional channels (CRR) for the calculation of satellite-based QPE proves to be beneficial and generally validates better than the single MSG channel method (HE).

5.3 RADAR-BASED PRECIPITATION ESTIMATION

5.3.1 Introduction

Weather radar provides an efficient means of measuring precipitation. Although its measurements are indirect and often biased, it remains the best alternative in capturing the spatial variability associated with precipitation on a high temporal and spatial resolution. With the implementation of the South African Flash Flood Guidance system (SAFFG) and the installation of 10 new S-band Doppler radar systems, a lot of emphasis has been placed on the performance of the radar's Quantitative Precipitation Estimation (QPE) field.

Due to the fact that radar QPE is the main source of precipitation input to the SAFFG, it has become absolutely vital that as many errors as possible are removed from the precipitation field to get the best possible estimates. The main sources of errors in precipitation measurements include:

- Homogeneity defects of the targets themselves, such as different precipitation types (rain or hail), particle size distributions (especially those that fall in the Mie region), the presence of the

melting layer or Bright Band (BB) and the presence of non-hydrological targets (birds, planes, etc.);
- The change of precipitation between the regions in the atmosphere where it is measured to where it will ultimately land. Evaporation and growth as well as vertical and horizontal movements of the target through the atmosphere can be contributing factors;
- Propagation of the radar beam where attenuation, refraction, curvature of the earth and occultation of the beam can all lead to errors in the reflectivity;
- Radar calibration faults and measurements errors, etc. (Sauvageot, 1992).

Clearly, the only way to reduced errors in precipitation measurement is through careful attention to many details. The South African Weather Service (SAWS) has opted to use a similar strategy as the Australian Bureau of Meteorology (BoM) as a first option to see if an improvement can be made in terms of QPE. Changes that have been made that differ from the precipitation output used by the current TITAN system is the use of a single Constant Altitude Plan Position Indicator (CAPPI) reflectivity map (1.5km above the radar) and a convective/stratiform classification scheme (explained in more detail in section 2.1) is introduce as well. This will allow the reflectivity to be converted into rain rate with the use of different Z-R relations depending on the classification of the rainfall type (Chumchean *et al.*, 2008). The result from these techniques, which will be incorporated in the radar QPE calculation, are then tested against rain gauge data as well as the TITAN precipitation that currently feeds the SAFFG.

5.3.2 Classification scheme

It can be a challenge to provide guidance to forecasters in selecting the appropriate Z-R relation for any giving precipitation type. Thus, automating the selection process through a classification scheme can drastically simplify the Z-R conversion. Radar equivalent reflectivity (Z_e) can be converted into rain rate using an appropriate Z-R relation. The purpose of the classification scheme is to assign a different Z-R relation to the classified rainfall types of convective and stratiform rainfall.

The classification scheme selected was originally proposed by Steiner *et al.*, (1995) and later adapted by Chumchean *et al.*, (2008). It uses instantaneous radar reflectivity to separate convective from stratiform reflectivity values. A pixel will be classified as a convective pixel when:

- The reflectivity value of that pixel is greater than 42dBZ. This is higher than Steiner *et al.* (1995) originally used due to the higher spatial resolution of the data available.
- If a pixel is not identified as a convective centre and the reflectivity is greater than 35dBZ it can still be classified as convective if:

$$Z_{bg} > Z_c \quad (1)$$

and $$Z - Z_{bg} > \Delta Z \quad (2)$$

Z_{bg} is the background reflectivity (see Figure 5.28) i.e. the average reflectivity in an 11km radius surrounding the pixel. Z_c is the minimum convective reflectivity, which is set at 35dBZ. ΔZ is dependent on the background reflectivity and the minimum convective reflectivity as shown in equations (3) and (4)

$$\Delta Z = 10 - \frac{Z_{bg}^2}{P} \qquad (3) \qquad\qquad and \quad P = max\left(\frac{(Z_c+2.5)^2}{10}, 140\right) \qquad (4)$$

If the criteria are met and the pixel is classified as a convective region the surrounding pixels are then influenced by the convective core and will be classified as convective (see Figure 5.28). This region is dependent on the background reflectivities listed in table 5.5. The result of the algorithm described above can be seen in Figure 5.29.

Table 5.5: The relationship between mean background reflectivity and convective radius for instantaneous pixel classification (Chumchean *et al.*, 2008)

RELATIONSHIP BETWEEN MEAN BACKGROUND REFLECTIVITY AND CONVECTIVE RADIUS					
Mean Background reflectivity (dBZ)	15-25	25-30	30-35	35-40	40-50
Convective Radius (km)	2	2	3	4	5

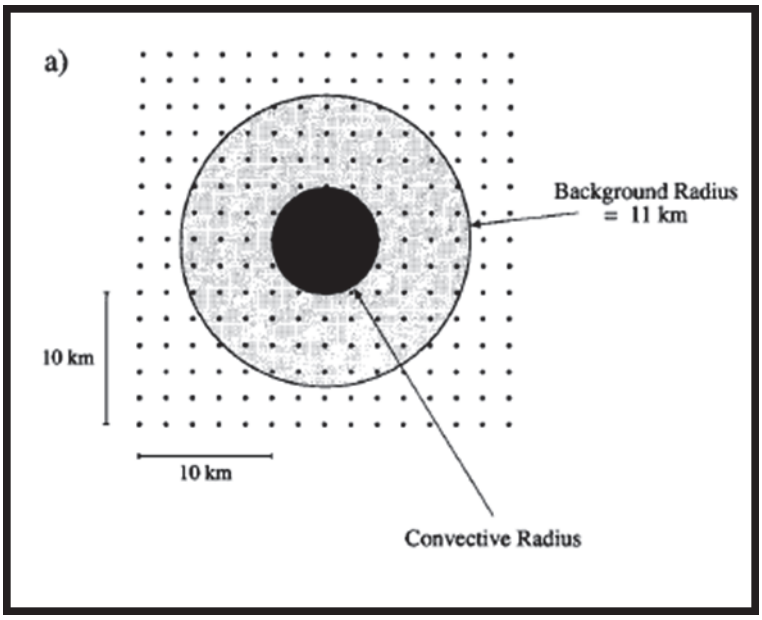

Figure 5.28: Illustration of the background reflectivity and convective radius around a pixel on a reflectivity map, after Steiner et al, 1995.

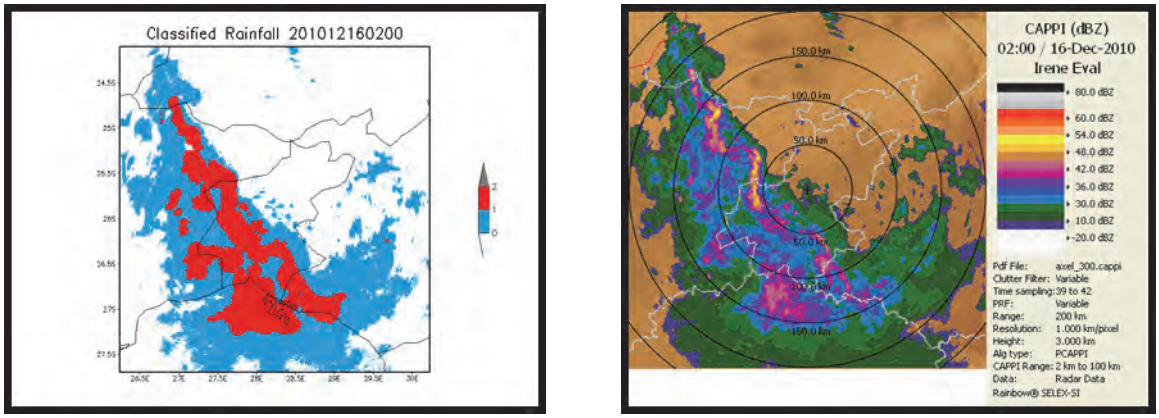

(a) **(b)**

Figure 5.29: (a) shows the convective and stratiform regions as red and blue respectively, calculated from the dBZ field in (b), using the reflectivities in Table 5.5.

5.3.3 Z-R relations

The equivalent reflectivity (Z_e) depends on the composition, size and number of precipitation particles. This is useful because precipitation rate R also depends on the same variables. Consequently, most researchers have utilised the empirical expression of the form, $Z = AR^b$.

Z is the reflectivity factor, *R* the rain rate in millimetres per hour, and *A* and *b* are constants. The most widely used Z-R relationship is that derived by Marshall and Palmer (1948) which can be expressed as $Z=200R^{1.6}$. Z-R relationships are associated with differences in geographic locality as well as different rain types and different synoptic conditions. There can even be appreciable differences from one storm to the next. When information in the characteristics of the above-mentioned is lacking, it is common practice to use the Marshall Palmer relation. However, it should be possible to increase the accuracy of radar measurements of rainfall by identifying the type of rain through the characteristics of the returned reflectivity (Battan, 1973). Hence, the use of the classification scheme as discussed in the previous section. By classifying the radar reflectivity into convective and stratiform rainfall, an appropriate Z-R equation can be selected in order to increase the accuracy of rainfall estimates.

Five relationships were selected for testing as listed in Table 5.6. The BoM default stratiform and convective relations were selected due to SAWS considering the BoM QPE methodology (personal communication with BoM staff). The remaining three are (1) the most commonly used Marshall Palmer equation, (2) the deep convection equation (used by the American NMQ system (Zhang *et al.*, 2011)) and (3) a tropical relationship often used for flash flood forecasting (Fulton *et al.*, 1998 and Rosenfeld *et al.*, 1993).

Table 5.6: Names of Z-R relations and their formulas associated with them.

Z-R relationship	Formula
BoM default Stratiform	$Z = 84R^{1.5}$
BoM default Convection	$Z = 260R^{1.5}$
Marshall-Palmer	$Z = 200R^{1.6}$
Deep Convection	$Z = 300R^{1.4}$
Rosenfeld Tropical	$Z = 250R^{1.2}$

Battan (1973) lists over 50 derived Z-R relationships, most of which are only appropriate for the specific time, location and case for which they were derived. The reality is that most Z-R relationships are similar and only a few need to be considered when working with rain types. Figure 5.30 illustrates that the difference in rain rate only becomes significantly noticeable at the higher reflectivity measurements.

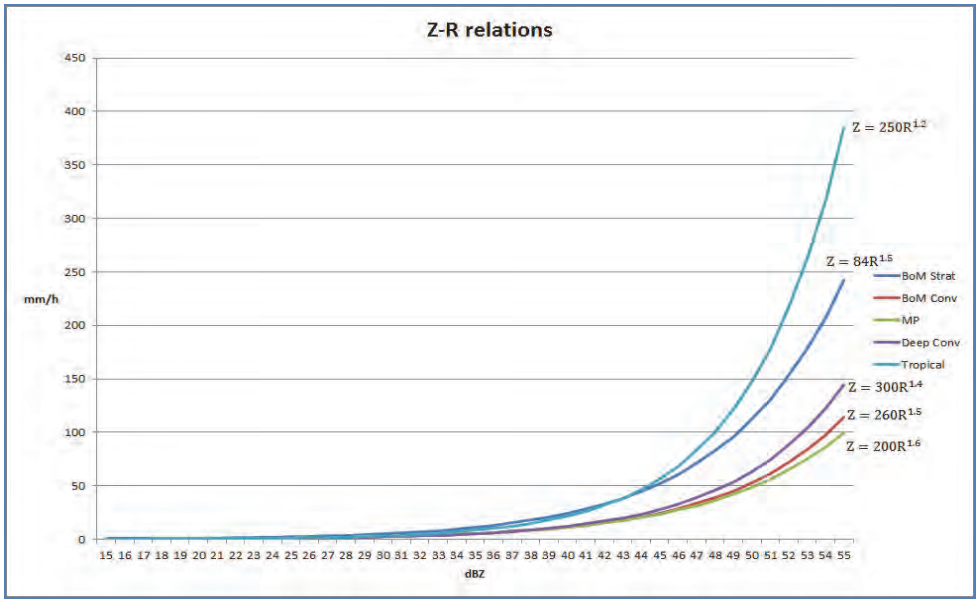

Figure 5.30: Rain rate associated with the radar reflectivity when using Z-R relationships

Even with the best possible fit of a Z-R relationship, there can still be significant errors. Atlas and Chmela (1957) illustrated that rain rates of 33 mm/h and 11 mm/h can be associated with the same reflectivity. Radar calibration can also be a factor. Unreliable calibration can result in a different Z-R relationship for different radars at the same location (Doviak & Zrnić, 1984). Thus, Z-R relationships are extremely sensitive to all physical properties of the radar and must be utilised with caution. It is also one of the most important steps in the QPE process and needs to be as accurate as possible.

5.3.4 Data and methods

Data from the Irene and Port Elizabeth (PE) radars were selected for the study. Reasons for the selection include a reliable dataset and a number of hourly rain gauges that are available within the radar coverage. The dataset selected stretches over the entire year of 2011.

Since the 20th of October 2010, the Irene radar scan strategy has been optimised to run at 6-minute intervals, which gives 10 volume scans per hour. The scans consist of 12 elevation scans that start at the top azimuth scan of 30° elevation and ends at the bottom with a 0.5° elevation. Output from the radar is in the format of raw Gematronic volume files created by the Rainbow software. Post processing of the data includes the use of a Doppler filter which deletes high reflectivity's at low level with zero velocity. In essence, this removes most of the ground clutter from the data.

The PE radar operates at 5-minute scan intervals, which gives 12 volume scans per hour. The scans consist of 18 elevation scans that start at the top azimuth scan of 47.8° elevation and ends at the bottom with a 1° elevation. One of the reasons for the difference in scan strategies is because the radar at PE does not have Doppler capability and thus does not suffer from the effects of the Doppler dilemma, which allows the free use of Pulse Repetition Frequency (PRF). It makes use of a predetermined clutter map to remove ground clutter, thus the radar still suffers from the effects of Anomalous Propagation (AP) from time to time. Another drawback of the PE radar is that it operates in the C-band frequency range in a populated area. Thus, it suffers from radio LAN (RLAN) interferences, which over-saturates the receiver giving false readings. A filter is applied in an attempt to remove most of the interference.

The RLAN filter currently running at the PE radar has the tendency to remove too much information. This is particularly the case with stratiform precipitation (Figure 5.31). Figure 5.31 shows two images that are successive scans at the PE radar with the filter switched on in the first image (left) and switched off in the second image (right). It is evident that valuable weather information is lost if the filter is activated. New techniques need to be investigated in order to improve precipitation estimates in this scenario, which will be part of subsequent research.

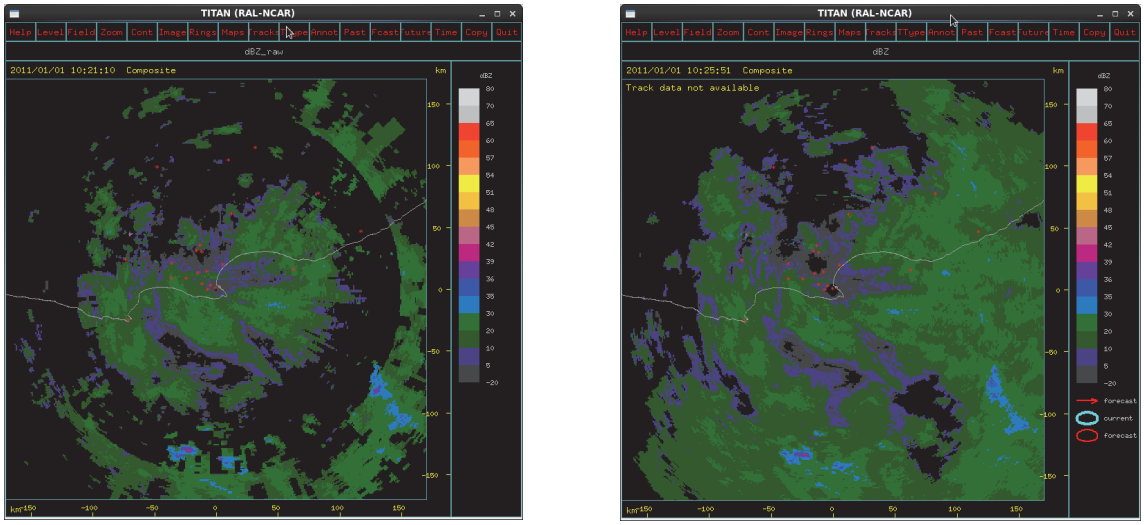

Figure 5.31: Consecutive scans at the PE radar with the RLAN filter switched on (left) and off (right).

The Meteorological Data Volume (MDV) format files were then utilised and the CAPPI level 1.5km above the radar was extracted using TITAN software. Using a CAPPI level to calculate the rain rate helps to eliminate the effects of the Bright Band (BB) as the freezing level during the summer months rarely drop that low. This reflectivity field is fed into the QPE algorithm where it is classified into convective/stratiform rainfall. The output is then tested against rain gauge data.

Four different algorithms were tested:

- The first is the standard precipitation field used by TITAN. This involves the Marshal-Palmer relationship and the selection of the maximum dBZ value within a 0km-5km vertical column at each grid point and converting that reflectivity into rain rate;
- The second is similar to the first except the tropical relationship has been used;
- The BoM default Z-R relationship was applied to the classification scheme to convert the reflectivity values to rain rate for the third algorithm;
- The final algorithm tested was to use the Z-R relationship from the American National Mosaic and Multi-Sensor QPE (NMQ) System, the deep convection and Marshall-Palmer relationships were applied to the classification scheme as convective and stratiform precipitation Z-R relationships respectively.

All algorithms also correct for hail by using a hail cap of 53 dBZ. All reflectivity values higher than this value will be set to 53 dBZ as they are considered to be hail contaminated. This parameter is also dependent on the geographic location of the radar and synoptic system associated with the precipitation event. It usually falls between the range of 51 and 55 dBZ most of the time so it is standard practise to fall back to a default 53 dBZ. However, the choice of hail threshold can significantly affect the rain estimates. (Fulton *et al.*, 1998)

One-hour accumulations are then compared against the readings of a number of hourly rain gauges within 140 km radius of the radar. The maximum range that rain gauges are considered is minimized to reduce the errors associated with radar gauge estimates due to beam elevation.

5.3.5 Results

The results are split into two parts. The first was where a vertical reflectivity profile (VRP) is used to test the classification scheme. For this purpose a heavy rainfall event on the 15th and 16th of December 2010 at the Irene radar was selected. The second part was where the rainfall estimates are compared to the relevant rain gauge data.

5.3.5.1 Vertical reflectivity profile (VRP)

Figure 5.32 shows two graphs of 5-minute rain rates as measured by the gauges for the 48 hours of the case study period. These stations were selected because the reflectivity over the rain gauge was continuously classified as either convective or stratiform precipitation for a period of an hour or more. This was done so that the average VRP for that period (which are extracted from radar volume scans every 6 minutes) can be calculated and compared to the rain rates of the gauges (available every 5 minutes). The ideal situation will be that the high spikes in rain rate are classified as convective precipitation (green line), the low continuous rain rates as stratiform (red line) and the zero rain rates no classification at all (blue line).

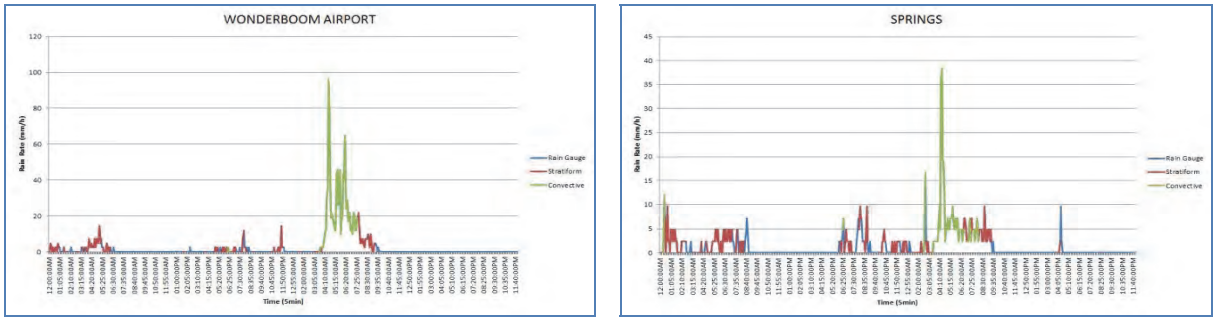

Figure 5.32: The Figure shows 5-minute rain rates at selected rain gauges for the 48 hour period of the 15th and 16th of December 2010. The blue line represents no classification from the radar at the corresponding time. The green and red line represent the period where the reflectivity was classified as convective or stratiform respectively.

The Wonderboom airport rain gauge was classified as convective rainfall for three consecutive hours. For a convective profile, the reflectivity must not show any evidence of a BB (an increase in reflectivity at the freezing level). A profile with similar reflectivity as it increases with height and then a steady drop in intensity once past the freezing level will be the ideal convective VRP. In Figure 5.33 such profiles can be observed over the rain gauge indicating that the classification scheme is correct. This also coincides with the high rainfall rate measured by the rain gauge (green line fig 5).

The Springs rain gauge had a total of 3 stratiform classified hours and 2 convective classified hours. Looking at the VRP in Figure 5.34 the BB is clearly visible near the freezing level, which is a very good indicator of stratiform rainfall, and thus the classification will be correct. With the convective classified period the VRP showed a typical convective profile at 0500Z but a BB is present with the 0600Z period. This shows that the classification scheme does not always work flawlessly.

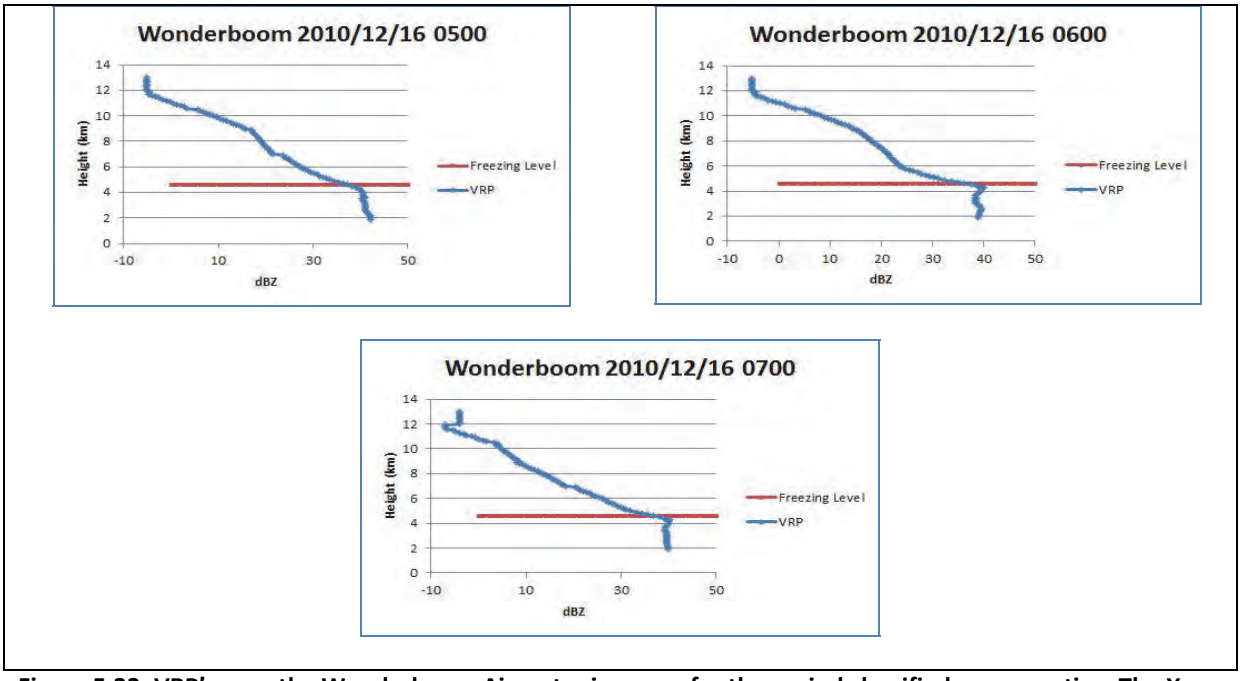

Figure 5.33: VRP's over the Wonderboom Airport rain gauge for the period classified as convective. The X-axis indicates reflectivity while the y-axis indicated the height AMSL. The red line is the freezing level taken from the balloon assent done at Irene weather office.

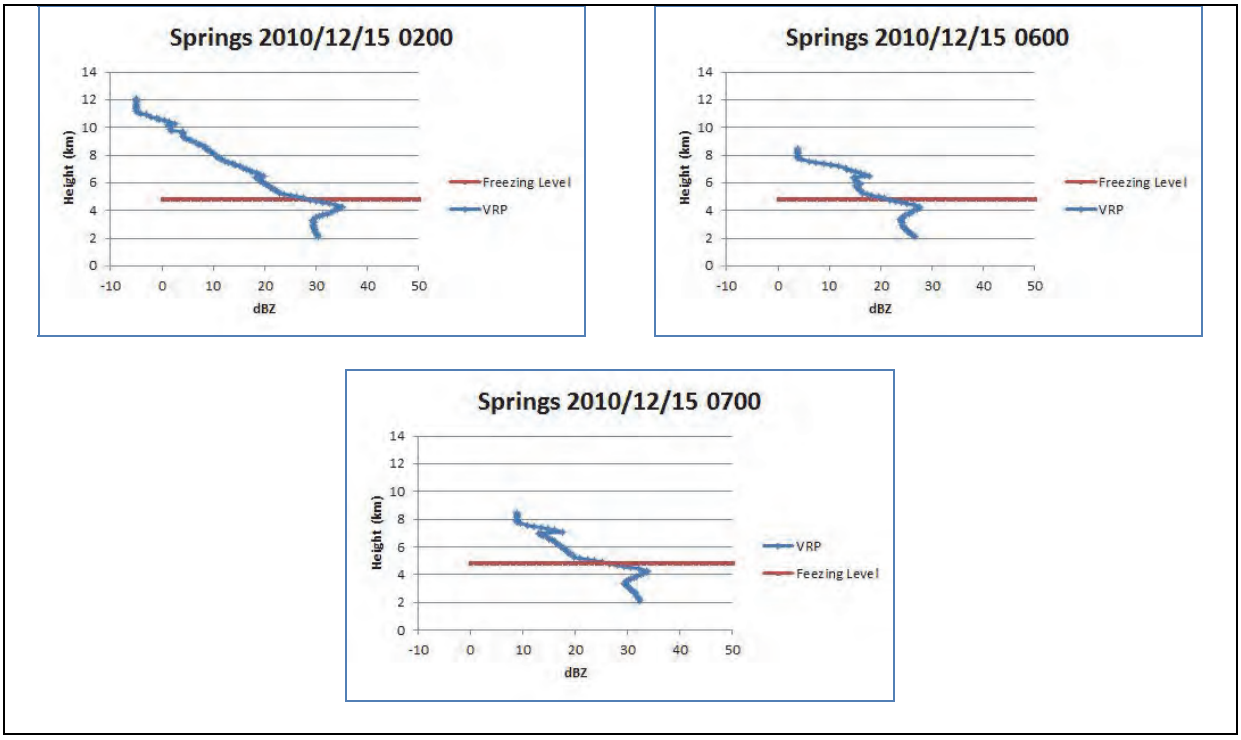

Figure 5.34: VRP's over the Springs rain gauge for the period classified as stratiform. The X-axis indicates reflectivity while the y-axis indicated the height AMSL. The red line is the freezing level taken from the balloon assent done at Irene weather office.

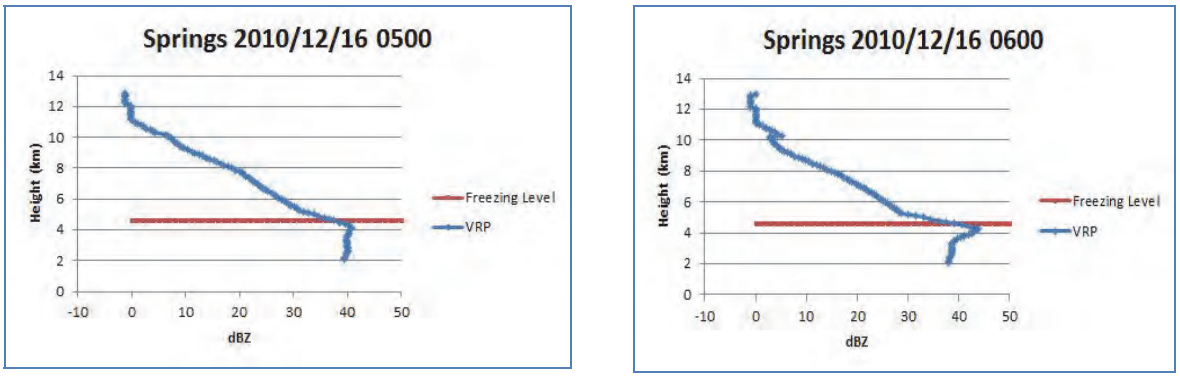

Figure 5.35: VRP's over the Springs rain gauge for the period classified as convective. The X-axis indicates reflectivity while the y-axis indicated the height AMSL. The red line is the freezing level taken from the balloon assent done at Irene weather office.

Parts of the classification algorithm still classify stratiform precipitation as convective as was illustrated by the VRP's above. Figure 5.36 below shows a large stratiform region of reflectivity to the south-east of the radar, as clearly indicated by the cross-section with the presence of the BB. Further studies will be necessary to optimise the classification scheme for the SA radar network.

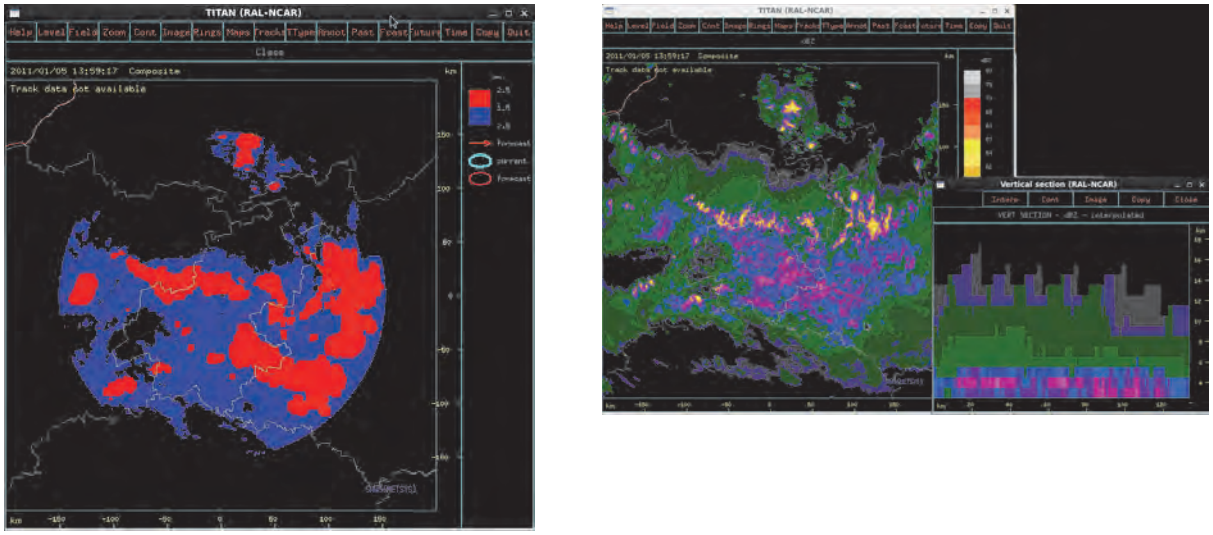

Figure 5.36: Classified field with red as convective and blue as stratiform precipitation. Reflectivity values of the classified field with a cross-section indicating the presence of a BB.

5.3.5.2 Precipitation

Continuous variable verification scores were selected to perform the evaluation of the precipitation algorithms against the rain gauges. The scores include:

- The Mean Absolute Error (MAE), which gives the average magnitude of the error without indication the direction of the deviation;
- The multiplicative bias (BIAS), which indicates the direction of the error is used and has a perfect score of 1. It is best suited for quantities that have 0 as a lower or upper bound such as rainfall measurements.
- The Root Mean Squared Error (RMSE), which places more emphasis on larger outliers and is a good score to use when comparing radar with gauges as large errors are undesirable with rainfall measurements.
- The Correlation Coefficient (CORR) was then also used to show the linear association of the data. (Wilks, 2006)

5.3.5.2.1 Irene

For the Irene radar, a selection of 47 days during 2011 was tested. The 47 days were selected when a rain gauge reported more than 50 mm in a 24 hour period and was termed “heavy rainfall days”. The current Marshall-Palmer ($Z=200R^{1.6}$) relationship was tested against the classification algorithm assigning convective ($Z=260R^{1.5}$) and stratiform ($Z=84R^{1.5}$) Z-R relationships used by BoM as defaults. Figure 5.37 shows the continuous variable scores calculated from 43 gauges surrounding the radar. The Marshall-Palmer Z-R relationship outperformed the classification algorithm on all levels (Figure 5.37), scoring better with the MAE, BIAS, RMSE and CORR. The BoM default relations were clearly not an improvement over the Marshall-Palmer relationship.

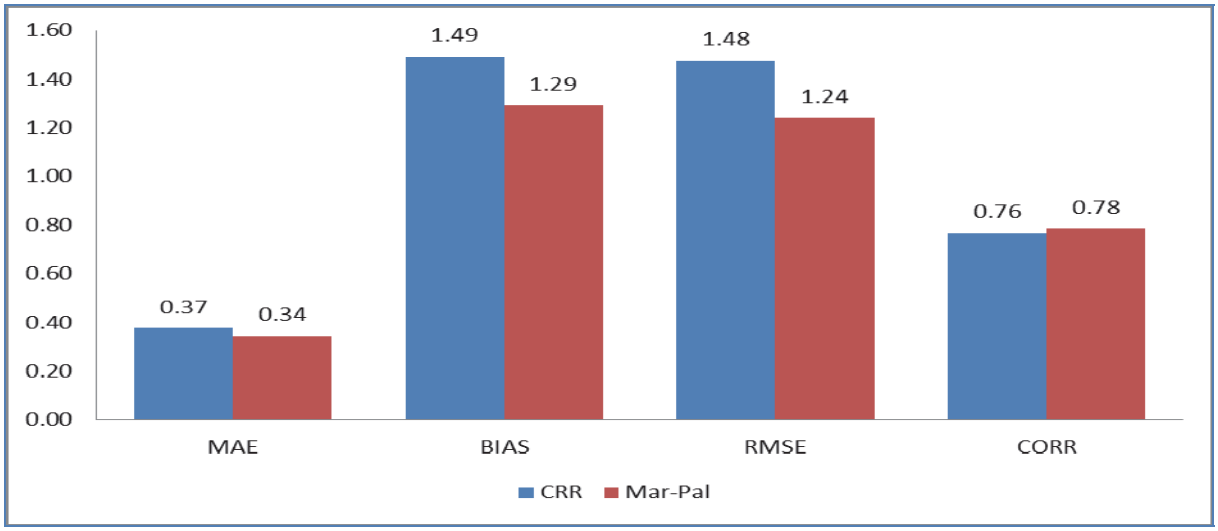

Figure 5.37: Continuous Variable Scores at Irene radar using 47 heavy rainfall days

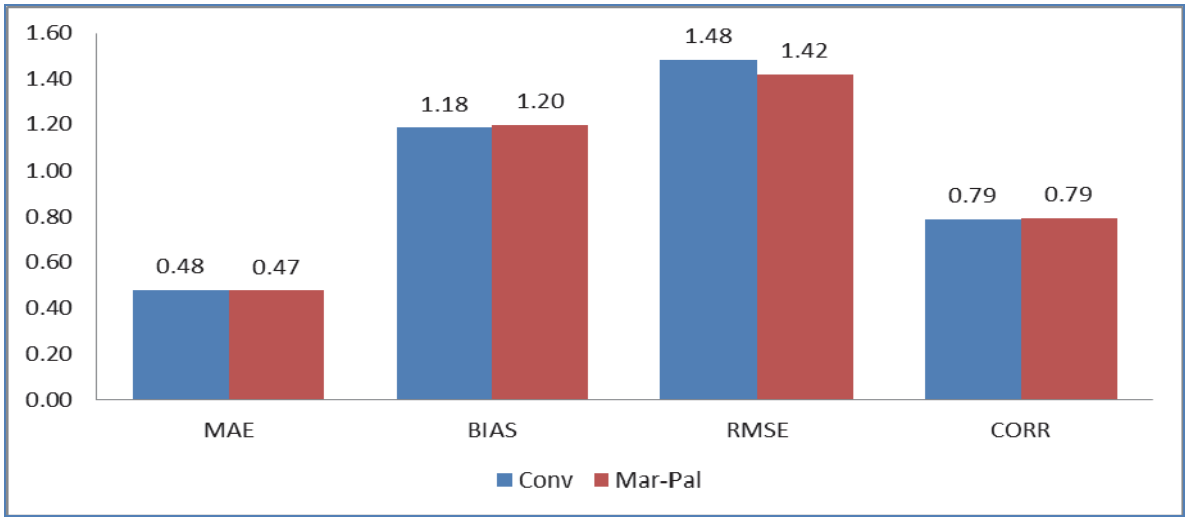

Figure 5.38: Continuous Variable Scores at Irene radar using 6 primarily convective days of the 47 heavy rainfall days

The BoM convective Z-R relationship ($Z=260R^{1.5}$) was then considered and tested with the Marshall-Palmer relationship using 6 of the 47 heavy rainfall days during 2011 where there was mostly convective weather with not much stratiform precipitation present. Tested over 39 gauges the results are quite similar and still the BoM convective Z-R relationship has a larger error as seen in Figure 5.38.

Figure 5.39 and 5.40 shows the same scores at Irene radar tested over 6 months of 2011 incorporating most of the rainfall season. Figure 5.39 depicts the period January-March (JFM) while Figure 5.40 depicts October-December (OND). During JFM 30 gauge pasted quality control while 38 were used during OND. The results of comparing the gauges to the tropical, Marshall-Palmer and the classification algorithm assigning convective ($Z=300R^{1.4}$) and stratiform ($Z=200R^{1.6}$) Z-R relationships is illustrated in the above mentions figures. Here the classification algorithm produces favourable results. Although it has a slightly weaker correlated during JFM with similar RMSE, it still

outperforms with a better BIAS as well as a lower MAE. During OND, the classification algorithm outperforms the Marshall-Palmer relationship on all scores. The tropical Z-R relationship correlates well but the error it makes is too great to be considered for everyday use. The classification algorithm assigning the deep convective Z-R relationship ($Z=300R^{1.4}$) as convective and the Marshall-Palmer relationship as stratiform ($Z=200R^{1.6}$) definitively show an improvement over the Marshall-Palmer Z-R relationship for Irene.

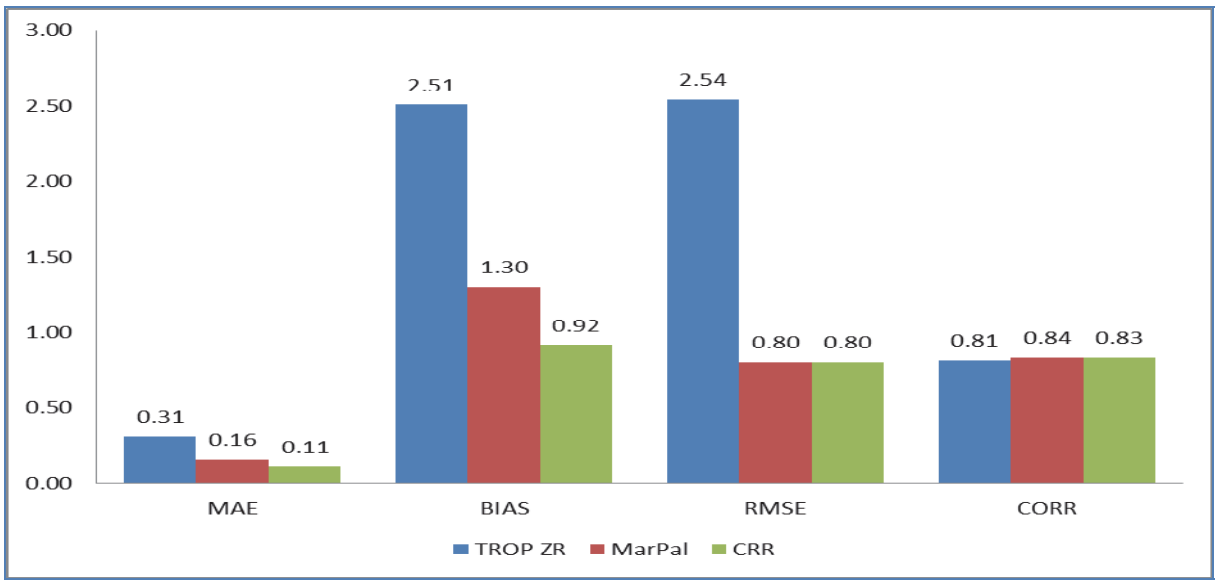

Figure 5.39: Continuous Variable Scores at Irene radar using January-March 2011

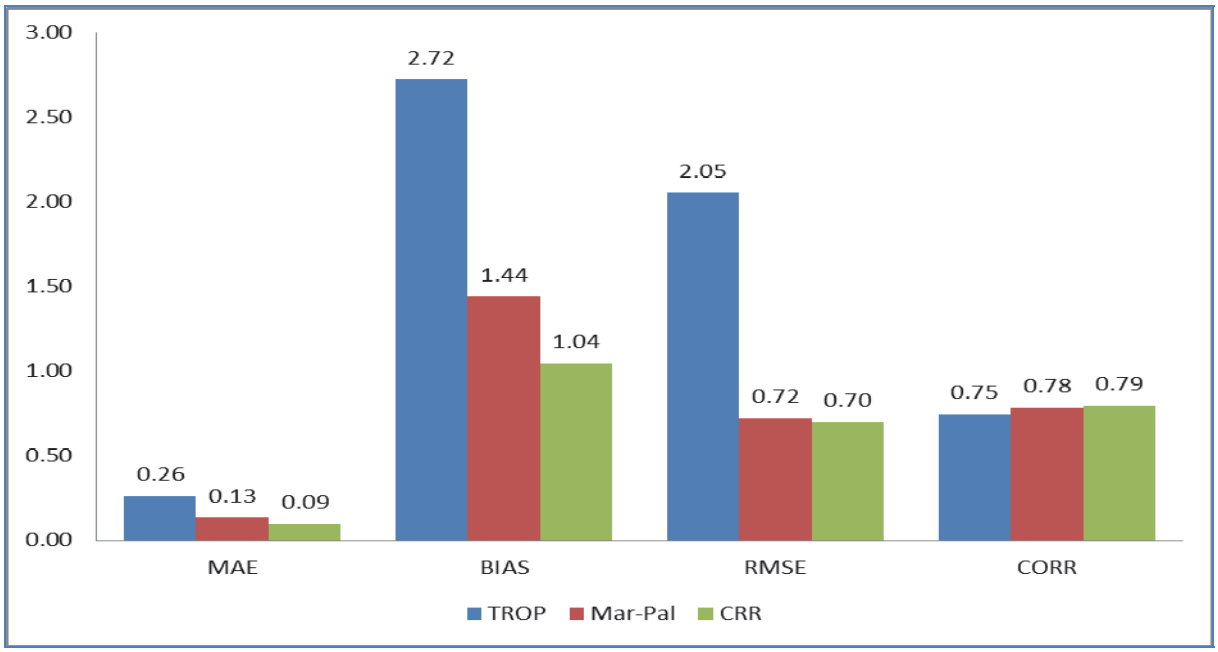

Figure 5.40: Continuous Variable Scores at Irene radar for October-December 2011

5.3.5.2.2 Port-Elizabeth (PE)

At PE more than 50 mm in a 24-hour period was reported in 41 different days during 2011 and were selected for testing. The standard Marshall-Palmer ($Z=200R^{1.6}$) relationship was tested against the classification algorithm assigning convective ($Z=260R^{1.5}$) and stratiform ($Z=84R^{1.5}$) Z-R relationships used by BoM as defaults. Figure 5.41 shows the continuous variable scores calculated from 23 gauges surrounding the radar. The Marshall-Palmer Z-R relationship in this case did not outperform the classified rain rate. The classification algorithm performed slightly better for all the scores. The under estimations shown by the BIAS and low correlations remain a concern. It is not clear that the classified rain rate is better. Since the Irene radar performs poorly with the BoM Z-R relationship, a similar test was done with the BoM stratiform Z-R relationship on the PE radar data as with the convective Z-R relationship on Irene radar data.

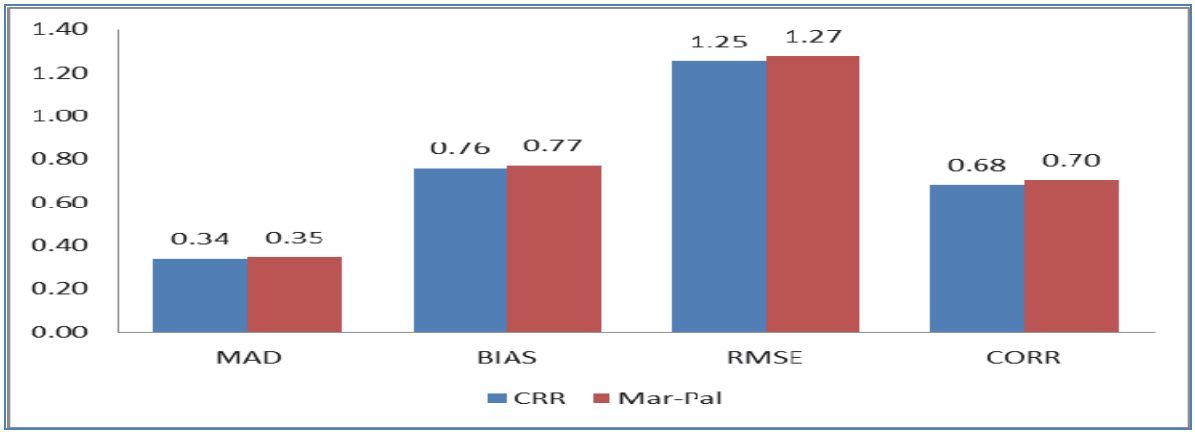

Figure 5.41: Continuous Variable Scores at PE radar using 41 heavy rainfall days

The BoM stratiform Z-R relationship ($Z=84R^{1.5}$) was then considered and tested against the Marshall-Palmer relationship using 10 of the 41 heavy rainfall days. Tested over 21 gauges the results show that Marshall-Palmer relationship outperforms the stratiform Z-R relations with a smaller error than the BoM stratiform Z-R relationship. Again, the results are not conclusive due to the good performance of the stratiform Z-R relationship in the BIAS test. The same test performed at Irene radar over the 6 months of 2011 was then performed at PE radar to compare results.

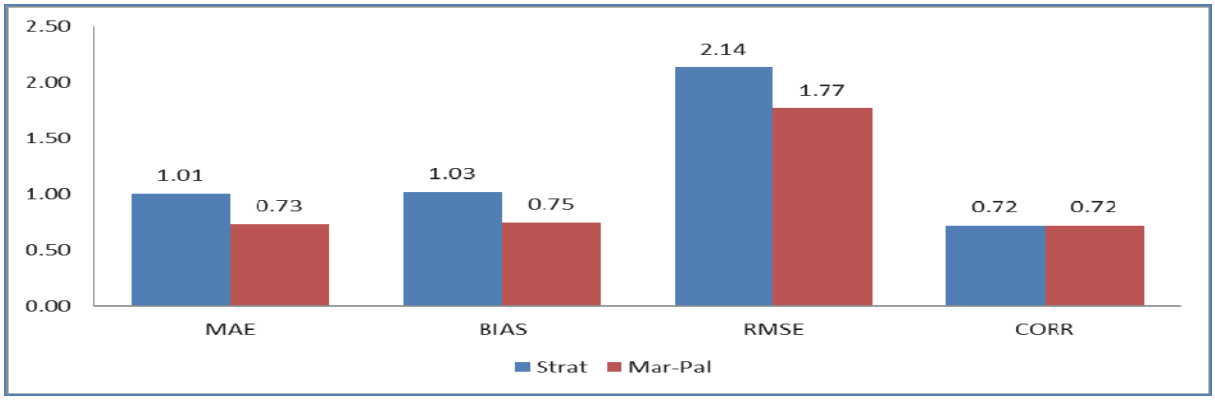

Figure 5.42: Continuous Variable Scores at PE radar using 10 of the 41 heavy rainfall days

Figure 5.43 and 5.44 depict periods JFM and OND respectively. During JFM 23 gauges provided useful data while 22 were used during OND. The results of comparing the gauges to the tropical, Marshall-Palmer and the classification algorithm assigning convective ($Z=300R^{1.4}$) and stratiform ($Z=200R^{1.6}$) Z-R relationships is illustrated in the above-mentioned figures. The results again are contradictory. During JFM, the classified rain rate performs much better with a smaller errors and higher correlation, while during OND the opposite is true, when the Marshall-Palmer relationship performs better.

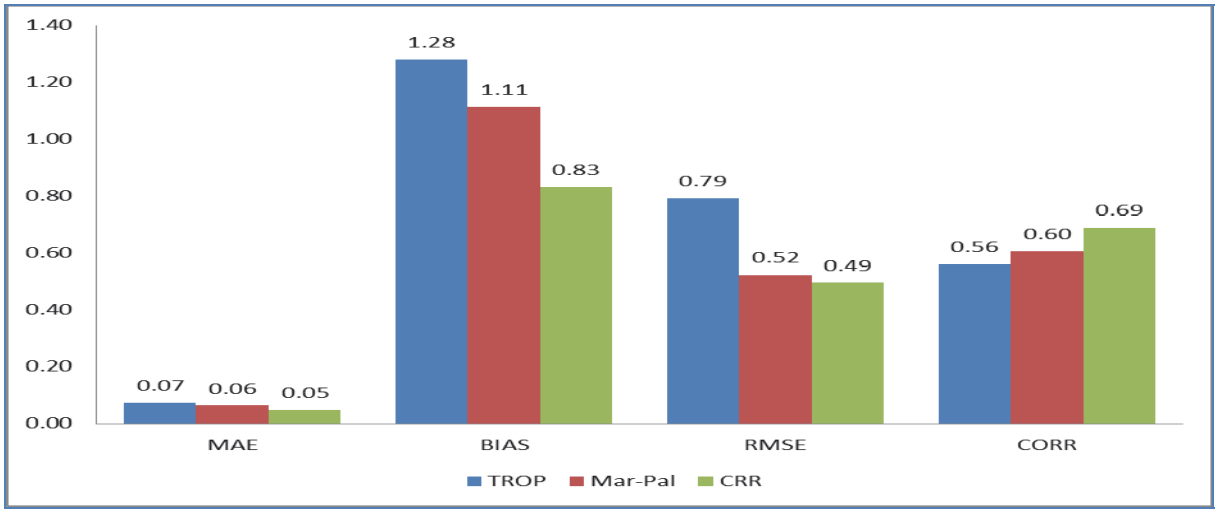

Figure 5.43: Continuous Variable Scores at PE radar using January-March 2011

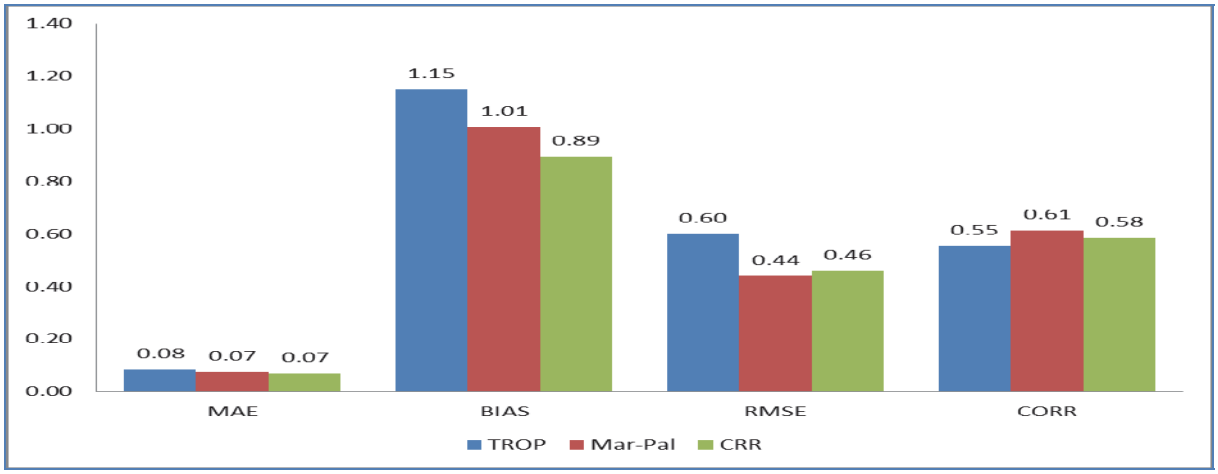

Figure 5.44: Continuous Variable Scores at PE radar using October-December 2011

5.3.6 Conclusions

5.3.6.1 Irene Radar

Results from the VRP comparisons show that the classification scheme works relatively well. Improvements are possible with a proper study to see if better results can be obtained if a bright band filter is added or adjustment to the thresholds in the classification criteria is needed.

From the results obtained, it is recommended to use the classification algorithm with the same Z-R relationship as that used by the NMQ system in the United States – thus a Z-R relationship of $Z=300R^{1.4}$ for convective rainfall and a Marshall-Palmer Z-R relationship of $Z=200R^{1.6}$ for stratiform rainfall. This classified rainfall field has the tendency to be slightly better than using just the Marshall-Palmer relationship. The tropical and BoM default Z-R relationships clearly did not perform better than the Marshall-Palmer relationship did.

The tropical Z-R relation is primarily used for extreme cases where the forecaster is able to switch to the appropriate Z-R relation prior to a heavy rainfall event (Fulton *et al.*, 1998). This will not be a practical solution in South Africa.

5.3.6.1 PE Radar

The PE radar seems to perform better with the classified algorithm with the American NMQ system Z-R relationship, even though it shows mixed results. With a low correlation and an underestimating bias, there is a strong indication that the radar is not very efficient or suitable for precipitation measurement. The RLAN interference negatively influences precipitation data and the filter does not help much in improving the measurement. Further studies needs to be done to improve the quality of data at the PE radar before a definitive answer on Z-R relations can be reached.

5.3.7 Summary

In summary:

- The classification scheme is working well with some room for improvement, by adjusting thresholds and introducing a bright band filter;
- The classification scheme with the deep convective Z-R relationship of $Z=300R^{1.4}$ for convective rainfall and a Marshall-Palmer Z-R relationship of $Z=200R^{1.6}$ for stratiform rainfall works best for the Irene radar and is an improvement on the current TITAN system;
- The PE radar is not suitable for precipitation estimation due to the RLAN interference and the filters in use to remove the corrupt data. Until new filtering techniques are introduced, the PE radar cannot be used for Z-R relation testing;
- The fact that the classification scheme improves the Irene radar precipitation estimates does not mean this will be the case for all radars. Each radar will have to be tested – especially the coastal radars – in order to find the best possible relation.

5.4 PRECIPITATION NOWCASTING

5.4.1 Background

This section explores the improvement of rainfall nowcasting opportunities to 6 hours, based on remote sensing and NWP. Quantitative Precipitation Forecasts (QPF) to 6 hours are aimed for use within the South African Flash Flood Guidance (SAFFG) and its SADC regional counterpart (SARFFG). Currently SAFFG and SARFFG employ persistence of the current 6-hour rainfall measurement into the next 6-hours as a nowcasting mechanism. This is however unrealistic, since rainfall systems move with time, particularly thunderstorms which grow and decay in a fraction of this interval. Therefore, a radar based precipitation nowcasting system that takes movement and development of the rain-bearing system into account is the preferred option.

A significant amount of work has been done in the field of Numerical modelling to produce probabilistic and deterministic forecasts of precipitation. Techniques that range from model output statistics to ensemble prediction systems have been utilized for this purpose (Bowler *et al.*, 2006). Comparatively little work has been done on Quantitative Precipitation Forecast (QPF) regarding Nowcasting. The main reason for the use of nowcasting techniques is that they can fully benefit from the spatial and temporal resolution that radars and satellites provide, because the execution time for a 6± hour lead-time forecast is much less than what a NWP model would be able to produce at the same spatial and temporal resolution. Therefore being able to produce and timeously update precipitation forecasts can significantly benefit both forecasters and use of hydrological models. This more immediate forecast will ensure sufficient time for warnings to reach the public, who will in turn be enabled to take precautions to limit or prevent damage to property and the loss of human life.

5.4.2 Nowcasting systems used internationally

5.4.2.1 Storm tracking, Auto-Nowcast and GANDOLF systems

A number of techniques are in use to produce nowcasts for precipitation. One of the most used methods involves extrapolation or translation of the precipitation fields. This mostly involves feature tracking based on the velocity and direction determined from the displacement of the feature identified in the precipitation or radar echo field. Cross correlation is most often used, and recently Optical Flow Constraints (OFC) vector calculation has been introduced to motion tracking. Used primarily for motion sensing in robotics, it allows for a motion vector for each pixel of the given resolution to be calculate (Bowler *et al.*, 2004).

A well-known example of a tracking algorithm available in use in South Africa is the TITAN algorithm (Figure 5.45) from NCAR (Dixon and Wiener, 1993). The biggest challenge with tracking algorithms is the forecast of growth and decay of storms. Linear extrapolation has shown to work best but a trend of at least 30-minutes needs to be established for it to be trusted (Mecklenburg *et al.*, 2002). Although tracking algorithms provides a forecaster with an abundance of information on storm size, movement, orientation and intensity, it still does not provide a reliable probabilistic and more importantly a deterministic field, which hydrological models use.

Systems like the Auto-Nowcast system (AN) from NCAR as well as the GANDOLF system is what are known as knowledge-based nowcasting systems. They make use of observational data and conceptual models that are based on studies done to gain information and understanding about the initiation, development and dissipation of precipitation (Mecklenburg *et al.*, 2002).

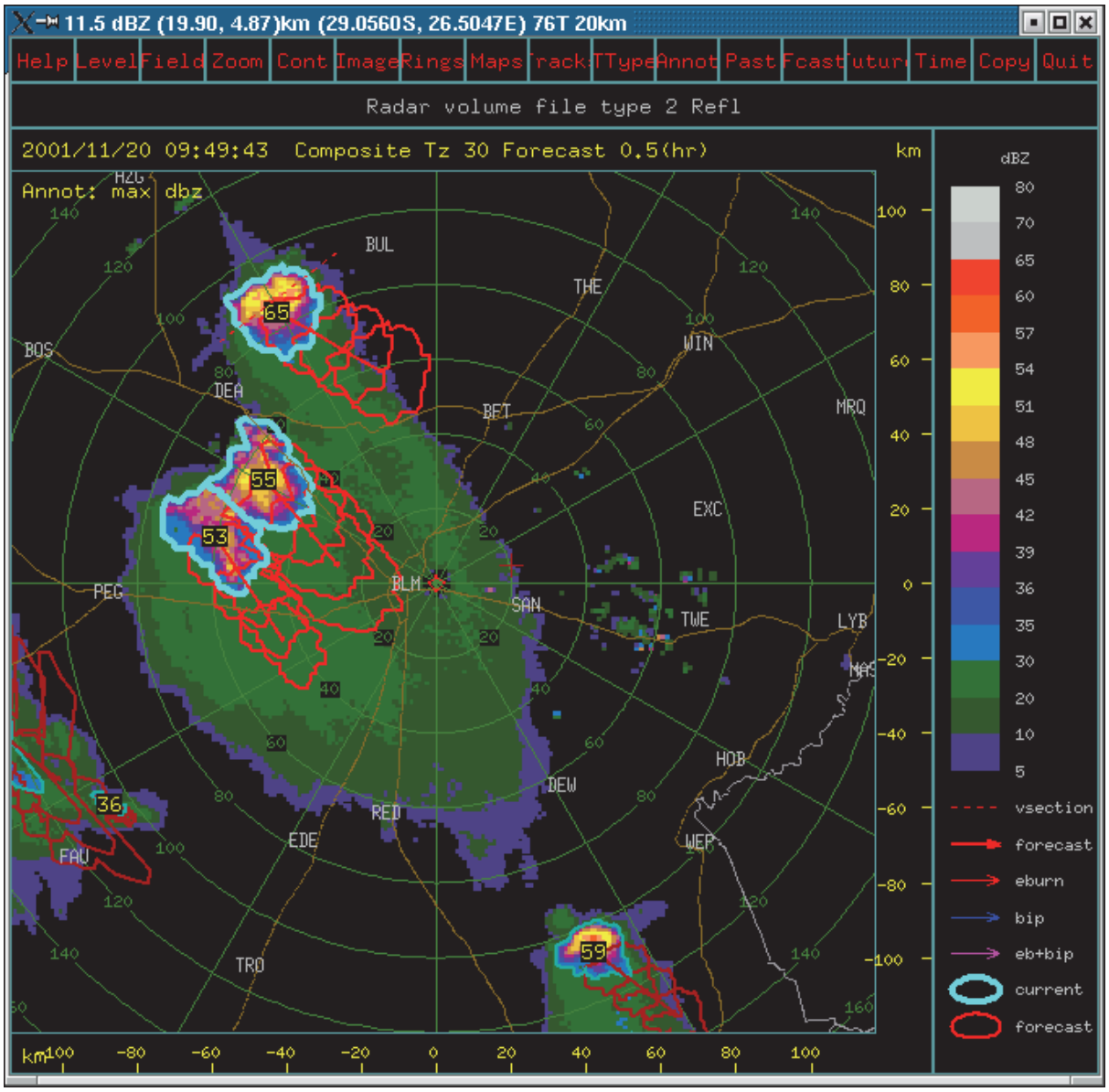

Figure 5.45: Example of the TITAN tracking algorithm

5.4.2.2 STEPS system

One of the most modern nowcasting systems is the Short-Term Ensemble Prediction System (STEPS) used by the Australian Bureau of Meteorology (BoM). A significant advantage of the STEPS system is that it includes some of the latest in nowcasting techniques, which can produce a probabilistic as well as deterministic precipitation forecast. STEPS is a powerful tool that incorporates extrapolation

techniques, Spectral Prognosis (S-PROG), Numerical Weather Prediction (NWP) blending, as well as ensemble prediction techniques that can produce deterministic and probabilistic forecasts of precipitation. These forecasts normally have a lead-time of up to 6 hours.

The STEPS system also uses extrapolation to produce its nowcast of precipitation. Extrapolation, however, has a number of sources that cause uncertainties in the evolution and motion of the Nowcast. Uncertainties in the evolution come from the basic assumption that coincides with extrapolation techniques, while uncertainties in the motion may come from within the calculations of the scheme. To try to minimize the errors associated with extrapolation growth and decay, STEPS uses the Spectral Prognosis (S-PROG) model (Seed, 2003). The evolution of precipitation is modelled by separating the large- and small-scale features in the precipitation pattern. The different spatial scales can then be treated independently. Large-scale features usually persist for longer periods while small-scale features, typically the least predictable, are replaced by stochastic noise. Thus, the assumption is made that large-scale features will persist while small-scale will be dominated by noise early on. The S-PROG model splits the field into additive cascades. Usually, eight different cascades (Figure 5.46) with small to large resolutions are created by means of a fast Fourier transform. An inverse transform returns the Fourier component back into the spatial domain. The result is a real-space decryption of the filtered data and not a Fourier representation. All the calculations of the evolution of the precipitation pattern within the forecast model are then performed on the cascades. The evolution of the field at each level in the extrapolation cascade is modelled using a second-order autoregressive (AR-2) process (Bowler *et al.*, 2006).

Advection velocity for precipitation from a sequence of rain analyses is determined by using an optical flow algorithm. Optical flow constraints are calculated by means of an advection equation that make the assumption that features in an image sequence only change shape and do not change in size or intensity. The velocity and motion for each pixel is then solved by a least squares approximation (Bowler *et al.*, 2004).

The STEPS system derives its Nowcasts from both radar based rain analyses and NWP model forecasts. To merge them with uncertainty estimates, three cascades are maintained: an extrapolation forecast cascade (as discussed above), an NWP model forecast cascade and a noise cascade. Estimates of the skill of the 2 forecast cascades determines the relative weights given to each cascade that allow a linear combination of the three cascades. Extrapolated forecast will become less skilful as the forecast persist especially at the smaller scales. To produce a useful forecast of at least 6 hours it is necessary to merge STEPS with NWP forecasts. This merging will allow the resultant precipitation nowcasts to maintain the large-scale dynamical evolution of the atmosphere on the precipitation field. Ensembles are then generated by choosing each member to have a different noise cascade.

NWP forecasts are made by the UK mesoscale model with resolution of 12km. Analysis on a 3-hour cycle uses 3D-Var analysis scheme. This is similar to what SAWS is running, with exception of the 3 hour cycle (SAWS runs it on a 6 hour cycle, but only once in 24 hours). Moisture Observation Pre-processing System (MOPS) and Latent Heat Nudging (LHN) are ingested into the models runs, thus reducing problems with spin up (Bowler *et al.*, 2006).

One of the central themes that drives much of the STEPS is the use of climatology. STEPS make real-time estimates on quantities like NWP skill and uses them in production of forecasts. The real-time

values are regressed to the climatology values as the lead-time increases. Figure 5.47 illustrates an example of a STEPS probabilistic nowcast.

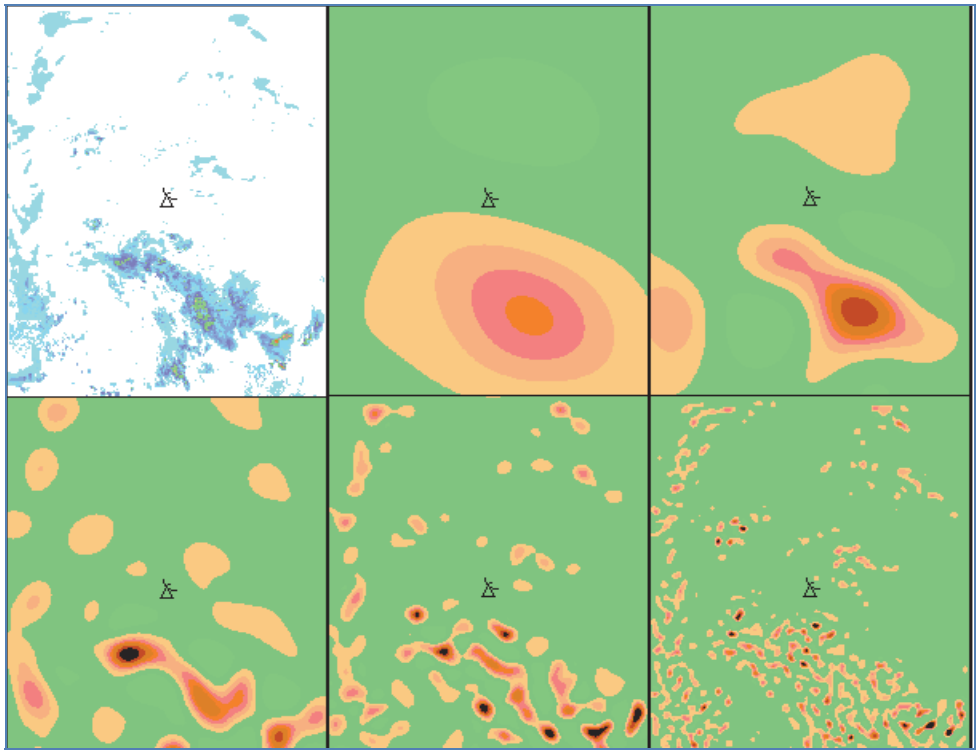

Figure 5.46: An example of S-PROG cascades within the STEPS system (Seed, 2009)

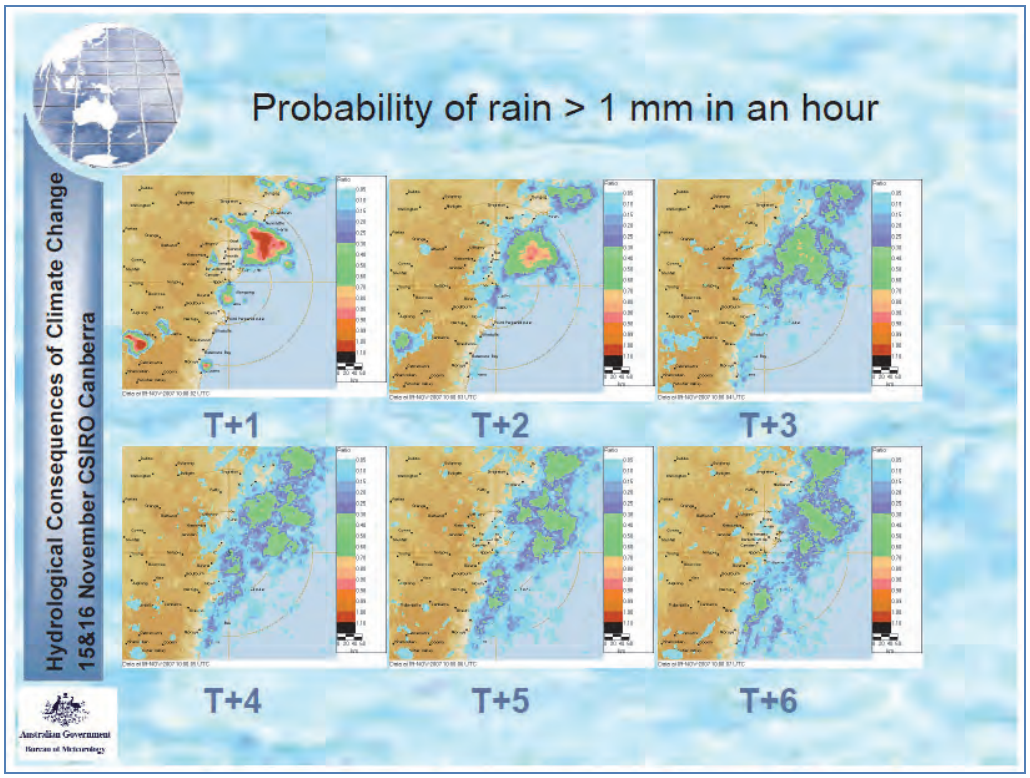

Figure 5.47: An example of a forecast from the STEPS system (Seed, 2007)

5.4.2.3 Rainbow "RainENCAST" product

The Rainbow software package uses the STEPS methodology in its RainENCAST (Ensemble Nowcasting) product. The RainENCAST uses radar rainfall from the Rainbow hydrology package to produce a forecast. No NWP blending is done at this moment in time. This means that only a lead-time of 2 hours can be achieved.

Ensemble forecasts are generated from variations of the input data (simulation of an observation error), variation of the advection fields (simulation of an inaccuracy of the tracking method) and variation of the rain data with each forecast step. This is to simulate an unknown development of precipitation (initiation, intensification and decay). The amount of this variation also depends on the skill of the ensemble nowcast derived from previous steps. The final product is a probabilistic and deterministic precipitation field shown in Figure 5.48.

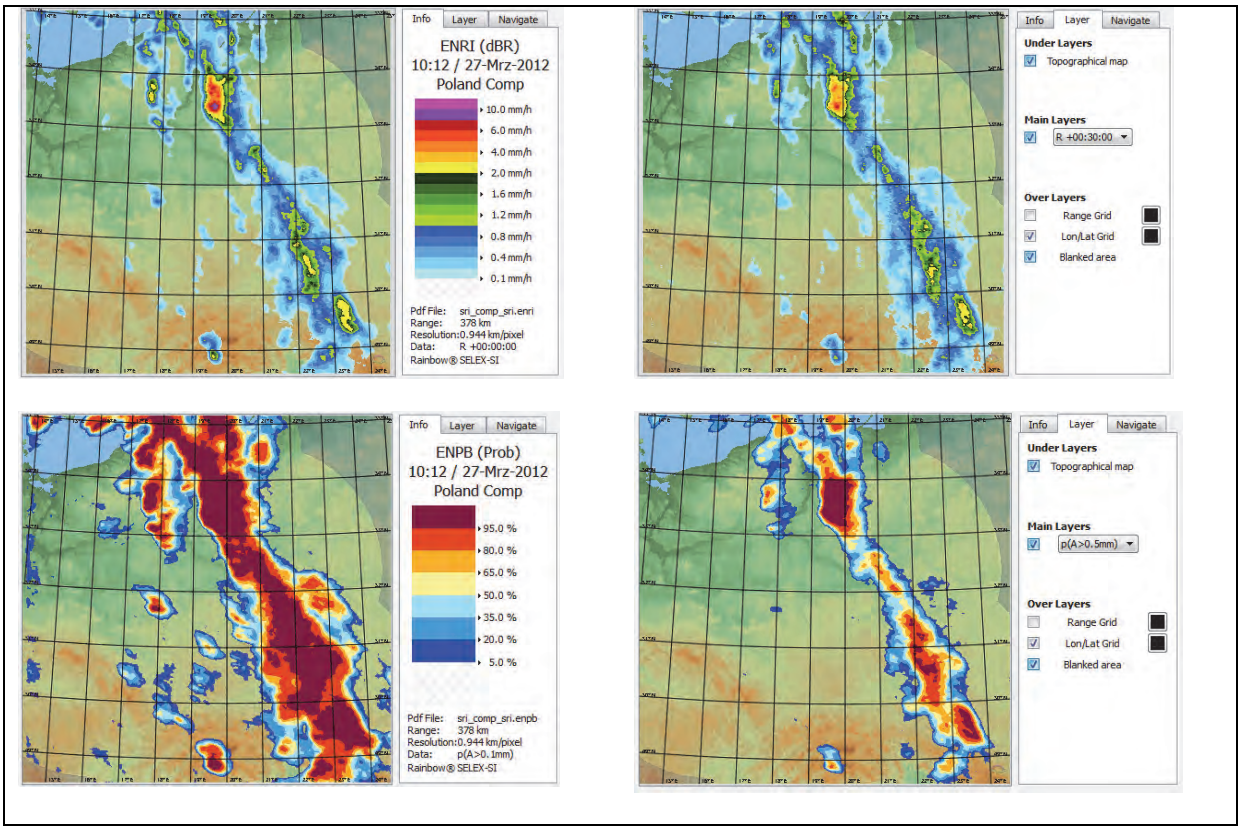

Figure 5.48: An example of Rainbow product output. Rain rate in mm/h (top left) with a 30min forecast (top right). A probability forecast of the area to receive more the 0.1 mm of rain (bottom left) and more than 0.5 mm (bottom right); (extracted from the Rainbow product manual).

5.4.2.4 Integrated Nowcasting through Comprehensive Analysis (INCA)

The Integrated Nowcasting through Comprehensive Analysis system (INCA) from the Central Institute for Meteorology and Geodynamics in Austria is a nowcasting system that uses observational data from weather stations, satellite and radar to produce an analysis field at a 1km grid resolution. It is specifically designed to aid in hydrological forecasts, support civil protection

activities and improve road safety. Observations are updated at 15 minute or 1 hour intervals depending on the parameter. Forecasts are computed based on two components. The first component is an extrapolation of the observation. The second component is the transition from the observation extrapolation to NWP model forecast, using a linear weighted function. Full weight is given to the extrapolated observations up to two hours ahead and is then linearly weighted to zero at 6-hour lead-time (Wang *et al.*, 2011). Figure 5.49 illustrates an example of the INCA temperature forecast. The system is web-based, which makes it easy to visualize and can produce multiple forecast parameters such as temperature, precipitation, wind, etc.

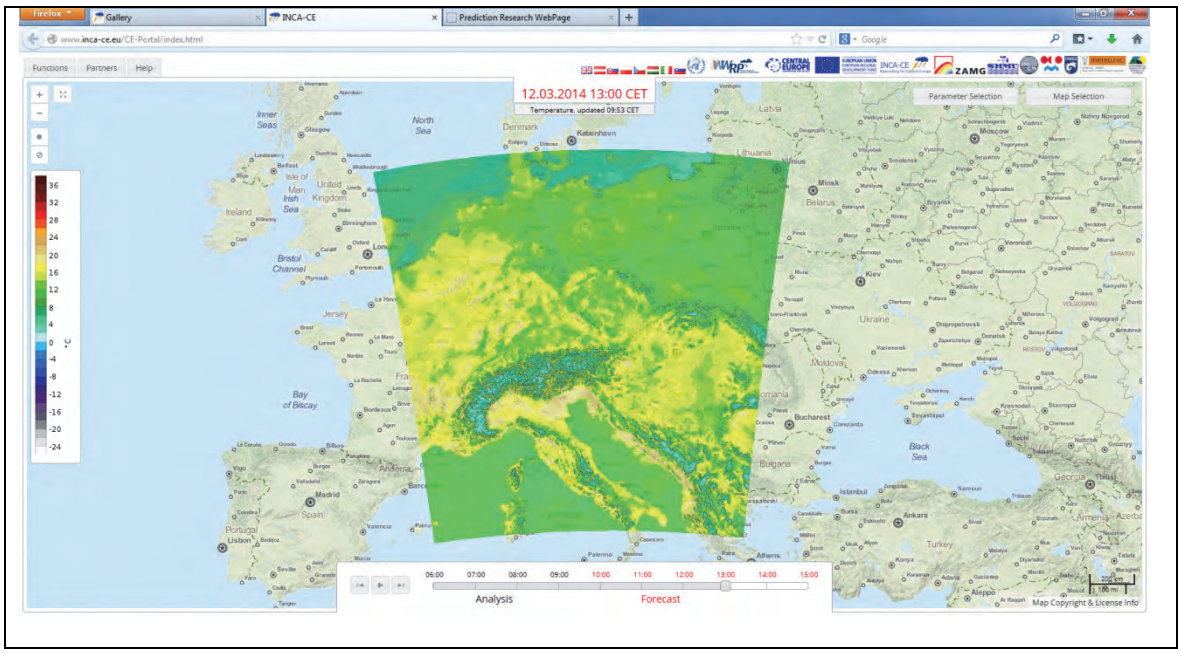

Figure 5.49: An Example of the INCA-CE nowcast output. Displayed is the temperature field +4 hours lead-time.

5.4.2.5 Using numerical weather prediction as a precipitation nowcasting tool

In the absence of viable radar-based precipitation nowcasting solutions (like STEPS or INCA), a less accurate option to provide a nowcast for the next 6 hours for the SAFFG and SARFFG systems, is the application of NWP forecasts. The NWP system to be used is the 12-km version of the Unified Model of the UK Met Office, run by SAWS under license over the SADC domain (UM-SA12). The UM-SA12 runs once a day, based on the midnight (00:00 UTC) model analysis, and predicts weather patterns and phenomena at an hourly output frequency for 48 hours on a 12 km grid.

NWP precipitation forecasts could be used in two different ways as 6-hour nowcasts in SAFFG and SARFFG. The first methodology implies the use of the accumulation of the relevant hourly rainfall forecasts from the deterministic model output into 6-hourly totals to produce a nowcast for the next 6 hours from the latest hour of the day as available in the SAFFG or SARFFG. This is demonstrated in Figure 5.50. This process is already operationally implemented in both SAFFG and SARFFG. As expected, the results are mixed, due to the inherent forecast uncertainty associated with NWP

rainfall forecasts. Examples of NWP deterministic model forecasts used in SARFFG are shown in Figure 5.51.

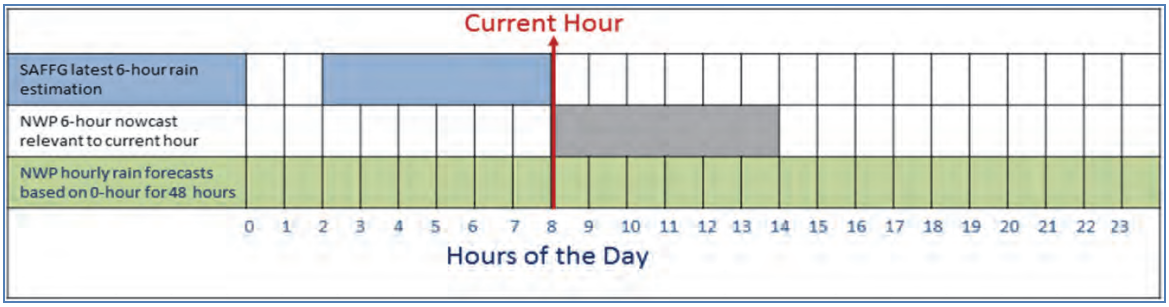

Figure 5.50: Graphical illustration of the 6-hour nowcast relevant to the current hour, say 08:00, based on an accumulation of the relevant NWP hourly forecasts for the next 6 hours from the current hour.

The second methodology uses an ensemble prediction system, which is a combination of different NWP forecasts to provide probabilistic forecasts of rainfall. In the absence of various NWP forecasts, an approach such as the Hybrid Ensemble Prediction system (HyEPS) as described in Section 6 could be used. HyEPS provide 30 ensemble members from a deterministic model for each basin, by using the mean areal precipitation of the nine surrounding basins as additional members, as well as the similar ten basins MAP for the previous 6-hours and those for the next 6-hours (see Figure 5.52). By comparing these 30 ensemble members with the FFG value, the potential flash flood threat can be determined as the percentage of members exceeding the FFG value for the basin. The HyEPS thus allows for the forecast uncertainty associated with NWP rainfall forecasting both in space (surrounding basins) and time (previous and next 6-hours basins), and thus produces a probabilistic forecast of the flash flood threat in the next 6 hours (see Figure 5.53).

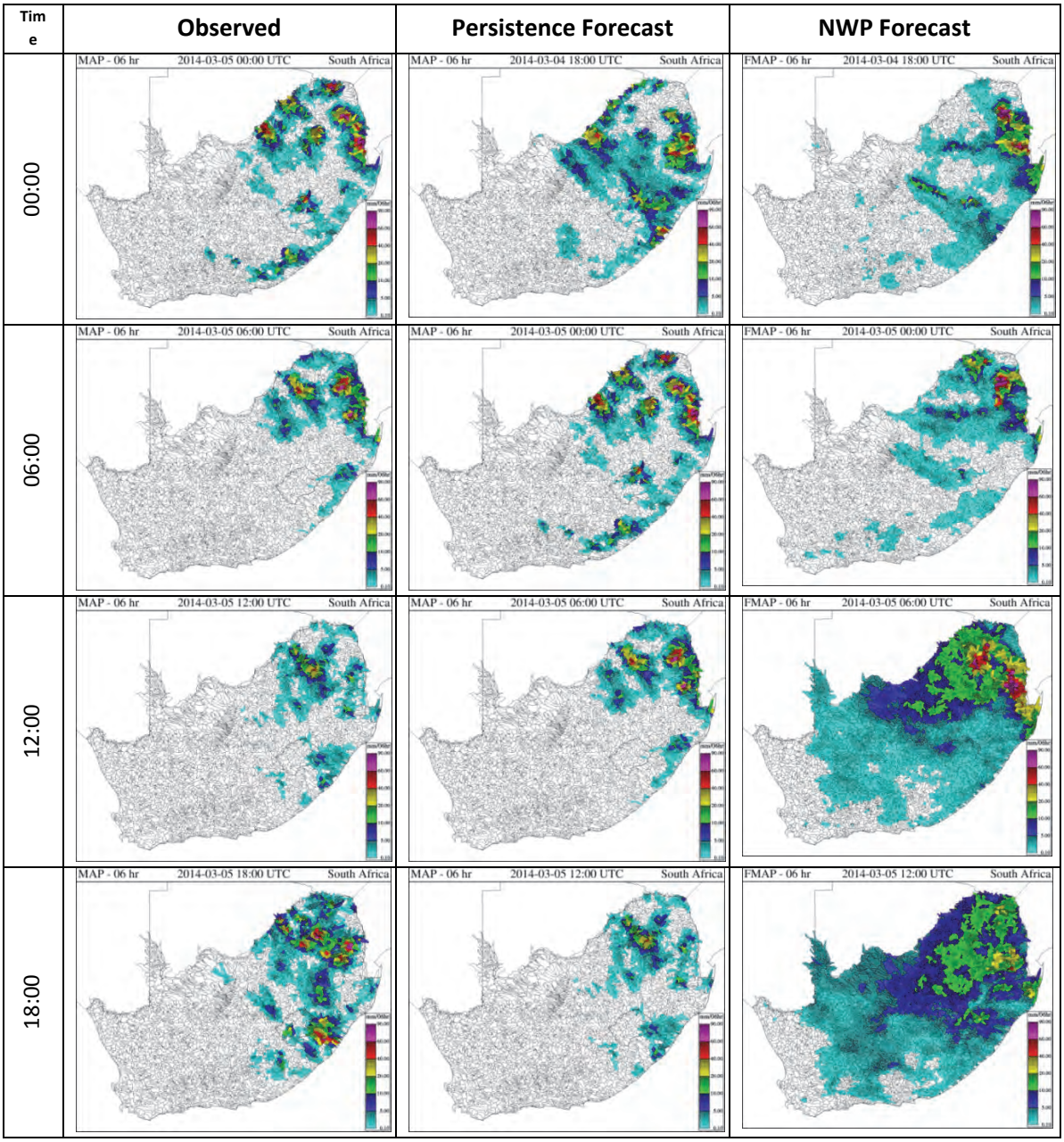

Figure 5.51: Example of NWP deterministic forecasts for 4 March 2014 used within the SARFFG to predict rainfall for the next 6 hours (right) compared to the corresponding SAFFG satellite observed 6-hour rainfall totals (left). The middle column is the persistence forecast using the previous six-hour satellite estimation.

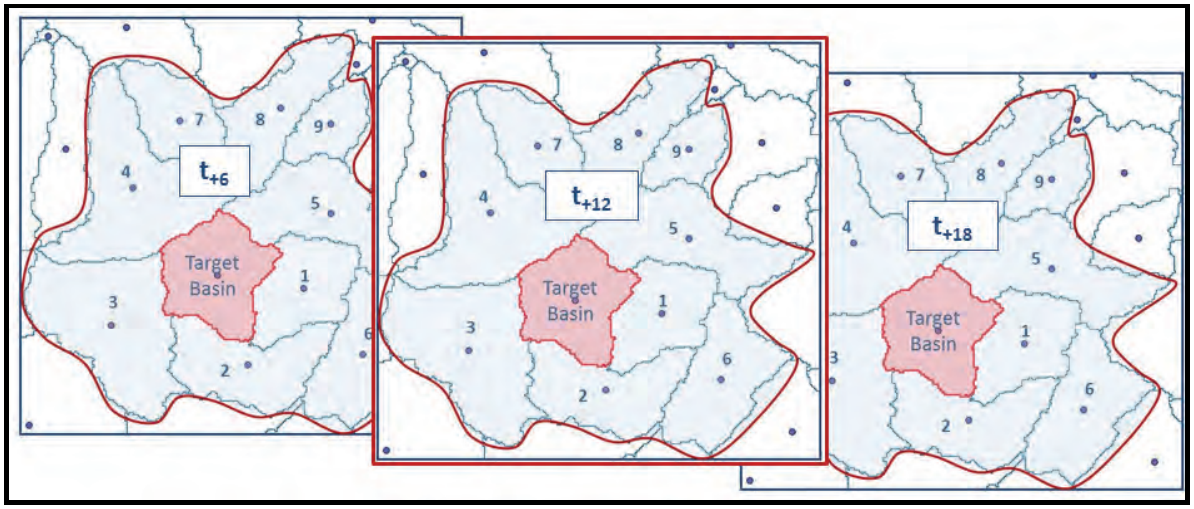

Figure 5.52: Graphical examples of 10 SAFFG ensemble member basins for the t+12 NWP forecast period associated with the target basin, and the associated basins of the previous 6-hour period and 6-hour subsequent period. This provides in total 30 EPS members for the target basin for the target t+12 forecast period (Poolman, 2014).

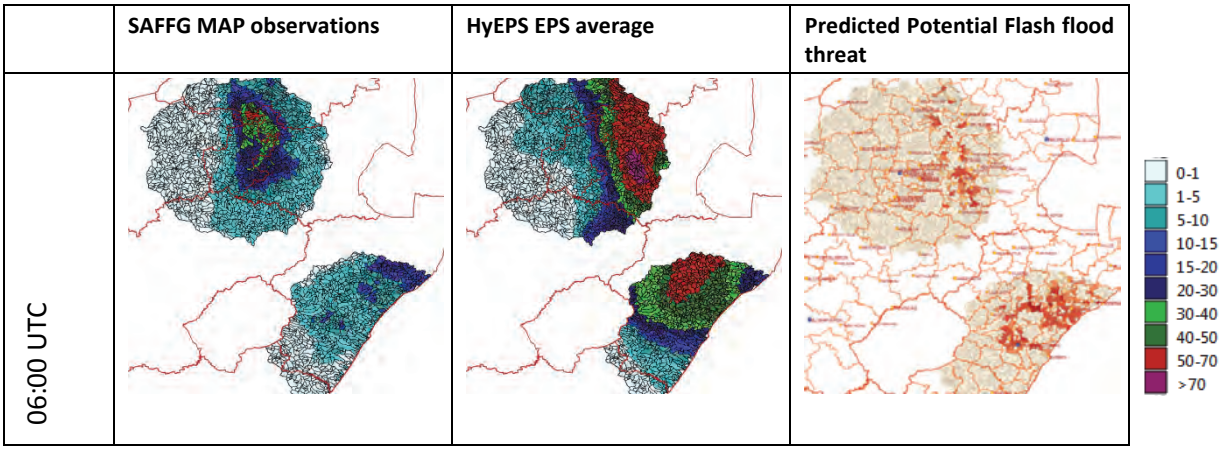

Figure 5.53: Comparison of the SAFFG MAP rainfall observations with the UM-SA12 xaang deterministic forecast and the HyEPS EPSave for 6:00 UTC and 12:00 UTC on 7 September 2012 (Poolman, 2014).

5.4.3 Summary

Various nowcasting systems are in operation worldwide, such as STEPS, Auto Nowcaster, INCA, etc. These systems are complex in nature and expensive to develop or implement. They rely heavily on real-time observational data and on skilled human resources.

Although the preferred method would be to use radar-based systems like STEPS or INCA, an alternative option is to use the hybrid EPS system, HyEPS, described in Section 6 to provide an objective rainfall nowcast for the 0-6 hour period, to be used in the flash flood guidance systems. A basic deterministic forecast from NWP is currently used in both SAFFG and SARFFG as predicted Mean Areal Precipitation fields, yielding reasonable results in many cases, and will continue to be used until the resources are available to upgrade to the stochastic forecasting tools.

6. INTEGRATED DISASTER MANAGEMENT APPLICATIONS TO ENHANCE DECISION MAKING

6.1 INTRODUCTION

The ISDR (2005a) emphasized that better local management and decision-making in the warning process is critical, even more so than promoting more advanced technology. Auld (2008) pointed out that a successful warning system will result in effective response mechanisms. This approach needs comprehensive information be conveyed to the user to enable a meaningful translation of the warning into disaster risk information a specific environment to allow life-saving decisions to be made. Improvements to the decision-making process, right through the early warning chain in the short-term forecasting time scale using meteorological information, will lead to more effective and earlier responses from the disaster management structures. This could lead to increasing the lead-time of useful decisions and in so doing contribute to saving lives and property.

The challenge of making effective communication of forecasts to users is a growing concern of hydrometeorological communities. Various publications highlight the need to improve the communication of forecasts to enable users to make effective decisions in their particular environments (Auld,2008; ISDR, 2005a; WMO, 2008; NRC, 2006; Golding, 2009; Joslyn *et al.*, 2009a, 2009b, 2010; Morss *et al.*, 2008, 2010; Demuth *et al.*, 2009; Vogel and O'Brien, 2006). These users range from the ordinary householder to specialized decision makers such as disaster managers.

The challenge to scientific service organizations, such as SAWS, is to provide user-friendly products in a way that users can directly use them within their decision support systems. This includes conveying a message of forecast uncertainty to users in such a way that it can have a significant influence on their decision-making, as long as it is conveyed in an understandable way. More often than not weather related products tend to be too scientific and not tuned to the specific needs of the users.

Added to the above is the continuous requirement of increasing the lead-time of forecasts and warnings of hazardous weather. This requires innovative application of NWP and EPS capabilities. The development of increasing lead-time of flash flood events is particularly complex, since it requires a combination of meteorological modelling and hydrological applications such as SAFFG, taking into account forecasting uncertainty associated with both.

The SAFFG is described in detail in Chapter 3. In Figure 6.1 typical images of the SAFFG system are presented, with a comparative image of the FFG for SARFFG. The latter represents the entire South Africa at a larger resolution (Section 3.1). The following discussion on forecast uncertainty and improving the lead-time originates from Poolman (2014), and addresses the forecast uncertainty in the SAFFG system through the Hybrid Ensemble Prediction System (HyEPS).

6.2 IMPROVING THE LEAD-TIME OF FLASH FLOOD GUIDANCE TO END-USERS

6.2.1 Forecast uncertainty within the SAFFG system

Addressing the problem of forecast uncertainty in an integrated system such as the SAFFG is a complex process. Eventual forecast uncertainty in the SAFFG system is a combination of uncertainty associated with different model elements throughout the chain from data ingestion and model components to the eventual presentation and use of forecast products by the disaster manager. Table 6.1 presents a high-level overview of the major uncertainty components in the SAFFG modelling chain, together with the likely sources of uncertainty in each component, and how these might be (or are) mitigated to minimize uncertainty as far as possible.

Neither SAFFG, nor SARFFG provides flash flood guidance information, beyond the next 6 hours, or over the next 24 hours, that could provide longer lead-time on potential flooding in small river basins. Consequently, an outlook methodology needs to be developed to project the latest available 6-hour FFG values in 6-hour steps to 24 hours ahead, and then to compare this series of 6 hour FFG values with predicted rainfall for similar 6-hour periods (see Figure 6.2). Basins where an excess of rain over and above the FFG value is predicted could then be deemed to be in potential danger of flash flooding in the next 24 hours, given the current state of soil moisture.

An important assumption of this methodology is that the persisted FFG values will remain the same in the subsequent 6-hour periods as were predicted by SAFFG (see Figure 6.2). Additional rain can actually increase a basin's soil moisture fraction and thus the potential for flooding, or a lack of rain will do the opposite. This problem can only be corrected by major modifications to the SAFFG hydrological modelling system to include predicted rain over the subsequent 6-hour periods; this work is outside the scope and capability of this project. However, it is suggested that the main purpose of this extended "advisory" period (18 to 24 hours) is to identify areas of potential flooding as an alert to disaster managers for early preparation, and therefore not necessarily down to the detail of the individual SAFFG basins. This assumption is used in the development of final products of the outlook methodology in subsequent sections of the project.

The challenge of the outlook methodology is to predict accurately the amount of rain likely to fall in 6-hour periods in the next 24 hours. This can currently only be addressed by means of numerical weather prediction (NWP) models. The NWP model used in the South African Weather Service (SAWS) is the 12 km resolution Unified Model (UM SA12) of the UK Met Office run by SAWS, covering Southern Africa. This model runs in hydrostatic mode, with a rainfall parameterization scheme to determine hourly amounts of rainfall at grid points. By definition, the amount of rainfall at a grid point represents the average amount of rain predicted over a box with the size of the model resolution (12 x 12 km^2) and centred over the grid point.

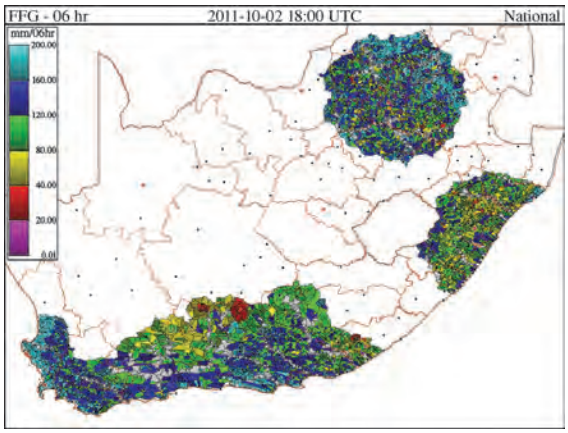

(a)

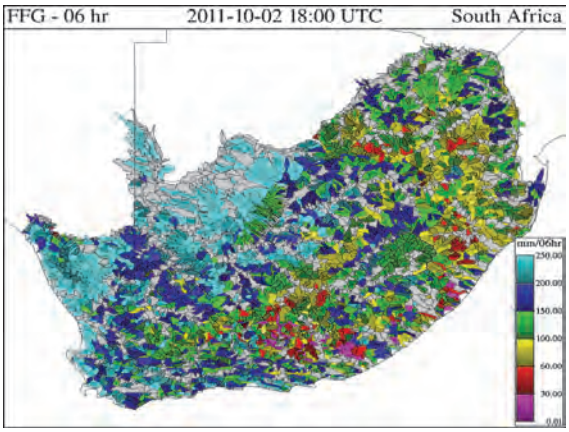

(b)

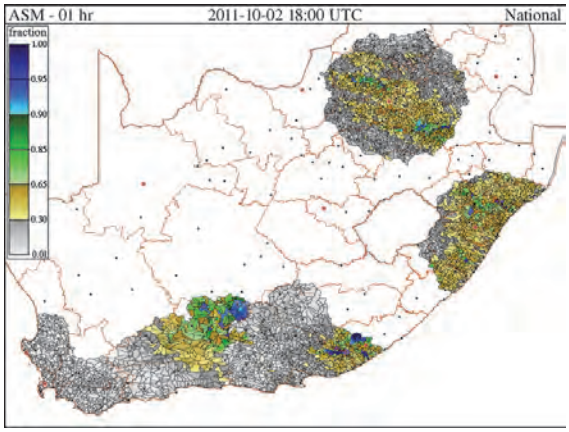

(c)

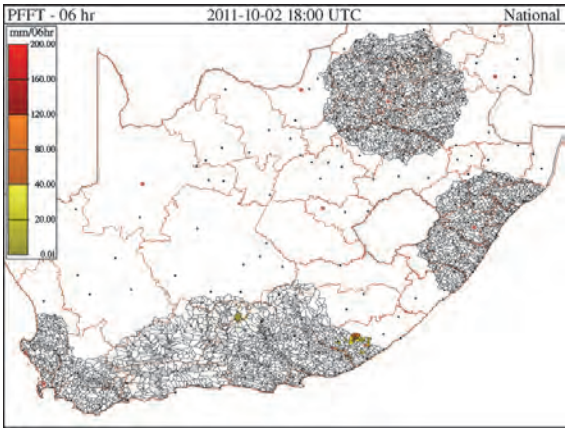

(d)

Figure 6.1: On the top left (a) is a typical 6 hour flash flood guidance (FFG) field of the SAFFG, illustrating the domain of SAFFG, as well as the small basins and what an FFG field indicates. The image on the top right (b) is a similar image, but from the WMO regional SARFFG system covering entire South Africa with larger basins. Image (c) is the fraction of soil moisture in the upper layer due to recent precipitation. Image (d) is the flash flood threat (FFT) indicating only basins where an excess of rain might occur if the precipitation of the past 6 hours is persisted for the next 6 hours corresponding with the FFG period.

Table 6.1: Major components of forecast uncertainty in the SAFFG system (Poolman, 2014)

SAFFG system Component	Sources and impacts of uncertainty in the system modelling chain	Mitigation of uncertainty
1. Basin delineation and hydrological feature representation	Satellite resolution, quality of GIS information used for parameterization of basin and soil properties in 50 km^2 basins, assumptions regarding the stream cross section properties	Meticulous preparation of parameterization and basin properties by developer (HRC) using best available information
2. Radar and satellite estimation of rainfall, and bias correction, calculation of mean areal precipitation (MAP)	Radar and satellite are both covering the basin with indirect measurements of rainfall bias corrected by actual point measurement by available gauges. Inherent quality of the radar and satellite information, including radar calibration, rainfall algorithms, etc., impacts on uncertainty.	Continuous efforts in improving the methodology and algorithms of rainfall calculations from remote sensing platforms. Technical care of radar, satellite and rain gauges.
3. Hydrological modelling of soil moisture and flash flood guidance	Inherent uncertainty in hydrological modelling based on remote sensing information	Careful adjusting of hydrological modelling during development phase by developer (HRC)
4. Prediction of rainfall for the next 1, 3 and 6 hours	The basic SAFFG system has no rainfall prediction capability, the previous 1, 3 and 6 hour rain are persisted to the coming 1, 3 and 6 hours as a first guess	Ensemble forecasting methods of remote sensing information, such as STEPS
5. Forecaster interpretation of SAFFG products	Forecaster ability to combine uncertainty of rainfall prediction with flash flood guidance (FFG) of required rainfall per basin.	Effective use of NWP as deterministic or ensemble systems.
6. Effective use of forecaster information and SAFFG products in decision-making by disaster management.	Perception and understanding of forecaster products by disaster manager. Complexity of SAFFG products hamper effective use in end-user decision making. Inability of system to project flash flood potential beyond the next 6 hours is a major source of uncertainty affecting disaster management planning.	Tailored products to suit end-user decision making, including impact forecasting. Using NWP ensemble prediction methodology to project flash flood potential beyond 6 hours to support disaster management early preparation and planning.

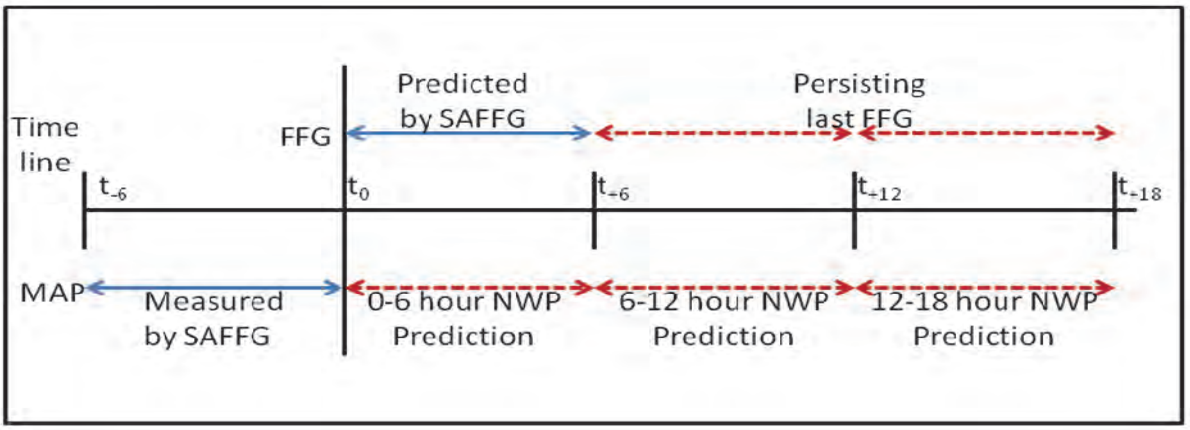

Figure 6.2: A graphical presentation of the timeline of events. At time t_0 the MAP of period t_{-6} - t_0 measured through the SAFFG system is used to calculate the predicted FFG field for period t_0 - t_6. This FFG field is then persisted for the next few 6-hour periods. It is compared with NWP ensemble predicted rain for the same 6 hour periods to determine where NWP predicts that a likelihood for rain to be in excess of the FFG rain exists, indicating a potential flash flood threat (Poolman, 2014).

Numerical models are notorious for their inaccuracy of precipitation forecasts in terms of exact location, the timing of particularly convection, and even the total amount of rainfall (Theiss, *et al*, 2005). This level of inaccuracy also differs between model configurations, for example when the same basic model system is used but with different initial conditions. When attempting to use a single numerical model to accurately predict rainfall for small river basins, this uncertainty linked to model prediction of rainfall is significant and can becomes problematic. This problem can be addressed by using an ensemble of NWP forecasts that attempt to predict the uncertainty of the exact location of convective elements, given the added problem of timing of convective precipitation during the day. Since a high-resolution ensemble consisting of 20 or 30 model runs is not available, a "poor man's ensemble" concept has to be applied. Ebert (2001) has found the "poor man's" ensemble approach more skilful than any of the individual model runs in her study. She actually found the greatest improvement using this ensemble in its ability to improve the accuracy of locating the rain pattern, by reducing the displacement error by 30%. She also found that at least seven members of a "poor man's" ensemble are needed to produce the best forecast skill. In the South African context, 2 to 3 versions of the Unified Model are readily available, and therefore a different approach was needed. This approach combines the available members (2 to 3 UM models) with the approach of Theis *et al.* (2005) of defining probabilistic precipitation forecasts from a deterministic model. In this way the "hybrid ensemble system" (HyEPS) was conceived.

6.2.2 Methodology

The HyEPS scheme was developed using a hybrid ensemble of the 2 to 3 operational model configurations of the UM SA12 NWP to determining the likelihood of predicted mean areal precipitation (MAP) exceeding the FFG for the SAFFG basins. These configurations were:

- Xaana: output of the basic 12 km UM, running straight from the initial fields and boundary conditions as received from the UK Met Office. This model usually runs early in the morning and is the first prediction available to forecasters at about 6 o'clock in the morning;

- Xaang: similar to xaana, however an additional data assimilation cycle is done locally before the model runs. The products of this version are usually available around 8 o'clock.
- Xaant: an upgraded version of the UM model, running with data assimilation during the morning, available by midday.

The first step was to determine a MAP value for every small river basin, from the model-predicted rainfall data, of each of the different UM SA12 configurations. These NWP based MAP values needed to be bias corrected before they could be used to compare against the SAFFG system's FFG rainfall values. Then a hybrid ensemble prediction system, which combines the MAP amounts of the different models as well as those of surrounding basins, was developed to predict probability of precipitation in the basin exceeding its particular FFG amount. The following sections elaborate on these three steps.

6.2.2.1 Determining a Mean Areal Precipitation (MAP) value from numerical models for each SAFFG basin

Hourly precipitation forecasts of the UM SA12 model, integrated into 6-hour totals, were used to calculate UM-predicted mean areal precipitation (UM-MAP) values for each SAFFG river basin. This was done for all three available UM SA12 model configurations separately, in preparation for the NWP ensemble system output following later. The basic process is similar to the process employed in the SAFFG system (Sperfslage *et al.*, 2010, and personal communication with K. P. Georgakakos). By definition, a precipitation value at an NWP model grid point represents the average rain at a grid box around the grid point (see Figure 6.3(a) and (b)).

GIS shape files of both the SAFFG basins and the UM SA12 gridded rainfall data were loaded into a QGIS system. Using a function in QGIS, the relevant NWP grid points associated with each river basin were identified. At the relatively high resolution of 12 km, the small size of SAFFG basins implied that it would be difficult to find more than even one grid point in many river basins. This was overcome by interpolating the 12 km grid to a 4 km grid using an equal block approach. This implies that the 4 km grid boxes within an initial 12 km grid box are allocated the same value as the associated 12 km grid box (Figure 6.3 (b) and (c)), but represent now only a 4x4 km domain. In this way it was possible to calculate UM-MAP for most SAFFG basins as a simple average from at least four grid boxes of the 4 km resolution grid that resides within the basin. For those few basins still not having at least four associated grid points the nearest four 4 km grid points were identified through a FORTRAN computer program and an inverse weight scheme used to determine their relative contribution to that basin's UM-MAP.

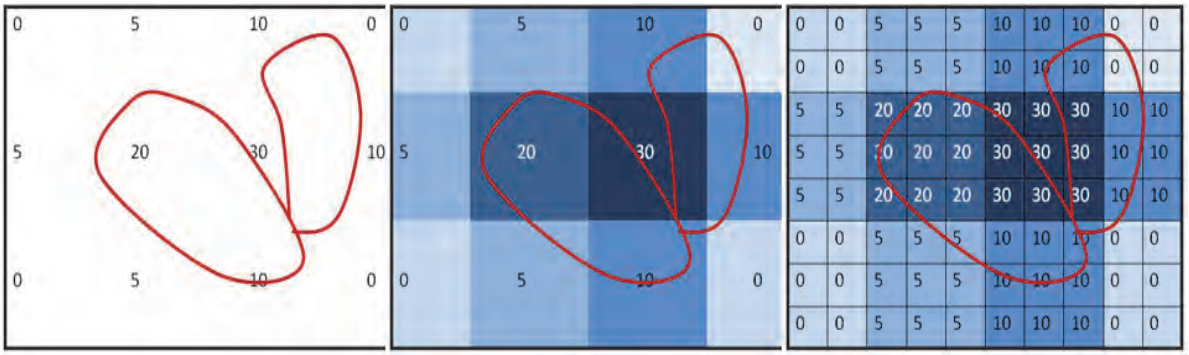

(a) **(b)** **(c)**

Figure 6.3: Example of interpolation of 12 km grid boxes to 4 km grid boxes for calculation of UM SA12 Mean Areal Precipitation (UM-MAP) amounts. (a) Distribution of 12 km grid points relative to imaginary SAFFG basins. (b) Representative grid boxes of 12 km precipitation grid points. (c) Interpolation of 12 km grid boxes to equal 4 km grid boxes used to calculate UM-MAP amounts (Poolman, 2014).

6.2.2.2 Bias correcting the mean areal precipitation forecasts

A major problem encountered was the inability of the NWP models to predict accurately the amount of rain that will fall in a basin. The mean areal precipitation (UM-MAP) was severely underestimated by all model configurations, and differed between UM configurations. Figure 6.4 (a) and (b) show vast underestimation of 6-hour rainfall amounts, averaged over 25 cases, compared with the corresponding SAFFG MAP totals in Gauteng in 2011. This emphasized the need for bias correcting each NWP model's UM-MAP to enable fair comparison with FFG values for the same basins from the SAFFG system.

Bias correction factors (BCF) for each model were calculated by determining the ratio of the sum of UM-MAP values of a large number of basins for a large representative region, summed over 25 cases in 2010, with the similar sum of the observed MAP of the corresponding basins of the SAFFG system for the same 25 cases. The formula computing BCF is: $BCF = \frac{\sum_{i=1}^{25}(\sum_{i=1}^{2101}(MAPum))}{\sum_{i=1}^{25}(\sum_{i=1}^{2101}(MAPobs))}$ where *MAPum* are the UM-MAP amounts per basin and *MAPobs* are the MAP values determined by SAFFG from radar, satellite and gauge observations.

In the case summarised in Figure 6.4, the large representative region used was the area covering all 2101 basins under the radar footprint of the Irene radar. The SAFFG observed MAP amounts of the SAFFG system were derived from radar observations or from satellite rainfall estimation data, bias corrected using rain gauges. Thus, the MAP values of the SAFFG system were assumed "observations" against which the UM-MAP can be bias corrected. This was thought to be acceptable, since the FFG product of the SAFFG was determined using the same radar/satellite based MAP values of SAFFG to calculate soil moisture and ultimately the FFG values. The UM-MAP must be compared against these MAP values, using the same reference scale, namely SAFFG basins.

Figure 6.5 presents a comparison of the sum of all UM-MAP amounts under the Irene radar for one day (10 Jan 2012) with the sum of the same SAFFG basin MAP amounts for the xaana and xaang UM SA12 model configurations before and after bias correction.

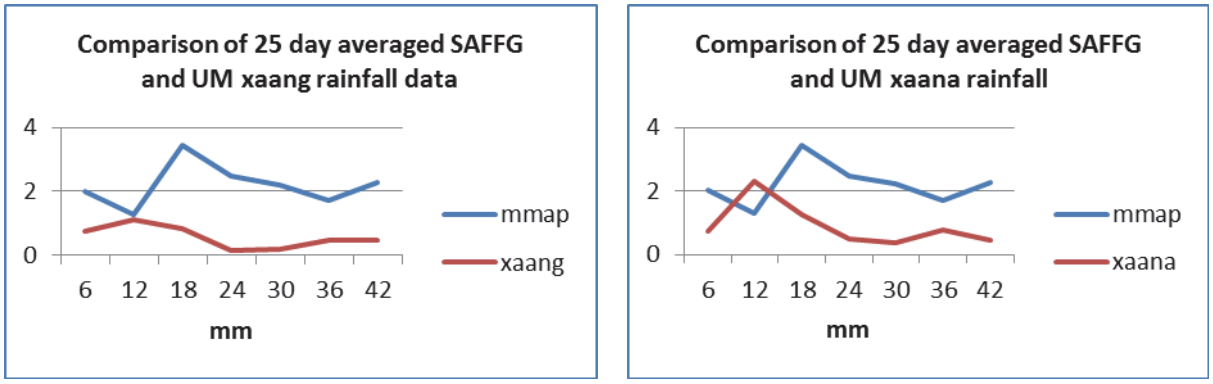

(a) (b)

Figure 6.4: Comparison of the sum of all UM-MAP amounts (um) under the Irene radar, averaged over 25 cases, with the sum of the same SAFFG basin MAP (mmap) amounts for the xaana and xaang UM SA12 model configurations. Panel (a) show the xaang model comparison and (b) the xaana model comparison.

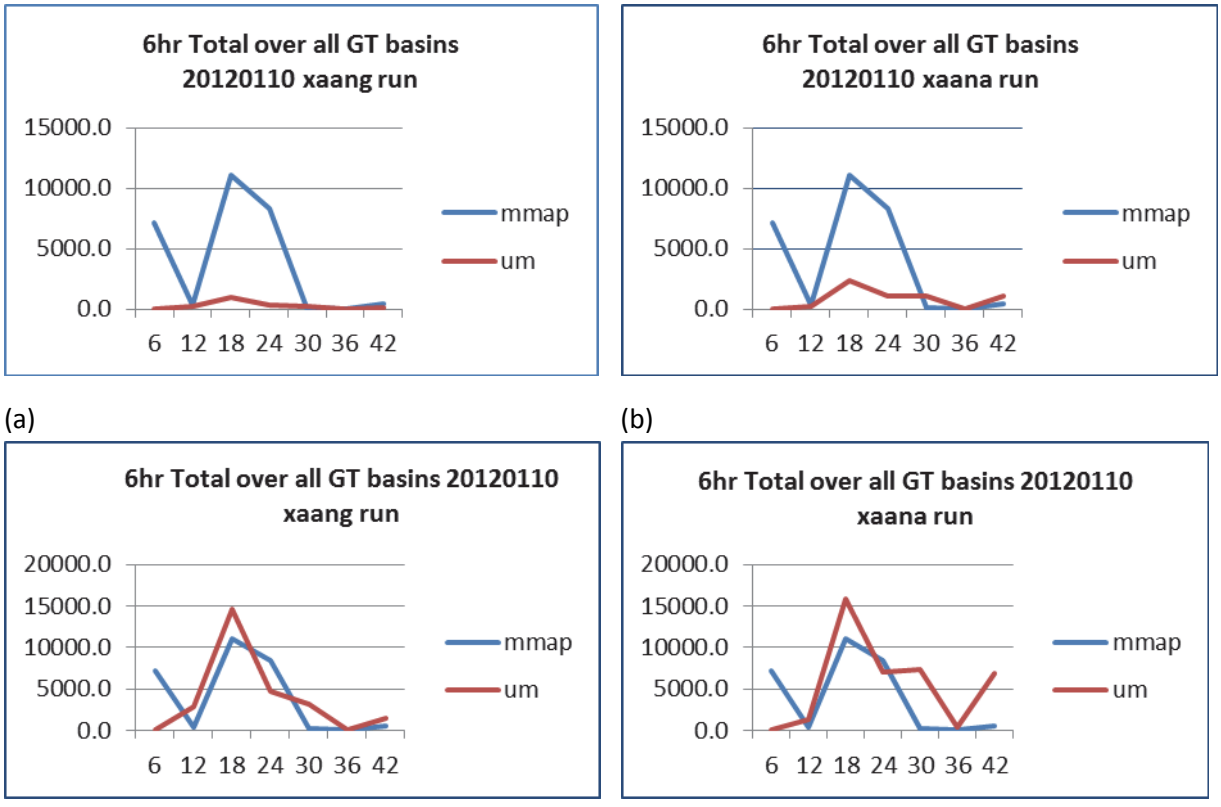

(a) (b)

(c) (d)

Figure 6.5: Comparison of the sum of all UM-MAP amounts (um) under the Irene radar for one day (20120110) with the sum of the same SAFFG basin MAP (mmap) amounts for the xaana and xaang UM SA12 model configurations. Panel (a) show the xaang model comparison and (b) the xaana model comparison before any bias correction. Panels (c) shows the xaang and (d) the xaana models comparison after individual bias correction factors were applied to the UM-MAP amounts as calculated for that specific day only.

6.2.2.3 Addressing uncertainty through a hybrid ensemble approach

Within each of the three versions of the NWP models, the problem of locating convection implies that even though the model may be quite accurate in predicting convection for a region, it may be misplacing the rain compared to where it actually occurred. In addition, NWP models tend to start convection too early in the day, so that timing within the correct 6-hour period may be quite wrong.

This is illustrated in a scatter plot for 10/01/2012 of the UM-MAP values and the corresponding SAFFG observed MAP values in Figure 6.6. The wide scatter of data in the two graphs illustrates the problem of accurate spatial distribution of NWP rainfall predictions, particularly for small areas such as the SAFFG basins. Since the model did predict convective rain for the day, it may well have the broad pattern in place, but the exact positioning of convective elements may be in neighbouring basins. This Figure also demonstrates an extreme case of underestimation where the highest model predicted value in the entire xaang configuration of the UM model domain was only about 5 mm, whereas SAFFG measured more than 71 mm as the highest. Other case days did not necessarily show such large underestimation.

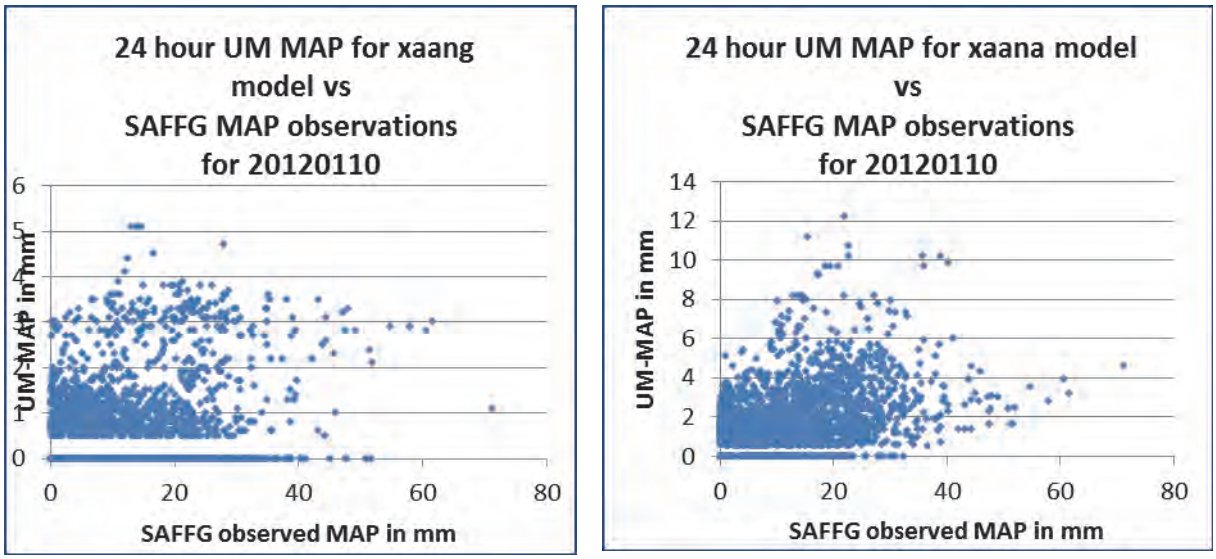

(a) (b)

Figure 6.6: Scatter plot of basin specific UM-MAP values for two model configurations, and the corresponding SAFFG observed MAP values, for 2102 basins under the Irene radar on 10/01/2012. (a) depicts the scatter plot for the xaang model and (b) for the xaana model

Both the spatial and the convection timing challenges were addressed through a hybrid ensemble approach as described by Theis *et al.* in 2005. They identified a "neighbourhood" of grid points from the same model around the target grid point whose rainfall values could just as well be associated with the target grid point. A methodology similar to the methodology of Theis *et al.* was adopted in the system described here covering an 18-hour period, except that SAFFG basins were used instead of NWP grid points as shown in Figure 5.52.

The nine closest SAFFG basins around each target SAFFG basin were identified using GIS and a FORTRAN program. These ten basins, providing ten ensemble members, accommodated the spatial uncertainty, i.e. the possibility that the precipitation predicted by the model over any neighbouring basin actually occurred over the target basin. Similarly, the potential offset in timing of the convection was addressed by including the same 10 basins from the next two 6-hour prediction periods into the ensemble set. In this way, the ensemble consisted of 30 basins based on precipitation forecast of one model, covering an 18-hour outlook period.

Using the approach of Theiss *et al.* (2005), the process in this study allowed the same methodology for two other available UM SA12 configurations to be used, providing in total 90 possible members, or solutions, for the target basin. From this ensemble set, the number of members whose UM-MAP exceeds the FFG value of the target basin could be determined which provides an estimate of the likelihood of flash flooding in that particular basin during the chosen 18-hour period. The Hybrid Ensemble Prediction System described here is referred to as the HyEPS.

6.2.2.4 Flash flood outlook products from the hybrid ensemble prediction system

From the HyEPS, probabilistic related information was extracted representing the 18-hour window period. These included the ensemble average (EPSave) and the ensemble maximum value (EPSmax) which is the highest UM-MAP value of all 90 members. Both values could be compared against the basin specific FFG value to identify the potential magnitude of flash flood events, with EPSmax representing the rainfall for the extreme scenario for the target basin. The Flash Flood Potential (FFP) of each basin over the 18-hour window period was calculated as the probability of the basin ensemble exceeding the last known FFG value of the basin. This was done by calculating the percentage of ensemble members in the 90-member basin ensemble set that exceeded the FFG value of the basin. Finally, the flash flood hazard index for a LM (LM-FFH) was determined as the percentage of SAFFG basins within a local municipality with a positive FFP. These parameters represented the basin specific potential for flash floods and the LM flash flood hazard risk over the 18-hour forecast period. For comparison, this was done for all the configurations of the UM-SA12 model.

The computations described above used the precipitation forecast products of a deterministic model and do not require large computer resources. Hence, it is quite suitable to be applied in smaller weather services, even those not running their own NWP model, which have access to the gridded rainfall output of a model run at a regional or global weather centre.

6.2.2.5 Projecting Flash Flood Guidance information to the next 18 hours

Referring to Figure 6.2, future 6-hour FFG values are needed to be compared with the predicted UM-MAP values in order to identify which basins could receive more rain than required for bank full at the basin outlet, and thus potential flooding. This implies that the soil moisture, and hence the FFG for future 6-hour periods, needs to be modelled based on the previous 6-hour's MAP. In the current configuration of the SAFFG modelling system available for this study, however, it is not possible to predict FFG values beyond 6 hours in advance. Although such an approach would be useful, it will require a substantial change to the hydrological modelling system.

Consequently, the only other approach is to extrapolate, or persist, the latest available 6-hour FFG values in 6-hour periods up to 18 hours in the future as shown in Figure 6.2. This approach assumes that the soil moisture content, and thus the FFG values in the basins, do not change significantly in the subsequent 12 hours. This assumption is not true, particularly if significant rain fell which could lead to saturation of the top soil, reducing FFG values. However, it is suggested as an acceptable assumption for this limited additional period based on Figure 6.7.

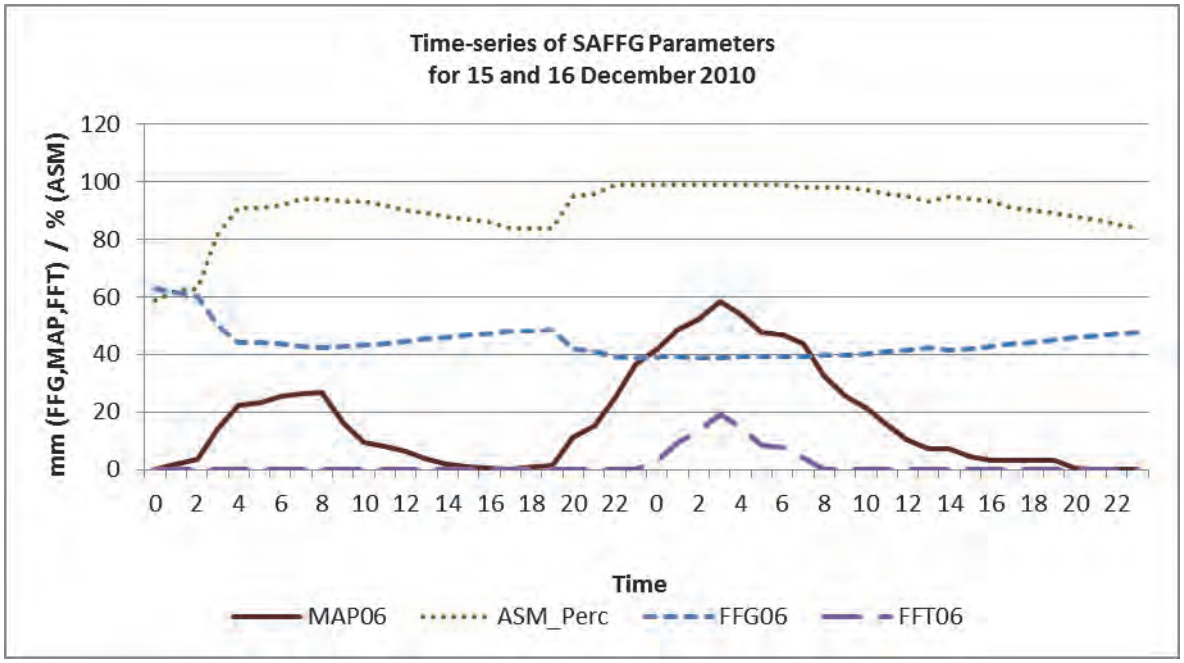

Figure 6.7: A graphical representation of the four main parameters of the SAFFG as they evolved during the flash flood event of 15 and 16 December 2010 for a specific basin in Dipaleseng Local Municipality. ASM_Perc is the saturation percentage of the top-layer soil moisture, MAP06 the 6 hour running total of MAP as observed by SAFFG from radar data, FFG06 is the 6-hour flash flood guidance, and FFT06 is the 6-hour flash flood threat if the MAP06 of the previous 6 hours is persisted for the subsequent 6 hours, obtained by subtracting FFG06 from MAP06.

Figure 6.7 is a graphical presentation of how the main relevant parameters in the SAFFG evolved hourly in a flash flooding situation in a typical SAFFG basin south of Johannesburg on 15 and 16 December 2010. Two rain episodes can be identified from the MAP06 graph in Figure 6.7. The first rain episode lasted from 02:00 to 10:00 UTC on the 15 December 2010, and the second rain episode lasted from 18:00 UTC on the 15th to 14:00 UTC on the 16th. The response of the SAFFG soil moisture saturation (ASM_Perc) and FFG06 parameters to the heavy rain (the solid line MAP06) is quite evident in both rain episodes. The soil moisture saturation level (ASM_Perc in top dotted line) jumped from 60% to about 90%, decaying slowly and then jumped from 85% to 100% where it stayed a while before decaying slowly again. The FFG06 was already at about 60 mm and dropped with the first rain episode to just over 40 mm. It again settled slowly to about 50 mm before it dropped again with the second episode to about 39 mm. Whenever the rainfall reduced or stopped the FFG06 rose relatively slowly. We are interested in the threat and this is indicated by the FFT06 line which is obtained by subtracting FFG06 from MAP06 and zeroing the negatives. Thus we identify a potential flooding threat between midnight and 7 am on 16 December.

If the FFG06 values were persisted at its level of 48 mm on 18:00 UTC on the 15 December 2010 for the next 12 hours it would have been too high at midnight when the actual values dropped to 39 mm due to the rain that fell between 18:00 UTC and 24:00 UTC. Thus, by keeping the FFG06 at a previous level in a period when more rain is expected a conservative estimate of potential flooding is created since the FFG06 is likely to drop due to the rain. If the FFG06 at 00:00 UTC on the 16 December 2010 was persisted at its value of 39 mm for the next 12 hours, it would have been too low compared to the slowly declining actual FFG06 to higher values. FFG06 rose in this situation, however, because no rain fell and the flash flood threat disappeared. Lastly, this case was a real extreme rainfall case where 133 mm of rain fell in that area between 18:00 UTC on the 15 December 2010 and 08:00 UTC on the 16 December 2010. Yet, the basins still responded relatively slow over the next 12 hours compared to rain episodes, particularly when the rain stops.

From this discussion, it is assumed that it is a reasonable approach to persist the FFG06 values for the next few periods in the absence of a capability to model its future values. An outlook of potential flash flooding can then be regarded as a conservative estimate.

6.2.2.6 Determining a Flash Flood Outlook for the next 18-hour window period

The 3-step *flash flood forecast modelling process* is summarized as follows:

Step 1: Prepare NWP-based probabilistic rainfall forecasts for each basin for the next 18 hours:

- Determine 6-hour UM-MAP for each basin from the gridded deterministic NWP 6-hourly output;
- Perform a bias correction on these UM-MAP values;
- Apply the hybrid ensemble approach to the MAP values to address forecast uncertainty for the 18-hour forecast window period.

Step 2: Project the last known 6-hour FFG values for each basin to the next 18 hours;

Step 3: Compare the forecast HyEPS rainfall information per basin for the 18-hour window period with the projected FFG values for the same period to determine the likelihood of potential flash flooding in a SAFFG basin (FFP), and in LM (LM-FFH) – see section 4.3.2.4 for more detail.

This process is followed for each of the SAFFG basins to provide a potential for flash flooding in the next 18 hours, and a risk of flash flooding in the corresponding LM. Results provided encouraging indications that this methodology could provide additional lead-time on the likelihood of flash flooding, based on NWP forecasts and FFG data from the SAFFG system. For the cases tested, the system did show indications of bias corrected UM-MAP values exceeding FFG values indicating potential excessive rain and areas in danger of flooding.

6.2.3 Results: Eastern Cape flash floods of 20 October 2012

6.2.3.1 Description of the event

On 20 October 2012, a cut-off low-pressure system caused heavy rain and flash flooding over the Eastern Cape Province of South Africa. Significant damage was caused to infrastructure and homes

near Port Alfred where people were forced to leave their homes due to flooding. Houses of 57 residents in the nearby informal settlement were damaged and hundreds of residents were without water or electricity (SAWS, 2012b). Cars were submerged and some houses were flooded with up to 2 m of water. A bridge was washed away and the damage to infrastructure and cars was estimated to be more than R1 billion. The N2 national road between Port Elizabeth and Grahamstown was washed away at a gully outside Grahamstown resulting in the road to be closed, severely disrupting traffic.

6.2.3.2 Simulating the rainfall outlook through HyEPS

The rainfall patterns as shown by the MAP images in Figure 6.8 were reasonably well forecast by the 20th 00:00 UTC run of the UM-SA12 xaana model configuration, although it underestimated the amount of rain that fell near Port Alfred 12 hours later. The UM-SA12 xaang run forecast much more rain, but misplaced the peak amounts to occur between 18:00 UTC and midnight on the 20th (Figure 6.9). These two runs therefore provided an opportunity for an interesting comparison of the application of the deterministic model pseudo-ensemble system by forecasts for the same event of two different model configurations.

For each basin, the 6-hour rainfall measured by SAFFG MAP was averaged for the three 6-hour periods within the relevant 18-hour window period. A comparison of the average rainfall for the 18-hour window periods of 0-18 and 6-24 is provided (Figure 6.10). The model average is the average of all 30 members of the ensemble (each 6 hours in length) relevant to the particular basin and covering the same 18-hour window period, done for xaang and xaana configurations respectively. It is quite evident that the UM-SA12 with the xaang configuration did not capture the average rain positioning correctly as compared with the SAFFG MAP average on the left hand side of Figure 6.10 for both periods. This was mostly due to the mistiming of the rainfall by the xaang configuration as the rainfall moved southeast out over the ocean. The xaana configuration, however, performed better in capturing the timing, although the total amounts were a bit low.

The main purpose of this case study was to determine the potential for flash flooding in small river basins from NWP forecasts. Consequently, the most important product was the FFP of each basin over the 18-hour window period, calculated as the probability of the basin ensemble UM-MAP values (or the percentage of members) exceeding the representative FFG values of the basin for the same 18-hour window period. This implies that the members with the highest values for each basin will be important to identify, since they have the best chance of exceeding the FFG value of the basin. A chart with the highest rainfall value of all ensemble members for a particular basin is a simple representation of this methodology from a rainfall perspective. Figure 6.11 shows rainfall maps of the maximum 6-hour rainfall value from all 30 members of the ensemble for each basin for the two 18-hour window periods under discussion using the two model configurations. The SAFFG MAP observation maximum was just the highest of the three relevant observed 6-hour periods for the basin. Again the xaang model configuration overestimated the rainfall in the wrong areas, although the xaang configuration's 6-24 hour window period provided quite good forecasts for the areas that did received the highest rainfall in this period around Port Alfred. The xaana model configuration performed much better with the highest values in the Port Alfred area, though much lower values than experienced.

	SAFFG MAP observations	UM-SA12 xaang deterministic model	UM-SA12 xaana deterministic model
06-hour	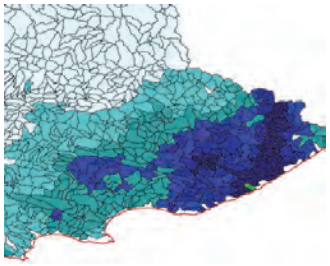	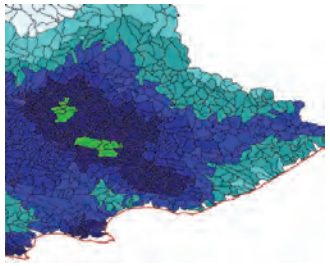	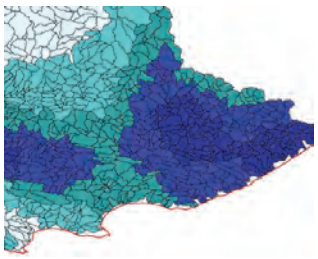
12-hour	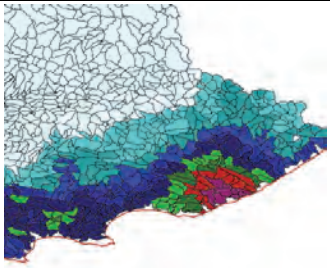	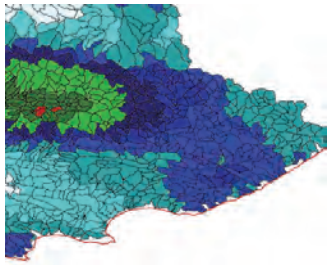	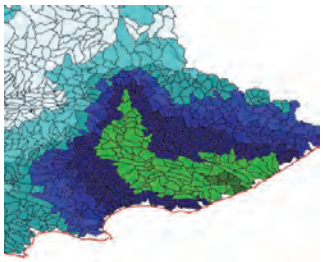
18 hour	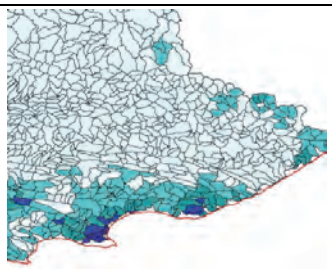	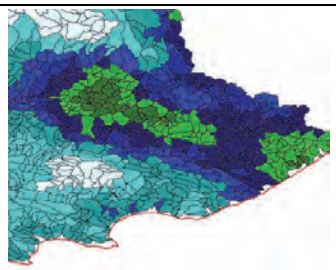	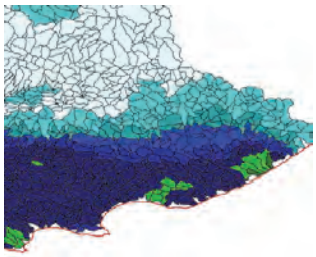
24 hour	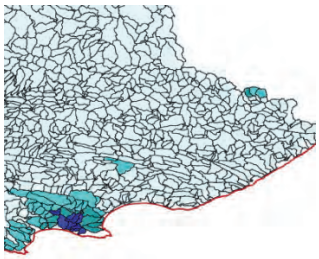	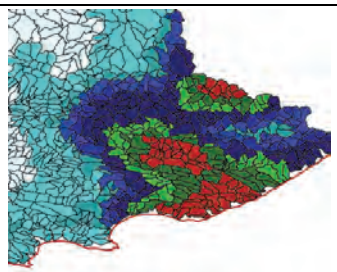	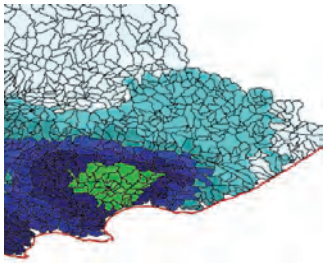

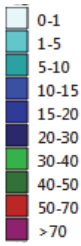

Figure 6.8: Comparison of the SAFFG MAP rainfall observations with the UM-SA12 xaang deterministic rainfall forecast and the UM-SA12 xaana deterministic rainfall forecast of the 20th 00:00 UTC model runs for 06-, 12-, 18- and 24-hours.

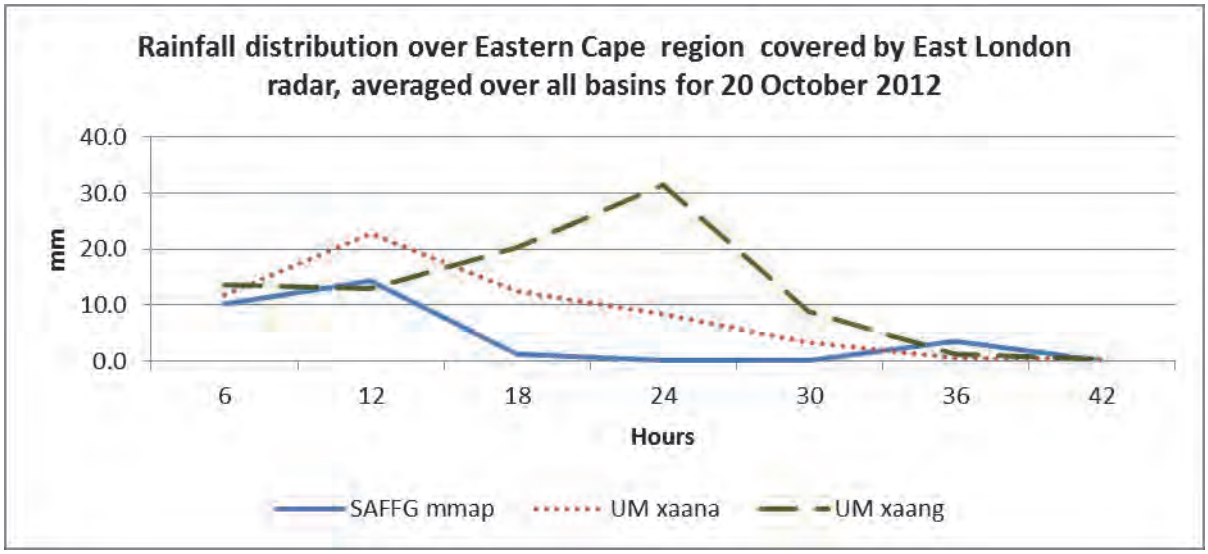

Figure 6.9: The rainfall distribution averaged over all the basins in the East London radar region of the Eastern Cape Province of South Africa on 20 October 2012. The solid line shows the observations as represented by SAFFG MAP. The dotted line is the rainfall forecast of the xaana configuration of the UM-SA12 initiated at 00:00 UTC and the dashed line the associated UM-SA12 forecasts using the xaang configuration

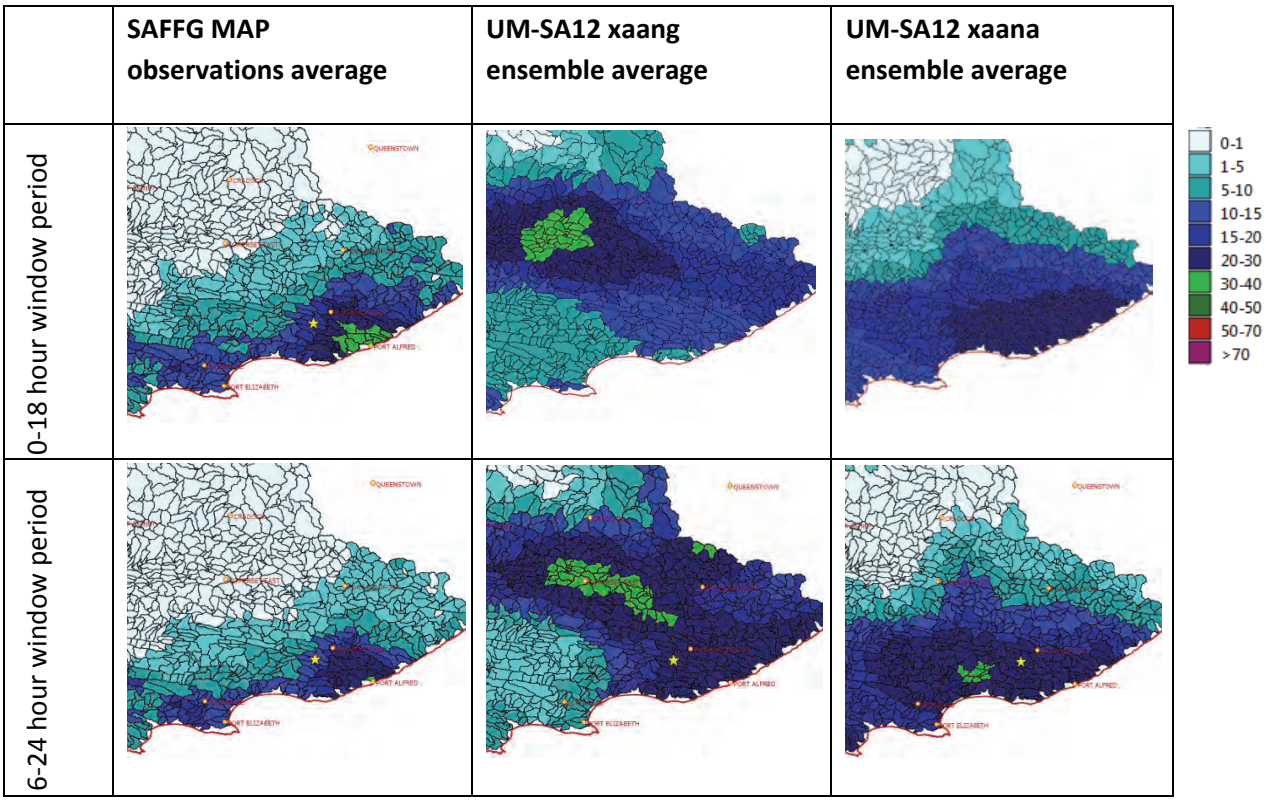

Figure 6.10: Comparison of the 6-hour SAFFG MAP average rainfall observations over the relevant 18-hour window periods with the average UM-SA12 xaang and UM-SA12 xaana ensemble forecasts for the same periods for 20 October 2012. The start shows the location where the N2 was washed away.

	SAFFG MAP observations maximum rain	UM-SA12 xaang ensemble maximum rain	UM-SA12 xaana ensemble maximum rain
0-18 hour window period	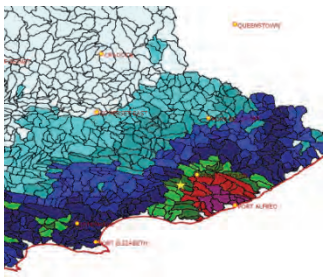	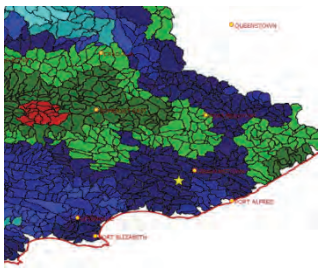	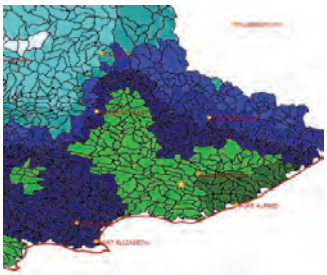
6-24 hour window period	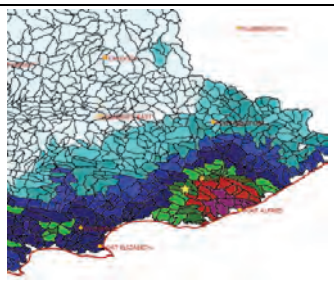	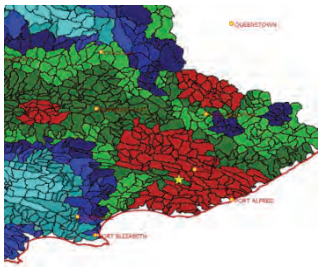	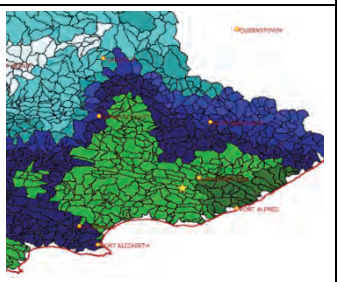

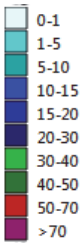

Figure 6.11: Comparison of the 6-hour SAFFG MAP maximum rainfall observations over the relevant 18-hour window periods with the maximum UM-SA12 xaang and UM-SA12 xaana ensemble forecasts for the same periods of the 20 October 2012.

Verification metrics were calculated for both the ensemble average and the ensemble maximum rainfall fields of the UM-SA12 forecasts using the xaana and xaang configurations compared to observed SAFFG MAP fields for the two 18-hour window periods. The domain covered is the same as in the images in Figure 6.11 and involved 432 small river basins. A contingency table was prepared for each forecast, determining event "Hits", "False alarms", "Misses" and "Correct Non-events". This data was used to calculate a variety of scores including the Critical Success Index (CSI), Hanssen-Kuipers Score (KSS) and Heidke Skill Score (HSS) (Wilks, 2006; Jollife and Stephenson, 2012).

These three scores were used because they measure the attributes of quality, namely

- "Accuracy" (i.e. the level of agreement between forecasts and observations, measured by CSI),
- "Discrimination" (i.e. the ability of forecasts to distinguish between occurrences and non-occurrences of the event, or tells a user if he can rely on the forecast, measured by KSS), and
- "Skill" (i.e. the accuracy of forecast compared to the accuracy of being correct by chance, measured by HSS). For CSI, KSS and HSS a score of "1" is a perfect score.

Figure 6.12 depicts a graphical illustration of the verification results. From all three indicators it is evident that the xaana configuration of the UM-SA12 performed the best. The xaang configuration performed the worst with the 0-18 hour forecast actually being misleading, particularly for the higher thresholds beyond 15 mm. This applied for all three attributes of accuracy, discrimination and skill. The xaang configuration 6-24 hour forecast performed better at higher thresholds than lower

thresholds for skill and discrimination as measured by HSS and KSS respectively. Consequently, though the UM-SA12 forecasts for the 18-hour forecast window were not precisely accurate, the xaana configuration, particularly, produced useful forecasts. The xaang 6-24 hour showed some skill above pure chance and the ability to discriminate between occurrences and non-occurrences at the higher thresholds. It can thus be concluded that the HyEPS ensemble rainfall forecasts provided useful outlooks for the rainfall over the two 18-hour window periods in this particular case study.

6.2.3.3 The 18-hour flash flood outlook

The probabilistic FFP values for the case study of 20 October 2012 are presented in Figure 6.13 (left panels) of both the xaana and xaang configurations of the UM-SA12 for the 6-24 hour window period. FFP was calculated as the percentage of ensemble members that would have exceeded the persisted 12:00 UTC FFG value for the particular basin. The right hand panels (LM-FFH) in Figure 6.13 indicates the number of SAFFG basins in the FFP products that show an outlook of potential flooding in a local municipality compared to all the basins of the particular local municipality and is aimed purely as a "heads up" of likely adverse conditions.

Based on the HyEPS forecasts both the xaana and xaang configurations of UM-SA12 identified by 12:00 UTC that the Ndlambe local municipality (which includes the town of Port Alfred) had a high likelihood of potential flash flooding in the 6-24 hour window period. Both model runs also forecast a higher FFP potential in the Kowie River running into Port Alfred, with the xaana configuration indicating more than 66% of the members expected more rain than required for potential flash flooding in this basin during this period.

The LM-FFH and FFP thus accurately provided an early outlook of the flash flooding in Port Alfred that occurred later that day. As a reference, the SAFFG system in hindsight identified the same basins would have flooded given the rainfall as estimated from the East London radar.

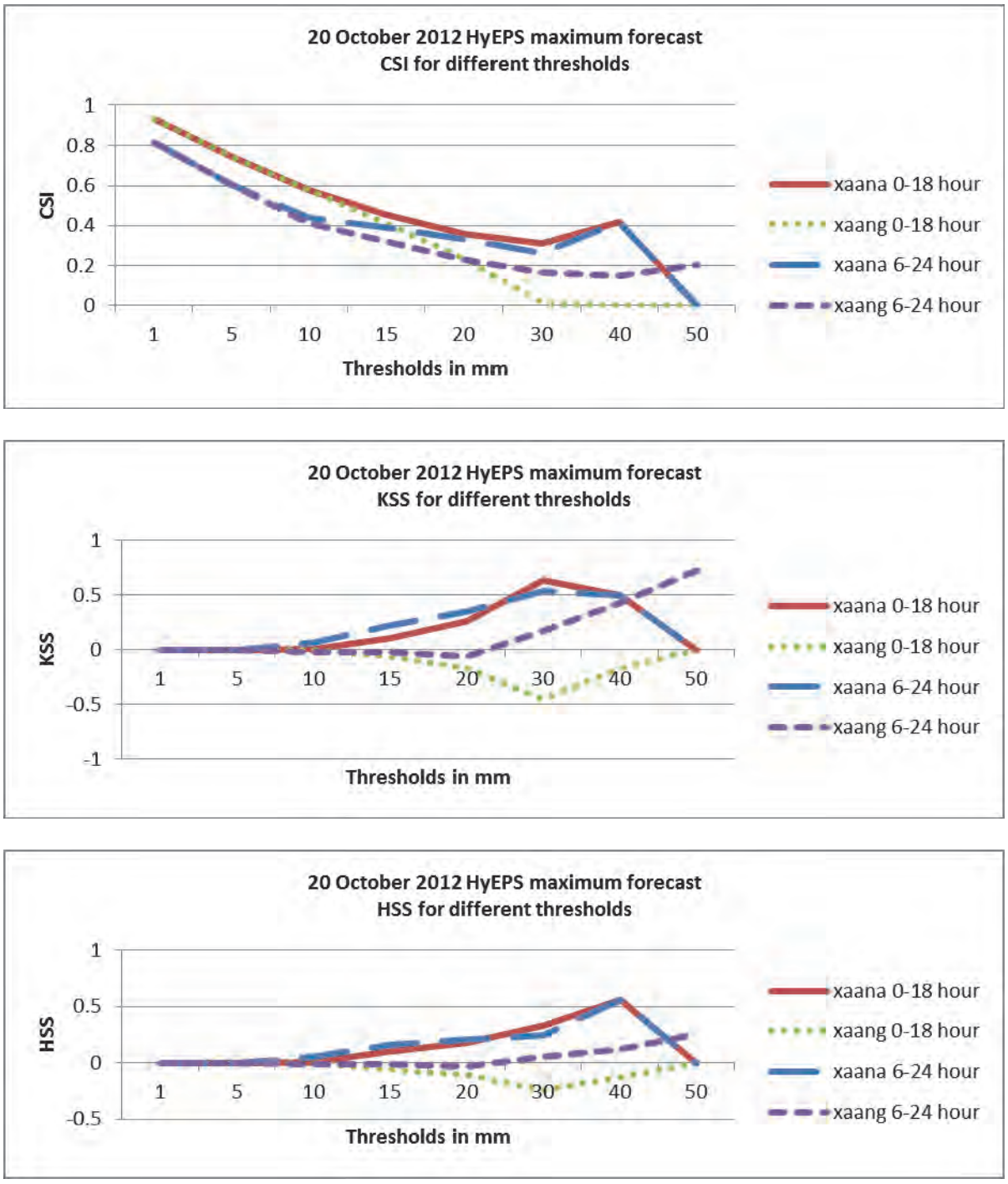

Figure 6.12: Verification statistics for the HyEPS maximum forecasts for the UM-SA12 xaana and xaang configurations for the 0-18 and the 6-24 hour window periods for different rainfall thresholds on 20 October 2012. The top panel shows the CSI, the middle panel the KSS and the bottom panel the HSS.

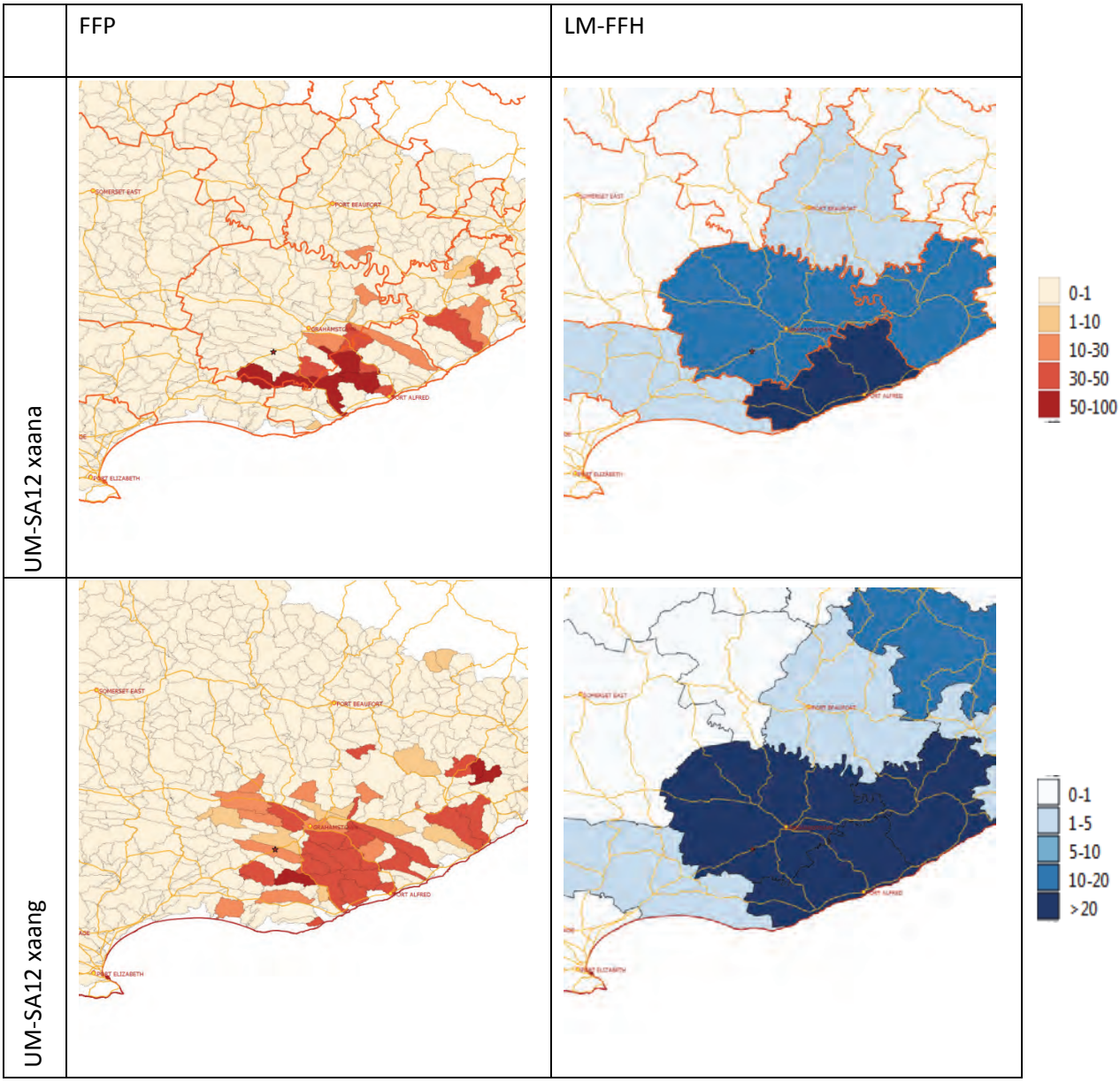

Figure 6.13: 6-24 hour FFP (left) and LM-FFH (right) fields of the UM-SA12 xaana and UM-SA12 xaang runs of 20th 00-hour based on the 12-hour FFG.

6.3 ENHANCED APPLICATION PRODUCTS FOR USER DECISION SUPPORTING SYSTEMS

6.3.1 Introduction

Various severe weather-warning products are available to disaster management structures from SAWS which are applicable to flood and flash flood warnings. These include the standard severe weather warnings issued to the media and disaster management, specific products from radar, satellite and other related systems, and the products from the SAFFG system itself. From previous experience, the basic products provided by the SAFFG system are technically too complex to be used optimally by disaster managers who do not have the time to familiarize themselves with the technical complexity of the products each time a flood hazard exists. This problem can only be addressed through a collaborative activity between SAWS and the relevant users, in this case disaster management structures. This aspect of the study is addressed in this section.

6.3.2 User decision making in early warning systems

6.3.2.1 Understanding decision-making by disaster management during early warnings

Typically, disaster managers have to decide when and where to initiate proactive or response activities in the face of likely flooding or wildfire hazard based on weather forecasts and warnings. Personal discussions invariably reveal that they do not want complex information, "just tell me what is going to happen, when, where and how serious it is".

However, probability information, linked to their particular decision making scenarios, will give the disaster managers far more valuable information to prompt their decisions than a deterministic "rain" or "no rain" forecast. Forecasters tend unintentionally to withhold valuable uncertainty information from users (Morss *et al.*, 2008, 2010; NRC, 2006). In some cases, forecasters argue that communicating uncertainty will negatively affect their integrity. In this way, a weather forecaster, to some extent, actually makes a decision *for* disaster managers instead of letting them decide at what uncertainty level they will react. This was typically the case in the Red River flooding in 1997 (Pielke 1999, cited in NRC, 2006, p12) when the lack of uncertainty information in the forecast, which could have made a difference, contributed to insufficient preparation of authorities and the general public.

6.3.2.2 User need for uncertainty information

The level of sophistication of users implies different levels of requirements for weather forecast information, and particularly for uncertainty information. Users that are more sophisticated, have a better understanding of the reasons for forecast uncertainty will more easily grasp how to use the information in their decision-making processes (WMO 2008). As scientists begin to understand the complexities of forecast uncertainty and find ways to quantify it through, for example, probability distributions from EPS, the question about the need for conveying uncertainty information has risen dramatically. Many authors describe, or call for, research around this topic. In the field of disaster management, the ISDR (2005a) appeals for more research in developing user-friendly products, with attention given to assimilate forecast uncertainty into the decision-making toolkits of disaster managers. According to Joslyn (2009b), some scientists argue that all public forecasts should have an indication of forecast uncertainty, and others question the kind of uncertainty information needed by the users. The reality is that very few forecasts provide any information on forecast

uncertainty, apart from maybe probability of precipitation (Roulston, 2006; Joslyn 2009b; Morss *et al.*, 2010). Moreover, even after being exposed to probability of precipitation for many years, few users really understand what is meant by 60% chance of precipitation. However, it is intriguing how users unknowingly interpret deterministic forecasts with a measure of uncertainty, presumably based on their experience. In their study, Morss *et al.* (2010) found that when users are provided with a deterministic forecast of rainfall or temperature approaching a critical threshold, many of them will chose protective action even if the threshold has not yet been reached. An earlier study by Morss *et al.* (2008) revealed similar results when 95% of respondents chose a range of temperatures around a given deterministic value as the most probable temperature expected. The authors' conclusions in these two papers were that these users interpreted the forecast with an uncertainty factor. However, this uncertainty was interpreted differently between the respondents. It is clear that the challenge lies in providing uncertainty information in such a way that it is understandable and makes a real difference to the decision-making of the user (NRC, 2006).

There are various reasons why uncertainty information needs to be conveyed to users (WMO, 2008; NRC, 2006). On a daily basis users need to make decisions based on the weather forecast affecting their lives and livelihoods. Even though they may request a specific deterministic forecast, they still need to weigh their options for a particular action or different contingencies. Depending on the decision-making context, different users will also harbour their own thresholds of forecast uncertainty for the same forecast that will prompt a particular reaction. These differences depend also on their differing cost/loss scenarios (costs of protection or action versus the potential losses due to the impact of the event). Because different users have different needs for uncertainty depending on their context, cost/loss and other decision-making considerations, the overall conclusion of various studies (Morss *et al.*, 2010; NRC, 2006; WMO, 2008; ISDR, 2005a) is that users should receive all the uncertainty information they need to make their own decisions, rather than be provided with recommended decisions from forecasters with generalized thresholds. In basic terms: by keeping uncertainty information away from the users, forecasters are actually making decisions on the users' behalf.

Apart from improving decision-making, forecast uncertainty information can help to manage user expectations and promote user confidence (WMO, 2008). Users generally expect that a forecast must always be correct. By providing a deterministic forecast (for example: the temperature will be 24°C) the forecasting community actually promotes such an expectation. However, since some situations are more predictable than others there is a need for better information sharing to create more realistic expectations and understanding of the situation. That is why forecasters generally feel comfortable talking to a user face-to-face or, on the phone, when they can convey their confidence through their choice of words and the user can get a sense of the uncertainty of the situation. It is well known that users who receive uncertainty information openly and who have a better feeling for the inherent uncertainty in weather forecasting are more likely to have more confidence in the weather forecaster (WMO, 2008).

Despite the previous arguments in favour of providing uncertainty information, disaster managers sometimes argue that all they want is a simple answer and that they do not have the time to interpret results (WMO, 2008; Poolman, 2009). The question therefore remains: do disaster managers really need and want uncertainty information to improve their decision making as argued by some authors (Auld, 2008; NRC, 2006), or should forecasters provide them with deterministic

forecasts because that is what they want and need? This fundamental question needs to be answered before we can investigate the format in which uncertainty information should be packaged for them. Morss *et al.* (2008) investigated this question as it applies to the public. Their findings were that a significant majority of respondents could use uncertainty information, and that many preferred uncertainty information in some or other form in the forecasts. It seems one needs to discriminate between technical and uncertainty information transfer.

6.3.3 Understanding user needs for effective decision making in flood warning systems

6.3.3.1 Assessment methodology

In order to develop appropriate user products for disaster management structures, it is necessary to have some understanding of their decision-making processes and decision support systems. This required various personal contact sessions with disaster management structures using surveys and small group meetings.

Results of a survey conducted with four groups of disaster managers during capacity building workshops in 2009 are provided in section 6.3.3.2. These results are quite pertinent to the questions and provided useful insight on the decision making needs and preferred products.

Feedback is provided in sections 6.3.3.3 to 6.3.3.5 of meetings conducted during 2012 and 2013 with representatives of disaster management centres of a number of district municipalities, a meeting with officials from the national Department of Water Affairs (DWA), and discussions with a representative of the Kruger National Park (KNP).

6.3.3.2 Results of an earlier survey on the disaster manager needs regarding flash flood warning information

6.3.3.2.1 Methodology

During a first round of capacity building workshops by SAWS with disaster managers in 2009 as part of the implementation phase of the SAFFG, the author did a survey among all disaster management officials attending the four workshops in Cape Town, George, Port Elizabeth and Midrand (Poolman, 2009) to determine their requirements related to the flash flood warning system. A questionnaire was completed by 67 officials from district, metro and provincial disaster management centres in these different regions. There were 22 officials among the 67 who were experienced disaster managers in leadership positions in their respective disaster management centres, and involved in authoritative disaster management related decision-making during disaster situations, which included the authority to order community evacuations if deemed necessary. Of the remainder, 28 were junior disaster management officials working on disasters, and the other 17 were GIS specialists, water engineers, four police and traffic officers, a medical doctor and three fire fighters, all of who were involved in disaster management supporting activities or decision-making in their own environments.

Apart from questions regarding the operational needs for the future SAFFG flash flood warning system, the questionnaire also sought for details of the decision-making processes during a flood situation and the disaster managers' need for uncertainty information in warnings from forecasters.

6.3.3.2.2 Results relating to decision making principles

Respondents were asked to choose between two different options, knowing that a weather forecast can go wrong, particularly at longer lead-times:

- Do they prefer that a weather forecaster issue a warning with a longer lead-time even if he could be wrong (i.e. provide some lead-time at the expense of accuracy, thus the potential for a false alarm, or "crying wolf", exist) as long as the event is not missed;
- Alternatively, do they prefer that forecasters wait until they are very sure what would happen before issuing a warning (which implies a short lead-time), as long as the warning is mostly correct.

Analysis of the responses to the first question (see Figure 6.14) revealed that the majority of disaster managers conceded that they should rather be prepared for an eventuality, and stand down when it does not occur, than risk not being prepared when a disaster struck. They can live with a false alarm, but do not want an event to be missed and be unprepared. Supporting staff, on the other hand, who do not have to make live-saving decisions, are of a different opinion: they do not want false alarms, and prefer that the forecasters wait until they are very sure before issuing a warning, in the process sacrificing lead-time. Their feeling was that false alarms will eventually lead to people not believing the warnings. The disaster managers did not share this concern regarding their own decision-making, and they seem to have had a better understanding of the complexity and uncertainty associated with forecasting.

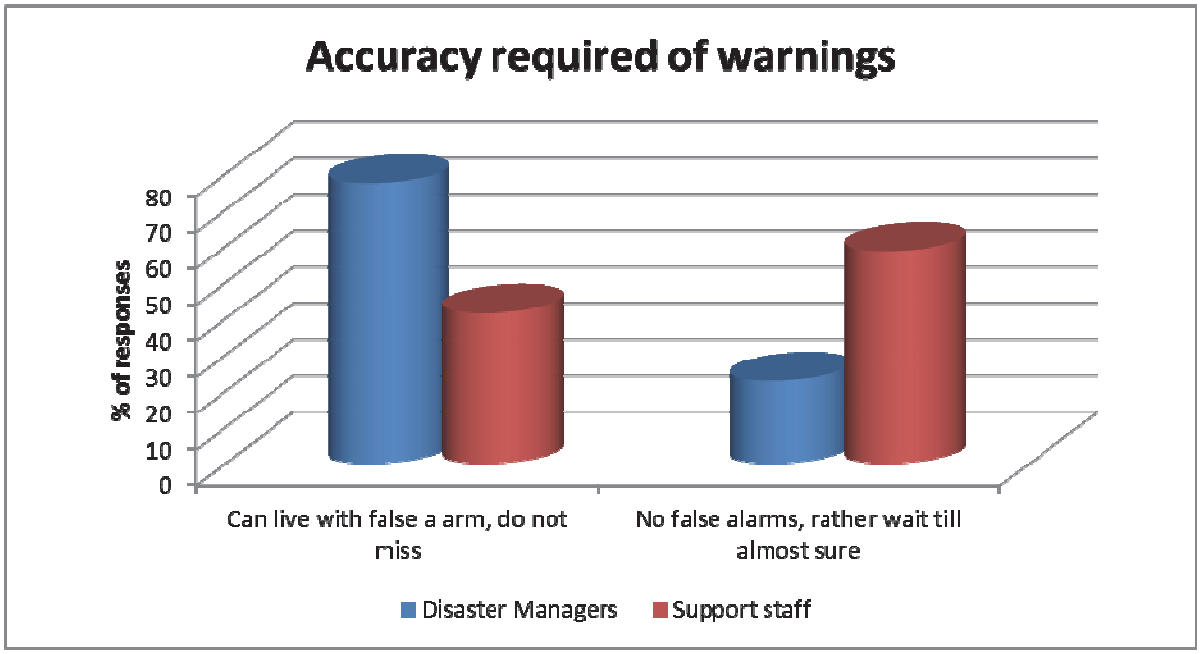

Figure 6.14: Responses from disaster managers versus supporting staff on the issuing of warnings with longer lead-time at the risk of higher false alarms (left) or issuing warnings with a short lead-time but with high accuracy.

6.3.3.2.3 Results relating to uncertainty information

Respondents were also asked, given the fact that forecasting accuracy decreases with increasing lead-time, if they could use probabilistic information of flooding (10%, 30%, 60% or 80%) in their decision making for planning purposes 2 or more days in advance to make useful decisions. This question was asked without explaining the meaning of forecast probabilities.

Responding to this question the vast majority (more than 94%) of both disaster managers and support staff were positive about their own ability to use probabilistic information on flooding two or more days in advance in their particular decision making environment. Their preferred threshold for action was 60% (47% of the respondents) with 30% probability regarded as their threshold by 30% of the respondents. This survey did not investigate what they understood by a 60% probability, however, Morss *et al.* (2010) concluded that even though many people may not interpret probability information correctly, they still are able to use it in decision-making within their own contexts.

6.3.3.3 Results of small group meetings with disaster management structures

6.3.3.3.1 Overview

Three meetings with representatives of disaster management centres of four district municipalities were held during visits to their individual Disaster Management Centres (DMCs). These district municipalities were City of Cape Town Metro, Cape Winelands, Overberg and West Coast. Official that attended these meetings were all involved in decision making during disasters. In all cases the predominant disaster was flooding associated with flash floods, or river floods, or pooling (particularly in the Cape Town Metro) as indicated by the representatives, and confirmed from disaster databases or lists such as CRED and CAELUM.

6.3.3.3.2 Results relating to impact of flooding

As can be expected there are some differences between the impacts experienced by the rural DMCs (Cape Winelands, Overberg, West Coast) versus the metro DMC (City of Cape Town).

- For all DMCs, deaths and disruption of people's livelihoods are the biggest impact of flooding. The causes for this differed in some aspects between the metro and the rural districts, as can be expected.
- In the Metro DMC the major issues are road flooding due to among others storm water system problems that cause traffic problems, and pooling that flood informal settlement houses and roads. They also experience problems with mudslides and rock falls in Constantia and the Chapman's Peak area.
- For the rural DMCs, road flooding and bridges washed away that lead to small towns being cut off for short periods were a major issue. In many cases this led to evacuation of small communities, or the need for relief operations, many times through the involvement of helicopters.
- In all cases, adverse impacts to schools and hospitals are a major concern.
- Another important impact for the rural regions was damage to agriculture and its communities.

6.3.3.3.3 Results relating to decision making

Within 1-2 days, prior to receiving a flood warning, DMCs advise municipalities to clean storm water systems, and road sections to inspect their problem areas. It is important to inform the administrative heads of municipalities, and generally to create awareness of what can happen. The request is "rather provide too much data, and do not miss the event". Information needed for these preparation activities include:

- A heavy rain watch at least at Local Municipality (LM) level;
- Historical information of similar events in the past to define typical impacts;
- Reaction measures on the web.

When a warning is received, indicating that flooding is imminent within 24 hours, various activities take place. DMCs pass the warnings to municipalities, line departments, emergency services (including traffic departments and police), the defence force, the public, media and the agriculture sector. Causeways, bridges and roads are closed where necessary, helicopters put on standby, information sent to people alongside rivers, preparations are made for possible evacuation. At this stage, the lead-time is limited to a few hours for critical decisions to be made. Information needed includes:

- warnings and updates at LM level that are meaningful, for example the severity, duration and expected dissipation of hazardous event;
- satellite and radar imagery showing position and movement of weather system;
- information at micro level (ward) regarding where flooding could occur, rain amounts and intensity;
- flash flood threat information at for small basins;
- Information over mountainous areas;
- Rain-rate information from ARS (automatic rainfall station) networks in real-time per LM;
- Access to information in a user-friendly format that could also easily be used (cut and paste) for onward sending to other decision makers.

6.3.3.4 Results of a small group meeting with water management officials from the Department of Water Affairs (DWA)

A training workshop was held for water officials of DWA to introduce them to basic concepts of weather forecasting. In a specific session, they were introduced to the South African Flash Flood Guidance (SAFFG) system and its products. During a discussion session, they were asked specific questions relating to their requirements of tailored products. These included products at different scales and were important for decision making in river flood situations and for reservoir management:

- A need to have an overview of the bigger picture through synoptic weather charts and satellite imagery were expressed;
- The need for access to rainfall observations from rain gauges, but also from radar and satellite estimations were highlighted;

- A need was also expressed to have access to the rainfall and soil moisture products of the SAFFG.

6.3.3.5 Results of a small group meeting involving the Kruger National Park (KNP) following tropical cyclone Dando

A workshop involving officials from SAWS, KNP and DWA was held in 2012 following the serious river flooding event caused by tropical cyclone Dando over eastern South Africa and Mozambique. A clear need was expressed by the KNP for advanced warning of river flooding to allow enough time for planning and evacuation of camps alongside the rivers. The problems were highlighted in the following questions:

- When and where the flood is going to occur (time and location):
    - When to evacuate?
    - How much time is available for the evacuation?
- How high will the flood be:
    - How far do they need to evacuate?
    - What are the flood lines?
- When will the flood subside:
    - What is happening upstream?
    - Is more rain expected?

What was evident is that a riverine flood warning system needs to be developed for regions such as Mpumalanga and Limpopo, involving stakeholders like the KNP, DWA, SAWS and the relevant Disaster Management Centres (DMCs). Coordinating guidelines between different stakeholders will be needed to clarify different roles in terms of early warning, prior and during a flood event.

The principle requirement was at least a basic model that can provide advance advisories of potential flooding in the rivers. The requirement of rainfall products at quaternary basin level and FFG basin level was emphasized. These products are now becoming available through the FFG systems. However, a rainfall run-off and flood routing system for the rivers in the region to integrate the FFGS basin average rainfall was not available and need to be developed.

6.3.4 Development of user friendly products

The wealth of information that was received provided excellent input for the process of developing user-friendly products for DMCs in line with their requests. At the time of preparation of the report, product development is still on-going. These products range from the large scale (weather outlooks and forecasts, advisories and watches) to the small scale (warnings, radar, satellite and rainfall) to micro scale (specially prepared flash flood guidance products from the SAFFG system). A new international drive focussing on the prediction of the potential impact of flash flooding is currently under development. With regard to all the products, an attempt will be made to provide these in a user-friendly way according to the needs received from the users. Due to the number of products, the best way to present this data will be through a dedicated website that will be developed in SAWS, complementing the NDMC's Early Warning website they are developing, but focussing more on specific weather information that could be tested within disaster management structures. Some of the products are presented below:

- In reaction to the need for local municipality (LM) river level watches and warnings, SAWS has modified its severe weather warning system to issue watches and warnings for most hazards, including heavy rain and flash flooding, in future at LM level. This will be implemented within the first half of 2013 as a new warning generator becomes operational.
- As a specific example, a product was developed to provide a heads-up of potential flooding according to the SAFFG in any small catchment in a district municipality (see Figure 6.15). Should the 6-hour flash flood threat indicate any basin that could potentially receive minor, moderate or serious flooding, then the entire municipality will be highlighted in an appropriate colour to attract attention. The more detailed flash flood threat product, at SAFFG basin level, will also be available at the next higher level for further scrutiny if required.
- Another example is the development of NWP observed and predicted Mean Areal Precipitation (MAP) products at both SAFFG and quaternary catchment levels. Where the former is intended to support the SAFFG system with additional lead-time, the quaternary catchment MAP product is aimed as additional information for DWA and other users (such as the KNP) for river flooding issues.

These products are only a few examples of a suite of products that together would aim to provide more holistic information to the disaster management structures to enhance their decision-making.

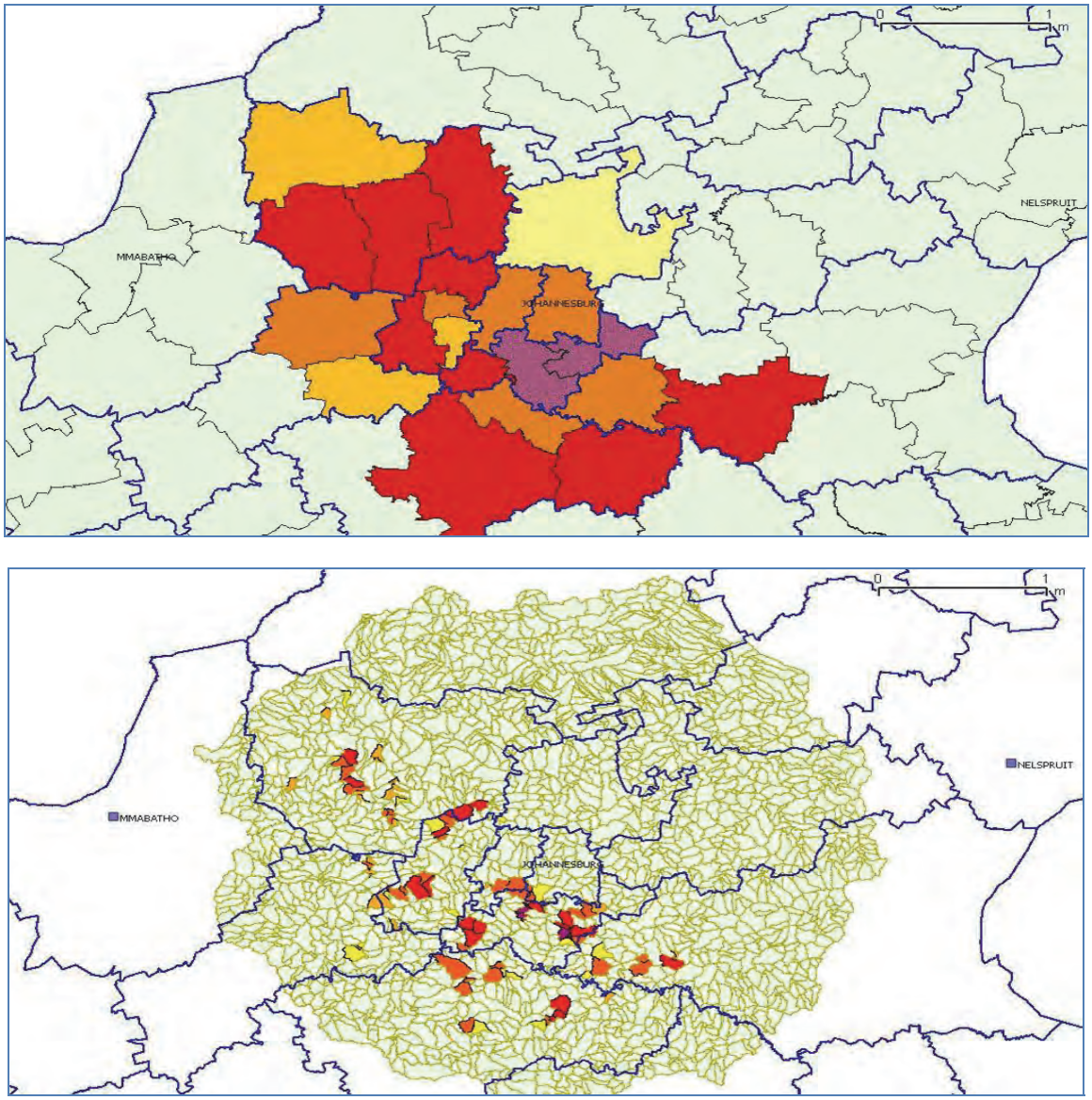

Figure 6.15: 6-hour flash flood potential indicated at local municipality (LM) level (top) versus the detailed SAFFG catchment calculated flash flood threat for the same area (bottom). The LM flash flood potential is determined by setting its potential to the highest level (colour) of any SAFFG catchment within the LM. This product provides a quick heads-up of potential flooding within the next 6-hours, with the ability to drill to more detail if required.

6.4 SUMMARY

The investigations described in this section highlighted the problem that the standard products available from the SAFFG system are technically too complex. Therefore, there is a dire need for developing more user-friendly products that will support the decision making of disaster management structures. These products need to present forecast uncertainty in practical ways without confusing the users, providing the basic needed information, but allowing them to make their own decisions in the face of uncertainty.

It is evident that disaster managers would like to know as early as possible of potential hazardous events such as floods and flash floods, even before absolute certainty about the event is established. They are willing to accept a level of uncertainty as long as they can receive the information with enough lead-time to allow them to be prepared should the event strike. This appears to be in contradiction to the need of the public of absolute certainty of an event before they are warned to avoid "cry wolf" situations. Disaster management related officials (from DMCs, DWA, and other stakeholders such as KNP) require products at various scales depending on the type of decision making at the time and on the lead-time available. These vary from large scale (synoptic products), to small scale (radar and satellite products, rain gauge information, local municipality level) to micro scale (SAFFG basin level, ward level and even smaller).

The products vary between users but include also spatial scale rainfall products, flood and flash flood potential indicators, and indications of the likely severity and impact of the floods and flash floods. This is a daunting task and development and testing of products will continue for a long time. Some of these products have already been developed, while others will take some time to complete. A mechanism to provide these products to the user needs to be developed, and include specialized web-portals.

Nevertheless, through this study, very useful insight has been gained into the decision-making processes of stakeholders, and their requirements for products that will support these decision support systems. This process needs to be kept dynamic to ensure continuous relevance of products provided for the early warning against floods and flash floods in South Africa.

7. CONCLUSIONS

7.1 GENERAL

Flash flood warnings are issued by default by the SAWS due to the short lead-time of 6 hours associated with flash floods, and SAWS operating on a 24-hour basis. An effective flash flood warning system, however, has to include all four phases of early warning systems, i.e. risk identification, monitoring and warning preparation, and warning dissemination and response activities. This fact was also emphasized by Du Plessis (2002) and Pegram *et al.* (2007) in their investigations for the WRC on flood warning systems. The latter proposed the implementation of a pragmatic national flood nowcasting system, taking into account institutional capacities, roles and responsibilities and appropriate technological systems, focussing on the main metropolitan areas in South Africa. Unfortunately, at the time of the proposal, this vision was not realizable on a technical or institutional level.

The implementation of the SAFFG system in 2010 and the SADC regional SARFFG in 2014, as hydrometeorological guidance tools for weather forecasters, has initiated a new approach for issuing flash flood warnings in South Africa. This brought South Africa more in line with international approaches emphasizing the importance of information on the hydrological response of the soil and small streams to heavy rain as a prerequisite for effective flash flood warnings. Both SAFFG and SARFFG are technological systems roughly along the lines envisaged by Pegram *et al.* (2007). They are based on the flash flood guidance modelling approach favoured by the WMO for developing regions with large ungauged areas and regions with little radar coverage.

As expected, the introduction of a flash flood warnings system did not occur without its share of challenges. These challenges occurred in all four phases of EWS mentioned above, and particularly with crucial components of the modelling system, uptake by forecasters, and user-friendly products that can support the decision-making of users such as disaster managers and vulnerable communities. The main purpose of the study presented in this report was to enhance the end-to-end flash flood warning system, particularly the SAFFG modelling system and the development of more effective user-oriented products. This was addressed through four main thrusts:

- Analysing the SAFFG modelling system through a climatological analysis of its products since 2010;
- A thorough comparative study of the soil moisture modelling of the SAFFG modelling system;
- Studies to improve the crucial aspect of precipitation estimation using radars and satellites;
- Investigation and development of more user-oriented products, particularly aimed at disaster managers.

The activities that addressed these four thrusts led to significant enhancements in the SAFFG system either as immediate outcomes, or to be addressed through subsequent activities. The main findings of these thrusts are summarized below.

7.2 OVERVIEW OF THE RESULTS

7.2.1 The SAFFG system in general

Based on a climatological analysis of the main products of the SAFFG:

- Rainfall estimation is a crucial input variable into the SAFFG modelling system. It therefore has to be done as accurately as possible. Any inaccuracies in the rainfall field have an adverse impact on all the other products produced by model components downstream, such as soil moisture fraction, flash flood guidance and flash flood threat, since these models accept the rainfall field to be the best estimate at the time.
- It is evident that the rainfall measured by the S-band radars of East London, Irene in Gauteng, and Durban in KwaZulu-Natal generally showed more realistic rainfall patterns, although they appears to be overestimating the rainfall. There is thus a need to recalibrate this part of the bias correction within SAFFG.
- The C-band radars at Port Elizabeth, and the one used for a short time in Durban, vastly underestimate the rainfall. This is due to attenuation and filtering to reduce the excessive radio LAN interference. These radars should rather be replaced with S-band radars, which are not affected by radio LAN frequencies.
- The Hydro-Estimator satellite rainfall estimation underestimates the rainfall significantly over the south-western region of South Africa, where rainfall is mostly stratiform in nature linked to frontal weather systems in the winter. Adjustments to the Hydro-Estimator methodology are needed to find a more suitable rainfall estimation system for this part of the country. Currently, the hybrid NWP/Hydro-Estimator technique developed in Section 5 is one such option.
- The soil moisture modelling results, particularly under the Irene radar in Gauteng, respond quite slowly to rainfall events, and as a result basins seldom indicate potential for flash flooding, even though it does occur more often. This should be investigated.
- A pattern of areas that are more prone to flash flooding is emerging, particularly for KwaZulu-Natal, and the eastern parts of the Eastern Cape, where S-band radars provided useful rainfall estimation.

There have been also a number of cases where the SAFFG provided positive guidance to forecasters, particularly in KwaZulu-Natal, and the eastern parts of the Eastern Cape. If the deficiencies mentioned above can be properly addressed, then SAFFG will be able to provide useful guidance information to forecasters.

7.2.2 Soil moisture modelling intercomparison

The following conclusions can be drawn from the model intercomparison study conducted:

- The SAFFG rainfall is similar to the TRM 3B42RT product, which forces PyTOPKAPI, but is about twice as heavy when averaged over a contemporaneous 21-month period.
- Filtering the upper layer (compared to the lower layer) of the SACRAMENTO model always gives an improvement in the R^2, when compared to the PyTOPKAPI estimates of Soil Moisture, irrespective of that model's forcing. Presumably, this is because the upper layer of the SAFFG model responds to the rainfall input more directly than the lower.
- The SAFFG lower and upper layers are more highly correlated when PyTOPKAPI is forced by TRMM than by the SAFFG input

- Given that the radar gives nearly twice the rain that TRMM offers, it is surprising that the SAFFG soil moisture estimates are so much lower than those of PyTOPKAPI. This observation applies to both the upper and lower layers of the SACRAMENTO model.
- Overall, the correlations are disappointingly low, mainly because of the explanation in the next paragraph.

A distinct plateau is observed in all of the time series of the SAFFG Soil Moisture traces, more obvious in the upper layer than the lower one. This is a worry, because when a soil store is above zero and there is no input, evapotranspiration and drainage do not switch off – that would be physically impossible. This paradox has been shared with the developers of SAFFG for possible explanation or modification if needed.

7.2.3 Radar- and satellite-based quantitative precipitation estimation

For any flood of flash flood warning system such as the SAFFG hourly accumulations of both radar rainfall and satellite based rainfall should be used. Unfortunately, radars do not cover the entire South Africa and are very scarce in the rest of Africa. The SAFFG requires input of rainfall observations on time scales of less than 6 h in order to provide a nowcast of such events. Rainfall fields from rain gauges, radar rainfall as well as satellite rainfall are used as input to the SAFFG on an hourly, 3-hourly and 6-hourly basis. Satellite precipitation estimates (SPE) offer an excellent way to compensate for some of the limitations of other rainfall data sources such as point measurements by gauges or radar rainfall. Geostationary satellites such as Meteosat Second Generation (MSG) provide updated information every 15 minutes and offer a full view of the African continent. The quality of satellite based precipitation estimations for South and southern Africa are crucial to ensure the accuracy of flood and/or flash flood warnings.

The Hydroestimator (HE), running operationally over southern Africa since 2007, is a satellite base precipitation estimator run in real time making use of a single channel (IR10.8) of Meteosat Second Generation (MSG) to estimate rainfall based on cloud top temperatures and input from numerical weather prediction models.

- In order to provide a more accurate and more comprehensive satellite precipitation based input field, a new combination product was developed. The new product aims to combine the strengths of the Hydroestimator (HE) in estimating convective rain and the stratiform precipitation field from the Unified Model (UMS).
- Given the improvement shown on a daily basis, it is believed that the combination of HE and UMS rainfall field should benefit the nowcasting of precipitation as well as enhance input to the South African Flash Flood Guidance system if it is used on an hourly, 3-hourly and 6-hourly basis as a supplement to input from radar rainfall and rain gauge data.

Another geostationary satellite based algorithm which also runs operationally (mostly in European countries) is the Convective Rainfall Rate product, which was developed by the Nowcasting and Very Short Range Forecasting SAF, (or SAFNWC). The CRR makes use of either two (IR108 and WV062) or three MSG channels (including VIS006 during day light hours). The CRR was tested using the Nowcasting SAF (version 2012) software was installed at SAWS during 2013 for running case studies.

- Although the 2012 version of the CRR is better than the 2011 version, it still lacks more cloud microphysical properties in the algorithm. The latter is included in the 2013 version of the CRR.

The 2013 version is scheduled for installation at SAWS during the course of 2014 and the CRR from this version should show considerable improvement to the 2012 version.

- Using additional channels (CRR) for the calculation of satellite-based QPE proves to be beneficial and generally validates better than the single MSG channel method (HE).

Weather Radar offers South Africa an efficient means of measuring precipitation. Although its measurements are indirect, it remains the best alternative in capturing the spatial variability associated with precipitation on a high temporal and spatial resolution. Due to the fact that radar QPE is the main source of precipitation input to the SAFFG, it has become absolutely vital that as many errors as possible are removed from the precipitation field to get the best possible estimates.

- The Z-R relationship classification scheme tested is working well with some room for improvement, by adjusting thresholds and introducing a bright band filter;
- The classification scheme with the deep convective Z-R relation of $Z=300R^{1.4}$ for convective rainfall and Marshall-Palmer a Z-R relation of $Z=200R^{1.6}$ for stratiform rainfall works best for the Irene radar and is an improvement on the current TITAN system;
- The PE radar is not suitable for precipitation estimation due to the RLAN interference and the filters in use to remove the corrupt data. Until new filtering techniques can be introduced the PE radar cannot be used for Z-R relation testing;
- The fact that the classification scheme improves the Irene radar precipitation estimates does not mean this will be the case for all radars. Each radar will have to be tested – especially the coastal radars – in order to find the best possible Z-R relation.

The improvement of rainfall nowcasting opportunities to 6 hours, based on remote sensing and NWP, was explored. Various nowcasting systems are in operation worldwide, such as STEPS, Auto Nowcaster, INCA, etc. These systems are complex in nature and expensive to develop or implement. It relies heavily on real-time observational data and on skilled human resources. Whereas the preferred method would be to use radar-based systems like STEPS or INCA, an alternative, more cost effective but less accurate, option is to use the hybrid EPS system, HyEPS, described in Section 6 to provide an objective rainfall nowcast for the 0-6 hour period to be used in the flash flood guidance systems. A basic deterministic forecast from NWP is currently used in both SAFFG and SARFFG as predicted Mean Areal Precipitation fields, yielding reasonable results.

7.2.4 User-oriented product development

Improvements of the decision-making process right through the early warning chain in the short-term forecasting time-scale using meteorological information will lead to more effective and earlier responses from the disaster management structures. This could lead to increasing the lead-time of useful decisions and in so doing contribute to saving lives and property. Various consultations with users were held. The exercise highlighted several aspects related to improving the link between scientific forecasting systems and users, particularly around the flash flood warning system and SAFFG:

- The investigations described in this report highlighted the problem that the standard products available from the SAFFG system is technically too complex and that there is a dire need for developing more user-friendly products that would support the decision making of disaster management structures.

- These products need to present forecast uncertainty in practical ways without confusing users, providing the basic needed information, but allowing them to make their own decisions in the face of uncertainty.
- It is evident that disaster managers would like to know as early as possible of potential hazardous events such as floods and flash floods, even before absolute certainty about the event is established. They are willing to accept a level of uncertainty as long as they can receive the information with enough lead-time to allow them to be prepared should the event strike. This appears to be in contradiction to the need of the public of absolute certainty of an event before they are warned to avoid "cry wolf" situations.
- Disaster management related officials (from DMCs, DWA, and other stakeholders such as KNP) require products at various scales depending on the type of decision making at the time and on the lead-time available. These vary from large scale (synoptic products), to small scale (radar and satellite products, rain gauge information, local municipality level) to micro scale (SAFFG basin level, ward level and even smaller).

The products vary between users but include also spatial scale rainfall products, flood and flash flood potential indicators, and indications of the likely severity and impact of the floods and flash floods. This is a daunting task and development and testing of products will continue for a long time. Some of these products have already been developed, while others will take some time to complete. A mechanism to provide these products to the user needs to be developed, and include specialized web-portals. From this investigation, basic developments supporting disaster management requirements include:

- A methodology to increase the outlook lead-time of flash floods based on the SAFFG and NWP was developed and tested. This methodology could contribute to increase the lead-time of warnings so desperately required by disaster management;
- The development of basic user-oriented flash flood guidance products, including "dashboard" products to alert forecasters and disaster managers of potential problems in a local municipality;
- The first concepts in South Africa of an Impact-based Forecasting system to highlight hotspots of potential higher risk of flash flooding;

These developments, however, only tested basic concepts and need to be further refined to enhance the application of user-friendly services.

Through this study, very useful insight has been gained into the decision-making processes of stakeholders, and their requirements for products that will support these decision support systems. This process needs to be kept dynamic to ensure continuous relevance of products provided for the early warning against floods and flash floods in South Africa.

7.3 RECOMMENDATIONS

The applications and modifications developed in this project have the ability to make a significant improvement to the SAFFG and SARFFG systems. Some of these applications and modifications have already been introduced into the SAFFG modelling system. Others have to be addressed in subsequent activities.

A principal recommendation, however, is that the improvement of the entire flash flood warning system, of which SAFFG is but one component, should be investigated. This is also in line with the recommendations made by Du Plessis (2002) and Pegram *et al.* (2007) in their investigations for the WRC on flood warning systems. Now we are in a position when technological development and related research allow the development of a more comprehensive, integrated, flood warning system. This system should cover all forecasting timescales from seasonal forecasts right down to the nowcasting of severe weather in the next hour or two:

- Seasonal-range (months): A seasonal streamflow forecasting system.
- Medium-range (multi day): Providing outlooks for the next 2-10 days of river flood and flash floods.
- Short-range (up to 24 or 36 hours): flood and flash flood outlooks based on NWP rainfall forecasts and remotely sensed rainfall estimations.
- Nowcasting time-range (out to 6 hours): Providing guidance from the SARFFG and SAFFG systems based on remotely sensed rainfall estimations.
- Nowcasting detail information (0-2 hours): Complete run-off and inundation models in a few selected high-risk small catchments based on hydrological streamflow models, providing detailed information on the expected flash flooding in these basins.
- Socio-economic impact-based forecasting products to support disaster management decision-making, tailored for each different timescale.
- A seamless product system with a user-oriented display system should be developed from the different systems covering all these timescales.

Such an integrated flood warning system should be developed in a partnership between relevant role-players, including the South African Weather Service (SAWS), the Department of Water Affairs (DWA), disaster management structures, and other relevant role players that can contribute to the efficiency and success of this system. Operational application of this integrated flood and flash flood warning system will also require effective partnerships between the main role players, particularly SAWS, DWA and disaster management structures.

8. REFERENCES

AMS, 2012: American Meteorological Society Glossary of Meteorology, http://amsglossary.allenpress.com/glossary

Atlas, D., and Chmela, A. C., 1957: Physical-synoptic variations of drop size parameters. *Proc. Weather Radar Conf.*, 65th, 1957 pp. 21-30

Auld, H., 2008: Disaster Risk Reduction under current and changing Climate Conditions. *WMO Bulletin*, Vol. 57(2): 118-125

Battan, L. J., 1973: Radar Observations of the Atmosphere*. University of Chicago Press.*, 324 pp.

Bowler, N. E. H., C. E. Pierce, and A. Seed, 2004: Development of a precipitation nowcasting algorithm based upon optical flow techniques. *Journal of Hydrology*, 288, 74-91.

Bowler, N., C. Pierce, and A. Seed, 2006: STEPS: A probabilistic precipitation forecasting scheme which merges an extrapolation nowcast with downscaled NWP. *Quarterly Journal of the Royal Meteorological Society,* 132, 2127-2155.

Caelum, 2010: South African Weather Service,

Carpenter, T. M., Sperfslage, J. A., Georgakakos, K. P., Sweeney, T., & Fread, D. L., 1999: National Threshold Runoff Estimation Utilizing GIS in Support of Operational Flash Flood Warning Systems. *Journal of Hydrology*, 224, 21-44.

Chumchean, S., A. Seed, and A. Sharma, 2008: An operational approach for classifying storms in real-time radar rainfall estimation. *Journal of Hydrology*, **363**, 1-17

COMET, 2010: COMET MetEd UCAR Community Programs. www.meted.ucar.edu

CRED/EMDAT, 2010: Centre for Research on the Epidemiology of Disasters International Disaster Database, Université Catholique de Louvain, Brussels, Belgium. http://www.emdat.be/

Davis, R. S., 2001: Flash Flood Forecast and Detection Methods. *AMS Meteorological Monographs*, Vol 28, No 50, Ch 12: 481-526

De Coning, E., and E. Poolman, 2011: South African Weather Service Operational Satellite based Precipitation Estimation Technique: Applications and Improvements. *Hydrol. Earth Syst. Sci*., No 15, 1131-1145.

De Coning, E., 2013: Optimizing satellite-based precipitation estimation for nowcasting of rainfall and flash flood events over the South African domain. *Remote Sens.* 2013, *5*, 5702-5724; doi:10.3390/rs5115702.

Demuth, J.L., B.H. Morros and J.K. Lazo, 2009: Weather Forecast Uncertainty Information – An Exploratory Study with Broadcast Meteorologists. *Bulletin of the American Meteorological Society*, Nov 2009, 1614-1618

Deyzel I.T.H., G.G.S. Pegram, P.J.M. Visser and D. Dicks, (2004). Spatial Interpolation and Mapping of Rainfall (SIMAR), Volume 2. Radar and satellite products. Water Research Commission, Report WRC 1152/1/04, ISBN 1-77005-160-0.

Dixon, Michael Wiener, G., 1993: TITAN Thunderstorm Identification, Tracking, Analysis, and Nowcasting – A Radar-based Methodology. *Journal of Atmospheric and Oceanic Technology*, 10, 785-797.

Doviak, R., and D. Zrnić, 1984: Doppler Radar and Weather Observations, *Academic Press*, 458 pp.

DPLG, 2002: National Disaster Management Act No 57 of 2002. *Department of Provincial and Local Government, Pretoria, South Africa*, 32 pp.

DPLG, 2005: National Disaster Management Framework of 2005. *Department of Provincial and Local Government, Pretoria, South Africa*, 270 pp.

Du Plessis, L. A., 2002: A review of effective flood forecasting, warning and response system for application in South Africa. *Water SA*, 28, No 2, April 2002, 129-137.

Fulton, R., J. Breidenbach, D.-J. Seo, D. Miller, and T. O'Bannon, 1998: The WSR-88D rainfall algorithm. *Wea. Forecasting*, **13**, 377-395

Georgakakos, K. P., 2004: Mitigating Adverse Hydrological Impacts of Storm on a Global Scale with High Resolution: Global Flash Flood Guidance. *Proceedings of the International Conference on Storms, Storms Science to Disaster Mitigation, Brisbane, Australia*, 5-9 July 2004.

Georgakakos, K.P., 2006: Analytical Results for Operational Flash Flood Guidance. *Journal of Hydrology*, 317, 81-103

Georgakakos, K. P., 2011: Overview of FFGS and Recent Developments. *Presentation at SARFFG Steering Committee Meeting, Pretoria, South Africa*

Golding, B.W., 2009: Uncertainty propagation in a London flood simulation. *Journal of Flood Risk Management,* 2 (2009), 2-15

Holloway, A., G. Fortune, V. Chasi, 2010: RADAR Western Cape 2010 – Risk and Development Annual Review. *Creda Communications*, 101 pp.

ISDR, 2005a: Living with Risk: A Global Review of Disaster Reduction Initiatives. *ISDR*

ISDR, 2006b: Global Survey of Early Warning Systems. *A Report Released at the Third International Conference on Early Warning*, 27-29 March 2006, Bonn, Germany.

ISDR, 2010: Terminology: Basic Terms of Disaster Risk Reduction. http://www.unisdr.org/eng/library/lib-terminology-eng%20home.htm

IPCC, 2011: Summary SREX Summary for Policymakers: IPCC Special Report on Managing the Risks of Extreme Events and Disasters to Advance Climate Change Adaptation. http://ipcc-wg2.gov/SREX/ , Geneva, Switzerland, 29 pp.

Joslyn, S., L. Nadav-Greenberg, R. M. Nichols, 2009a: Probability of precipitation: assessment and enhancement of end-user understanding. *Bulletin of the American Meteorological Society*, Feb 2009, 185-193.

Joslyn, S., L. Nadav-Greenberg, M. U. Taing, R. M. Nichols, 2009b: The effects of wording on the understanding and use of uncertainty information in a threshold forecasting decision. *Applied Cognitive Psycholog*, 23: 55-72.

Kroese, N.J. (2004). Spatial interpolation and mapping of rainfall (SIMAR), Volume 1. Maintenance and upgrading of radar and raingauge infrastructure. Water Research Commission, Report WRC 1151/1/04, ISBN 1-77005-161-9.

Liu Z. and Todini E., 2002: Towards a comprehensive physically-based rainfall-runoff model. *Hydrol. Earth Syst. Sci***. 6**(5) 859-881.

Marshall, J.S., and W.M.K. Palmer, 1948: Distribution of Raindrops with Size*, J. Meteorology*, **5**,165-166

Meirold-Mautner, I., Y. Wang, A. Kann, B. Bica, C. Gruber, G. Pistotnik, S. Radanovics, (2010): "Integrated Nowcasting System for the Central European Area: INCA-CE", Data and Mobility, *Advances in Intelligent and Soft Computing*, 2010, Volume 81/2010, 107-114, DOI: 10.1007/978-3-642-15503-1_10

Mecklenburg, S., J. Anna, S. Jan, and O. Katerzyna, 2002: Quantitative precipitation forecasts (QPF) based on radar data for hydrological models.

Morss, R. E., J. L. Demuth and J. K. Lazo, 2008: Communicating Uncertainty in Weather Forecasts: A Survey of the U.S. Public. *Weather and Forecasting*, 23: 974-991

Morss, R. E., J. K. Lazo and J. L. Demuth, 2010: Examining the use of weather forecasts in decision scenarios: results from a US survey with implications for uncertainty communication. *Meteorological Applications*, 17: 149-162

National Research Council, 2008: Integrating Multiscale Observations of US Waters. *National Academies Press*, Washington, DC, 210 pages, pp 74-76)

Pegram GGS. (2004). Spatial interpolation and mapping of rainfall (SIMAR), Volume 3. Data merging for rainfall map production. Water Research Commission, Report WRC 1153/1/04, ISBN 1-77005-159-7.

Pegram, G., S. Sinclair, M. Parak, D. Sakulski, N. Nxumalo, 2007. National Flood Nowcasting System: towards an integrated mitigation strategy. *WRC Project 1429/1/06,* Water Research Commission, Pretoria, South Africa.

Pegram, G., Sinclair, S., Vischel, T., and Nxumalo, N., 2010: Soil Moisture from satellites: Daily maps over RSA for flash flood forecasting, drought monitoring, catchment management & agriculture. Technical Report, Water Research Commission Report No. K5-1683, *Water Research Commission*, Pretoria, South Africa.

Poolman, E. R., 2009: Analysis of DMA questionnaires from 2009 SAFFG workshops. *SAFFG Internal Report SAFFG-Gen-007.1*, South African Weather Service, Pretoria

Poolman, E. R., 2014: A probabilistic impact-focussed early warning system for flash floods in support of disaster management in South Africa. *Unpublished PhD Thesis*, University of Pretoria, Pretoria

Rosenfeld, D., D. Wolff, and D. Atlas, 1993: General probability-matched relations between radar reflectivity and rain rate*. J. Appl. Meteor.*, **32**, 50-72

Roulston, M.S., G.E. Bolton, A. N. Kleit and A. L. Sears-Collins, 2006: A Laboratory Study of the Benefits of Including Uncertainty Information in Weather Forecasts. *Weather and Forecasting*, 21: 116-122

Sauvageot, H., 1992: Radar Meteorology*. Artech house*, 366 pp.

SAWS, 2011: Guidelines for a Storm Surge Early Warning System. *MHEWS Report submitted to NDMAF*, NDMC, Pretoria, South Africa.

SAWS, 2011a: Guidelines for a Tsunami Early Warning System for South Africa. *MHEWS Report, NDMC,* Pretoria, South Africa.

Seed, A., 2003: A dynamic and spatial scaling approach to advection forecasting. Journal of applied meteorology, 42, 381-388.

Seed, A.,2007: Short-term hydrological forecasting using weather radar, hydrological consequences of climate change, *15 & 16 November CSIRO*, Canberra

Seed, A.,2009: Recent Advances in Nowcasting, *SAWS*, Pretoria

Sperfslage, J., C. Spencer and K. Georgakakos, 2010: South African Flash Flood Guidance System User's Guide. *HRC Limited Distribution Report No. 32*, Hydrologic Research Centre, San Diego, CA, USA, 210 pp

Steiner, M., R. A. Houze Jr, and S. E. Yuter, 1995: Climatological characterization of three-dimensional storm structure from operational radar and rain gauge data. *Journal of Applied Meteorology*, **34**, 1978-2007

Vogel, C., and K. O'Brien, 2006: Who can eat information? Examining the effectiveness of seasonal climate forecasts and regional climate-risk management strategies. *Climate Research*, 33: 111-122

Wang, Y., A. Kann, I. Meirold-Mautner, and B. Bica, 2011: A Central European Initiative for Severe Weather Warnings and Improved Communication Strategies on a trans-national Level. http://www.incace.eu/index.php?option=com_jdownloads&Itemid=138&view=finish&cid=210&catid=29

WMO, 2006: Preventing and Mitigating Natural Disasters. *WMO-No 993*, Geneva, Switzerland

WMO, 2006a: Symposium on Multi-Hazard Early Warning Systems for Integrated Disaster Risk Management. *EWSSymposium2006OutcomeReport.pdf*, WMO, Geneva, Switzerland.

WMO, 2007: Prospectus for the Implementation of a Flash Flood Guidance System with Global Coverage. *WMO CBS-MG-VII/Doc 5(7)*, Geneva, Switzerland.

WMO, 2008: Guidelines on the Communication of Forecast Uncertainty. *WMO TD No. 1422*, Geneva, Switzerland

WMO, 2008: Guide to Hydrological Practices, *Vol II, Chapter 7*. WMO, Geneva, Switzerland

WMO, 2011: Manual on Flood Forecasting and Warning. *WMO No. 1072*, Geneva, Switzerland

Worldbank, 2010. Data finder: population total. http://datafinder.worldbank.org/

Wilks, D.S., 2006: Statistical Methods in the Atmospheric Sciences, *Elsevier 2nd edition*, pp. 627

Zhang, J., Howard, K., Langston, C., Vasiloff, S., Kaney, B., Arthur, A., van Cooten, S., Kelleher, K., Kitzmiller, D., Ding, F., Seo, D.J., Wells, E., Dempsey, C., 2011: National Mosaic and Multi-Sensor QPE (NMQ) Systems: Description, Results, and Future Plans, *Bulletin of the American Meteorological Society*, vol. 92, issue 10, pp. 1321-1338